INVESTIGATION OF MICROSTRUCTURAL CRACKING OF RIVETED AND HEAT-TREATED AL7075 ALLOYS UNDER CONSTANT FATIGUE LOADING

BY

ROBERT KIPCHUMBA RUTTO

A thesis submitted in partial fulfilment of the requirements for the degree of Master of Science in Industrial Engineering, Department of Manufacturing, Industrial & Textile Engineering, School of Engineering, Moi University

2023

DECLARATION

Declaration by the Student

This thesis is my original work and has not been presented for a degree at any other University.

11th November 2023

Robert Kipchumba Rutto Date

ENG/MIE/3988/20

Declaration by Supervisors

This thesis has been submitted for examination with our approval as University Supervisors.

11th November 2023

Prof. Diana Madara Date

Moi University, Eldoret, Kenya

11th November 2023

Dr J . K . Kiplagat Date

Moi University, Eldoret, Kenya

DEDICATION

I dedicate this work to my entire family. They have always been there to lift me when I fall and to celebrate with me when I succeed.

ABSTRACT

The unique properties of the strength-to-weight ratio of aluminium make them the preferred material aircraft design with safety margins and improved payload. Fatigue cracking of Al7075 poses major issues in administering ageing aircraft structures. Understanding the effect of fatigue on rivet hole geometry and heat treatment on aircraft structures helps identify crack mitigation measures, making aluminium continue operation with high assurance levels. The main objective was to investigate microstructural cracking of riveted and heat-treated Al7075 used in aerospace stringers and frames under constant fatigue loading and develop crack mitigation measures. The specific objectives were to evaluate crack growth and propagation under constant fatigue loading of Al7075-O/T6/T7; to determine crack propagation under constant fatigue loading in 100^{o} Countersunk rivet hole and perpendicular rivet hole geometry of Al7075-O/T6/T7; to characterize cracking of Al7075 under (a) varied heat treatment conditions in terms of crack-path and crack surface morphology, and (b) under 100^{o} countersunk rivet hole and perpendicular rivet hole geometry in terms crack surface morphology; to identify mitigating actions to microstructural cracking Al7075. Al7075-O/T6 were procured from Smiths Advanced Metals U.K., and Al7075-T6 was converted to Al7075-T7 as per Boeing standard BAC562 at Kenya Airways mechanical workshop, Nairobi. High-cycle-fatigue testing was performed at the University of Nairobi Mechanical Engineering workshop. The crack surface morphology was observed via the Tescan Vega-3 scanning electron microscope. The sample size for heat treatment was 6, for hole orientation 12, and for scanning electron microscope analysis 72. Middle-tension specimen geometry was utilized for crack growth rates as per ASTM E647-13.

Crack initiation samples for different rivet hole orientation were prepared as per (ASTM E8, 2010). Paris-region material parameters were Paris exponent; 10.069, 10.869, 9.663 and Paris constants; 3E-07, 4E-07, 1E-06 for Al 7075-T7, Al 7075-T6, Al 7075-O respectively. Crack propagation curves for 100^{o} countersunk and perpendicular rivet holes were parallel for the same heat-treated condition. Al7075-O had trans-granular and deflecting angles of about 30^{o}, 45^{o}, and 70^{o} crack paths. Al7075-T6 and Al7075-T7 exhibited trans-granular, minimal deflection crack paths. Internal tissue flaws or stress concentration initiated fatigue cracks. The fatigue crack propagation comprises two phases: crack initiation, occurring along the primary slip plane to inside metal, and crack propagation, displaying fatigue strips with widths 0.28μm, 0.36μm and 0.68μm for 7075-T7, 7075-T6, and 7075-O respectively. The final fracture surfaces were coarse with mixed ductile-brittle fractures of tearing ridges. The dimple size increased with heat treatment from 7075-O to 7075-T6 to Al 7075-T7. The study concludes that fatigue strength increases with heat treatment of Al 7075. The countersunk and perpendicular rivet holes exhibit similar fatigue cracking for the same heat-treated condition. Micro-cracks inducing fracturing start from zones where inclusions, coarse, secondary-stage particulates, and micro-structural flaws are present. The zone of quasi-cleavage planes and fatigue strip widths declines with increasing heat treatment. The final fracture area is attributed to dimples whose dimensions become larger. From the study, it can be concluded that Microstructural impurities majorly cause microstructural cracking. To mitigate against fatigue cracking of aircraft stingers and frames, the study recommends using high-purity Al7075, and should be heat-treated to reduce stress concentrations.

TABLE OF CONTENTS

LIST OF TABLES

LIST OF FIGURES

ACKNOWLEDGEMENTS

My sincere gratitude goes to the Almighty God for the gift of life and good health, guiding me through this journey and granting me sufficient grace and wisdom every step of the way.

This thesis was prepared under the supervision of Professor Diana Madara and Dr. Joseph Kiplagat of the School of Engineering at Moi University. I am grateful to my advisors and reviewers for providing crucial advice, direction, and criticism during my research and report writing.

I also take this opportunity to thank the staff of the Department of mechanical engineering at the University of Nairobi, especially Dr Thomas Ochuku Mbuya, Prof. George Rading, Mr John Ngugi Kahiro, Mr Luke Mwafwali Wangai, Mr David Mwangi. In addition, the Faculty of Engineering at Busitema University, especially Mr. Tumusiime Godias (Busitema), for the technical support and guidance that enabled me to conduct my experiments.

I also acknowledge the financial and technical support from Moi University through the Africa Centre of Excellence in Phytochemicals, Textile and Renewable Energy (ACE II-PTRE) for making this research possible.

Finally, I would like to thank the postgraduate teaching team in the School of Engineering at Moi University for their unwavering assistance throughout my academic career. I also want to thank my friends and co-workers, who have always been there for me.

ABBREVIATIONS AND ACRONYMS

AMM: Aircraft Maintenance manual

AOG: Aircraft on Ground

CPS: Crack Propagation Slow

CPF: Crack Propagation Fast

FF: Final Failure

SEM: Scanning Electron Microscope

SRM: Structural Repair Manual.

CHAPTER ONE: INTRODUCTION

1.1 Introduction

This chapter will look at the background of the study, the problem statement, the study objectives, and the research justification.

1.2 Background of the Study

The unique properties of aluminium alloys and their strength-to-weight ratio make it the preferred choice for designing aircraft with design safety margins and improved payload (Gloria et al., 2019). Colossal resistance to extension of fatigue cracks and enhanced formability of the alloys permits low manufacturing costs and reduced process flow time.

Alloy 7075-T6 is used where compressive strength is the critical design principle, e.g., stringers and frames of an aircraft.

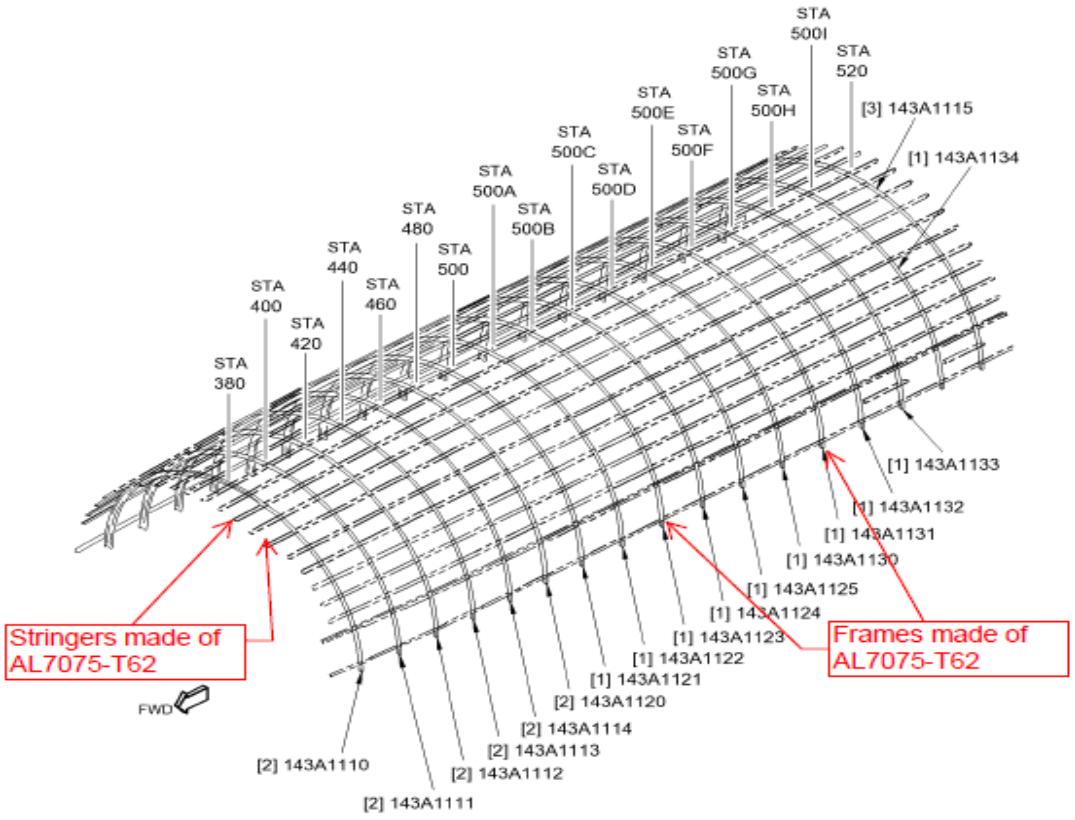

Figure 1.1: Stringers and frames identification (Boeing 737-800 SRM).

1.3 Statement of the Problem

During maintenance inspections, several aircraft operators report the crack failure of parts made of Al 7075-T6, specifically frames and stringers, as seen in Figure 1.1. The current remedy is to repair or replace the parts before the next flight, which takes at least five days. The aircraft will be grounded for at least five days, leading to a loss of average revenue of KES 13,703,200.00 per day (Kenya Airways disruption rate, 2018, Kenya airways Cost-benefit analysis tool). Undetected cracks lead to compromised structural members that carry an aircraft's primary and secondary loads, making it unsafe to operate. The breakdown of structural elements of aircraft happens due to various determinants that may appear from microstructural flaws and/or employed static or cyclic stresses.

According to Boeing Multi Operator Message MOM-MOM-19-0536-01B, out of eighteen (18) airplanes, including both 737-700 and 737-800 variants, have been inspected, three (3) of them showed crack findings. One (1) reported cracks on the left-hand side and right-hand side frame fitting outer chords, and one (1) reported a crack on the right-hand side frame fitting the outer chord.

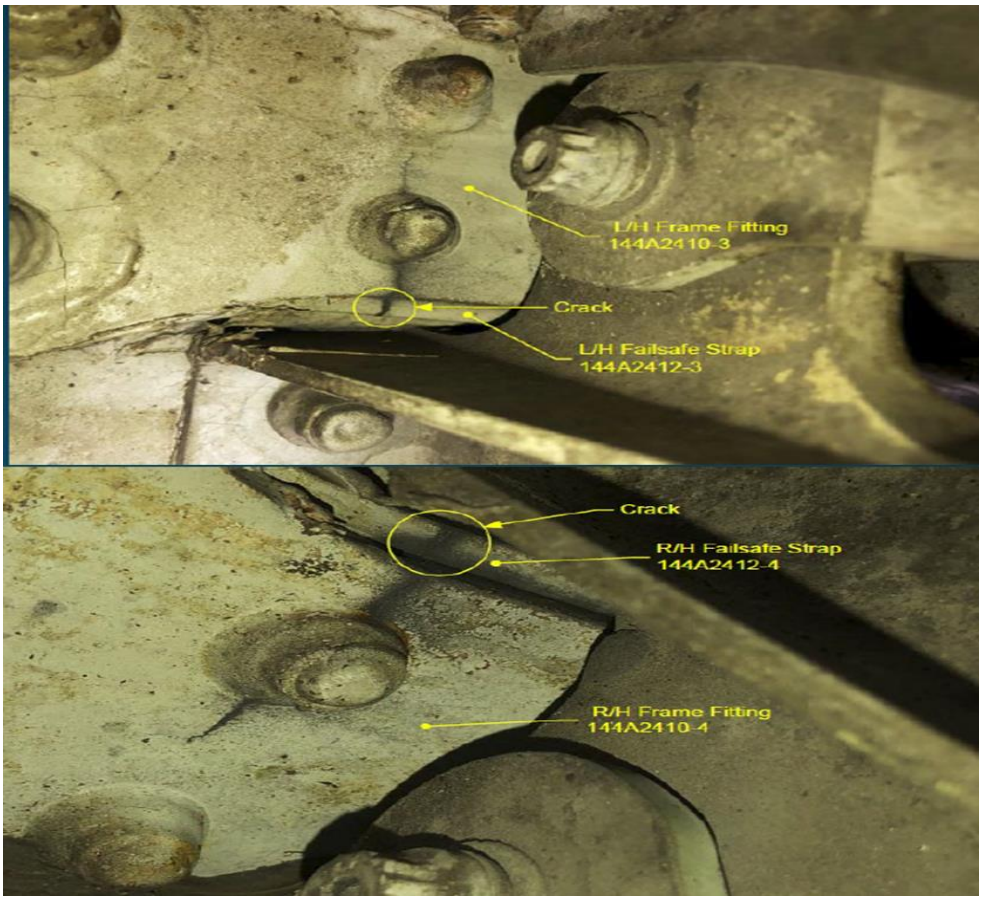

Figure 1.2: Example showing fitting/strap with cracks (Boeing Multi Operator Message MOM-MOM-19-0536-01B).

1.4 Significance of the Study

When the effect of fatigue on rivet hole geometry and heat treatment on aircraft structures is fully understood via laboratory data and identification crack mitigation measures, aluminium

alloys will continue to operate over many decades with a high level of assurance. During maintenance inspections, this will reduce or eliminate reported crack failure by aircraft operators of parts made of Al 7075-T6, specifically frames and stringers.

Since there will be a reduced cracking of Al 7075, the need to repair or replace parts will decline, and aircraft grounding will be reduced, leading to avoidance of revenue loss of average revenue of KES 13,703,200.00 per day (Kenya Airways disruption rate, 2018).

1.5 Objectives

1.5.1 Main Objective

To investigate microstructural cracking of riveted and heat-treated Al alloy 7075 used in aerospace stringers and frames under constant fatigue loading and develop crack mitigation measures.

1.5.2 Specific Objectives

1. To evaluate crack growth and propagation under constant fatigue loading of Al alloy 7075 under varied heat treatment conditions (-O,-T6,-T7)
2. To determine crack propagation under constant fatigue loading in a 100^{o} countersunk rivet hole and straight rivet hole geometry of Al 7075-O, Al 7075-T6, and Al 7075-T7 alloys specimens.
3. To characterize cracking of Al alloys 7075 under(a) varied heat treatment conditions in terms of crack path and surface morphology, and (b) under 100^{o} countersunk rivet hole and straight rivet hole geometry in terms of crack surface morphology.
4. To identify mitigating actions to microstructural crack growth and propagation of Al alloys 7075.

1.6 Justification of the Study

In this work, microstructure, nature of precipitates, rivet-hole geometry, and heat treatment affecting the fatigue performance of several aluminium alloys 7075-0/T6/T7 used in aerospace stringer and frames were studied through fatigue loading tests and micro-structural analysis. When the effect of fatigue on rivet hole geometry and heat treatment on aircraft structures is fully understood via laboratory data and identification crack mitigation measures, aluminium alloys will continue to operate over many decades with a high level of assurance. During maintenance inspections, this will reduce or eliminate reported crack failure by aircraft operators of parts made of Al 7075-T6, specifically frames and stringers.

Since there will be a reduced cracking of Al 7075, the need to repair or replace parts will decline, and aircraft grounding will be reduced, leading to avoidance of revenue loss of average revenue of KES 13,703,200.00 per day (Kenya Airways disruption rate, 2018).

This study proposes reducing the breakdown of aircraft structural elements typically due to various determinants that may appear from microstructural flaws and/or employed static or cyclic stresses. It also reduces the issue of undetected cracks that usually lead to compromised structural members that carry the primary and secondary loads in an aircraft, making them unsafe to operate.

1.7 Scope of the Study

This study focused on the Al 7075 alloy in three heat-treated conditions: O, T6 and T7. The study was also limited to constant fatigue loading and scanning electron microscopy on the cracking surfaces. The design of the specimen was done as per the standards ASTM 647. Data analysis, interpretation and discussion were done as per ASTM 647.

CHAPTER TWO: LITERATURE REVIEW

2.1 Introduction

This chapter reviews the literature related to the purpose of the study. It is organized according to the objectives developed in the previous chapter and discusses the theoretical framework upon which the study is based. It covers the background, aluminium alloy, fatigue crack theories and concepts, fatigue crack propagation models, and fatigue crack propagation studies directly related to 7075 alloys.

2.2 Background

Airports manufacturers face competition to keep operating costs low in the aviation industry. In most cases, the factors considered include better fuel efficiency, flight range, payload increase, extended service life, and efficient fuel consumption. Therefore, there has been an advancement of materials that each manufacturer focuses on using unique and better features. Research by Raghavender & Sahoo (2021) shows that manufacturers focus on weight reduction and prolonging the service life of aircraft components and structures. However, to lower the weight, there is a need to use sophisticated materials with superior wear and fatigue features, corrosion resistance, and a high tolerance to damage (Zhang et al., 2018; Dursun & Soutis, 2014; Warren, 2004).

The popular choice of material used for sub-sonic aircraft systems is Aluminium alloys. (Raghavender & Sahoo, 2021). Because of their low price, outstanding formability, and high strength-to-weight ratio, due to these characteristics, the alloys are excellent for minimalistic building designs. The use of these materials is limited by their inability to withstand high temperatures. Furthermore, the use of high-strength Aluminium alloys is determined by their susceptibility to stress corrosion cracking and their relatively poor fatigue strength.

In aviation, the selection of materials largely depends on the component type, geometric limits, environment, stress circumstances, production, and maintenance. For instance, while selecting structural elements, one factor considered would be its ability to withstand weight due to the aircraft's static and extra loads associated with activities such as turbulence, manoeuvres, taxing, take-off, and landing. Therefore, they must exhibit comparatively low densities to reduce weight overall. Another critical factor is the ability of the material to withstand harsh conditions of ultraviolet radiation, temperature, and humidity (Huda & Edi, 2013).

Riveting is the common practice for attaching sheet metal components in aeroplanes. (Cheraghi, 2008). Failure of a rivet can have severe consequences, like losing human lives and money. Loss of life and financial resources are just two potential outcomes of a failed rivet. Squeeze force, rivet length, rivet diameter, and hole diameter tolerance are just a few of the many characteristics of a riveting process that directly impact the quality of the rivets. Excessive residual stresses can be induced by incorrect selection or modifications in these parameters, resulting in stress concentration sites and the initiation of cracks, improper rivet head deformation, and, therefore, loose rivets.

2.3 Aluminium Alloys

For several ages, Al alloys have remained broadly utilized materials in aviation; nonetheless, the situation is swiftly advancing, as confirmed by Table 2.1, which indicates the estimated fundamental structure elements exploited through weight in Boeing aircraft. The data shows that the part played by composites is rising (Warren, 2004).

Table 2.1: Materials used in aircraft by the Boeing Company, weight percentage. (Warren, 2004).

Boeing Series	**747**	**757**	**767**	**777**	**787**
Al alloys	81	78	80	70	20
Ti Alloys	4	6	2	7	15
Steel	13	12	14	11	10
Composites	1	3	3	11	50
Others	1	1	1	1	5

Note: The phrase “Others” applies to materials in very minute quantities, including metal alloys, carbon, magnesium, and refractory metals.

In any case, notwithstanding the increasing application of composites, Al alloys remain the materials of primary relevance for structural use due to their lightweight, workability, and relatively economical cost. At the same time, appropriate enhancements have been accomplished for 7XXX and 2XXX AL-LI alloys.

In most cases, the 2XXX order alloys are used in areas where fatigue is crucial because they exhibit high tolerance to damage; the 7000 orders are employed wherever strength is the foremost necessity. Al-Li alloys get preference where parts require immense stiffness and incredibly low density.

2.3.1 7XXX order-(Al-Zn) [7075 Aluminium Alloy]

Amongst metals, zinc has the most incredible ability to be soluble in Aluminium, and its strength outcome is enhanced by raising the Zn substance. The 7XXX line alloys exemplify the most influential alloy of Al. They are used for aeronautic parts subjected to high stresses,

such as upper wing skins, stringers, and stabilizers, produced from alloy 7075 (Yield Strength = 510 MPa). Magnesium and Copper remain commonly applied in addition to Zinc to produce $MgZn_2$, Al_2CuMg, and AlCuMgZn precipitates, which make an alloy of good strength (Zeng et al., 2012). Nevertheless, there exist a few disadvantages to the 7XXX line of alloy. Particularly, reduction in fracture toughness, damage threshold, and corrosion endurance restrains the application of 7075 alloys in aeronautics. Nevertheless, varying the distribution can help enhance the features.

The best attributes of the 7XXX line of alloy are achieved when the Zinc/Magnesium and Zinc/Copper ratios are almost equivalent to 3 and 4 sequentially. The alloy of series 7085 is a practical substitute for the 7075 alloys in aerospace applications owing to its better mechanical features (Yield Strength = 504 MPa, elongation = 14%) and enhanced damage threshold. Due to its high strength/weight ratio, 7075 aluminium alloy has been widely used as an aerospace material. However, it has relatively low fatigue strength and low fracture toughness in the T6 condition (Albedah et al., 2020b).

Outline defects that aluminium alloys experience, including gas pores, micro-shrinkages, un-melted regions, defective micro-structures, and micro-cracks as the leading cause of fatigue failure. The second critical class of defects addressed is damage initiated within service, maintenance, or manufacturing (Zerbst et al., 2019). It consists of dents, scratches, sparling, and corrosion pits. Different defect types exhibit other fatigue crack commencement and extension rates. Conditions under which crack emanates from defects and the nature of crack arrest in terms of critical defect sizes are addressed.

A critical problem associated with using 7XXX line alloys is the fatigue response and research actions have been dedicated to the issue while considering various variables.

Discontinuities in materials are frequently linked to crack nucleation. At a micro-scale, precipitate and roughness shreds can play preference nucleation places; nonetheless, the major pressing issues arise at a macro-scale level. The coating covers owing to cladding, anodizing, and errors (scratches during machining and marks) created by the manufacturing method have been discovered to be the primary origin of failure (Merati & Eastaugh, 2007). The anodic oxidation process considerably decreased the performance of the 7075-T6 alloy in fatigue. In contrast, the degrading effect of the oxidation raises coating layer thickness increased by the deep micro-cracks that develop during the anodizing process, bringing about this considerable effect. Furthermore, the brittleness of the coating of oxide and variations under the coating help toward deterioration (Cirik & Genel, 2008).

2.4 Fatigue Crack Growth Theories and Concepts

Small cracks are shear-forced and are related to microstructure. Thus, continuum mechanics techniques are mainly used during its analysis. On the other hand, large cracks are tension-driven and are micro-structurally insensitive. Fracture mechanics models usually analyse these cracks. Figure 2.1 illustrates different stages of fatigue crack growth in a material.

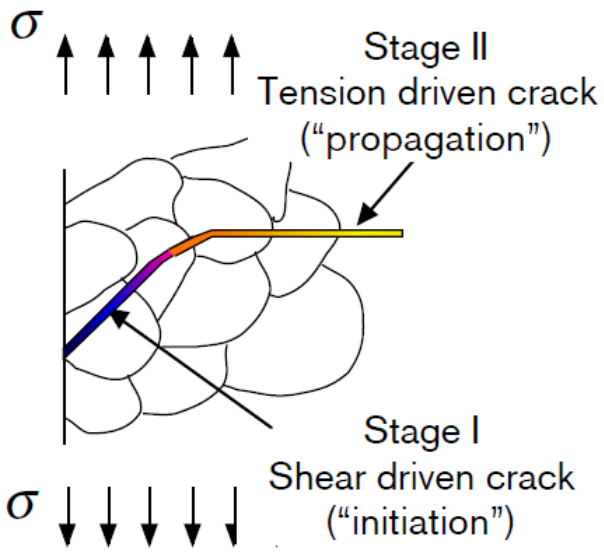

Figure 2.1: Phase I and phase II fatigue crack growth (Raghavender & Sahoo, 2021)

The stress intensity factor in static Loading for a small crack in a large sample can be represented as:

$$K_I = f\left(s, \sqrt{a}\right) \quad \text{(Eq.2.1)}$$

Where S- applied stress, a-crack growth, and f rely on the specimen geometry.

When the stress is maintained unchanged, the fracture for a specific crack length, $a = a_c$, will deliver $K_I = K_{IC}$. (Where: a_c - critical crack growth, K_I = stress intensity factor, K_{IC} = critical stress intensity factor).

A fracture is found in dynamic Loading if the stress intensity factor, for some moment time, surpasses $K_I = K_{IC}$. Nevertheless, for $K_I<K_{IC}$, crack propagation may transpire. This suggests that a (and K_I) will advance, and we will ultimately get a fracture when $a=a_c$. It is important to note that crack propagation has usually been examined as a function of the stress intensity factor in investigations.

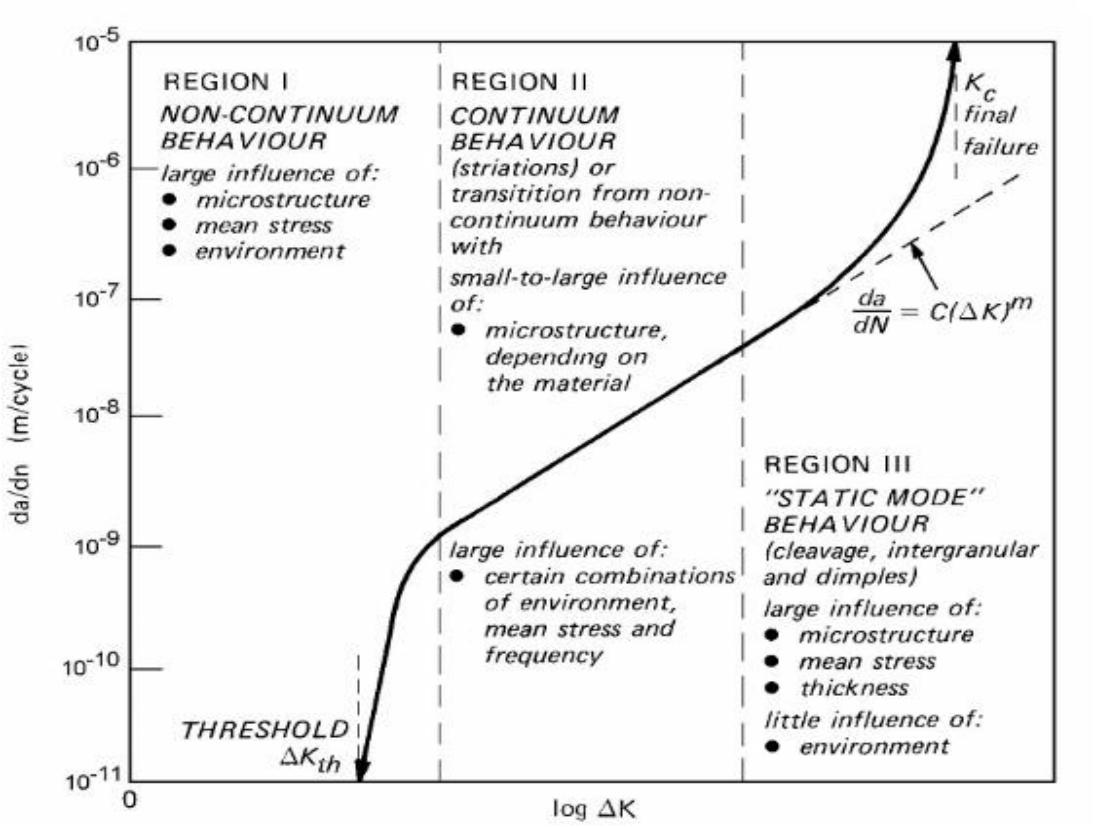

Figure 2.2: Features of the fatigue crack growth rate curve da/dN-ΔK.(Raghavender & Sahoo, 2021)

There is no spread of fatigue cracks below a particular stress intensity factor, ΔK. The fracture toughness of KC is approached, and material failure occurs when Kmax is close to KC. The relationship between log (da/dN) and ΔK is linear in Region II. It is important to remember that ΔK varies with the size of the crack, even if this is not reflected in the graph.

The fatigue life can be roughly divided into crack initiation, growth, and propagation. For these regions, the da/dN-ΔK curve on a double logarithmic scale, which plots the crack growth rate per cycle against the stress intensity span, displays a typical sigmoid shape, see Figure 2.2.

The following features are typical of fatigue in every metallic material:

Zone I: Fatigue crack initiation and stable threshold area

Zone II: Steady crack propagation is displayed as linear on a log-log scale.

Zone III: Crack propagation in an unsteady state.

Zone I: Fatigue crack initiation and threshold zone.

The initiation phase is referred to as where the fatigue procedure begins and where microscopically small cracks develop. Micro-cracks occur close to a discontinuity in the material during initiation, e.g., particles or voids, scratches, indents, and corners indicate sites of relatively high-stress concentrations. Micro-structurally short cracks are typical of the order of one or rare grains in length and propagate by shear mode (Mode II). Crack initiation governs the fatigue life of aluminium alloys: more than 90% of the life span is usually spent in this phase, depending on the stress variation. Materials such as steel and titanium have a limit where repeated stress does not lead to cause failure called fatigue limit. Infinitely small stress amplitudes will eventually induce failure, and the fatigue limit does not exist for most materials, including aluminium alloys. Near-threshold fatigue crack propagation refers to crack growth rates below 109 m/c, as seen in Figure 2.2.

Zone II: Stable crack propagation

Cracks propagate by mode I in Stage II. Distinct fatigue cracks mature from the first stage (I) to a second stage (II) crack, as shown by the schematic illustration in Figure 2.3 (Cicero et al., 2020). Stage II crack path is now practically perpendicular to the tensile stress axis. Linear association between da/dN against ΔK on a log-log-scale best describes crack

propagation in zone II, known as Paris' Law, where da – crack growth rate, dN-change in several cycles induced, and ΔK – stress intensity factor.

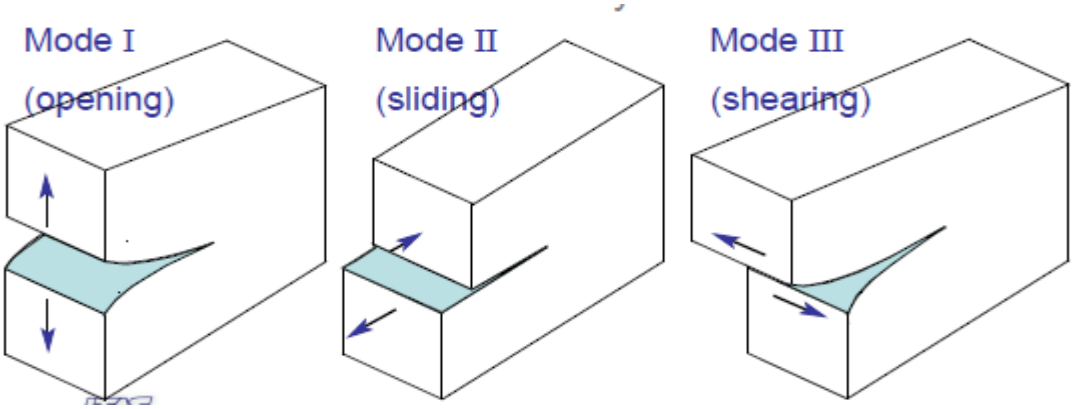

Figure 2.3: Different modes of crack surface displacements

Striations are the most characteristic feature on a microscopic scale during crack growth in Region II. the striations represent crack successive front positions, while one load cycle forms each striation (Kelly, 2020).

Zone III: Unsteady crack propagation

Region II exhibits steady fatigue crack growth; the driving force of the crack should be larger than the material's crack resistance. In zone III, the increased driving force can no longer resist the material resistance. The crack growth accelerates rapidly since it is an interaction between fatigue and static processes and is no longer a pure fatigue process.

The tensile stress axis is now an angle to the crack growth direction. The sum of the cycles devoured in various areas makes Total fatigue life, see Figure 2.4.

Compared to the total fatigue life, the duration of zone III growth is always shorter. Hence, fatigue life estimations can neglect Region III without significant loss of accuracy. Failure occurs once fracture toughness, $K_{C,}$ is reached by the maximum stress intensity factor K_{max}.

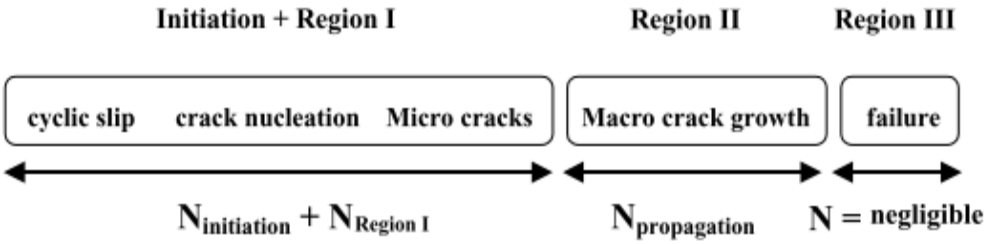

Figure 2.4: Fatigue life duration.(Raghavender & Sahoo, 2021)

2.4.1 Influence of Mechanical Properties

2.4.1.1 Microstructure

The impact of microstructure and fatigue crack growth agents is localized close to the crack tip. For instance, the following are related to microstructure: surface roughness, environmental interaction, and corrosion-induced closure. Fatigue properties related to microstructure are challenging to understand due to interaction with micro-structural features of the environment and loading system. Generally, at lower crack growth rates, microstructure has a more substantial influence on fatigue crack growth. The larger da/dN at high K dominates all other mechanisms (De et al., 2009).

2.4.1.2 Grain Size

Many researchers have examined how grain size affects fatigue crack development resistance and how cracks are arrested at grain edges (Chen et al., 2013). It was investigated by (Ma et al., 2022) that a shift in crack growth agency occasionally transpired when the monotonic plastic location size was roughly equivalent to the grain proportions. Grain edges can operate as deterrents and multiple stints, and fatigue cracks growth pace reduction is honoured in the threshold area (Chen et al., 2013).

The fatigue limit can be improved by grain refinement. Nonetheless, the threshold ΔK is frequently more significant for more extensive grains. Grain proportions deviations in a material result from earlier heat treatment and deformation. Furthermore, different micro-structural changes vary with processing; for example, texture and yield strength happen simultaneously. Evaluation of the underlying agents influencing the crack growth conduct for materials bearing various grain proportions becomes difficult due to these complex deformation-related and temperature-related transformations.

2.4.1.3 Effect of Yield Strength.

A concordance exists, typically in the threshold region, between the effect of the material's strength on fatigue crack propagation and the failure threshold itself; a higher yield strength for steel correlates to decreased plasticity and higher threshold significance. In contrast, a higher yield strength for non-ferrous metals correlates to reduced plasticity and lower threshold significances. Attempts have been made to explain the effect of hydrogen embrittlement steels where a small area is impacted by hydrogen around the crack tip. Hydrogen lowers threshold values since it weakens the metal and influences the environment.

2.4.1.4 Influence of Moisture

Investigations performed with low water vapour pressure have indicated that residual moisture due to low partial pressures can substantially influence crack growth paces, particularly in assortment with more elevated frequencies (Wang & Zhou, 2022). In the case of aluminium alloys, the formation of hydrogen atoms and oxide layers on the newly formed fracture surface occurs at the crack tip during the fatigue process.

Dislocation activities can move hydrogen atoms after diffusing into the plastic zone. Acceleration of crack formation at ultrasonic frequencies in the air (dots), dry air (circles), and a vacuum (triangles) at a load ratio R = -1 during trials of constant load amplitude near the threshold in different conditions or under different water vapour pressure requirements. Surface migration of water vapour molecules into the fracture tip can be used to characterize the disparity in crack propagation. By diffusion, water vapour from the surrounding air is transported to the crack tip, where it undergoes chemical reactions with the freshly created fracture surfaces, producing hydroxide, hydrated oxides, and the liberation of hydrogen. The cycle frequency and the partial pressure of water vapour controlled the surface reaction at the crack tip. Hydrogen atoms can either adsorb on the surface or in the initial few atomic layers, enhancing dislocation nucleation, or diffuse in front of the crack tip, both of which have embrittling effects (Pineau et al., 2016).

2.4.1.5 Influence of Temperature

Fatigue behaviour changes with temperature changes. Temperature plays a role in the rate of a chemical reaction (corrosion). Generally, with increasing temperature, the corrosion reaction becomes faster. Additional crack closure may result due to corrosion products on the crack surfaces.

2.4.2 Influence of the Loading System

2.4.2.1 Influence of Stress Ratio

The load ratio R strongly affects crack growth. There is a change to reduced ΔK values with rising R in crack growth curves; see figure 2.5 (Hassanifard et al., 2019). Elber developed crack closure theory to provide a physical rationale for such load-ratio consequences. For a qualitative explanation of the effects of the stress ratio, this analogy postulates that the crack

flanks come into touch with one another before the minimum load is reached. According to calculations, crack tip openings at R = 0.5 are more extensive than at R = 0.2. Under the condition where R = 0.5, the split widens. At R = 0.5, the distorting influence of crack surfaces on the roughness of the surface will be minimal, and it will improve with further decreases in R.

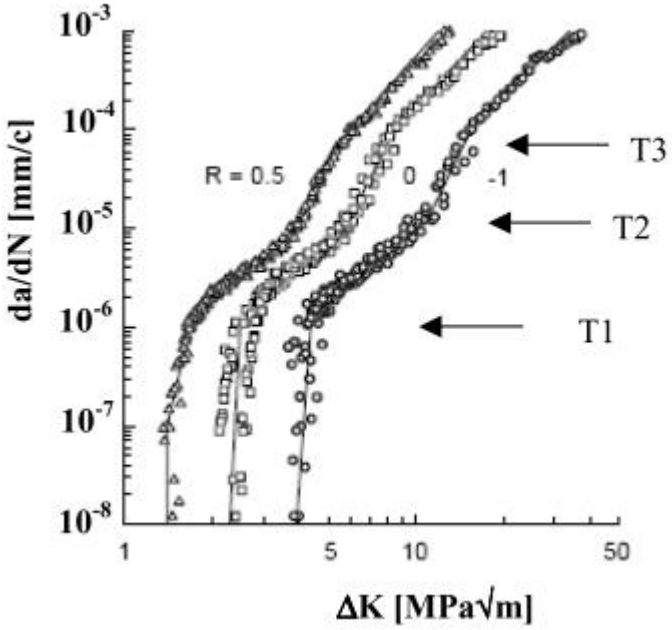

Figure 2.5: Stress ratio effect in Al 7075.(Raghavender & Sahoo, 2021)

2.4.2.2 Influence of Load Frequency

The crack development acceleration da/dN is caused by a confluence of mechanisms at the fracture tip, including time-dependent chemical processes, corrosion, hydrogen absorption, and diffusion. Compared to high-frequency experiments, low-frequency tests in corrosive fluids typically result in shorter lives measured in cycles. (Meischel et al., 2015).Higher frequencies cause a decrease in crack growth rate, expressed as da/dN, while reaction time for chemical mechanisms is repeatedly separated. If a time-dependent agent is applied and

overwhelms the collection of agents, various crack growth behaviour is anticipated with multiple frequencies. Generally, frequency effects are more pronounced at lower crack growth rates.

2.4.2.3 Influence of Loading History

A large plastic zone's formation is affiliated with an overload effect. Due to the stress, plastic deformation increases just before the crack point. An extensive plastic zone can lead to crack closure past the crack tip and compression before the crack tip. The effective stress intensity factor (ΔKeff) is predicted to decrease as closure increases and crack propagation should be slowed due to enhanced fracture resistance in the plastic zone of the material. Overload effects typically only last for a short time; as a crack progresses, the acceleration of its growth returns to its actual value, and the impact vanishes. An under-load can mitigate the adverse effects of an overload. Compression sets in when the load is reduced, and the plastic deformation is (at least) reversed. If an underload follows an excess, the crack growth is only marginally affected, but the opposite is true if the underload is followed by an overload (Cerny, 2012); (Albedah et al., 2020a).

2.5 Fatigue Crack Propagation Models

For dynamic loading of a crack, the three considerable essential elements defining the crack propagation of the crack are:

- Stress intensity spectrum, $\Delta K = K_{max} - K_{min}$
- Stress intensity proportion, $R = \frac{K_{min}}{K_{max}}$
- Stress history, H

Therefore, the crack growth advancement (i.e., growth per stress cycle) can be represented as:

$$\frac{da}{dN} = f(\Delta K, R, H) \quad \text{(Eq.2.2)}$$

Where crack growth per stress cycle is given by $\frac{da}{dN}$

2.5.1 Short Cracks

It is known that:

$$\frac{da}{dN} = f(\Delta K) \quad \text{(Eq.2.3)}$$

Where ΔK relies on the amplitude of the normal stress and geometry.

Nevertheless, short cracks are shear stress caused and invalid LEFM. There are two classes of short cracks: (1) mechanically short cracks propagate more quickly than large cracks with the identical ΔK, and (2) Micro-structurally short cracks that interact with the microstructure and extend fast, as illustrated in Figure 2.6.

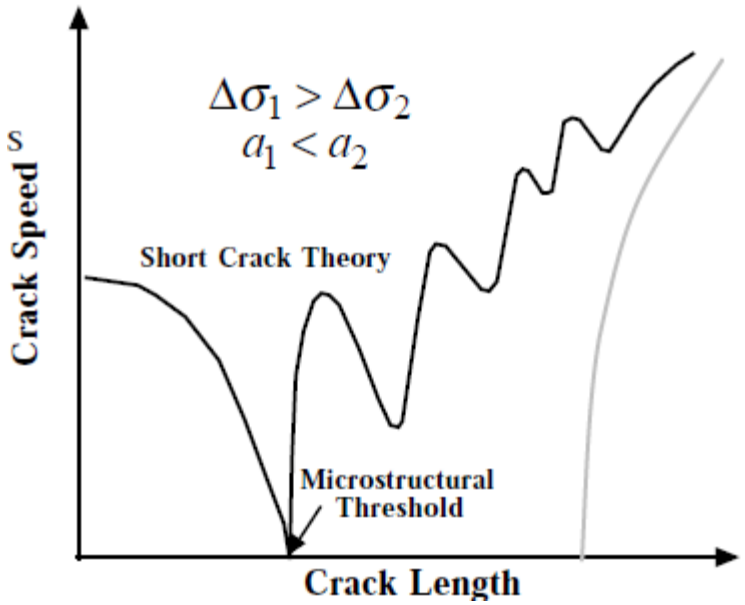

Figure 2.6: Short crack theory (Raghavender & Sahoo, 2021)

2.5.2 Retardation Models due to Overloads

A tensile overload will present compressive residual stresses. These residual stresses will affect ΔK and, consequently, the swiftness of crack propagation, as shown in Figure 2.7.

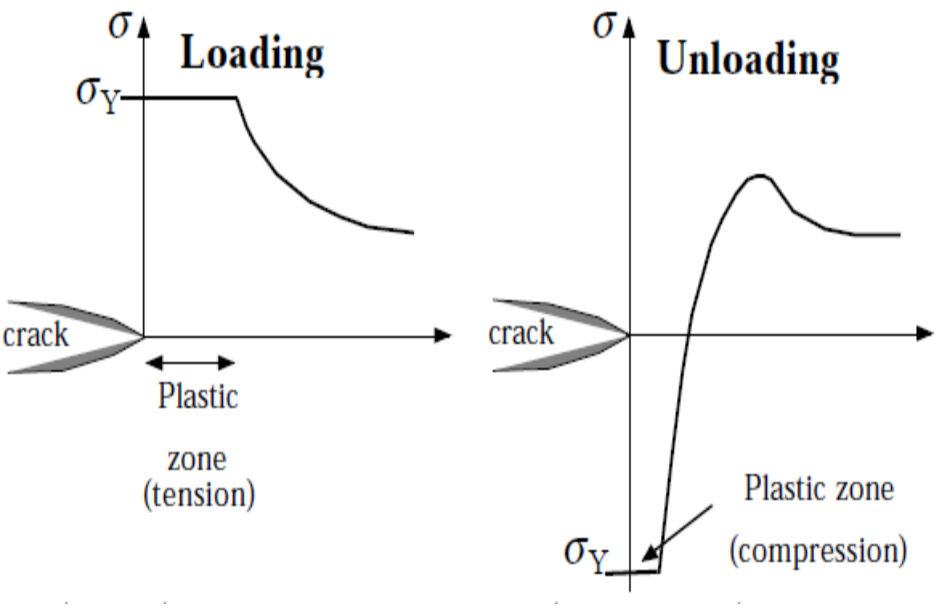

Figure 2.7: Forces induced in a material during loading (Raghavender & Sahoo, 2021)

The Wheeler model is utilized to determine the decrease of the crack growth acceleration due to an overload. The reduction of crack growth acceleration functions solely as long as the "current plastic zone" of the crack is within the plastic zone region from the overload.

2.5.3 Crack Closure.

In 1970, Elber uncovered that crack closure happens in cyclic loading, consistent for more significant loads than zero. This crack closure will reduce the fatigue crack growth acceleration by lowering the practical stress intensity span, hence the stress intensity pace:

$$\Delta K = K_{max} - K_{min} \qquad \text{(Eq.2.4)}$$

Where ΔK-stress intensity factor, K_{max}- maximum stress intensity applied, K_{min}- minimum stress intensity applied.

$$K_{min} = max[K_{min}, 0] \qquad \text{(Eq.2.5)}$$

Crack closure happens when $K = K_{op}$.

$$\Delta K_{eff} \equiv K_{max} - K_{op} \quad \text{(Eq.2.6)}$$

Where ΔK_{eff} –effective stress intensity factor.

Paris law utilizes an effective stress intensity rate given by the following;

$$\frac{da}{dN} = C\left(\Delta K_{eff}\right)^{m} \quad \text{(Eq.2.7)}$$

Where a = crack length, N = number of cycles, m = Paris exponent, and C = Paris constants.

The practical association is given by:

$$\mathrm{K_{op}} = \varphi(\mathrm{R})\mathrm{K_{max}} \quad \text{(Eq.2.8)}$$

Where $\mathrm{K_{op}}$ are a function of the stress ratio R and the maximum stress applied $\mathrm{K_{max}}$.

$$\varphi(R) = 0.25 + 0.5R + 0.25R^2 - 1 \leq R \leq 1 \quad \text{(Eq.2.9)}$$

The crack will be arrested when it has completed the stress cycle. A schematic relationship between K_{max}, K_{min}, $\mathrm{K_{op}}$, and ΔK_{eff} is shown in Figure 2.8 below.

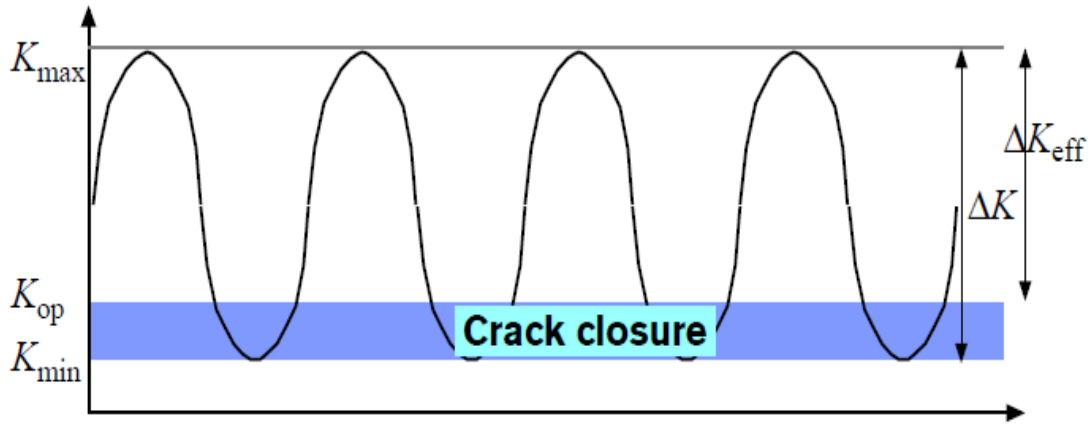

Figure 2.8: Principle of Elber's crack closure theory (Raghavender & Sahoo, 2021).

2.5.4 Paris Law

Paris' law is defined as

$$\frac{da}{dN} = C\Delta K^m \quad \text{(Eq.2.10)}$$

Where a = crack length, N = number of cycles, m = Paris exponent, and C = Paris constants

One of the foremost and considerably employed fatigue crack propagation standards compared to a general crack propagation criterion is equation 2.12. However, Paris' law does not consider mean stress consequences (expressed by the R-ratio) and historical impacts (presented by H). Additionally, Paris law is accurate in states with uniaxial loading, long cracks, and LEFM-states. The damage tolerant strategy is proposed to characterize a material's fatigue performance, and curves due to fatigue crack extension are applied together with design tools for dimensions of fatigue appearance (C. Chen & Li, 2020).

Chen & Li (2020) proposed that cracks progress for every cycle and fatigue crack growth speed relies on the stress intensity factor range ΔK. The expression is as shown in equation 2.12. The Paris law has been the widely adopted principle for FCG rate forecasting for decades. They can be utilized to evaluate the fatigue life of the alloy. The resulting equation found the stress intensity factor ΔK :

$$\Delta K = \frac{\Delta P}{B}\sqrt{\left(\frac{\pi a}{2W} sec \frac{\pi a}{2}\right)} \quad \text{(Eq.2.11)}$$

Where P =load; B= sample thickness, W=width; a = half–crack length (2a=w).

Investigation of fatigue experienced by metal relies on a practical strategy because of the evolution of LEFM. Tang et al. (2016) adopt the most commonly used log-log plot. Log (da/dN) vs. log (ΔK) is a log-log plot that displays the relationship between the fatigue crack extension rate da/dN and the stress intensity factor ΔK. Both the y-intercept and the gradient of this assumed line will be used as the two operational parameters in the ΔK model. Crack

model linearization is given by taking logarithmic methods on Equation 2.12 on both sides presents:

$$Log\left(\frac{da}{dN}\right) = logC + mlog(\Delta K) \quad \text{(Eq.2.121)}$$

Where a = crack length, N = number of cycles, m = Paris exponent, and C = Paris constants.

Log C gives a Y-intercept, and the gradient is provided by m. The following external and internal fatigue impacts are: specimen, material, temperature, environments, and geometry are represented by the two experimental parameters C and m.

2.6 Fatigue Crack Propagation Studies Directly Related to 7075 Alloys.

2.6.1 Thermomechanical Processing and Cyclic Pre-Loading

The reviews by Raghavender & Sahoo (2021) on the improvements in features that have been acquired in Al alloy 7075 at the Air Force Materials Laboratory via the use of easy thermo-mechanical treatments demonstrated that due to the more high strength likely via thermo-mechanical methods, the over-aged state always retains strength grades extremely near to that of traditional T6. Information explaining the improvements in fatigue strength, stress corrosion resistance, and fracture toughness achieved by employing these techniques is presented. Fatigue life examinations indicate that all four thermos-mechanical approaches examined by Albedah et al. (2020b) increase fatigue life at low-stress classes but decline at elevated stress levels.

The fatigue crack propagation acceleration of the alloy with a wide precipitate-free zone (PFZ) was discovered to be identical to the alloy with a narrow PFZ under similar states of cyclic loading. The alloy with the wide PFZ revealed a higher fracture toughness value than the alloy with the bit of PFZ. When materials undergo thermo-mechanical treatments,

insoluble dispersants may be formed from the added elements, hence playing a significant role in re-crystallization control, or refined precipitates introduce hardening structurally, increasing static metal features (Tang et al., 2016).

2.6.2 **The Impact of the Degree of Ageing on Fatigue Crack Propagation**

Leng et al. (2018) demonstrate that precipitation intervals narrow before widening with increasing aging time. This trend is followed by a progressive rise in hardness and a progressive decrease in tensile strength. Fatigue strength optimizes as yield strength rises because fatigue strength increases first and then decreases.

When heat treated to condition T651, hardness and tensile features are optimum, while the fatigue life is the briefest (Yang et al., 2017a). After being subjected to a solution, the hardness and the extension suffer the most. An increase in aging temperature from 150 to 190 °C improves high cycle fatigue (HCF). The subsurface impurity particles cause the cracking. The most comprehensive crack propagation and the location of the quasi-cleavage plane both occur at the 170-degree heat treatment. Dimple proportions of fracture surfaces eventually grow more extensive and resonant as the aging temperature rises.

Aging has been linked to faster growth rates and lower threshold stress intensities (ΔKth weights), which correlate with lower assessed grades of fracture closure and lessening crack route tortuosity (Albedah et al., 2020b). Corrosion was shown to play a modest role in the closure of cracks in this alloy, according to an investigation on crack growth in humid room air.

Extreme slip reversibility and enhanced roughness-induced crack closure and deflection from more tortuous crack paths were found to be responsible for the underaged

microstructures' exceptional fatigue resistance (compared to overaged structures of identical strength and peak-aged structures of more high strength). As the deformation mode is a non-homogeneous planar slip, alloy systems toughened by coherent shearable precipitates are encouraged to exhibit such properties.

A shift in fracture surface morphology and crack growth curves are seen in the heat-treated conditions T 651 and T 7351 in the near - threshold region (Wang et al., 2023). Crack closure measurements rely on surface roughness, which explains why, except for the T 7351 alloy, ΔKth does not rely on load ratio. For a microstructure with a single deformation mode, an equation of fracture development rate to the fourth power of Keff is in good agreement with the reported crack propagation curves.

Over-aging temper has no positive or negative effect on the environmental fatigue fracture propagation rate in the 7000-series aluminium alloy/aqueous-chloride solution process, depending on the loading frequency (Leng et al., 2018). For peak and overaged AA7075 specimens, Paris zone fatigue crack growth rates are accelerated up to 10-fold by cyclic loading in 3.5% NaCl solution compared to fatigue in moist air for the SL-crack orientation. Crack growth is inter-sub-granular for the T6 microstructure but trans-granular-brittle for the T7 case. Cracking at low f is dominated by corrosion product-induced crack closure enhanced by over-aging. At intermediate to high f, environmental fatigue is due to hydrogen embrittlement and rate limited by H diffusion over a crack tip process zone distance established by local stress.

2.6.3 The Impact of PFZ on Fatigue Crack Propagation

Under an identical state of cyclic loading, alloy with wide PFZ and alloy with narrow PFZ were found to have roughly the same fatigue crack propagation rate. A higher fracture toughness value was exhibited on the alloy with the wide PFZ than those with the narrow PFZ (Louthan, 2018).

2.6.4 The Effect of Riveting Parameters on the Formed Rivet Quality.

Cheraghi (2008) study was performed on an aluminium sheet with dimensions of 0.125" diameter rivet and thickness of 0.064". The outcomes demonstrated that under standard deviations in the riveting procedure parameters, most rivets constructed would not fulfil the quality conditions when utilizing the suggested countersunk 0.042″ rivet hole depth. The most significant reason for this is the separation of the produced rivet and the resulting hole. The range of hole and rivet diameter tolerances and squeezing force that can be used without violating quality standards expands when the countersunk depth is lowered to 0.032 inches (Cheraghi, 2008).

2.6.5 Effect of Loading.

Retardation effects (Al 7075-T7351 alloy) of overloads of the extent 2.7 stints and 3.0 stints of the most significant load in the steady span fatigue loading were consequential in the investigations by Cerny (2012). The effect of overload causes substantial crack closure. However, this did not happen instantly but merely after additional fatigue crack elongation, similar to plastic zone size.

2.6.5.1 Effects of Overloads.

The overload application induced a plastic zone in aluminium alloys 2024-T3 and 7075-T6 when the investigation was performed with single overload under unchanging-amplitude loading on the fatigue crack growth (Albedah et al., 2020). The developed plastic zone is three stints more extensive in the subject of 2024-T3 analogized to 7075-T6; therefore, consequential crack retardation was formed for 2024-T3. This retardation impact caused by the overload for 2024-T3 and 7075-T6 prevailed for approximately 10 mm and 1 mm, respectively, from the moment of overload induction.

2.6.5.2 Impact of Stress Proportion and Thickness on Crack Closure.

The crack growth behaviour of heat-treated aluminium alloys relies primarily on whether the prevailing closure agent is caused by plasticity or roughness (Borrego et al., 2010). Roughness improves aluminium alloys' crack development resistance by closing up cracks that might otherwise grow. Aluminium alloys that have been age-hardened in either a natural or artificial way with higher concentrations of Mn and Cr components have a far more difficult time closing cracks due to surface roughness. Plasticity-induced fracture closure is standard in artificially aged alloys, and so is the utilization of a limited selection of Mn and Cr alloying components. The effects of a critical stress ratio and material dependencies on the development of fatigue cracks were analyzed. The crack growth behaviours of alloy 2017-T4 are indifferent to sample thickness. Whether plasticity or roughness, the dominant closure agent determines the fracture development styles of heat-treated aluminium alloys. By closing off potential crack entry points, roughness further inhibits crack formation. Crack closures due to plasticity are common in artificially aged alloy 6082, which also has a smaller range of Mn and Cr components. Crack closures caused by roughness overwhelm crack

closures in naturally aged alloys and artificially aged 6082 alloys with more elevated scopes of Mn and Cr components.

Scale segmentation involves multiple ranges. Impacts of R ratios on the crack advancement due to the fatiguing nature of alloy 7075-T6 Al sheets are exhibited as a subject of discussion on the proposed da/dN–DS model. Varied R ratios introduce changes in TFs, and the fatigue cracks advancement nature of 7075-T6 Al sheets is influenced appreciably; complete fatigue models currently do not exist. As the physical models differ, so does the explanation variation of the same test results. This work was within the scope of only the micro–macro scale range of alloy 7075-T6 Al sheets. Microstructure material deterioration at lower scales remains uncertain; there is still a need to extend the approach to lower levels (Tang et al., 2016).

2.6.6 Effect of Heat Treatment Temperature & Process

The fatigue life of aluminium alloy samples was significantly enhanced compared to those of non-treated samples (Imam et al., 2015a). It was demonstrated that after heat treatment at three different temperatures, 420°C, 460°C, and 500°C, fatigue cracks are probably to be retarded by the sample surface because fatigue cracks have been honoured to begin first at the surface and after that to propagate. SEM and EDS investigation outcomes indicated that (MgZn2) grade constituted the microstructure following the HTTP, RRA, and T6 heat treatment methods. The highest fatigue strength was observed in artificially aged (T6) specimens, and the lowest fatigue strength was observed in the annealed (O) specimens (Fakioglu et al., 2013a).

2.6.7 The Effect of Effect of Notch Geometry and Mean Stress

Results by Benachour et al. (2013) on Al alloys 7075 T6 and 7075 T71 under invariant amplitude loading indicate that fatigue life is related to crack initiation. Crack initiation is connected to mean-induced stress, stress concentrations, and material features. An upsurge in mean stress raises total fatigue life. The initiation phase of the crack is prevalent, corresponding to the fatigue crack growth phase.

2.6.8 Effects of Solution Treatment

Liu et al. (2017) discovered that a more extended solution treatment period of 7075 aluminium alloy greatly affects the high-cycle ($N \geq 10^5$) fatigue attributes of the Al-Zn-Mg-Cu alloy. Under the loading stress of 240 MPa, the fatigue life was roughly 95.7%, 149%, and 359% for the solution treatment of 2 hours, 1.5 hours, 1 hour, and 0.5 hours, respectively. SEM and TEM microstructure observations were as follows: re-crystallization appears in the grains under solution treatment, and the grains become significant with the length of solution treatment time increases. Cracks primarily start from the substantial undissolved phases, and extending the solution time can facilitate the dissolution of the T grade and S grade, lower dislocations number, and decrease the pace of the initiation of fatigue cracks at the extensive undissolved stages because of dislocation glide and dislocation build-up. The observed outcome that fatigue striation widths evolve more limited with more extended solution treatment periods confirms the fatigue effects of the 7075-aluminium alloy, as the secondary cracks reduce the initiating force and the crack propagation rate during the second phase of crack propagation.

Moreover, the impacts of the fracturing method should be researched in developing crack propagation associations and deciding on crack closure stresses. Crack closure investigations

have employed thin samples and examined only the specimen surface. The crack closure aspects at centre thickness, comparable to plane strain states, may be distinct. Eventually, further crack propagation information is needed. It is evident that material substantially affects the consequence of mean stress, and few materials have been studied exhaustively. Brahami et al. (2018) concluded that fatigue resistance is affected by numerous factors, including microstructure, mechanical properties, nature, and phase distribution in secondary-state precipitates having high sensitivity to the elements added.

In this investigation, the microstructure, rivet hole size, and heat treatment effects on the fatigue of several alloys of aluminium 7075-0/T6/T7 are examined via mechanical characterization studies and microstructural examination. The impact of the nature and distribution of various elements on the crack advancement rate will be performed, and their chemical compositions will be examined via an SEM.

CHAPTER THREE: METHODOLOGY

3.1 Introduction

This chapter covers the research methodology for the study that was discussed under the following sub-headings: study area, method, and techniques used to achieve every objective in the form of fatigue testing equipment, specimen design, notch preparation, variables, and measurements, testing procedure, and framework for data processing and analysis of data.

3.2 Study Area

Two essential parts form part of this investigation: (1) a mechanical description based on fatigue crack extension to accurately recognize the principles of acts commanding the lifetime materials utilized, and (2) an examination microstructurally to establish and distinguish the elements of the varied forms by SEM.

3.2.1 Materials

The Al 7075 aluminium alloy, widely used in the aerospace industry because of its low mass, strong strength, and high electrical and thermal conductivities, was employed in the experiments. The materials adopted in this examination are 7075 heat-treated to 7075 -0, 7075 -T6, and 7075 -T7 aluminium alloys.

1) Al 7075-O is an untreated Al alloy 7075 condition
2) Al 7075-T6 was prepared as per Boeing standard BAC5602 - summarized below;
    I. To get Al 7075-T6, Al 7075 bare and clad sheet was heated in a furnace to 487 to 498^{o} C and maintained for 35-45 hours to get 7075-W (unstable condition)

II. Then Al 7075-W was heated to 115^{o}C to 127 ^{o}C and maintained at that temperature for 22 to 24 hours

NOTE: for this project, Al 7075-T6 was procured already heat-treated to Al 7075-T6

3) Al 7075-T7 was prepared as per Boeing standard BAC5602 - summarized below;

I. Al7075-T6 was heated in a furnace from 157^{o}C to 169^{o}C and maintained at that temperature for 26-28 hours at Kenya Airways mechanical workshop, Nairobi.

Table 3.1: Properties of Al 7075 alloy.

Properties	**Al alloy (7075)**
Tensile strength (MPa)	510–540 Mpa
Young's modulus (GPa)	71.7
Melting temperature (^{0}C)	650-800
Density (g/cc)	2.81 g/cc
Thermal conductivity (W/m-K)	196
Linear thermal expansion coefficient (K–1)	$2.36x10^{-5}$

Table 3.2: Chemical compositions of Al 7075 alloy (wt. %).

Mg	Si	Cu	Cr	Mn	Zn	Ti	Fe	Al
2.71	0.51	1.65	0.31	0.29	4.48	0.22	0.23	89.6

The typical properties of Al 7075 are shown in Table 3.1, and Chemical compositions in Table 3.*2* (Brahami et al., 2018). The material used in this study is equivalent to the material used in aircraft frames and stringers. Specimen material 7075 aluminium alloy was procured from Smiths Advanced Metals Stratton Business Park, London Rd, Biggleswade SG18 8QB, United Kingdom, in O and T6 conditions. At the same time, Al 7075-T6 was converted to Al 7075-T7 by heating as per Boeing standard BAC562 at Kenya Airways Mechanical Workshop.

3.3 Methods and Techniques to evaluate crack growth and propagation under constant fatigue loading of Al alloy 7075 under varied heat treatment conditions (-O,-T6,-T7)

Objective one intends to evaluate crack growth and propagation under constant fatigue loading of Al 7075 alloy under varied heat treatment conditions (-O,-T6,-T7) and was achieved as outlined below.

3.3.1 Fatigue Testing Equipment

A high cycle fatigue testing machine at the University of Nairobi (UoN), School of Engineering, Mechanical Engineering department, mechanical engineering workshop (strength of materials) was used to achieve objective 1, as shown in Figure 3.1.

Figure 3.1: Brute force axial-load fatigue testing machine.

The specimens were fixed in place using the three grip holes and fixtures shown in Figure 3.2. Good alignment in the force train was essential; thus, all grasping fittings had to be meticulously machined.

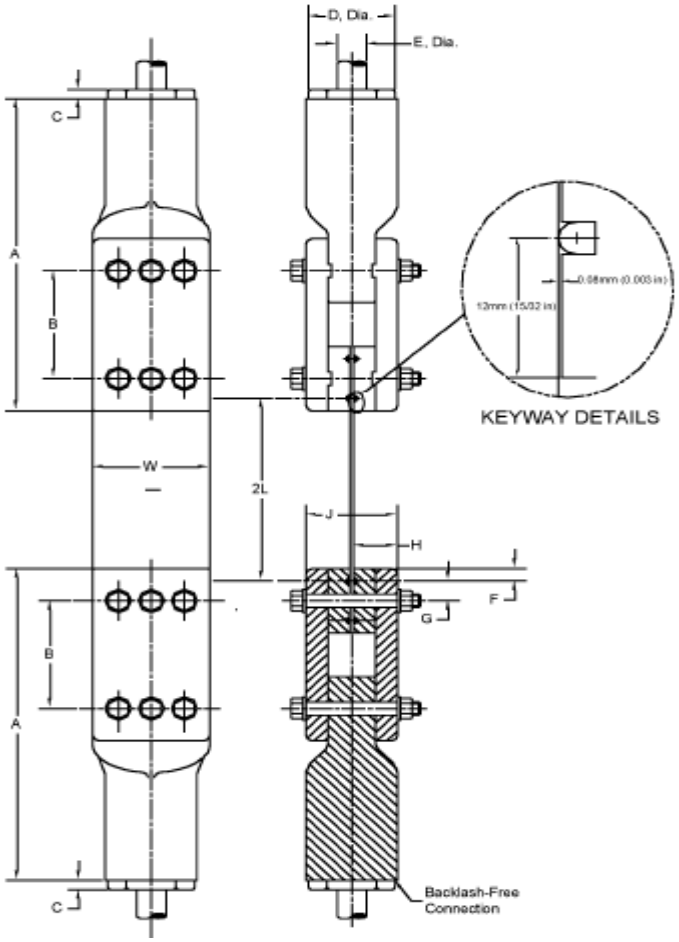

Figure 3.2: This illustration shows a typical 100 mm(4-in.) wide M (T) specimen bolt and keyway system used for a grip (ASTM E647−13, 2014).

3.3.2 Specimen Design

The geometry of the M (T) specimen was, as shown in Figure 3.3, in line with the gripping method. Three (6) pieces were machined to middle tension [M (T)] specimen of Standard test method for crack growth rates as per ASTM E647-13 refer to Figure 3.2. Two pieces in

each heat treatment condition: 7075-O condition, 7075-T6 condition, and 7075-T7 condition. Dimension a was measured from the perpendicular bi-sector of the central crack.

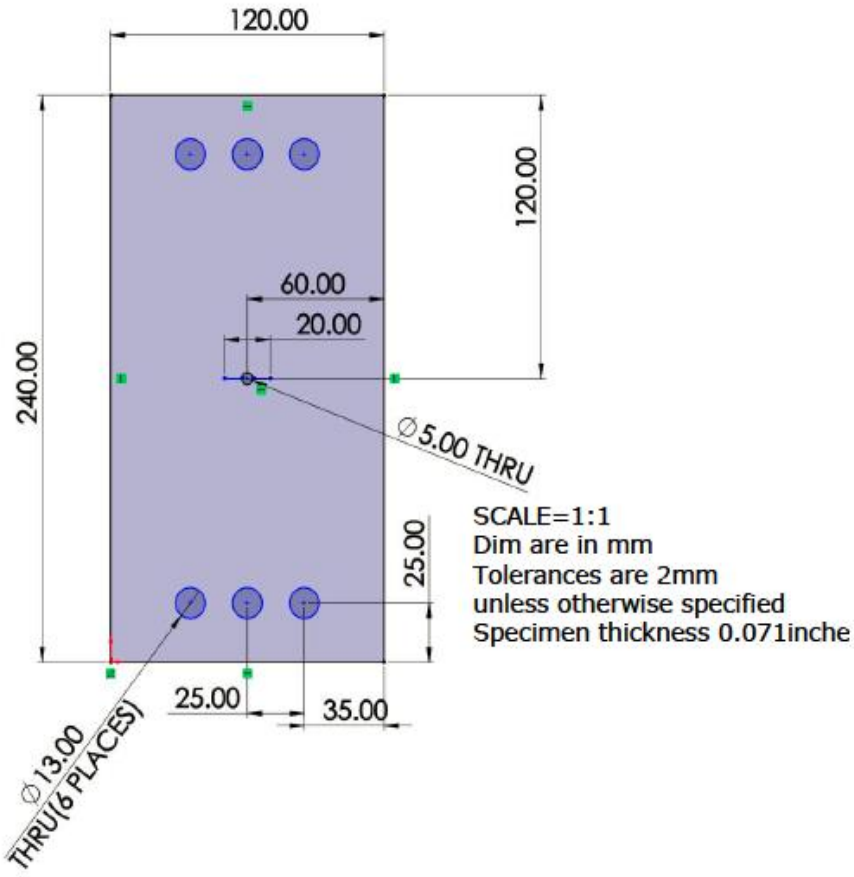

Figure 3.3: Specimen design used to study the effect of heat treatment on crack propagation-Al7075-0/T6/T7 prepared as per (ASTM E647−13, 2014).

3.3.3 Notch Preparation

The machined notch for the specimens was made by saw cutting, as is recommended for aluminium alloys. Notch and pre-cracking details for the samples are given in Figure 3.4.

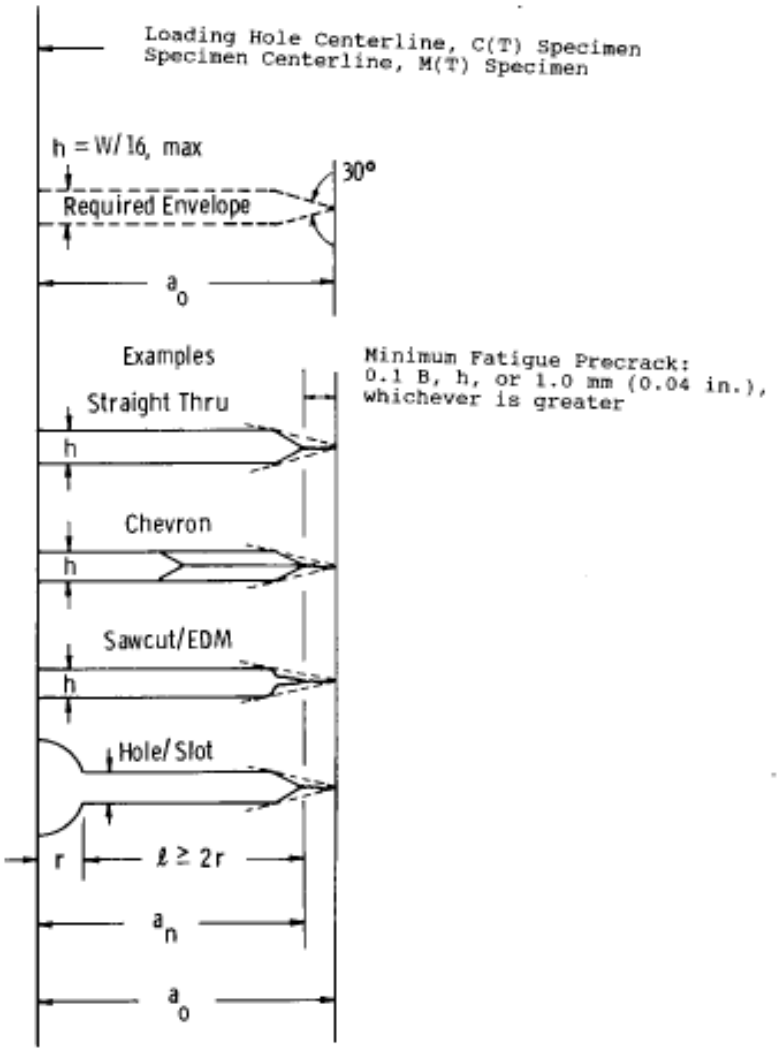

Figure 3.4: Notch details and minimum fatigue pre-cracking requirements (ASTM E647−13, 2014).

3.3.4 Variables and Measurements

A fatigue-testing machine was used to perform constant load amplitude at room temperature. An incremental crack length increase was measured and recorded with a variable in heat treatment (-0/T6/T7) and hole orientation.

Table 3.3: Objective number 1: variables studied and how they were collected

Variables	**Tools**	**Units of Raw Measured data**
Crack Length	Travelling Microscope	crack length (2a) mm
Min and Max Load(P_{min}, P_{max})	Load cell	newton (N)
Flywheel speed	Tachometer	RPM
Elapsed time to a specific crack length	Stopwatch	Minutes

3.3.5 Procedure

3.3.5.1 Number of Tests

The number of samples was chosen based on (ASTM E647−13, 2014) procedures of replicate tests. The number of samples was chosen as per (ASTM E647−13, 2014).

Table 3.4: Number of tests to determine the effect of heat treatment on specimens

HT conditions	**Number of tests**	**Response**
7075-0	2	crack length (2a) and Number of cycles
7075-T6	2	crack length (2a) and Number of cycles
7075-T7	2	crack length (2a) and Number of cycles

3.3.5.2 Fatigue Pre-cracking

Pre-cracking was vital in eliminating the effect of the machined starter notch on the K-calibration of the M (T) specimen by providing a sharpened fatigue crack of sufficient size, straightness, and symmetry. The sample was heat-treated to the state where the test would be performed before the fatigue pre-cracking was performed. The specimen used for studying fatigue initiation was subjected to pre-cracking via a saw cut as per Figure 3.4 (notch preparation).

3.3.5.3 Test Equipment Parameters Setting

The equipment for fatigue testing was such that the force distribution was symmetrical to the specimen notch.

1. The specimen was loaded onto the test machine
2. P_{min} was set as a 400N load cell indicator, then
3. The flywheel adjusted up until the load cell indicator was P_{max} =1201N
4. In that case, the R ratio was set as R=0.333 ΔP=1201N,
5. A stopwatch was used to determine the elapsed time (minutes) for each crack advancement that resulted in getting elapsed cycles.
    a. Elapsed cycles = Elapsed time (minutes) x Flywheel Speed (rpm)
6. A tachometer was used to measure the speed of the flywheel in RPM
7. A travelling microscope was used to measure the crack length (2a in millimetres)

3.3.5.4 Constant-Force-Amplitude Test Procedure for da/dN >10−8 m/cycle (ASTM E647).

This test procedure was chosen since it is well suited for fatigue crack growth rates above 10^{-8} m/cycle.

Therefore, each specimen was tested at a constant force range (ΔP) and a fixed set of loading variables (stress ratio=0.33 and frequency). All the tests were performed at room temperature and pressure conditions. Short-duration test interruptions during work stoppages while making crack size were employed to avoid transient growth rates without loading variable changes.

3.3.5.5 Measurement of Crack Size

The specimen test region was polished, and indirect lighting helped resolve the crack tip so that measurements could be taken visually. Then, a travelling microscope with a low magnification objective (between 20 and 50) was used to measure the crack's size. At least 0.25 mm of spacing was used between crack size measurements to ensure that the da/dN values were relatively uniformly distributed with regard to K (0.01 in.). The magnitude of the cracks in the specimen was measured from only one side (the face).

3.3.6 Framework for Processing and Analysis of Data

3.3.6.1 Theoretical Fatigue Test Model

All fatigue analyses were conducted following constant load amplitude at room temperature on a fatigue testing machine at the University of Nairobi, as shown in Figure 3.1. Crack propagation was observed via a travelling microscope. The specimens were tested using a load frequency of 1498Hz. Figure 3.3 depicts the geometry together with the dimensions of the samples. The expression in equation 4.1 defines the stress intensity factor: The maximum load and the load ratio of all materials used in the fatigue experiments were calculated before the test.

3.3.6.2 Theoretical Fatigue Crack Advancement Model

The data for fatigue crack advancement rate (da/dN) calculated experimentally against the range of SIF (ΔK) was generated via incremental technique. The experimental data were correlated using the Paris law, as shown in Equation 2.12. This was represented in a plot of Log-log (da/dN) against ΔK for all materials, as indicated in equation 4.2.

3.3.6.3 Determination of Crack Growth Rate

The secant method, also known as the point-to-point methodology, is applied to the crack size versus elapsed cycles data (a versus N) to compute the crack growth rate, which is as simple as determining the slope of the straight line connecting two nearby data points on the a versus N curve. Check out the 40-minute highlighted data in Table 3.5 as an example.

Table 3.5: Section of data collected from specimen Al 7075-T7 constant amplitude: ΔP =1201 N, R = 0.33

Time(Min)	Total Time(Min)	RPM	N (Cycles)	ΔN [Cycles]	ΔP [N]	a [mm]	Δa[mm]	da/dN (mm/cycle)	ΔK ($MNm^{-3/2}$)
0	0	1498	0	0	1201	20.6	0	0.00E+00	0
200	200	1498	299600	299600	1201	21.35	0.75	2.50E-06	1.44E+00
30	230	1498	344540	44940	1201	21.85	0.5	1.11E-05	1.45E+00
40	270	1498	404460	59920	1201	23.1	1.25	2.09E-05	1.50E+00
20	290	1498	434420	29960	1201	23.75	0.65	2.17E-05	1.52E+00
20	310	1498	464380	29960	1201	24.55	0.8	2.67E-05	1.54E+00
7	317	1498	474866	10486	1201	24.85	0.3	2.86E-05	1.55E+00
10	327	1498	489846	14980	1201	25.3	0.45	3.00E-05	1.56E+00

For the highlighted data, the raw data collected was Time = 40 min, resulting in a cumulative time of 230 + 40= 270 minutes.

To get the number of cycles=flywheel RPM X Total time=1498x270 =404460 Cycles for that instant.

Note that the flywheel rpm was captured via a tachometer.

To get the change in cycles ΔN, ΔN=Current total cycles –Immediate total cycles

ΔN = 404460 – 344540 = 59920 cycles

Alternatively, change in cycles can be given as Recording time (min) x RPM

ΔN = 40 x 1498 = 59920 Cycles

In millimetres, crack growth (2a) was recorded as raw data via a travelling microscope for each time (min).

Change in Δ2a was determined by = Current 2a reading - Immediate 2a reading

For our examples, Δ2a= (46.2 - 43.7) =2.5mm

Crack growth was determined by dividing 2a by two, i.e.

a = 2a/2 and for our example, a = (46.2/2) = 23.1mm

Change in a Δa was determined by current reading value – immediate reading value

And for our case Δa= (23.1-21.85) =1.25mm

Alternatively, Δa is given by diving Δ2a by two, i.e.

Δa= (Δ2a/2) = (2.5/2)=1.25mm

(Δa / ΔN) cracked growth rate da/dN (mm/cycle).

And for this example, da/dN (mm/cycle) = (Δa/ ΔN) = (1.25/59920) = 2.09E - 05mm/cycle

3.3.6.4 Determination of Stress-Intensity Factor Range, ΔK

For each crack size value, equation 4.1 was used to calculate the stress-intensity range corresponding to a given crack growth rate, which was found as follows;

Where, $\Delta P = P_{max}-P_{min}$ for R.>0 or $\Delta P = P_{max}$ for R <0, $\alpha = 2a/W$, B = thickness, W = Width (m), a = crack growth (mm)

For the highlighted data in Table 3.5,

$\Delta P = P_{max}-P_{min}$ = 1788N -587N = 1201N

Based on specimen design dimensions,

W = 120mm = 0.12m

B = 1.8034mm = 0.0018034m

a = 23.1mm = 0.0231m

Therefore

$$\Delta K = (\frac{1201}{0.0018034}\sqrt{(\frac{\pi x \frac{2x0.0231}{0.12}}{2x0.12} sec \frac{\pi x \frac{0.0231}{0.12}}{2}}))/1000000$$

ΔK ($MNm^{-3/2}$) = 1.50E+00

Examination of FCG rates for every cycle (da/dN) against stress-intensity factor, ΔK was presented in a log-log plot of (da/dN) versus ΔK. For example, data in column da/dN (mm/cycle) was plotted in the y-axis against column ΔK (MNm-3/2) in the X-axis, resulting in Figure 4.1 for 7075-T7 and Figure 4.2 for 7075-T6 is and Figure 4.3 for 7075-O.

A schematic representation of FCG rate, (da/dN), as against stress-intensity factor ΔK with various metallographic examinations at crack initiation. Slow crack propagation, fast crack propagation, and fatigue fractures formed the basis of the result analysis and discussion.

3.3.6.5 Determination of a Fatigue Crack Growth Threshold

a) A linear regression of log da/d N versus log ΔK was performed using a minimum of five da/dN, ΔK data points approximately equally spaced between growth rates of 109 and 1010 m/cycle to determine the best-fit straight line. This provided a range for the threshold stress-intensity factor, ΔKth, for fatigue crack growth. Since the fitting interval was defined in terms of da/dN, the dependent variable in determining this linear relationship had to be log ΔK.

   For example, the power equation for the Paris region for the 7075-T7 conditions, as indicated in Figure 4.1 7075-T7, gives y = 3E-07 x $^{10.069}$

   Representing the same on Paris equation 2.12,

   For 7075-T7, becomes

$$\left(\frac{da}{dN}\right) = 3E - 07(\Delta K)^{10.069}$$

b) The ΔK-value that corresponded to a growth rate of 10^{-10} m/cycle was calculated using the above-fitted line; this value of ΔK was defined as ΔK_{th}

   For example, for 7075-T7 conditions gave

$$10^{-7} = 3E - 07(\Delta K)^{10.069}$$

   ΔK_{th}=0.8966 MNm$^{-3/2}$

3.3.6.6 Analytical Methods

Examination of FCG rates for every cycle (da/dN) against stress-intensity factor, ΔK was presented in a log-log plot of (da/dN) versus ΔK with the guide of equation 4.2. A schematic representation of FCG rate (da/dN), as against stress-intensity factor ΔK, formed the basis of objective one analysis, discussion, and conclusion.

Activity flow chart to evaluate crack growth and propagation under constant fatigue loading of Al alloy 7075 under varied heat treatment conditions (-O,-T6,-T7)- Objective number 1

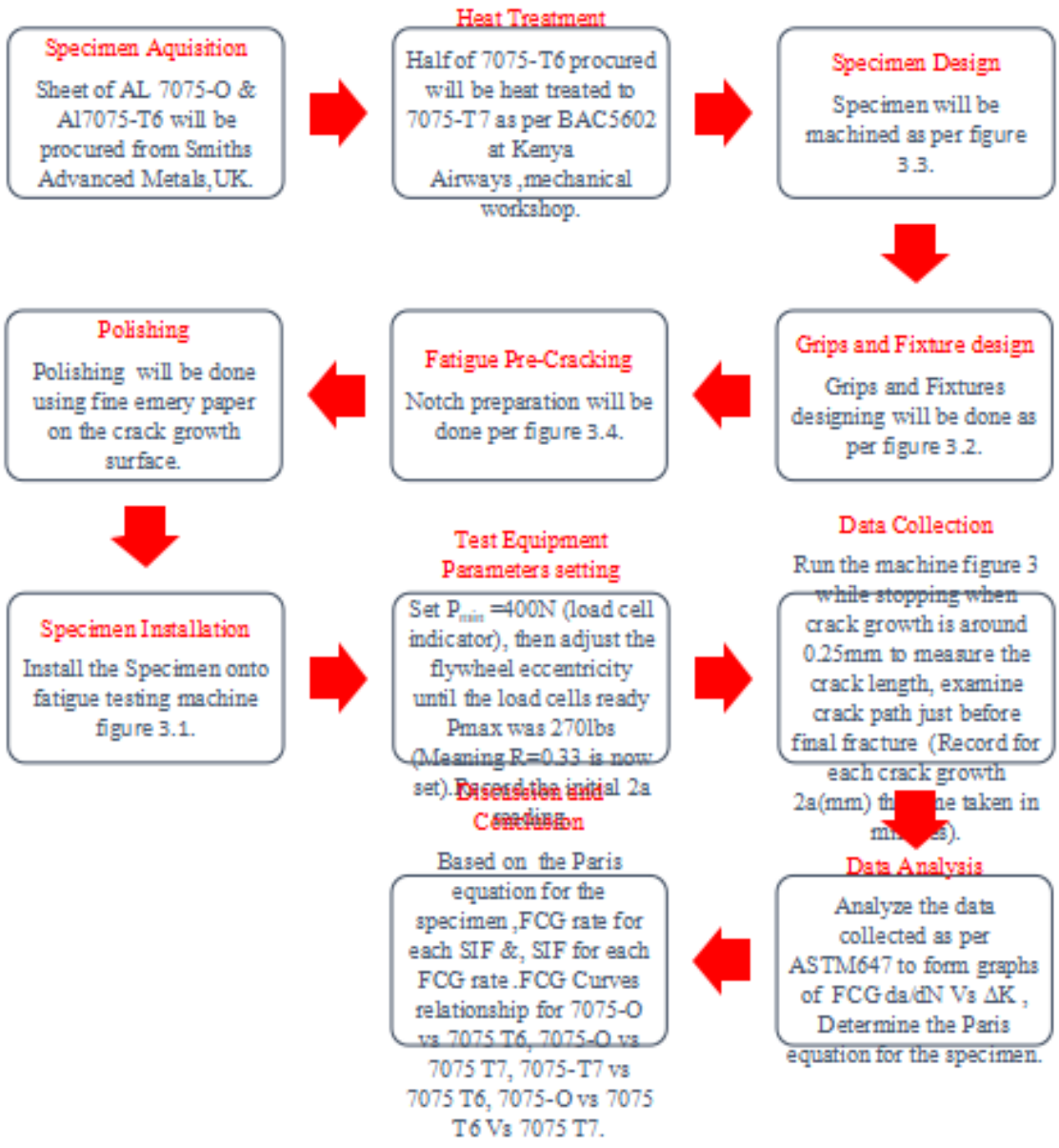

3.4 Methods and techniques to determine crack propagation under constant fatigue loading in a 100^{o} countersunk rivet hole and straight rivet hole geometry of Al 7075-O, Al 7075-T6, and Al 7075-T7 alloys specimens for objective No. 2

Objective two sought to determine crack propagation under constant fatigue loading in a 100^{o} countersunk rivet hole and straight rivet hole geometry of Al 7075-O, Al 7075-T6, and Al 7075-T7 alloy specimens.

3.4.1 Fatigue Testing Machine

A fatigue-testing machine used to study high cycle fatigue at the University of Nairobi, School of Engineering, Mechanical Engineering department, mechanical engineering workshop (strength of materials) was used to achieve objective 2, as shown in Figure 3.1. Grips and Fixtures: Three grip holes and fixtures were used for the specimens, as outlined in Figures 3-5 and 3.2. Grips were aligned by machining all gripping fixtures to achieve good alignment in the force train.

3.4.2 Specimen Design

Specimens designed for crack initiation at different rivet hole orientation was prepared as per (ASTM E8, 2010) to avoid specimens cracking at the gripping holes.

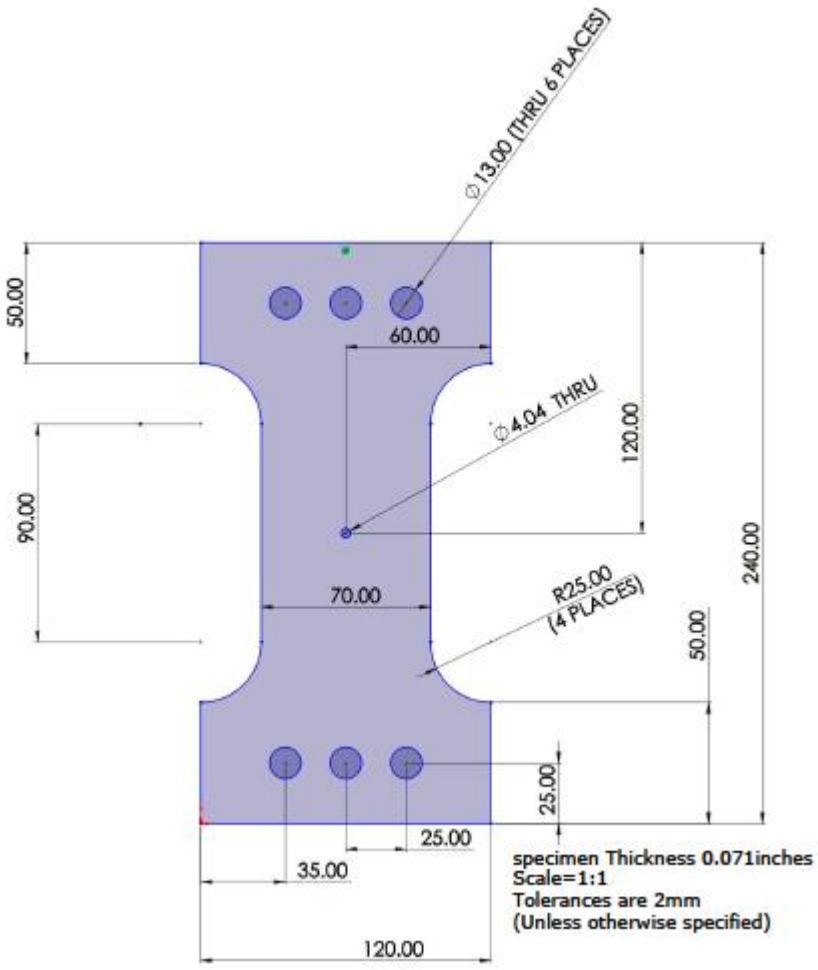

Figure 3.5: Specimen design used to study the effect of rivet hole orientation on crack initiation prepared as per (ASTM E8, 2010).

Hole geometry was drilled to achieve a 100^{o} countersunk rivet hole and straight hole, as shown in Figure 3.6.

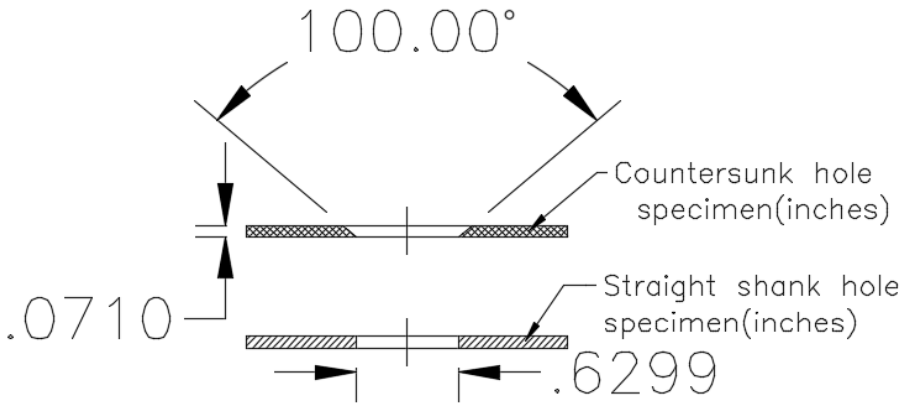

Figure 3.6: Hole geometries of specimens designed for the study of crack initiation

3.4.3 Variables and Measurements

A fatigue testing machine was used to perform constant load amplitude at room temperature. The incremental increase in crack length was measured and recorded with variables in heat treatment (-0/T6/T7) and hole orientation.

Table 3.6: Objective number 2: variables studied and how they were collected

Variables	**Tools**	**Units of measured data**
Crack Length	Travelling Microscope	crack length (2a) mm
Min & Max Load(P_{min}, P_{max})	Load cell	Newton (N)
Flywheel speed	Tachometer	RPM
Elapsed time to a specific crack length	Stopwatch	Minutes

3.4.4 Procedure

3.4.4.1 Number of Tests;

Dummy tests were performed before the actual test for each specimen; the number of tests were indicated in Table 3.7, chosen based on (ASTM E647−13, 2014) procedures of replicate tests used to study the effect of rivet geometry. The number of samples was determined based on the number of parameters to study under (ASTM E647−13, 2014).

3.4.4.2 Test Equipment Parameters Setting

The equipment for fatigue testing was such that the force distribution was symmetrical to the specimen notch.

1) The specimen was loaded onto the test machine
2) P_{min} was set as a 400N load cell indicator, then
3) The flywheel was adjusted until the load cell indicator P_{max} was 1201N.
4) In that case, the R ratio was set as R = 0.333 ΔP = 1201N.
5) A stopwatch determined each crack advancement's elapsed time (minutes), resulting in elapsed cycles.

   Elapsed cycles = Elapsed time (minutes) x Flywheel Speed (rpm)
6) A tachometer was used to measure the speed of the flywheel in RPM
7) A travelling microscope was used to determine the crack length (2a)

Table 3.7: Number of tests used to study crack initiation at different rivet orientation

HT conditions	Rivet hole orientation	Number of samples	Response
7075-0	Perpendicular	2	crack length (2a) and number of cycles
	Countersunk 100 degrees	2	crack length (2a) and number of cycles
7075-T6	Perpendicular	2	crack length (2a) and number of cycles
	Countersunk 100 degrees	2	crack length (2a) and number of cycles
7075-T7	Perpendicular	2	crack length (2a) and number of cycles
	Countersunk 100 degrees	2	crack length (2a) and number of cycles

3.4.4.3 Constant-Force-Amplitude Test Procedure for da/dN >10−8 m/cycle (ASTM E647−13, 2014)

This method was selected because it is applicable to fatigue crack growth rates greater than 108 m/cycle. Each specimen was tested at ambient temperature and pressure, with a stress ratio of 0.33 and a constant frequency. To prevent Transient growth rates from occurring

without changes in loading variables, tests were interrupted briefly during breaks in the manufacturing process of crack sizes.

3.4.4.4 Measurement of Crack Size

The crack tip was resolved using indirect lighting and a polished specimen test area for visual measurements. The size of the cracks was then evaluated with a low-powered (20 to 50) travelling microscope. As a result of taking measurements at regular intervals, the da/dN data show a nearly normal distribution around the value of ΔK, with a minimum of 0.25 mm (0.01 in.). The front of a specimen was used to take crack size measurements. Throughout the test, the crack never skewed more than +/-20 degrees from the symmetry plane over a width of 0.1W.

3.4.5 Framework for Processing and Analysis of Data

3.4.5.1 Theoretical Fatigue Test Model

All fatigue analyses were conducted following load amplitude that was constant at room temperature on a fatigue-testing machine, as shown in Figure 3.1. Crack propagation was observed via a travelling microscope. The specimens were tested using a load frequency of 1498 Hz. Figure 3.5 depicts the geometry together with the dimensions of the samples. The SIF was defined by equation 4.1: The maximum load and the load ratio of all materials used in the fatigue experiments were calculated before the test.

3.4.5.2 Theoretical Fatigue Crack Advancement Model

The data for fatigue crack advancement rate (da/dN) calculated experimentally against the range of SIF (ΔK) was generated incrementally. The experimental data were correlated using the Paris law in equation 2.12.

Where C and m are material features.

This was represented in a plot of Log-log (da/dN) against ΔK for all materials, as indicated in equation 4.2.

3.4.5.3 Determination of Crack Growth Rate

Data on crack size versus the number of cycles (a versus N) was used to compute the crack growth rate by determining the slope of the line joining two neighbouring data points on the a versus N curve. This method is also known as the secant method or the point-to-point technique. Consider the underlined information, for instance.

Table 3.8: Section of data collected from specimen Al 7075-O constant amplitude: ΔP =1201 N, R = 0.33

Time(Min)	Total Time(Min)	RPM	N (Cycles)	ΔN [Cycles]	ΔP [N]	a [mm]	Δa[m m]	da/dN (mm/cycle)	ΔK ($MNm^{-3/2}$)
0	0	1498	0	0	1201	2.05	0	0.00E+00	0.00E+00
69	69	1498	103,362	103,362	1201	3	1	9.19E-06	3.03E-01
1	70	1498	104,860	1,498	1201	6.7	4	2.47E-03	5.98E-01
5	75	1498	112,350	7,490	1201	8	1	1.74E-04	3.55E-01
2	77	1498	115,346	2,996	1201	10	2	6.68E-04	4.40E-01
3	80	1498	119,840	4,494	1201	11.5	2	3.34E-04	3.81E-01
1	81	1498	121,338	1,498	1201	14.65	3	2.10E-03	5.52E-01

For the highlighted data, the raw data collected was Time = 5 Min, which resulted in getting cumulative time, 70 + 5 = 75 minutes,

To get the number of cycles = flywheel RPM x Total time = 1498 x 75 =112350 Cycles for that instant. Note that the flywheel rpm was captured via a tachometer.

To get the change in cycles ΔN, ΔN = Current total cycles –Immediate total cycles.

$\Delta N = 112350 - 104860 = 7490$ cycles

Alternatively, change in cycles can be given as Recording time (Min) x RPM

$\Delta N = 5x1498 = 7490$ cycles

Crack growth (2a) mm was recorded as raw data via a travelling microscope for each Time (in Min).

Change in $\Delta 2a$ was determined by = Current 2a reading - Immediate 2a reading

For our examples, $\Delta 2a = (16-13.4) = 2.6$mm

Crack growth given was determined by dividing 2a by 2, i.e.

$a = 2a/2$ and for our example, $a = (16/2) = 8$mm

Change in a Δa was determined by current reading value – immediate reading value.

And for our case $\Delta a = (8-6.7) = 1.3$mm

Alternatively, Δa is given by diving $\Delta 2a$ by 2, i.e.

$\Delta a = (\Delta 2a/2) = (2.6/2) = 1.3$mm

Crack growth rate da/dN (mm/cycle) was given by $(\Delta a/ \Delta N)$.

And for this example, da/dN (mm/cycle) = $(\Delta a/ \Delta N) = (1.3/7490) = 1.74E - 04$ mm/cycle

3.4.5.4 Determination of Stress-Intensity Factor Range, ΔK

For each crack size value, equation 4.1 was used to calculate the stress-intensity range corresponding to a given crack growth rate, which was found as follows;

Where, $\Delta P = P_{max}-P_{min}$ for R.>0 or $\Delta P = P_{max}$ for R <0, $\alpha = 2a/W$, B = thickness, W = Width (m), a = crack growth (mm)

For the highlighted data in Table 3.8,

$\Delta P = P_{max} - P_{min}$ = 402 lbs. - 132 lbs. = 1201N, converting it to Newton becomes 1201 N

Based on specimen design dimensions,

W = 120mm = 0.12m

B = 1.8034mm = 0.0018034m

a = 8mm = 0.008m

Therefore,

$$\Delta K = (\frac{1201}{0.0018034}\sqrt{(\frac{\pi x \frac{2x0.008}{0.12}}{2x0.12} sec \frac{\pi x \frac{0.008}{0.12}}{2}))/1000000}$$

ΔK ($MNm^{-3/2}$) = 3.55E-01

Examination of FCG rates for every cycle (da/dN) against stress-intensity factor (ΔK) was presented in a log-log plot of (da/dN) versus ΔK. For example, data in column da/dN (mm/cycle) was plotted on the Y-axis against data in column ΔK ($MNm^{-3/2}$) on the X-axis, which resulted in Figure 4.2 -2 for the straight hole and Figure 4.2 -1 countersunk rivet hole for 7075-T7. Figure 4.2 -5 for a straight hole, Figure 4.2 -4 countersunk rivet hole for 7075-T6, Figure 4.2 -8 for the straight hole, and Figure 4.2 -7 countersunk rivet hole for 7075-O.

A schematic representation of FCG rate, (da/dN), as against stress-intensity factor ΔK with various metallography examinations at crack initiation. Slow crack propagation, fast crack propagation, and fatigue fractures formed the basis of the result analysis and discussion.

3.4.5.5 Analytical Methods

Examination of FCG rates for every cycle (da/dN) against stress-intensity factor, ΔK was presented in a log-log plot of (da/dN) versus ΔK with the guide of equation 4.2. A schematic representation of FCG rate (da/dN), as against stress-intensity factor ΔK, the formed basis of Objective 2 analysis, discussion, and Conclusion.

Activity flow chart to determine crack propagation under constant fatigue loading in a 100° countersunk rivet hole and straight rivet hole geometry of Al 7075-O, Al 7075-T6, and Al 7075-T7 alloys specimens. Objective no.2

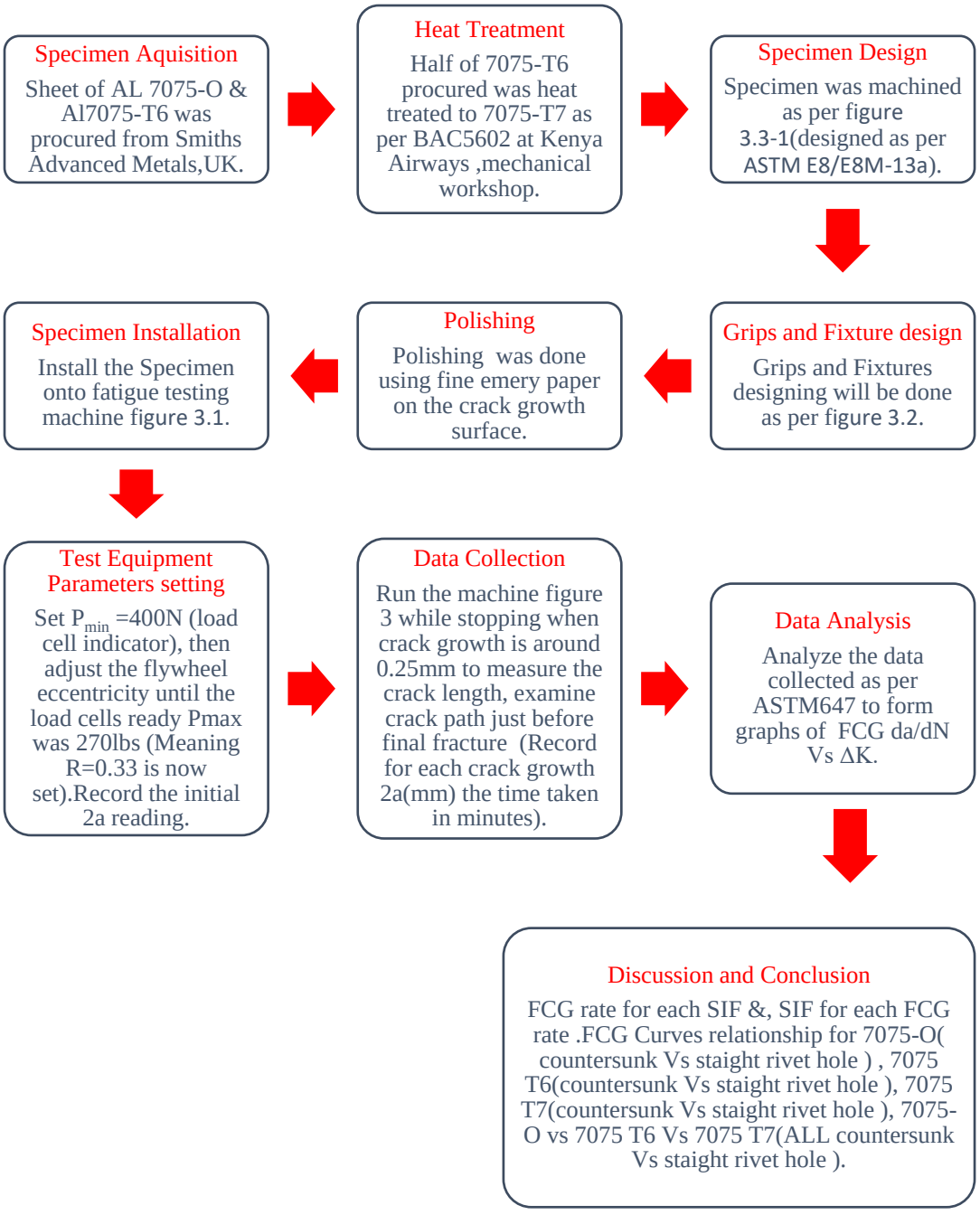

3.5 Methods and techniques to characterize cracking of Al alloys 7075 under (a) varied heat treatment conditions regarding crack path and surface morphology, and (b) under 100º countersunk rivet hole and straight rivet hole geometry in terms of crack surface morphology (Objective No.3).

To characterize the cracking of Al7075 alloy under varied heat treatment conditions (Al 7075-O, Al 7075-T6, and Al 7075-T7) in terms of Crack path and Crack surface morphology and Cracking of 100º countersunk rivet hole and straight rivet hole geometry of Al 7075-O, Al 7075-T6, Al 7075-T7 alloys in terms Crack surface morphology.

3.5.1 SEM Machine

The crack surface morphology or fractography was observed by a standard scanning electron microscope (Tescan Vega 3) with an acceleration voltage of 20 kV at Busitema University, Uganda.

3.5.2 Specimen Design

Fatigue tests were maintained until the samples broke. At the end of fatigue tests, fractured surfaces of samples were examined using a standard scanning electron microscope (SEM) (Tescan Vega 3) with an acceleration voltage of 20 kV at Busitema University, Uganda**.** The cracked surface will be cut with a shear cutter with a thickness of 2mm.

The cracked surface was cut into four pieces: (1) CI-Crack Initiation (6mm length), (2) CPS-Slow crack propagation (6mm length), (3) CPF-fast crack propagation (6mm length), (4) FF-Final fatigue fracture (6mm length) as per Figure 3.4-1. The Tescan specimen holder limited the dimension. The entire four specimens per sample were fitted onto a diameter of 15mm, the design size of the SEM specimen holder.

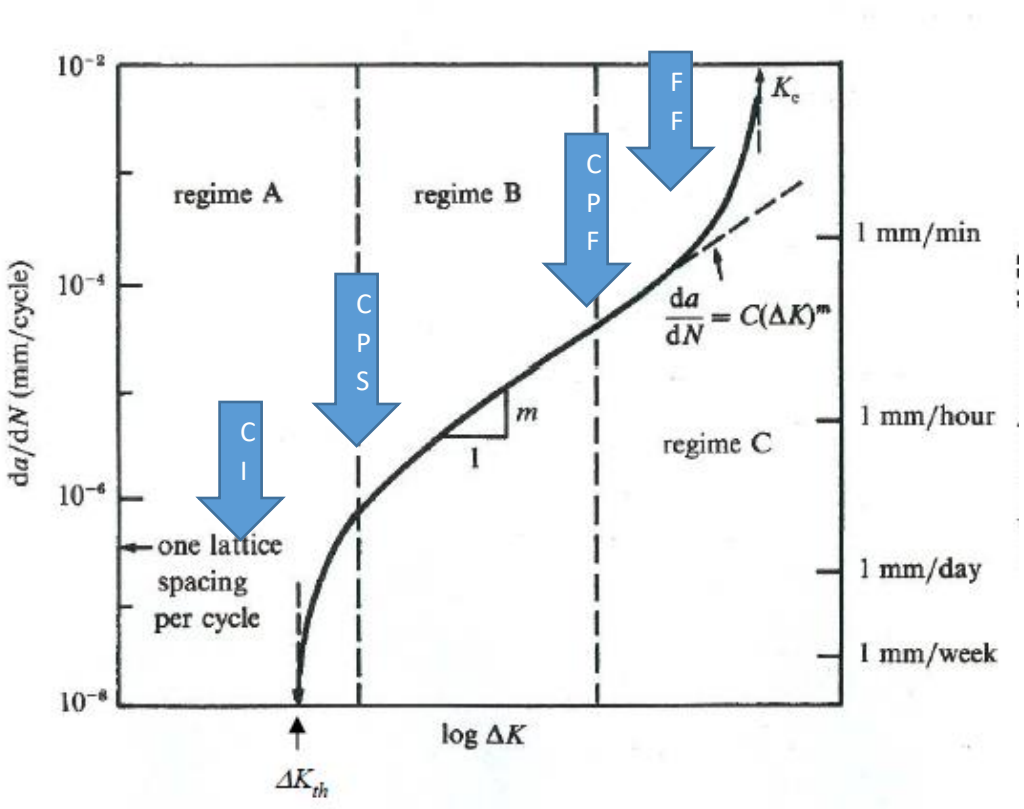

Figure 3.7: FCG curve showing areas where SEM Samples were collected (C. Chen & Li, 2020).

3.5.3 Variables and Measurements

SEM microstructure observation at the points where crack length dim was taken.

Table 3.9: Objective number 3: variables under study and how they will be collected

Variables	**Tools**	**Units of Raw Measured data**
Crack Surface	SEM	Crack Morphology, Elemental analysis
Crack Path	High-resolution camera	Images of the crack path (zigzag)

3.5.4 Procedure

3.5.4.1 Scanning Electron Microscopy -Microstructural Observation

All specimens undergoing microstructure investigation were prepared from the cracked surface with dimension length of 6mm, 2mm thickness, and width = 1.8mm. They were placed in a specimen holder with a diameter of 15mm in the order shown in Table 3.10

Table 3.10: Arrangement of specimen in SEM holder

How to set up SEM Specimens(Crack direction is critical)	
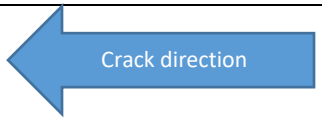	
CI	
CP-F	CP-S
FF	

Key; CI = Crack Initiation, CP-S = Crack propagation slow, CP-F = Crack propagation fast, FF = Final fracture

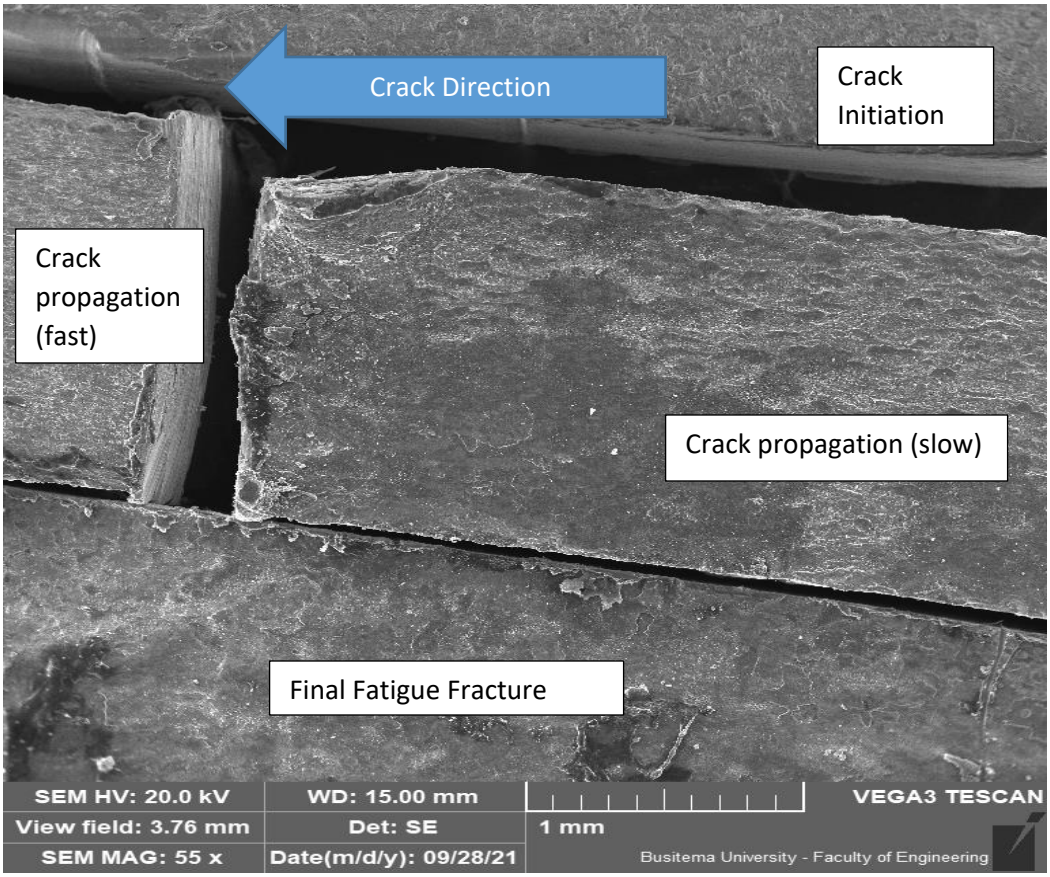

Figure 3.8: Example of specimen orientation in SEM specimen holder

SEM was utilized to scrutinize the metamorphosis of the microstructure and to conduct the investigation in order to define the element constituents for the materials and plot the crack route for all the parts.

3.5.5 Framework for Processing and Analysis of Data

Metallographic characterization formed the basis of the analysis, discussion, and conclusion of objective 3.

Activity flow chart to characterize cracking of Al alloys 7075 under (a) varied heat treatment conditions regarding crack path and surface morphology, and (b) under 100^{o} countersunk rivet hole and straight rivet hole geometry in terms of crack surface morphology. (Objective No.3)

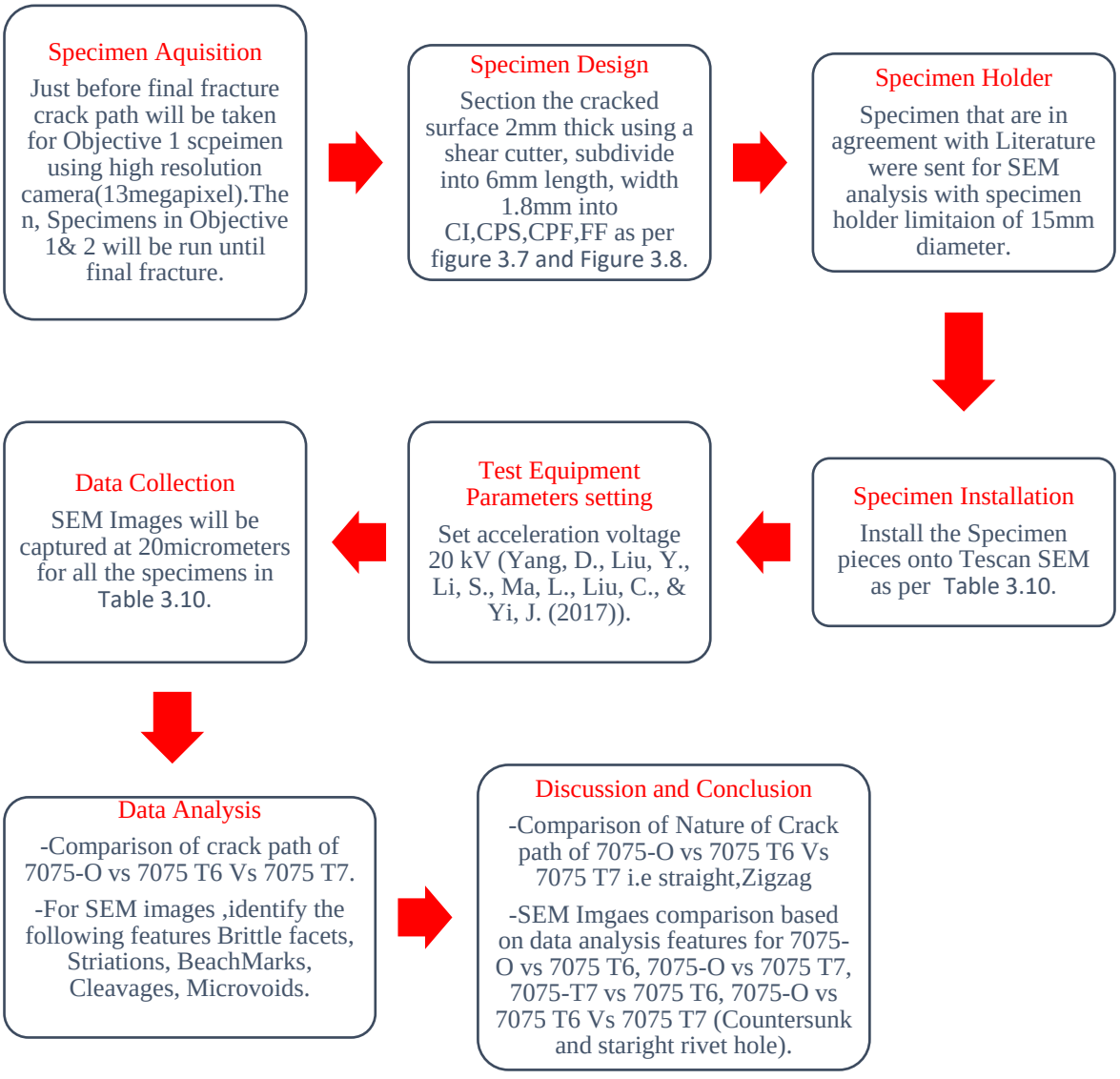

3.6 Methods and Techniques to identify mitigating actions to microstructural crack growth and propagation of Al alloys 7075 (Objective No.4).

To identify mitigating actions to microstructural crack growth and propagation Al alloys 7075-T6. The outcome of objectives 1, 2 & 3 in relation to the relevant literature formed the basis of analysis, discussion, and conclusion for objective no.4

3.6.1 Procedure

Identifying mitigating actions to microstructural crack growth and propagation Al alloys 7075-T6 were identified based on the following procedure:

Design of Objective: Entails all the results and discussion of Objectives 1, 2 & 3 and considerations from the literature

Data Collection: Results, discussion, and conclusion of Objectives 1, 2 & 3 -Design, in-service considerations of Aerospace Al alloys 7075-T6 -Advantages and limitations of using Al alloys 7075-T6.

Data Analysis: Fatigue design (safe-life structures, fail-safe structures) of Al alloys 7075-T6 in-service Experience (repair design, allowable cracks) of Al alloys 7075-T6.

Discussion and conclusion: design and repair considerations of the aerospace stringer and frame Al alloys 7075-T6 and in comparison, with the following from the literature

I. Fatigue Design: safe-life structures (elements without cracks) and fail-safe structures (cracks acceptable until they reach a critical size.)
II. Service Experience; repair and alteration design

Activity Flow chart to identify mitigating actions to microstructural crack growth and propagation of Al alloys 7075 (Objective No.4).

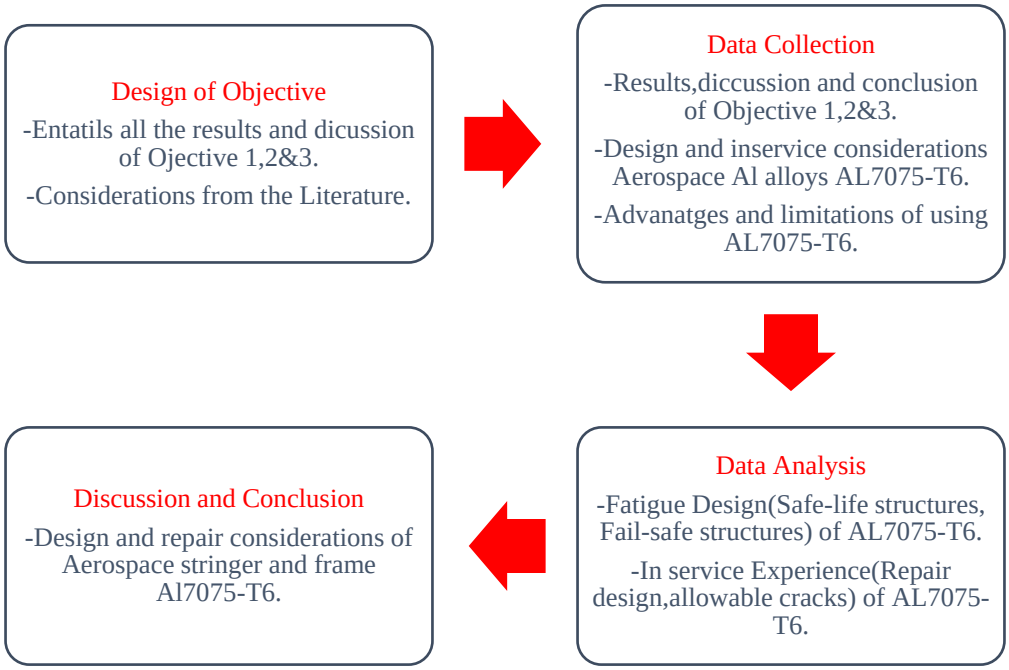

CHAPTER FOUR: RESULTS AND DISCUSSION

4.1 Introduction

This chapter analyses and interprets data collected from 18 fatigue sample tests and 36 SEM observations from Al 7075-O, Al 7075-T6, Al 7075-T7, and 100 ^{o} countersunk rivet hole and straight rivet hole geometry. This chapter also covers results and discussion regarding the impact of heat treatment of high cycle fatigue, the effect of rivet hole orientation, fractographic fatigue analysis, and mitigating actions to microstructural crack growth and propagation of Al 7075-T6.

4.2 Impacts of Heat Treatment on HCF

4.2.1 Crack Propagation Curves

The graph in Figure 4.1 shows the fatigue crack growth of Al 7075-T7.

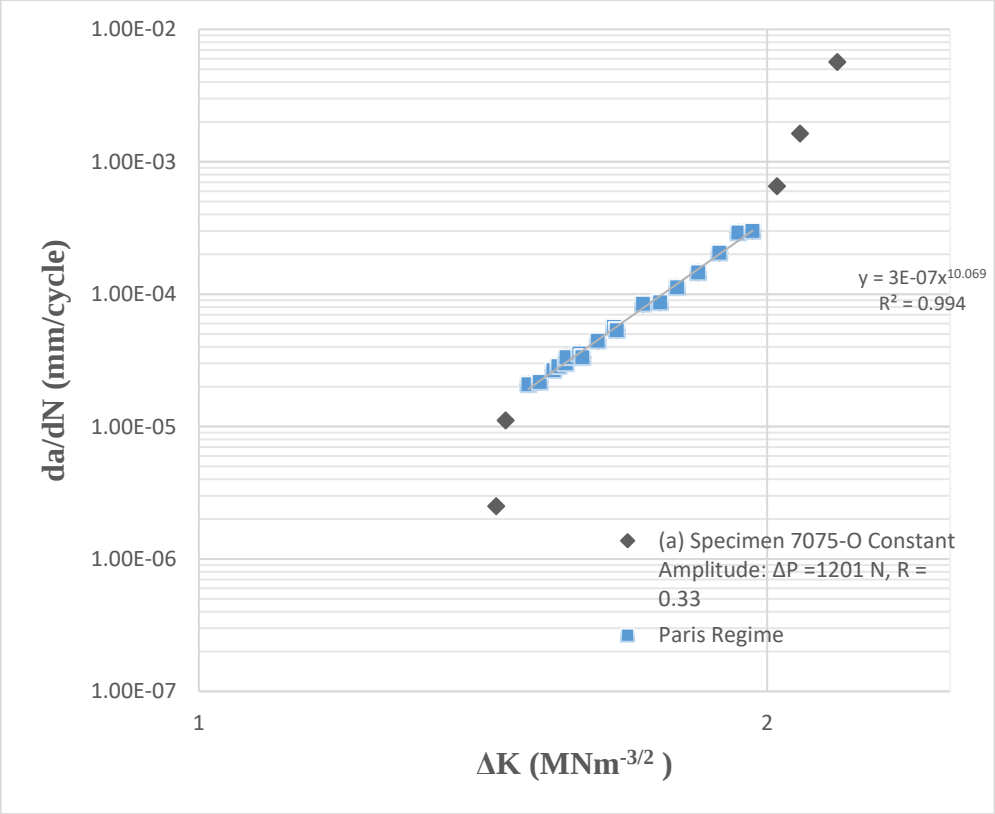

Figure 4.2: FCG Curve in log scale for Al 7075-T7

Table 4.1: Data for specimen Al 7075-T7 constant amplitude: ΔP =1201 N, R = 0.33

Time (Min)	Total Time (Min)	RPM	N (Cycles)	ΔN [Cycles]	ΔP [N]	a [mm]	Δa[mm]	da/dN (mm/cycle)	ΔK ($MNm^{-3/2}$)
0	0	1498	0	0	1201	20.6	0	0	0
200	200	1498	299600	299600	1201	21.35	0.75	2.50E-06	1.44E+00
30	230	1498	344540	44940	1201	21.85	0.5	1.11E-05	1.45E+00
40	270	1498	404460	59920	1201	23.1	1.25	2.09E-05	1.50E+00
20	290	1498	434420	29960	1201	23.75	0.65	2.17E-05	1.52E+00
20	310	1498	464380	29960	1201	24.55	0.8	2.67E-05	1.54E+00
7	317	1498	474866	10486	1201	24.85	0.3	2.86E-05	1.55E+00
10	327	1498	489846	14980	1201	25.3	0.45	3.00E-05	1.56E+00
1	328	1498	491344	1498	1201	25.35	0.05	3.34E-05	1.57E+00
15	343	1498	513814	22470	1201	26.15	0.8	3.56E-05	1.59E+00
4	347	1498	519806	5992	1201	26.35	0.2	3.34E-05	1.60E+00
15	362	1498	542276	22470	1201	27.35	1	4.45E-05	1.63E+00
13	375	1498	561750	19474	1201	28.45	1.1	5.65E-05	1.66E+00
2.5	377.5	1498	565495	3745	1201	28.65	0.2	5.34E-05	1.67E+00
15	392.5	1498	587965	22470	1201	30.55	1.9	8.46E-05	1.72E+00
10	402.5	1498	602945	14980	1201	31.85	1.3	8.68E-05	1.76E+00
8	410.5	1498	614929	11984	1201	33.2	1.35	1.13E-04	1.79E+00
8	418.5	1498	626913	11984	1201	34.95	1.75	1.46E-04	1.84E+00
6	424.5	1498	635901	8988	1201	36.8	1.85	2.06E-04	1.89E+00
4	428.5	1498	641893	5992	1201	38.55	1.75	2.92E-04	1.93E+00
3	431.5	1498	646387	4494	1201	39.9	1.35	3.00E-04	1.97E+00
2.5	434	1498	650132	3745	1201	42.35	2.45	6.54E-04	2.02E+00
1	435	1498	651630	1498	1201	44.8	2.45	1.64E-03	2.08E+00
0.5	435.5	1498	652379	749	1201	49.05	4.25	5.67E-03	2.18E+00

Table 4.2: Data for specimen Al 7075-T6 constant amplitude: ΔP =1201 N, R = 0.33

Time (Min)	Total Time(Min)	RPM	N (Cycles)	ΔN [Cycles]	ΔP [N]	a [mm]	Δa[mm]	da/dN (mm/cycle)	ΔK ($MNm^{-3/2}$)
0	0	1498	0	0	1201	20.4	0	0.00E+00	1.40E+00
57	57	1498	85,386	85,386	1201	20.95	0.55	6.44E-06	1.42E+00
12	69	1498	103,362	17,976	1201	21.3	0.35	1.95E-05	1.44E+00
18	87	1498	130,326	26,964	1201	22	0.7	2.60E-05	1.46E+00
12	99	1498	148,302	17,976	1201	22.5	0.5	2.78E-05	1.48E+00
24	123	1498	184,254	35,952	1201	23.9	1.4	3.89E-05	1.52E+00
10	133	1498	199,234	14,980	1201	24.55	0.65	4.34E-05	1.54E+00
9	142	1498	212,716	13,482	1201	25.25	0.7	5.19E-05	1.56E+00
8	150	1498	224,700	11,984	1201	26	0.75	6.26E-05	1.59E+00
8	158	1498	236,684	11,984	1201	26.8	0.8	6.68E-05	1.61E+00
7	165	1498	247,170	10,486	1201	27.65	0.85	8.11E-05	1.64E+00
5	170	1498	254,660	7,490	1201	28.4	0.75	1.00E-04	1.66E+00
2.4	172.4	1498	258,255	3,595	1201	28.7	0.3	8.34E-05	1.67E+00
5	177.4	1498	265,745	7,490	1201	29.55	0.85	1.13E-04	1.69E+00
10	187.4	1498	280,725	14,980	1201	31.75	2.2	1.47E-04	1.75E+00
5	192.4	1498	288,215	7,490	1201	33.5	1.75	2.34E-04	1.80E+00
3.5	195.9	1498	293,458	5,243	1201	35	1.5	2.86E-04	1.84E+00
4	199.9	1498	299,450	5,992	1201	37.5	2.5	4.17E-04	1.90E+00
2	201.9	1498	302,446	2,996	1201	39.5	2	6.68E-04	1.96E+00
1	202.9	1498	303,944	1,498	1201	40.5	1	6.68E-04	1.98E+00
1	203.9	1498	305,442	1,498	1201	42	1.5	1.00E-03	2.02E+00
0.75	204.65	1498	306,566	1,124	1201	44	2	1.78E-03	2.06E+00
0.5	205.15	1498	307,315	749	1201	48.5	4.5	6.01E-03	2.17E+00

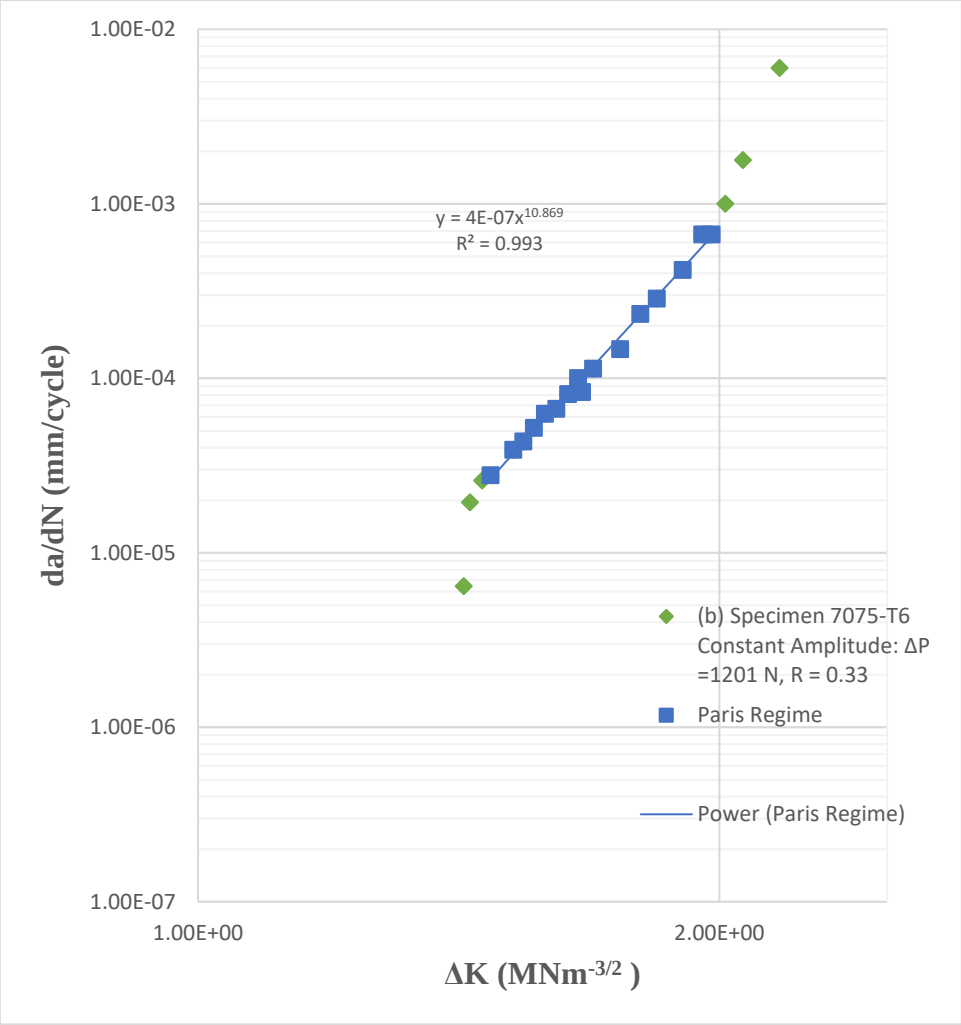

Figure 4.3: FCG curve in log scale for Al 7075-T6

Table 4.3: Data for specimen Al 7075-O constant amplitude: ΔP =1201 N, R = 0.33

Time (Min)	Total Time (Min)	RPM	N (Cycles)	ΔN [Cycles]	ΔP [N]	a [mm]	Δ a[mm]	da/dN (mm/cycle)	ΔK ($MNm^{-3/2}$)
0	0	1498	0	0	1201	19.95	0	0.00E+00	1.39E+00
45	45	1498	67,410	67,410	1201	20.95	1	1.48E-05	1.42E+00
10	55	1498	82,390	14,980	1201	21	0.05	3.34E-06	1.43E+00
7	62	1498	92,876	10,486	1201	21.45	0.45	4.29E-05	1.44E+00
8	70	1498	104,860	11,984	1201	22	0.55	4.59E-05	1.46E+00
13	83	1498	124,334	19,474	1201	23.25	1.25	6.42E-05	1.50E+00
8	91	1498	136,318	11,984	1201	24.1	0.85	7.09E-05	1.53E+00
5	96	1498	143,808	7,490	1201	24.75	0.65	8.68E-05	1.55E+00
5	101	1498	151,298	7,490	1201	25.4	0.65	8.68E-05	1.57E+00
4	105	1498	157,290	5,992	1201	26	0.60	1.00E-04	1.59E+00
6	111	1498	166,278	8,988	1201	27.15	1.15	1.28E-04	1.62E+00
5	116	1498	173,768	7,490	1201	28.2	1.05	1.40E-04	1.65E+00
3	119	1498	178,262	4,494	1201	28.75	0.55	1.22E-04	1.67E+00
3	122	1498	182,756	4,494	1201	29.5	0.75	1.67E-04	1.69E+00
2	124	1498	185,752	2,996	1201	30	0.50	1.67E-04	1.70E+00
3	127	1498	190,246	4,494	1201	31	1.00	2.23E-04	1.73E+00
2	129	1498	193,242	2,996	1201	31.9	0.90	3.00E-04	1.76E+00
1	130	1498	194,740	1,498	1201	32.35	0.45	3.00E-04	1.77E+00
2	132	1498	197,736	2,996	1201	33.5	1.15	3.84E-04	1.80E+00
2	134	1498	200,732	2,996	1201	34.6	1.10	3.67E-04	1.83E+00
1	135	1498	202,230	1,498	1201	35.4	0.80	5.34E-04	1.85E+00
1	136	1498	203,728	1,498	1201	36.5	1.10	7.34E-04	1.88E+00
1	137	1498	205,226	1,498	1201	37.5	1.00	6.68E-04	1.90E+00
1	138	1498	206,724	1,498	1201	39.75	2.25	1.50E-03	1.96E+00
0.75	138.75	1498	207,848	1,124	1201	42.65	2.90	2.58E-03	2.03E+00
0.25	139	1498	208,222	375	1201	45	2.35	6.28E-03	2.09E+00
0.1	139.1	1498	208,372	150	1201	47.5	2.50	1.67E-02	2.14E+00

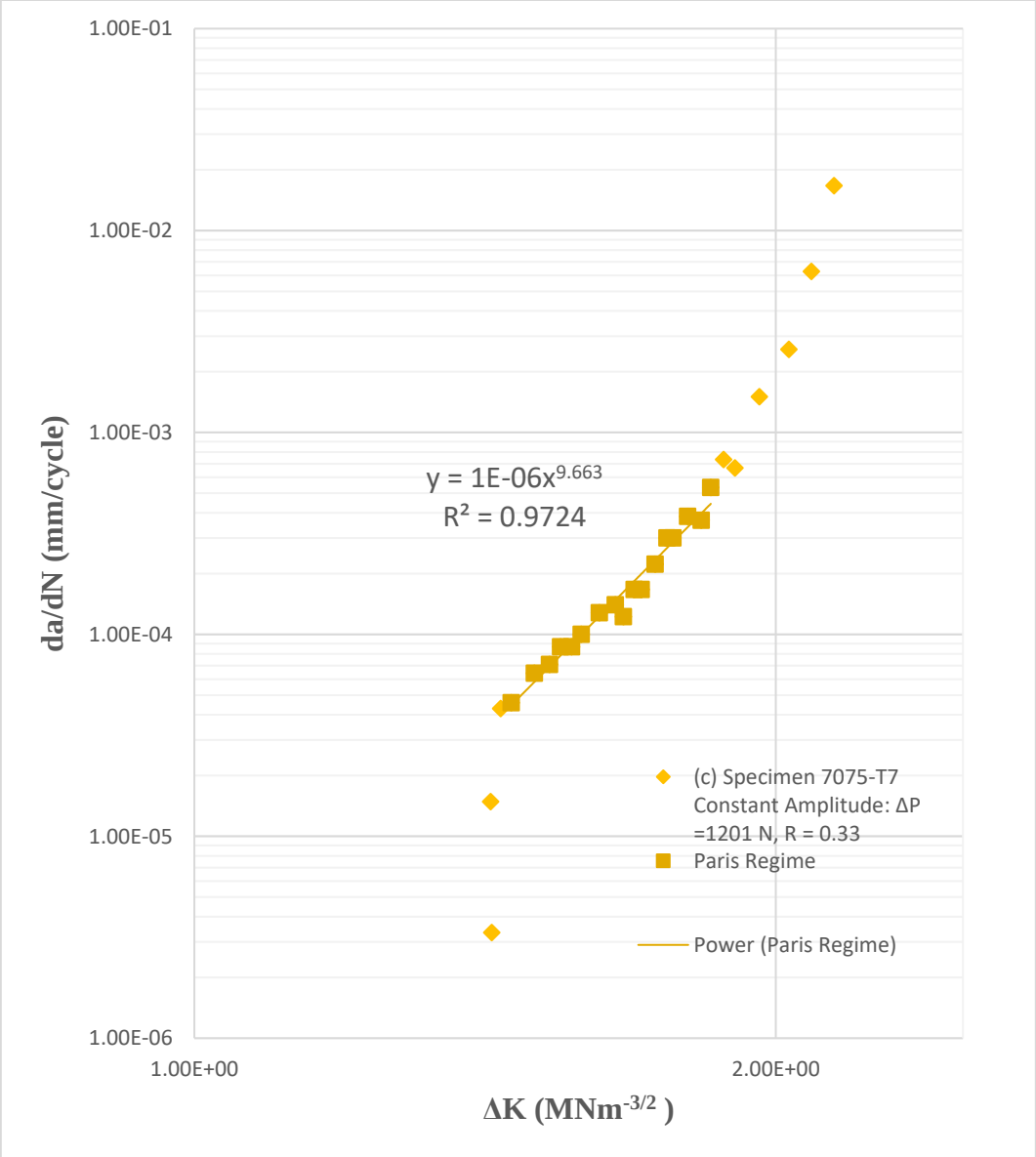

Figure 4.4: FCG curve in log scale for Al 7075-O

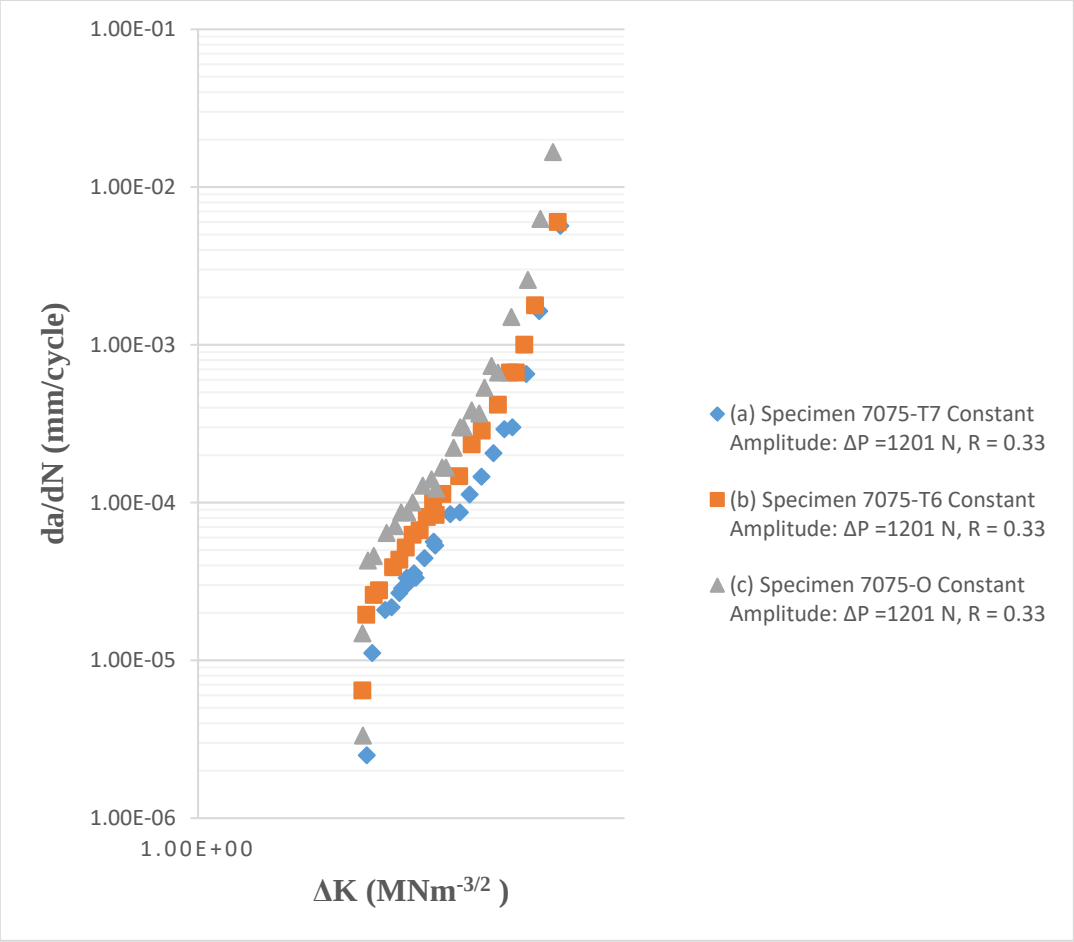

Figure 4.5: Superimposed FCG curves for Al 7075-O, T6 and T7

The propagation curves da/dN against ΔK are illustrated in Figure 4.1, Figure 4.2, and Figure 4.3 for Al alloys 7075-T7, T6, and O, respectively, for R, = 0.33 in the three heat-treated conditions. The curves concur with those acquired by Leng et al. (2018). Al alloys 7075-T7 condition demonstrates a more increased resistance against crack propagation than the Al alloys 7075-O Condition, the contrast advancing as the growth rates decline towards the threshold. Al alloys 7075-T6 condition displays an intermediate behaviour between Al alloys 7075-O and Al alloys 7075-T7 and grows towards Al alloys 7075-T7 above 1.00E-03mm/cycle.

Figure 4.4. Shows a superimposed FCG curve for the three heat-treated expressed in terms of ΔK. R = 0.33. The characteristic variation of da/dN with ΔK is exhibited for Al alloys 7075-O, 7075-T6, and 7075-T7 specimens at stress ratios R = 0.33 in Figure 4.1, Figure 4.2, and Figure 4.3. The FCG rates of Al alloys 7075-O, 7075-T6, and 7075-T7 specimens are compared for R = 0.33 in Figure 4.1, Figure 4.2, and Figure 4.3. The da/dN is greater while ΔKth is less for the Al alloys 7075-O state than for the Al alloys 7075-T7 one while Al alloys 7075-T6 is sandwiched amongst the two.

The monitored greater da/dN and less ΔKth under the Al alloys 7075-O condition than under the Al alloys 7075-T7 and 7075-T6 states, Figure 4.1, Figure 4.2, and Figure 4.3, are also registered by other researchers (Imam et al., 2015a). The crack propagation curves of the Al alloys 7075-O, 7075-T6, and 7075-T7 are represented for R = 0.33 by straight lines along the Paris region b, i.e.

The power equation for the Paris region for the three heat treatment conditions gives;

As indicated in Figure 4.1, Al alloys 7075-T7 gives $y = (3*10^{-07}) \text{ x } ^{10.069}$

As shown in Figure 4.2, Al alloys 7075-T6 gives $y = (4*10^{-07}) \text{ x}^{10.869}$

As indicated in Figure 4.3, Al alloys 7075-O gave $y = (10^{-06}) \text{ x}^{9.663}$

Representing the same on Paris equation 2.12,

For Al alloys 7075-T7 becomes

$$\left(\frac{da}{dN}\right) = (3 * 10^{-07})(\Delta K)^{10.069} \qquad \text{(Eq.4.1)}$$

For Al alloys 7075-T6 becomes

$$\left(\frac{da}{dN}\right) = \left(4 * 10^{-07}\right)(\Delta K)^{10.869} \quad \text{(Eq. 4.2)}$$

For Al alloys 7075-O becomes

$$\left(\frac{da}{dN}\right) = (10^{-06})(\Delta K)^{9.663} \quad \text{(Eq. 4.3)}$$

Assuming the Stress intensity factor is constant, for this case, let's take ΔK=2

For Al alloys 7075-T7,

$$\left(\frac{da}{dN}\right) = (4 * 10^{-07}) * 2^{10.869} \quad \text{(Eq. 4.4)}$$

$$\left(\frac{da}{dN}\right)_{7075-T7} = 3.22x10^{-4} \quad \text{(Eq. 4.5)}$$

For Al alloys 7075-T6,

$$\left(\frac{da}{dN}\right) = (4 * 10^{-07}) * 2^{10.869} \quad \text{(Eq. 4.6)}$$

$$\left(\frac{da}{dN}\right)_{7075-T6} = 7.48x10^{-4} \quad \text{(Eq. 4.7)}$$

For Al alloys 7075-O

$$\left(\frac{da}{dN}\right) = (4 * 10^{-07}) * 2^{10.869} \quad \text{(Eq.4.8)}$$

$$\left(\frac{da}{dN}\right)_{7075-O} = 8.10x10^{-4} \quad \text{(Eq. 4.9)}$$

The exact value of ΔK in the crack propagation rate of Al alloys 7075-T7 is consistently inferior to the crack propagation rate of Al alloys 7075-T6 and 7075-O, and they tend to

become identical beyond 1.0E-03mm/cycle. We again witness that, in this model, it is inconceivable to determine a point as an asymptotic boundary of the crack propagation curves.

Determining ΔK_{th} for different heat treatment materials.

For Al alloys 7075-T7 becomes

$$\left(\frac{da}{dN}\right) = (3 * 10^{-07})(\Delta K)^{10.069} \quad \text{(Eq. 4.10)}$$

$$10^{-7} = 3E - 07(\Delta K)^{10.069} \quad \text{(Eq.4.11)}$$

$\Delta K_{th} = 0.8966$ MNm$^{-3/2}$

For Al alloys 7075-T6 becomes

$$\left(\frac{da}{dN}\right) = (4 * 10^{-07})(\Delta K)^{10.869} \quad \text{(Eq.4.12)}$$

$$10^{-7} = 4E - 07(\Delta K)^{10.869} \quad \text{(Eq. 4.13)}$$

$\Delta K_{th} = 0.8802$ MNm$^{-3/2}$

For Al alloys 7075-O becomes

$$\left(\frac{da}{dN}\right) = (10^{-06})(\Delta K)^{9.663} \quad \text{(Eq.4.142)}$$

$$10^{-7} = 1E - 06(\Delta K)^{9.663} \quad \text{(Eq.4.15)}$$

$\Delta K_{th} = 0.7880$ MNm$^{-3/2}$

Table 4.4: Material parameters

Al alloys 7075 Material condition	C	m	ΔK_{th} (MNm$^{-3/2}$)	da/dN(Assumption, ΔK =2)mm/cycle
7075-T7	3*10^{-07}	10.069	0.8966	3.22x10^{-4}

7075-T6	$4*10^{-07}$	10.869	0.8802	$7.48x10^{-4}$
7075-O	10^{-06}	9.663	0.7880	$8.10x10^{-4}$

The interpretation of fatigue crack propagation rates da/dN against stress intensity span ΔK for Al alloys 7075-O, 7075-T6, and 7075-T7 conditions is shown in Figure 4.1, Figure 4.2, and Figure 4.3 for load ratio 0.33, constant amplitude. It is apparent that Al alloy 7075-T7 structures are close to threshold levels, which offer the most elevated fatigue resistance in spans of the low growth rates and the highest threshold point ΔK_{th} values. Likened with those for the Al alloy 7075-O configuration, the threshold ΔKth values in the current developments are approximately 11% and 14% more heightened in the Al alloy 7075-T6 and 7075-T7 configurations, respectively, at R = 0.33 (Table 4.4).

4.3 Effect of Rivet Hole Orientation

4.3.1 Crack Propagation Curves

Table 4.5: Data for Al 7075-T7 specimen constant amplitude: ΔP =1201 N, R = 0.33, countersunk 100^{o} rivet hole.

Time (Min)	Total Time(Min)	RPM	N (Cycles)	ΔN [Cycles]	ΔP [N]	a [mm]	Δa[mm]	da/dN (mm/cycle)	ΔK ($MNm^{-3/2}$)
0	0	1498	0	0	1201	1.9	0	0.00E+00	0.00E+00
70	70	1498	104860	104860	1201	2.75	0.85	8.11E-06	2.87E-01
2	72	1498	107856	2996	1201	5.05	2.3	7.68E-04	4.72E-01
4	76	1498	113848	5992	1201	6.4	1.35	2.25E-04	3.61E-01
7	83	1498	124334	10486	1201	7.5	1.1	1.05E-04	3.26E-01
3.5	86.5	1498	129577	5243	1201	9	1.5	2.86E-04	3.81E-01
2	88.5	1498	132573	2996	1201	11.85	2.85	9.51E-04	5.25E-01
1	89.5	1498	134071	1498	1201	15.1	3.25	2.17E-03	5.61E-01

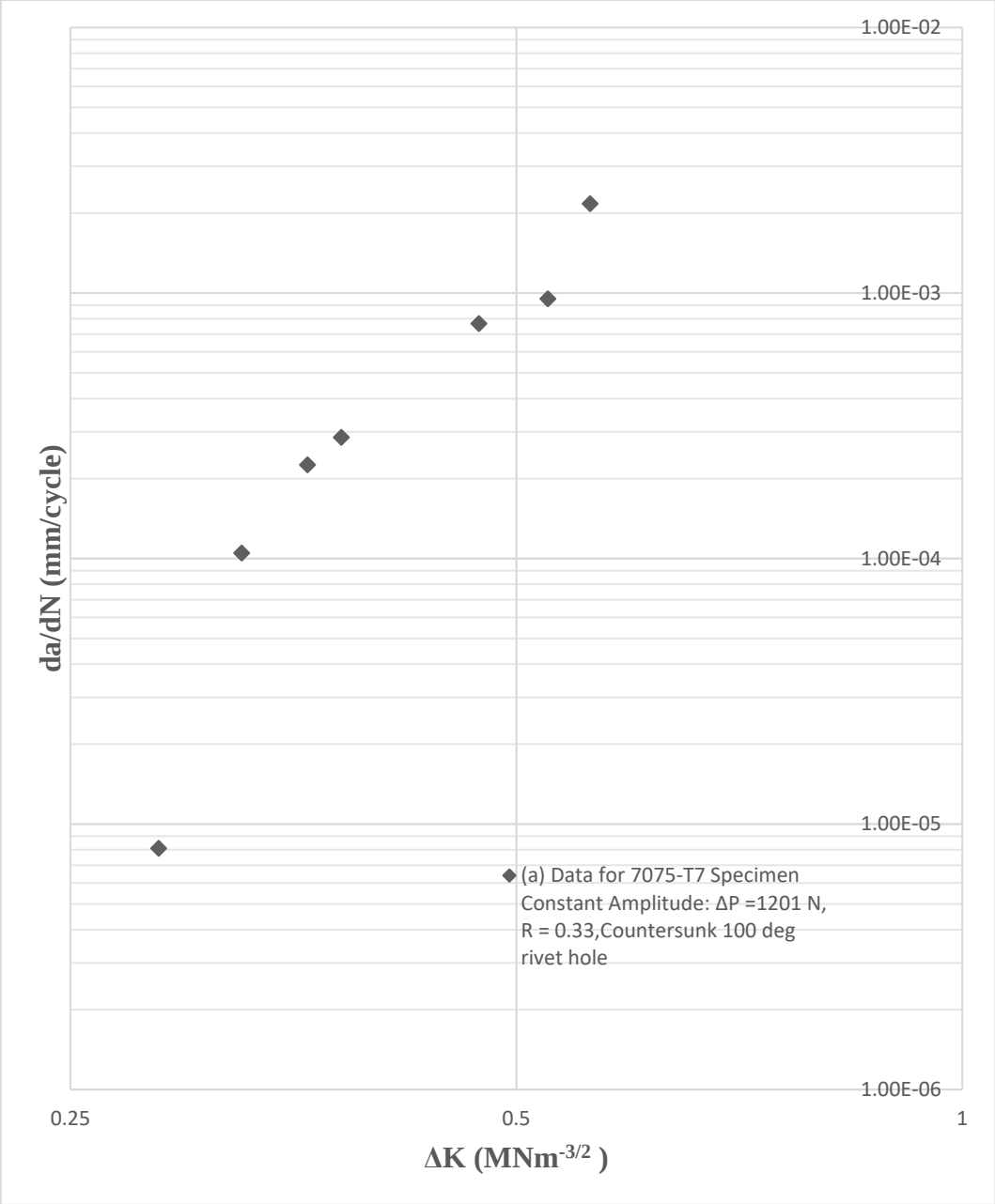

Figure 4.6: FCG of Al 7075-T7 with countersunk 100°.

Table 4.6: Data for Al 7075-T7 specimen under constant amplitude: ΔP =1201 N, R = 0.33, perpendicular rivet hole.

Time(Min)	Total Time(Min)	RPM	N (Cycles)	ΔN [Cycles]	ΔP [N]	a [mm]	Δa[mm]	da/dN (mm/cycle)	ΔK ($MNm^{-3/2}$)
0	0	1498	0	0	1201	2.05	0	0.00E+00	0.00E+00
69	69	1498	103,362	103,362	1201	3	1	9.19E-06	3.03E-01
1	70	1498	104,860	1,498	1201	6.7	4	2.47E-03	5.98E-01
5	75	1498	112,350	7,490	1201	8	1	1.74E-04	3.55E-01
2	77	1498	115,346	2,996	1201	10	2	6.68E-04	4.40E-01
3	80	1498	119,840	4,494	1201	11.5	2	3.34E-04	3.81E-01
1	81	1498	121,338	1,498	1201	14.65	3	2.10E-03	5.52E-01

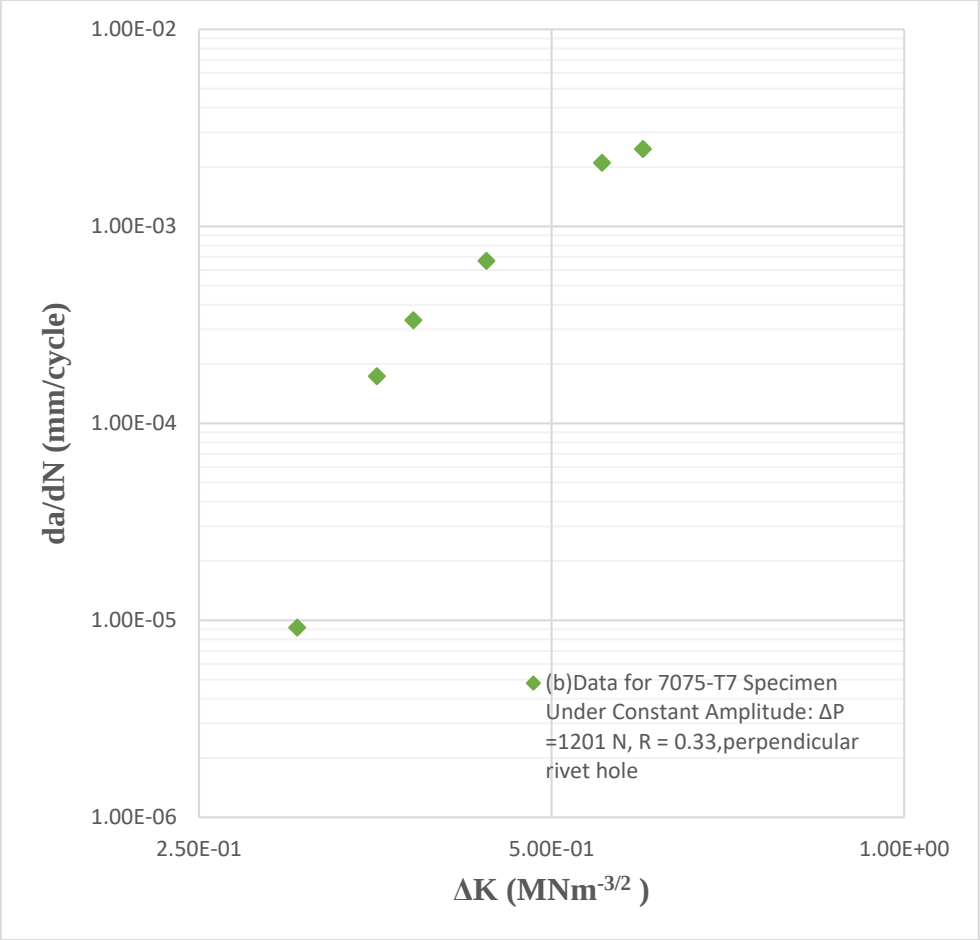

Figure 4.7: FCG of Al 7075-T7 with perpendicular rivet hole.

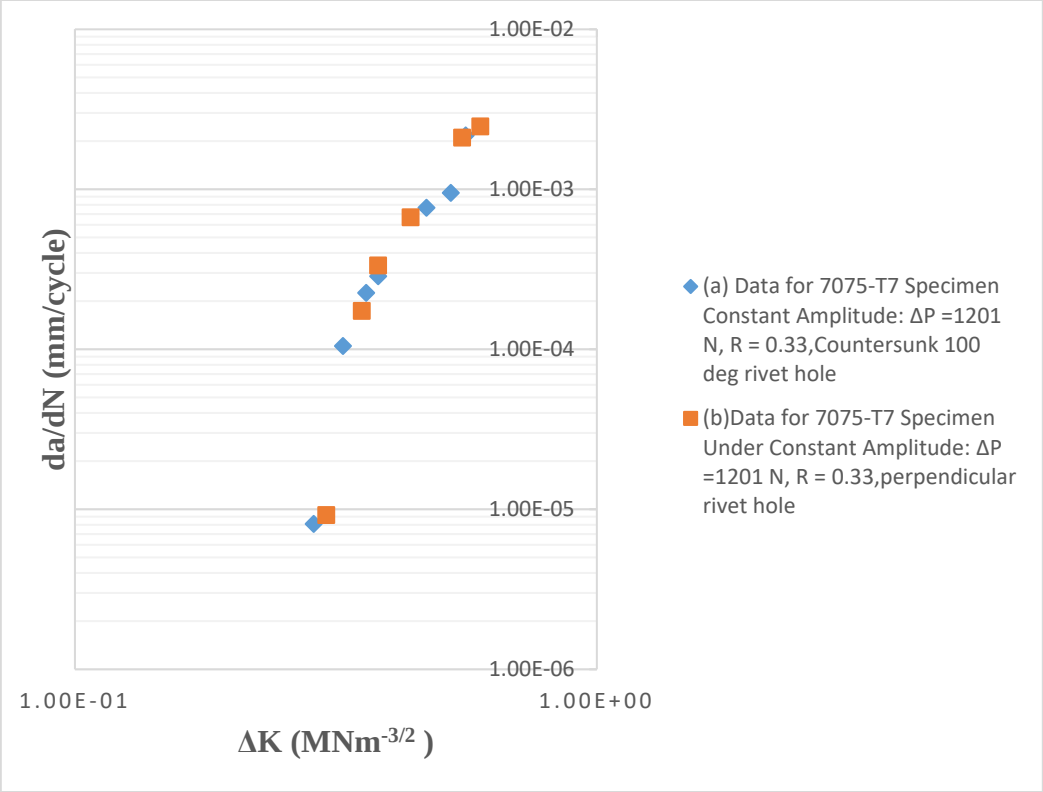

Figure 4.8: Superimposed FCG of Al 7075-T7 under countersunk and perpendicular rivet hole.

Table 4.7: Data for Al 7075-T6 specimen under constant amplitude: ΔP =1201 N, R = 0.33, countersunk 100^{o} rivet hole.

Time(Min)	Total Time(Min)	RPM	N (Cycles)	ΔN [Cycles]	ΔP [N]	a [m m]	Δa[mm]	da/dN (mm/cycle)	ΔK (MNm$^{-3/2}$)
0	0	1498	0	0	1201	2	0	0.00E+00	0.00E+00
55	55	1498	82,390	82,390	1201	2.7	0.70	8.50E-06	2.60E-01
1.5	56.5	1498	84,637	2,247	1201	4.25	1.55	6.90E-04	3.87E-01
10	66.5	1498	99,617	14,980	1201	5	0.75	5.01E-05	2.69E-01
3	69.5	1498	104,111	4,494	1201	6	1.00	2.23E-04	3.11E-01
0.5	70	1498	104,860	749	1201	8.9	2.90	3.87E-03	5.30E-01
0.75	70.75	1498	105,984	1,124	1201	11	2.10	1.87E-03	4.51E-01
0.25	71	1498	106,358	375	1201	14	3.00	8.01E-03	5.39E-01

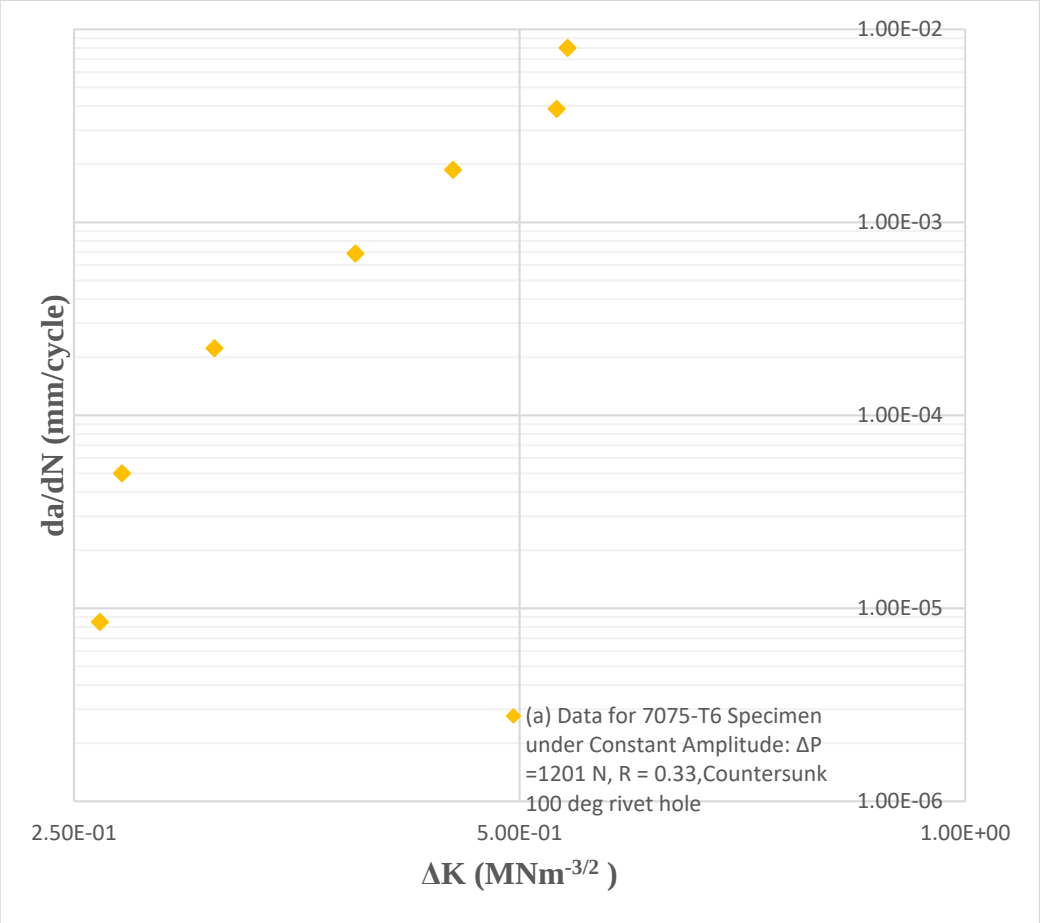

Figure 4.9: FCG of Al 7075-T6 with countersunk rivet hole.

Table 4.8: Data for Al 7075-T6 specimen under constant amplitude: ΔP =1201 N, R = 0.33, perpendicular rivet hole.

Time(Min)	Total Time(Min)	RPM	N (Cycles)	ΔN [Cycles]	ΔP [N]	a [mm]	Δa[mm]	da/dN (mm/cycle)	ΔK (MNm$^{-3/2}$)
0	0	1498	0	0	1201	2	0	0.00E+00	0.00E+00
65	65	1498	97,370	97,370	1201	2.65	0.65	6.68E-06	2.51E-01
1.25	66.25	1498	99,243	1,873	1201	4.25	1.60	8.54E-04	3.93E-01
10	76.25	1498	114,223	14,980	1201	5.05	0.80	5.34E-05	2.78E-01
15	91.25	1498	136,693	22,470	1201	5.8	0.75	3.34E-05	2.69E-01
0.25	91.5	1498	137,067	375	1201	8.9	3.10	8.28E-03	5.48E-01
0.75	92.25	1498	138,191	1,124	1201	11.8	2.90	2.58E-03	5.30E-01
0.75	93	1498	139,314	1,124	1201	14	2.20	1.96E-03	4.61E-01

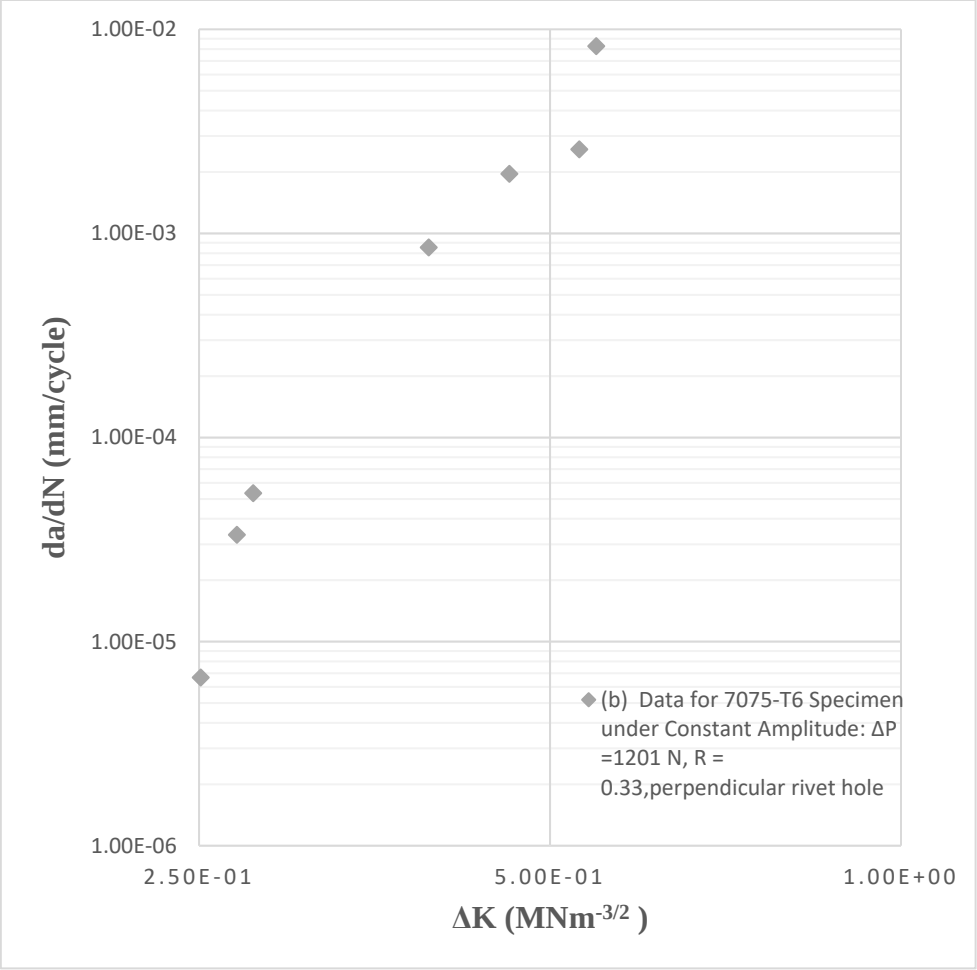

Figure 4.10: FCG of Al 7075-T6 with perpendicular rivet hole orientation.

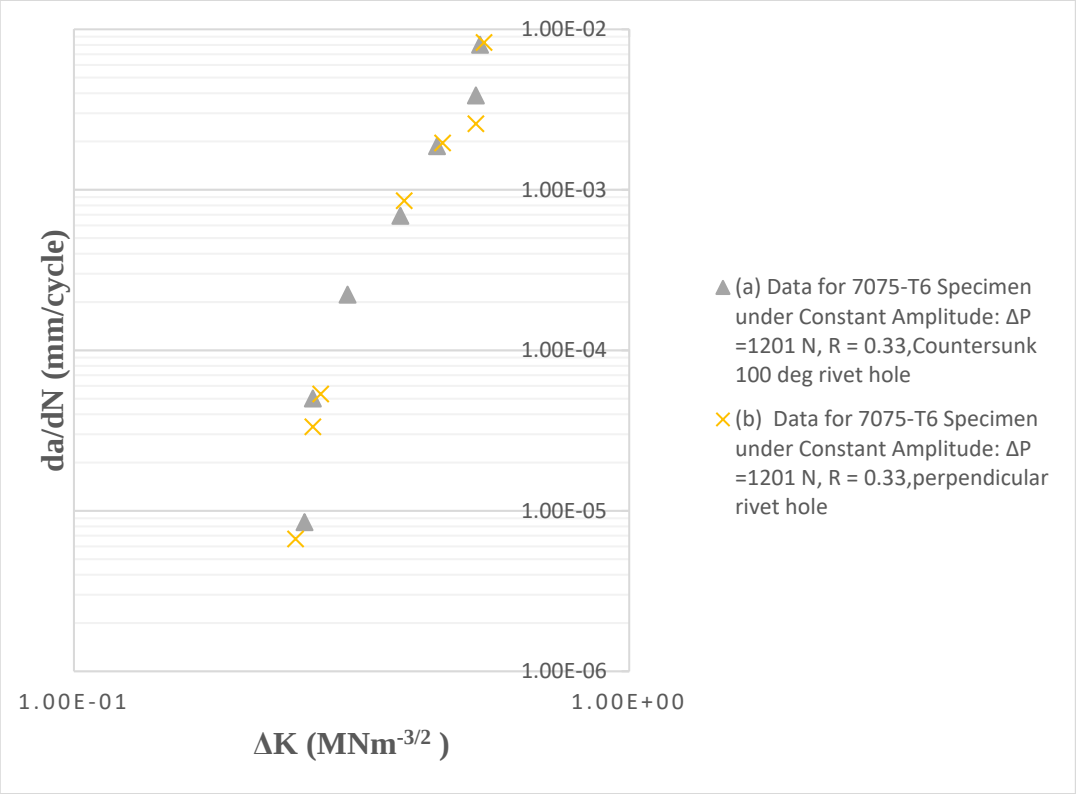

Figure 4.11: Superimposed FCG of Al 7075-T6 with countersunk and perpendicular rivet hole orientation.

Table 4.9: Data for Al 7075-O specimen under constant amplitude: ΔP =1201 N, R = 0.33, countersunk 100^{o} rivet hole.

Time (Min)	Total Time (Min)	RPM	N (Cycles)	ΔN [Cycles]	ΔP [N]	a [mm]	Δa[mm]	da/dN (mm/cycle)	ΔK (MNm$^{-3/2}$)
0	0	1498	0	0	1201	1.95	0	0.00E+00	0.00E+00
70	70	1498	104,860	104,860	1201	2.25	0.30	2.86E-06	1.70E-01
16	86	1498	128,828	23,968	1201	2.7	0.45	1.88E-05	2.09E-01
15	101	1498	151,298	22,470	1201	3.05	0.35	1.56E-05	1.84E-01
10	111	1498	166,278	14,980	1201	3.5	0.45	3.00E-05	2.09E-01
5	116	1498	173,768	7,490	1201	4.05	0.55	7.34E-05	2.31E-01
1.5	117.5	1498	176,015	2,247	1201	5	0.95	4.23E-04	3.03E-01
1	118.5	1498	177,513	1,498	1201	5.1	0.10	6.68E-05	9.84E-02
0.25	118.75	1498	177,888	375	1201	8.25	3.15	8.41E-03	5.52E-01
2	120.75	1498	180,884	2,996	1201	9.05	0.80	2.67E-04	2.78E-01

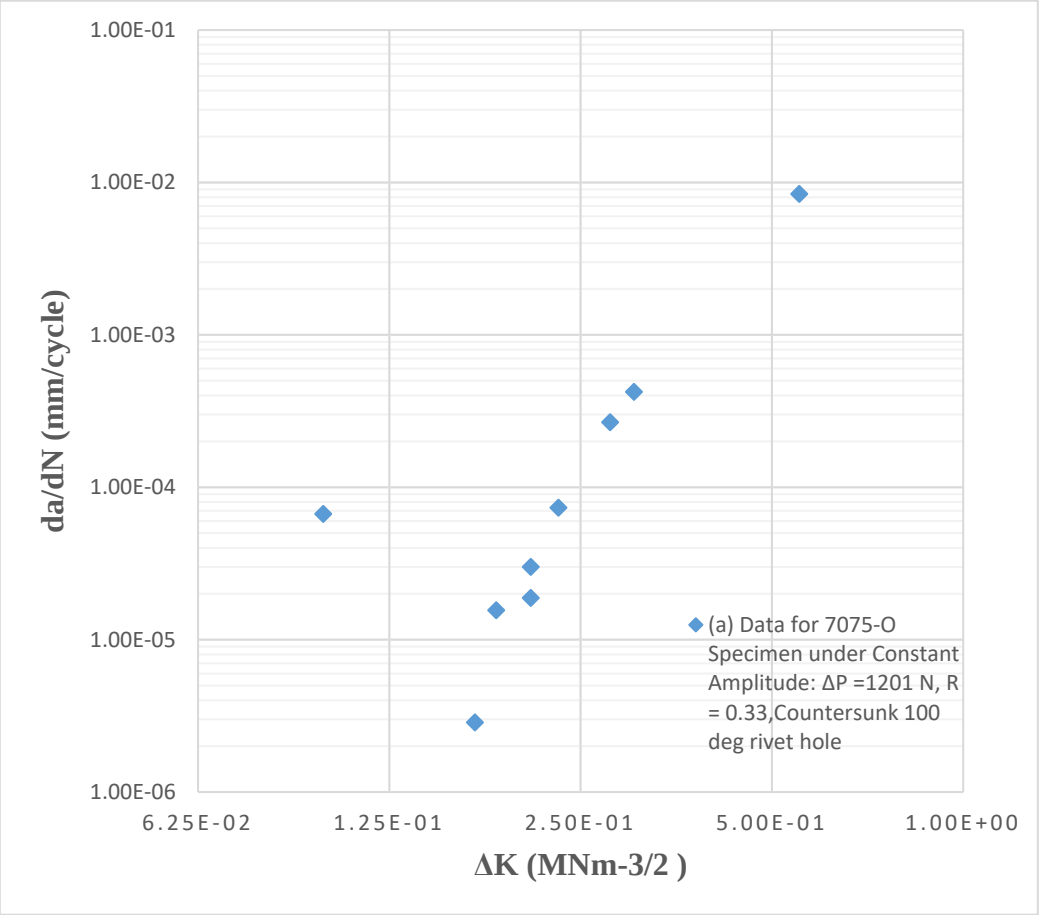

Figure 4.12: FCG of Al 7075-O with countersunk rivet hole orientation.

Table 4.10: Data for Al 7075-O specimen under constant amplitude: ΔP =1201 N, R = 0.33, perpendicular rivet hole.

Time(Min)	Total Time(Min)	RPM	N (Cycles)	ΔN [Cycles]	ΔP [N]	a [mm]	Δa[mm]	da/dN (mm/cycle)	ΔK ($MNm^{-3/2}$)
0	0	1498	0	0	1201	2	0	0.00E+00	0.00E+00
74	74	1498	110,852	110,852	1201	2.35	0.35	3.16E-06	1.84E-01
40	114	1498	170,772	59,920	1201	2.7	0.35	5.84E-06	1.84E-01
3	117	1498	175,266	4,494	1201	3.35	0.65	1.45E-04	2.51E-01
1.5	118.5	1498	177,513	2,247	1201	4.9	1.55	6.90E-04	3.87E-01
1	119.5	1498	179,011	1,498	1201	7.5	2.60	1.74E-03	5.02E-01
0.5	120	1498	179,760	749	1201	11.7	4.20	5.61E-03	6.37E-01
1	121	1498	181,258	1,498	1201	14	2.30	1.54E-03	4.72E-01

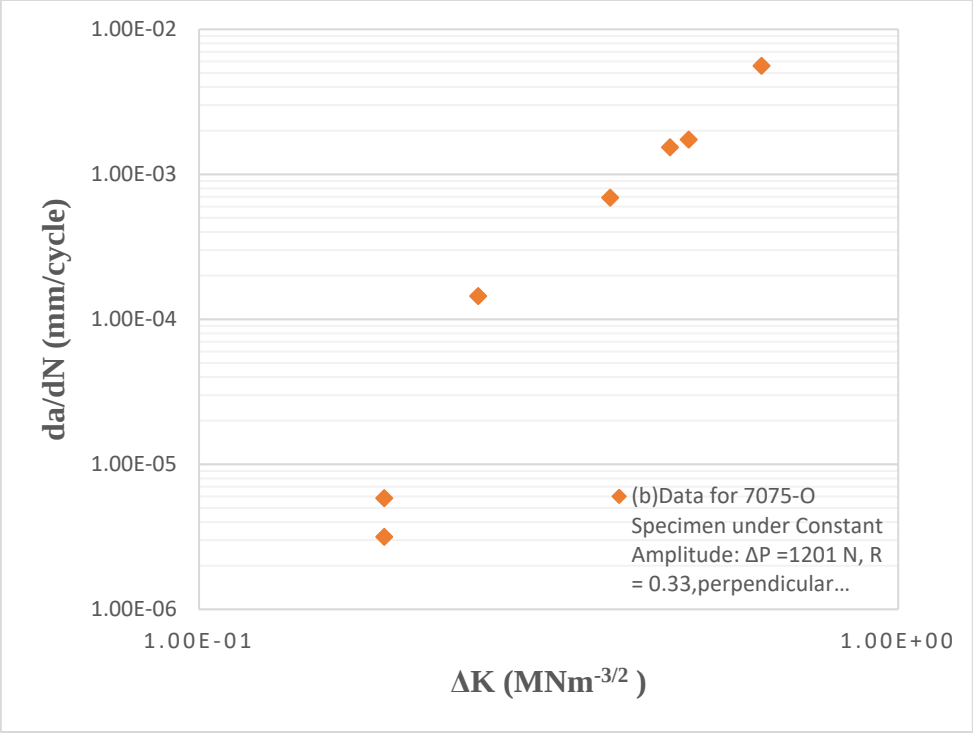

Figure 4.13: FCG of Al 7075-O with perpendicular rivet hole orientation.

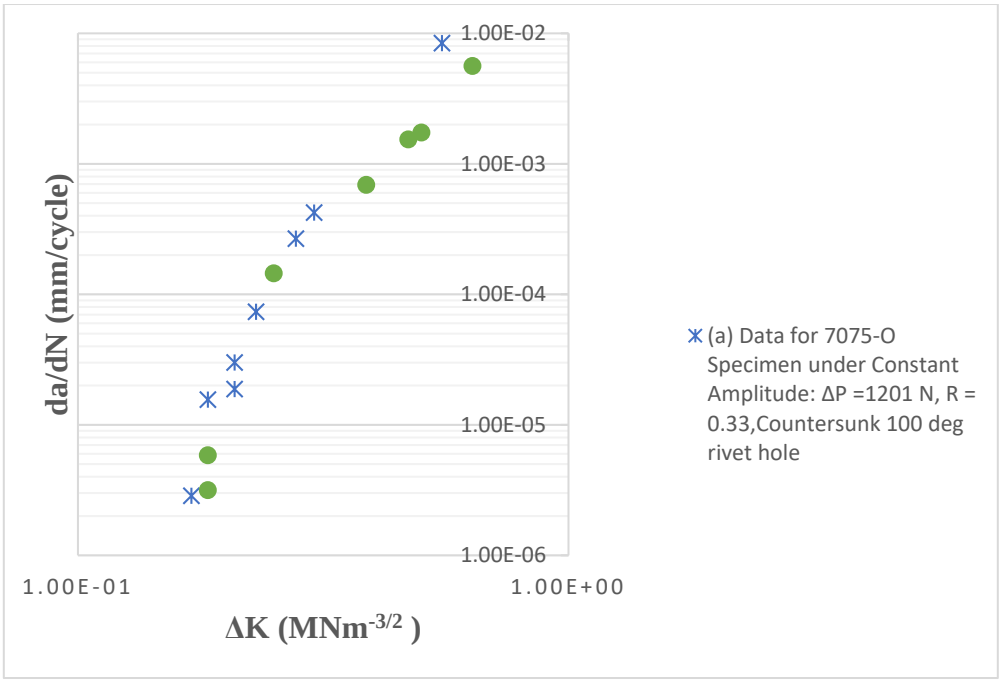

Figure 4.14: Superimposed FCG of Al 7075-O with countersunk and perpendicular rivet hole orientation.

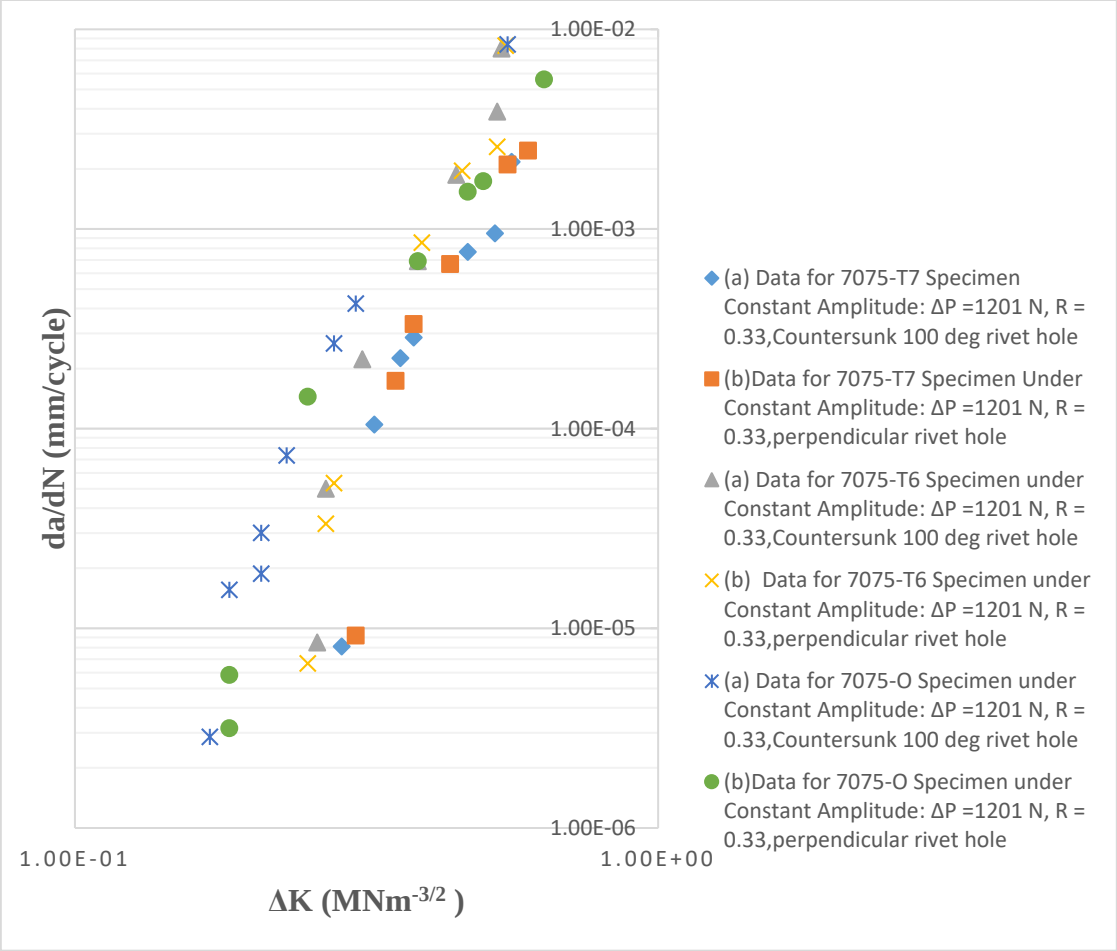

Figure 4.15: Superimposed FCG of Al 7075-O/T6/T7 with countersunk and perpendicular rivet hole orientation.

As witnessed in Figure 4.11 & Figure 4.12, the rivet hole geometry has a negligible impact on the fatigue lives of the countersunk and perpendicular rivet hole for Al alloy 7075-O.

The superimposed fatigue cracks growth graph for Al alloy 7075-O is depicted in Figure 4.13, showing the fatigue growth of the countersunk following the curve for perpendicular rivet hole orientation.

Figure 4.8 & Figure 4.9 depict fatigue crack growth for Al alloy 7075-T6 under countersunk and perpendicular rivet hole orientation. The two showed insignificant deviation from their FCG.

As shown in Figure 4.5 and Figure 4.6, the rivet hole geometry has a small impact on the fatigue lives of the countersunk and perpendicular rivet hole for Al alloy 7075-T7. Its superimposed graph, Figure 4.7, depicts the growth graph of countersunk and perpendicular are in line with each other. A superimposed graph of all three heat-treated conditions with different hole geometry showed that Al alloy 7075-T7 has higher and lower ΔK_{th} than Al alloy 7075-T6 and Al alloy 7075-O. Al alloy 7075-T6 is the bandwidth between Al alloy 7075-T7 and Al alloy 7075-T6, which agrees with the results found by other scholars (Imam et al., 2015b; Leng et al., 2018). Specimen geometry used to study hole geometry did not provide enough data to determine the Paris region.

4.4 Fatigue Fractographic Analysis

4.4.1 Impact of Heat Treatment on Crack Path of AL7075

Figure 4.16: Crack path for Al alloy 7075-O.

Figure 4.17: Crack path for Al alloy 7075-T6.

Figure 4.18: Crack path for Al alloy 7075-T7.

The typical crack paths in the Al alloy 7075-O, 7075-T6, and 7075-T7 specimens are shown in Figure 4.15, Figure 4.16, and Figure 4.17. In the Al7075-O sample, the crack path associated with fatigue is Trans granular, sharply angled and tortuous, deflecting, and branching, as shown in Figure 4-15. Most deflections, including zigzagging, are observed to have transpired at grain borders and precipitate particles. Measured deflection angles are about 30°, 45°, and 70°. Al alloy 7075-T6 and 7075-T7 samples exhibit Trans granular and nearly straight, linear with no deflection fatigue crack path as depicted in Figure 4.16 and Figure 4.17.

The failure analysis for the fracture surface is Trans granular in all subjects with proof of slip steps, ledges, and facets. Such facets are mainly enunciated in the Al alloy 7075-O form and have an appearance aspect of crystallographic fatigue surfaces (Fakioglu et al., 2013b; Yang et al., 2017b). Figure 4.15, Figure 4.16, and Figure 4.17 show crack profiles for the three conditions depicting Al alloy 7075-O structures with rougher or more tortuous nature of the crack path. In distinction with Al alloy, 7075-0 fractures displaying a zigzag appearance, Al alloy 7075-T6 and 7075-T7 are predominately linear, outlying fewer crack deflections crack paths.

4.4.2 Fatigue Fracture Morphology Observation of Al Alloy 7075-O/T6/T7

4.4.2.1 Fatigue Crack Initiation

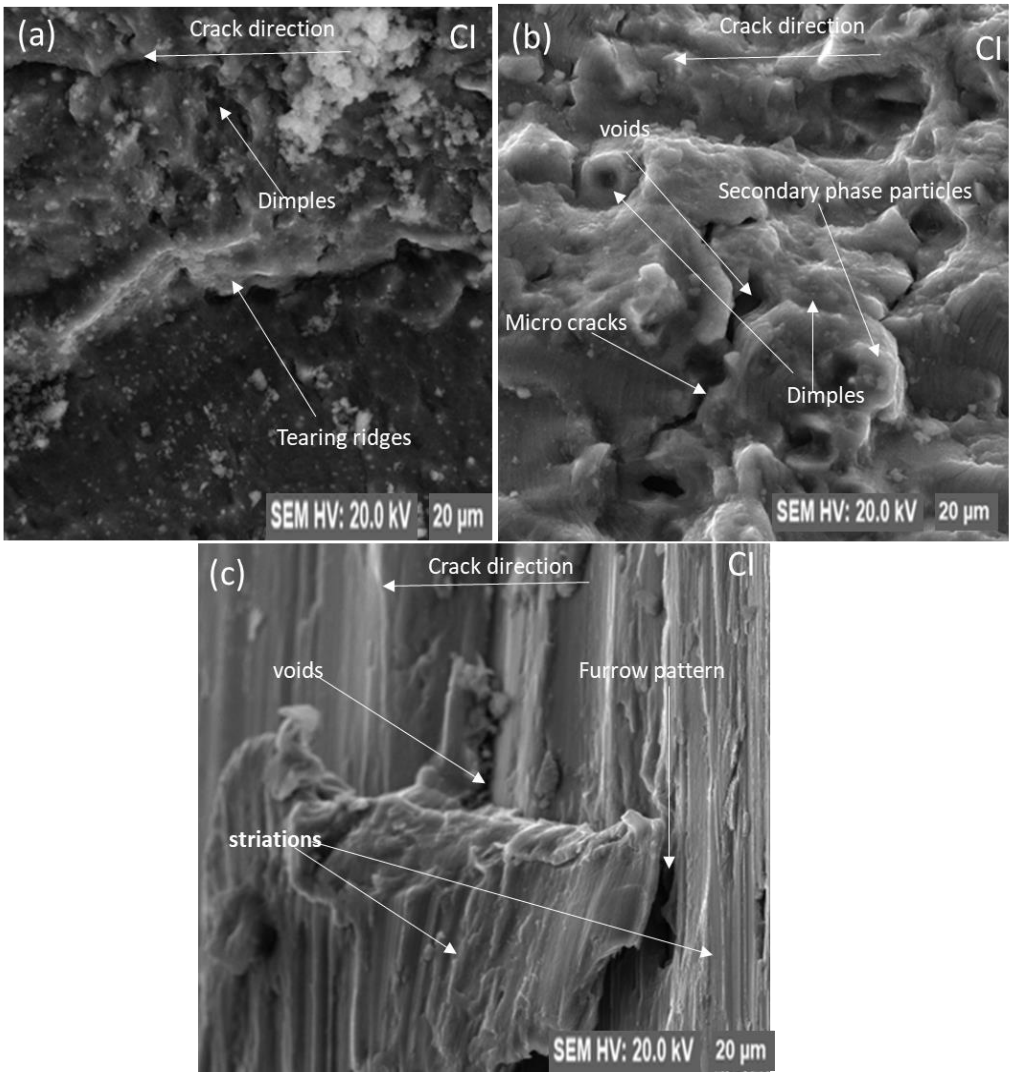

Figure 4.19: Fatigue-fractured surface morphology of the fatigue initiation of (a) Al alloy 7075-O, (b) Al alloy 7075-T6, (c) Al alloy 7075-T7.

The fatigue fracture surfaces of tests Al alloy 7075-O, 7075-T6, and 7075-T7 under R=0.33 were scrutinized by scanning electron microscopy (SEM). Figure 4.18 illustrates the all-around fracture surfaces and the fatigue crack initiation. The failure analysis for the fracture surfaces consists of fatigue crack initiation regions for the three heat-treated conditions.

As shown in the studies (Yang et al., 2017b; Fakioglu et al., 2013b), the stress concentration of the surface or subsurface commonly initiates fatigue crack for the samples without internal tissue flaws. Several factors lead to stress concentration, such as the flaws (the minute porosity and the surface scratches) and the impurities that develop when it undergoes smelting and heat treatment. In these tests, the impurity phase particles separated from the matrix under the cyclic loading were where the crack initiated. The compositions of those particles are high silicon compounds. (S. Y. Chen et al., 2014; Clemens et al., 2017) concluded that Particles in the impurity phase have a different Young's modulus, Poisson's ratio, and strength than the alloy matrix.

Under cyclic loading, the impurity phase particles slide and detach from the high silicon phase matrix, or the rich iron phase fractures itself, leading to a crack at the weak end of the critical zone, which propagates inward along the perpendicular loading direction. The propagation rate is low since the surfaces where fatigue cracks start to form are exposed to air. The repeated open and shut cyclic loading polishes and smoothens the fracture surface. As can be seen in Figure 4.18, cracks that have started in various planes eventually collide during propagation, leaving behind a series of radial steps.

4.4.2.2 Fatigue Crack Propagation

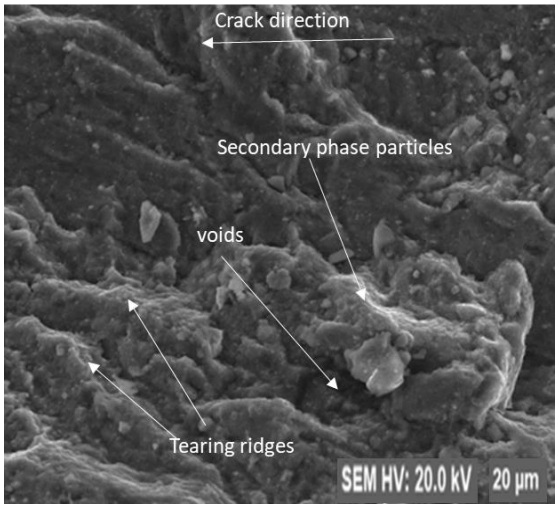

Figure 4.20: Fast fatigue crack propagation morphology of Al alloy 7075-O.

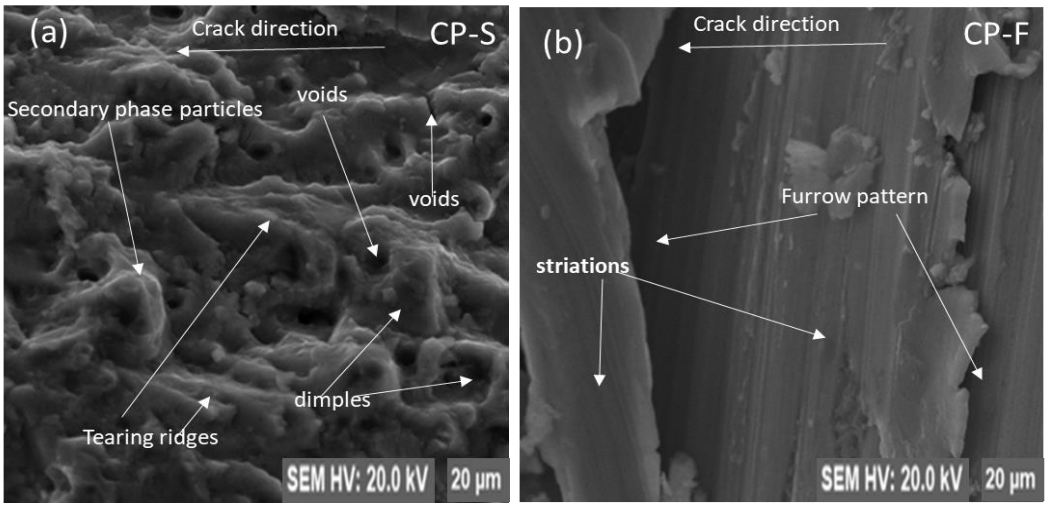

Figure 4.21: Fatigue crack propagation morphology of Al alloy 7075-T6, (a) slow crack propagation, (b) fast crack propagation.

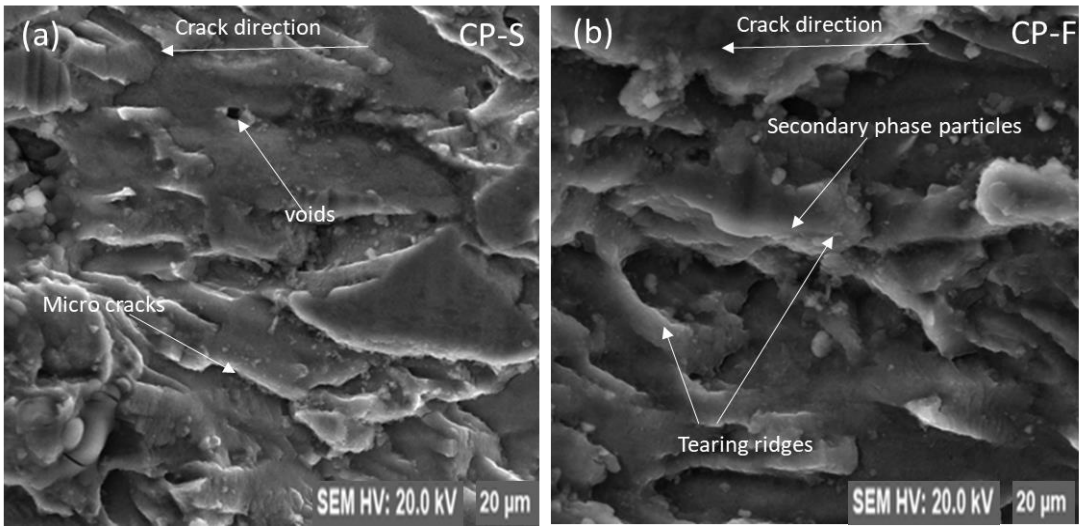

Figure 4.22: Fatigue crack propagation morphology of Al alloy 7075-T7, (a) slow crack propagation, (b) fast crack propagation.

Scanning electron micrographs of the locations where a fatigue fracture propagated at a stress ratio of 0.33 and a constant amplitude are depicted in Figures 4.19, 4.20, and 4.21. Figures 4.20 (a) and 4.21 describe the initial stage of fatigue crack propagation, which entails crack initiation and the subsequent propagation of cracks along the slip band's primary slip plane to the metal's interior by the pure shear manner (a). Figures 4.19, 4.20 (b), and 4.21 show the crack propagating a predetermined length before changing directions, the crack propagating in a direction perpendicular to the stress, and the onset of the second phase of fatigue crack propagation (b).

Fractography of aluminium alloy 7075 aged at different temperatures (O/T6/T7) (Figure 4.20 (a) and Figure 4.21 (a)) reveals a quasi-cleavage fracture plane and a parallel zigzag area. Crack propagation is halted, and substantial deformation occurs at crack boundaries after being aged to various Temper O, T6, and T7, leading to the combination of cracks by ripping them apart and creating a lamella fracture surface. Test Al alloy 7075-0 has the least extensive region of the quasi-cleavage fracture plane, whereas test Al alloy 7075-T7 has the

greatest. Grain size, precipitated phase type, size, and disbandment all have a role in determining the shape and size of the quasi-cleavage fracture plane, and the larger the grain, the more widespread the fracture plane.

Fatigue strips are present during the second stage of fatigue crack propagation. In figures 4.19, 4.20 (b), and 4.21, each strip represents a stress cycle and pinpoints the location of a crack tip during that cycle (b). Test Al Alloys 7075-O, 7075-T6, and 7075-T7 have typical widths of 0.28 µm, 0.68 µm, and 0.36 µm, respectively. Some secondary micro-cracks run parallel to the strips on the fatigue crack propagation surfaces. Particles in the second stage impede the crack's progress and change its direction of travel, yet the crack continues to spread after navigating around it.

The desquamation of the second-stage particles from the matrix causes the holes to be left behind after cyclic loading. The particles in the second stage have a diameter of 2-3mm (as measured by the holes' size), negatively affecting high cycle fatigue performance. Particles are dispersed in the matrix at a nanoscale-precipitated stage, which benefits high-cycle fatigue performance.

4.4.2.3 Final Fracture

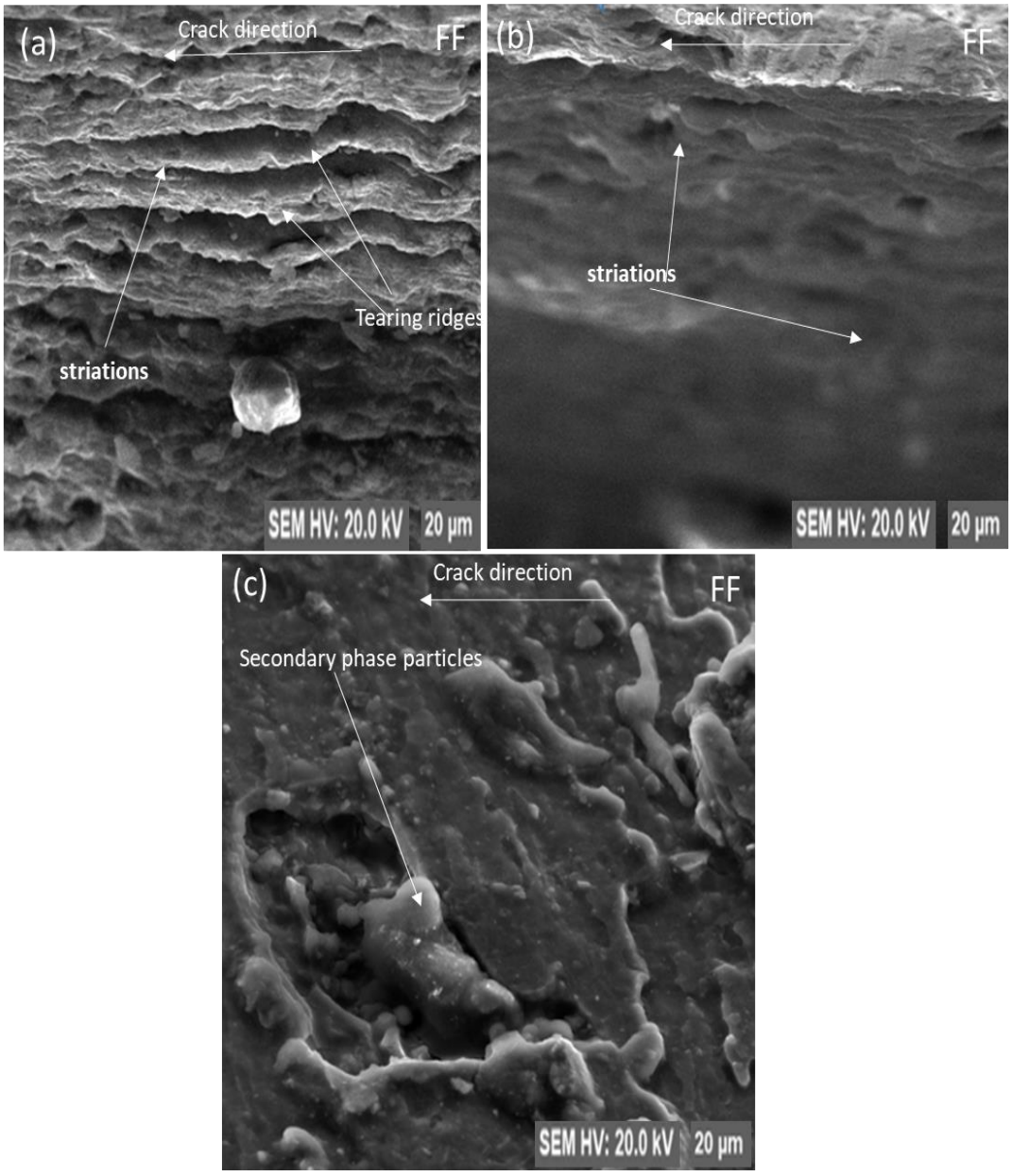

Figure 4.23: Final fatigue-fractured surface morphology of (a) Al alloy 7075-O, (b) Al alloy 7075-T6, (c) Al alloy 7075-T7.

The material cannot handle the cyclic loading when the crack length comes to the critical length, unstable crack propagation is experienced, and eventually, there is a transient material fracture. Final fracture SEM images are displayed in figure 4.22.

In Figure 4.22 (a), (b), and (c), we can see that the final fracture surfaces are rough and mixed ductile-brittle fractures with multiple ripping ridges (c). Test Al alloy 7075-O has the smallest dimple size and smallest dimple size number. According to the results, the dimple size and depth of Al alloy 7075 gradually improved from Al alloy 7075-O to Al alloy 7075-T6 and Al alloy 7075-T7. The particles in the precipitated stage are highly correlated with the number of dimples. The more pronounced the dimples, the better and finer the precipitated stage particles. It can be inferred that the more Al alloy 7075 is heat-treated, the more finely predicated phase particles occur.

4.4.3 Fractographic Analysis of Different Hole Orientations

4.4.3.1 Fatigue Crack Initiation to Study Hole Geometry

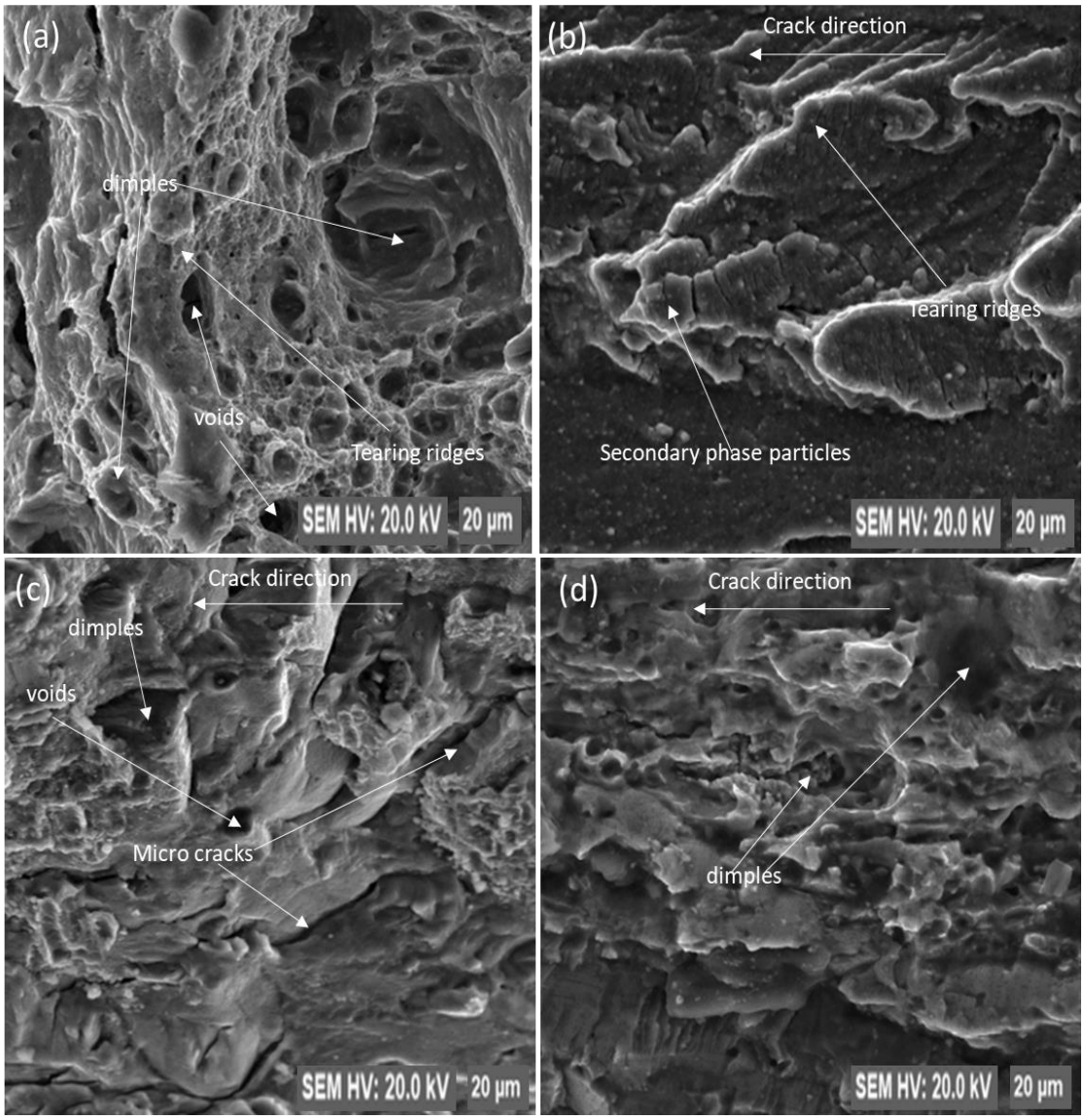

Figure 4.24: Fatigue crack initiation morphology of (a) Al alloy 7075-O countersunk rivet hole, (b) Al alloy 7075-O perpendicular rivet hole, (c) Al alloy 7075-T6 countersunk rivet hole, (d) Al alloy 7075-T6 perpendicular rivet hole.

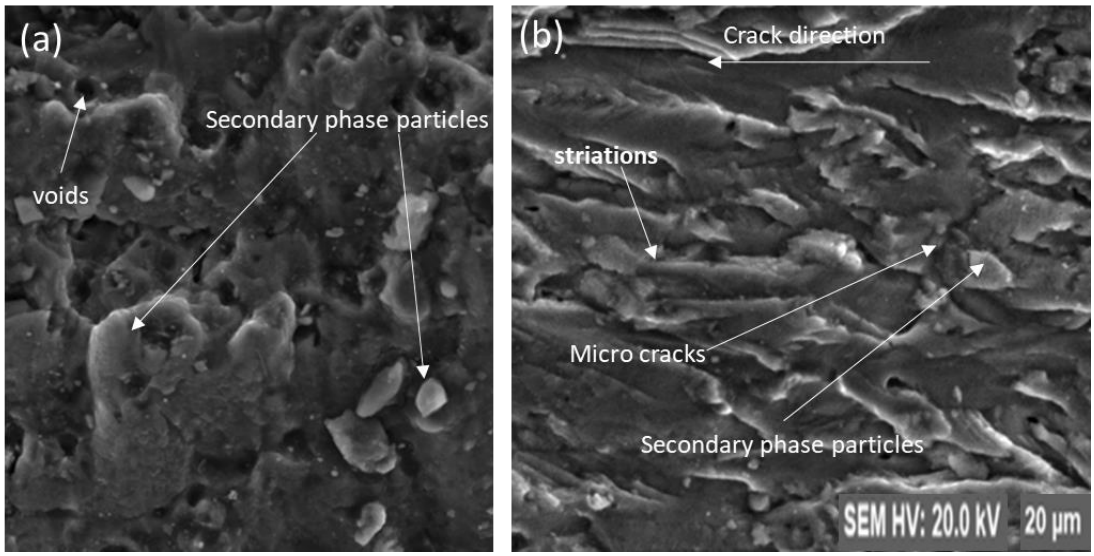

Figure 4.25: Fatigue crack initiation morphology of Al alloy 7075-T7, (a) countersunk rivet hole, (b) perpendicular rivet hole.

The SEM was used to look at the fracture's surface. Figure 4.23 and Figure 4.24 show specimens examined in the air displaying crystallographic faces characteristic of stage I growth. The countersink of a chamfered hole is the origin of fatigue cracking (after initiation on the other side, a crack is noticed propagating along the countersink after initiation on the opposite side in all cases).

The occurrence of some crystallographic facets that are expected during stage I growth does not alter the fact that crack initiation is typically Trans granular. Microscopic cracks link pits together beneath the surface of the fracture. Straight-hole and chamfer-hole samples exhibit micro-cracks originating from the cladding and/or the cladding/core metal interaction. The fracture surfaces are analyzed by scanning electron microscopy (SEM). Figure 4.23 and Figure 4.24 show crystallographic faces characteristic of stage I growth in the specimen.

4.4.3.2 Fatigue Crack Propagation to Study Hole Geometry

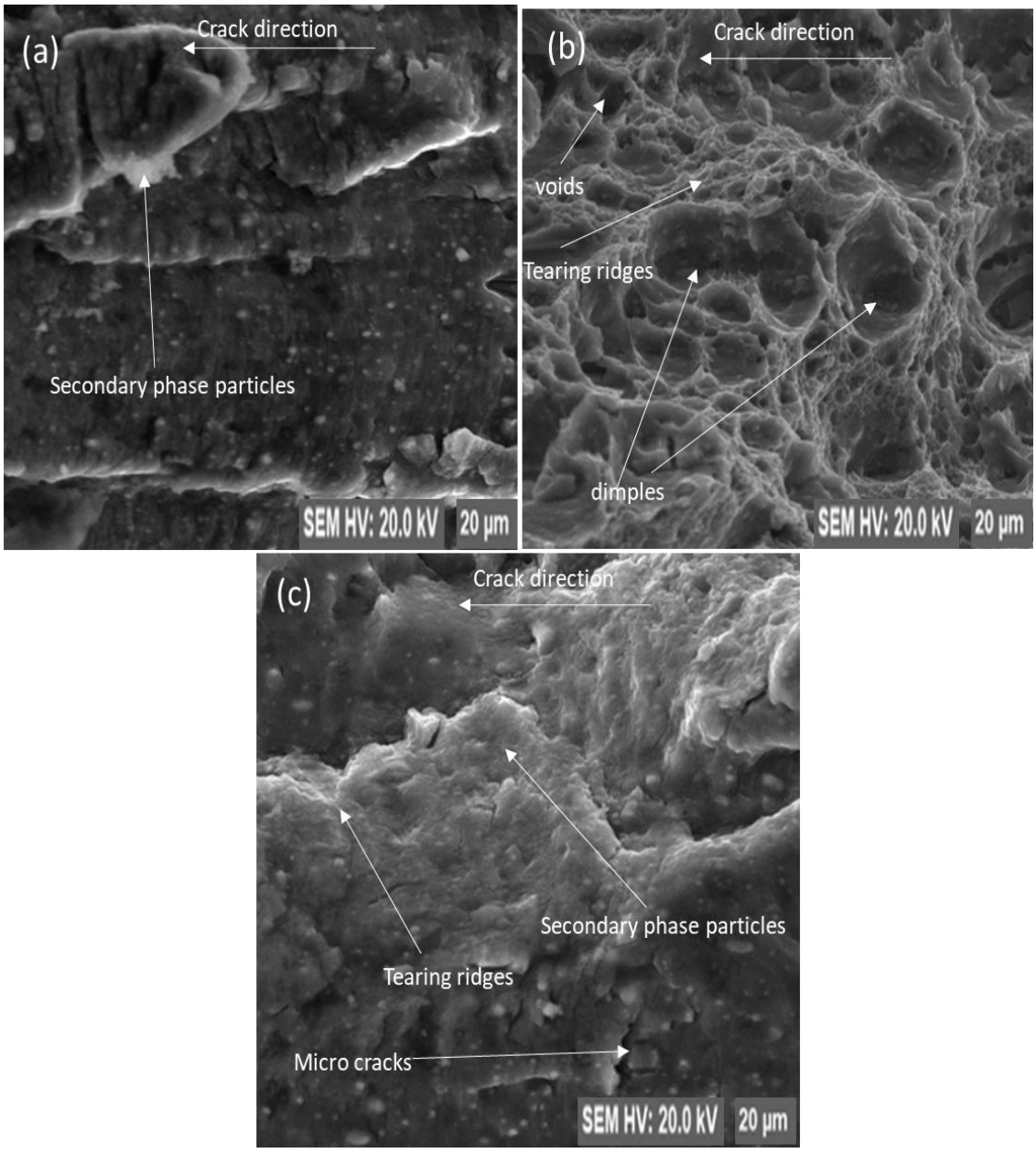

Figure 4.26: Fatigue crack propagation morphology of Al alloy 7075-O, (a) CPF-countersunk rivet hole, (b) CPS- perpendicular rivet hole, (c) CPF - perpendicular rivet hole.

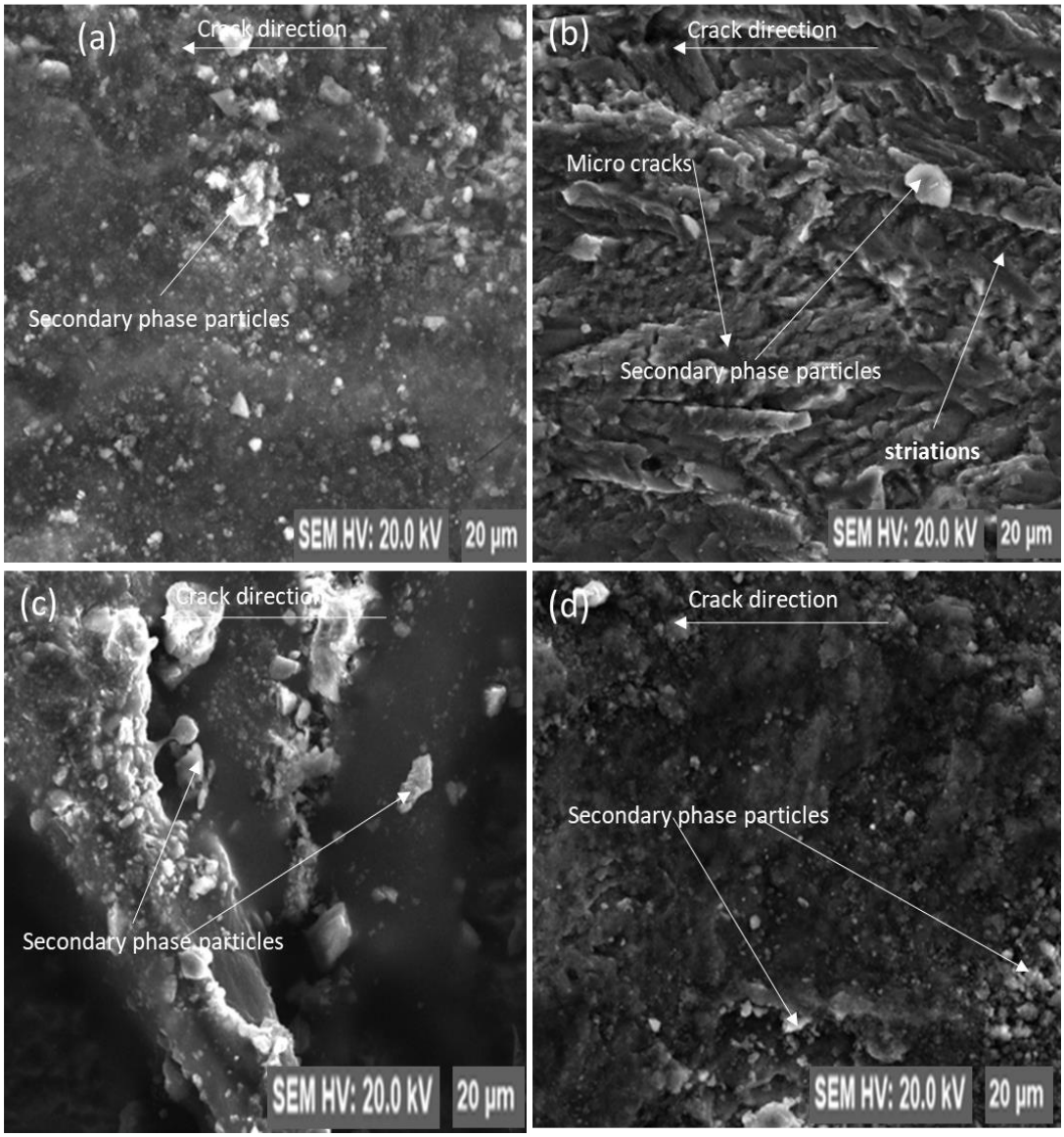

Figure 4.27: Fatigue crack propagation morphology of Al alloy 7075-T6, (a) CPS - countersunk rivet hole, (b) CPF -countersunk rivet hole, (c) CPS –perpendicular rivet hole, (d) CPF - perpendicular rivet hole.

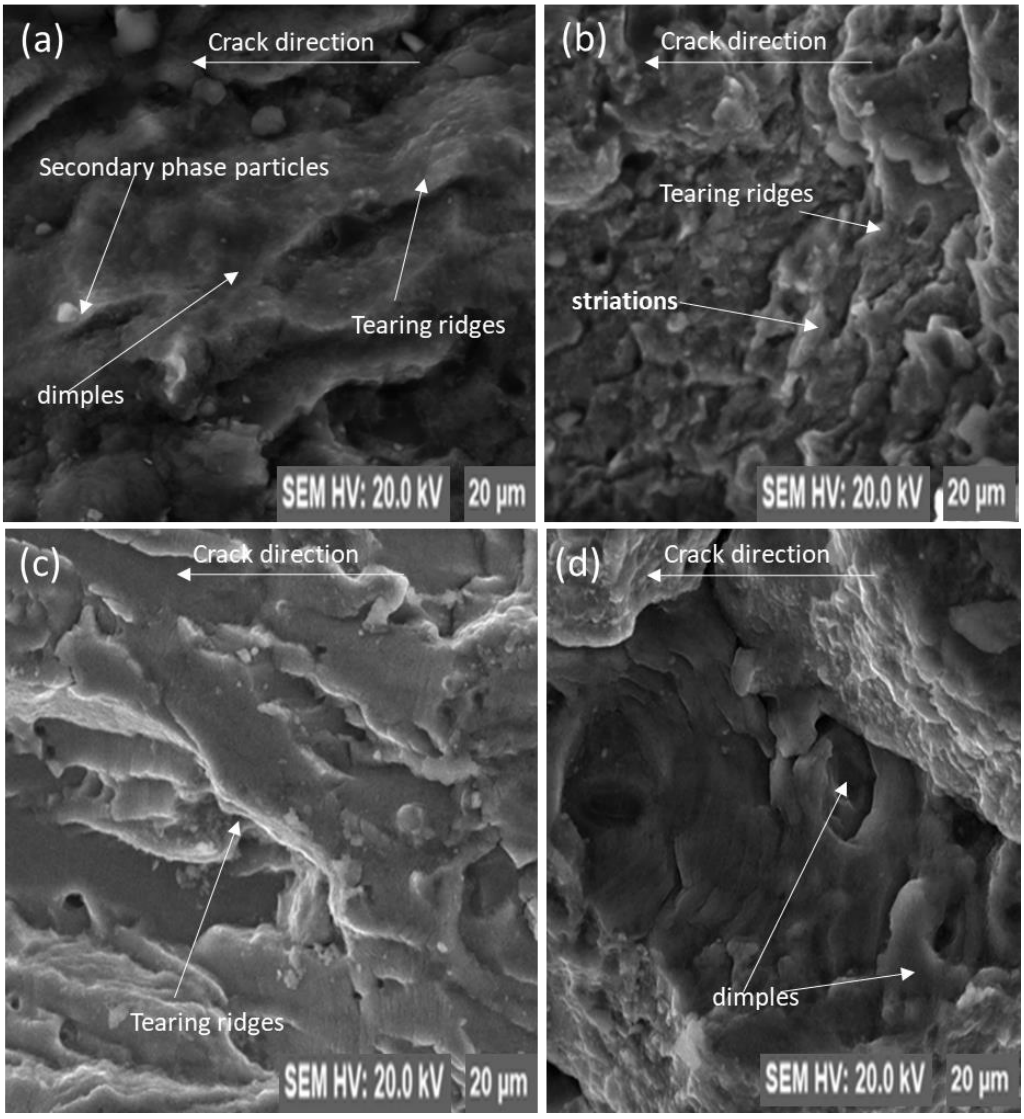

Figure 4.28: Fatigue crack propagation morphology of Al alloy 7075-T7, (a) CPS - countersunk rivet hole, (b) CPF - countersunk rivet hole, (c) CPS – perpendicular rivet hole, (d) CPF - perpendicular rivet hole.

A significant disparity is noticeable in fractographic attributes between the Al alloy 7075-O, 7075-T6, and 7075-T7 conditions and an insignificant difference between the countersunk and perpendicular rivet hole geometry. The typical fractographs of the Al alloy 7075-O, 7075-T6, and 7075-T7 specimens of stress ratios 0.33 are shown for two different rivet hole geometry (countersunk and perpendicular).

For slow crack propagation fatigue crack growth rates, fast crack propagation fatigue crack growth rates, in Figure 4.25 (b), Figure 4.26 (a), Figure 4.26 (c), Figure 4.27 (a), Figure 4.27 (c), slow crack propagation. Figure 4.25 (a), Figure 4.25 (c), Figure 4.26 (c), Figure 4.26 (d), Figure 4.27 (c), and Figure 4.27 (d) for fast crack propagation. More increased ΔK makes Crack propagation is entirely transgranular. There is clear visibility of beach marks at the base of a dimple that exists as a constituent particle, showing brittle behaviour.

A faceted fatigue crack growth depicts the Al alloy 7075-O state. The facets are constituted on crystallographic planes, their direction shifts from grain to grain, and the crack surface is relatively rough. They are compatible with a predominantly planar slip mode, which happens when the precipitates are shearable. The crack surface of the Al alloy 7075-T7 sample is relatively flat, displaying some regions without features, patches of faint striations, and dimples.

4.4.3.3 Final Fracture to Study Hole Geometry

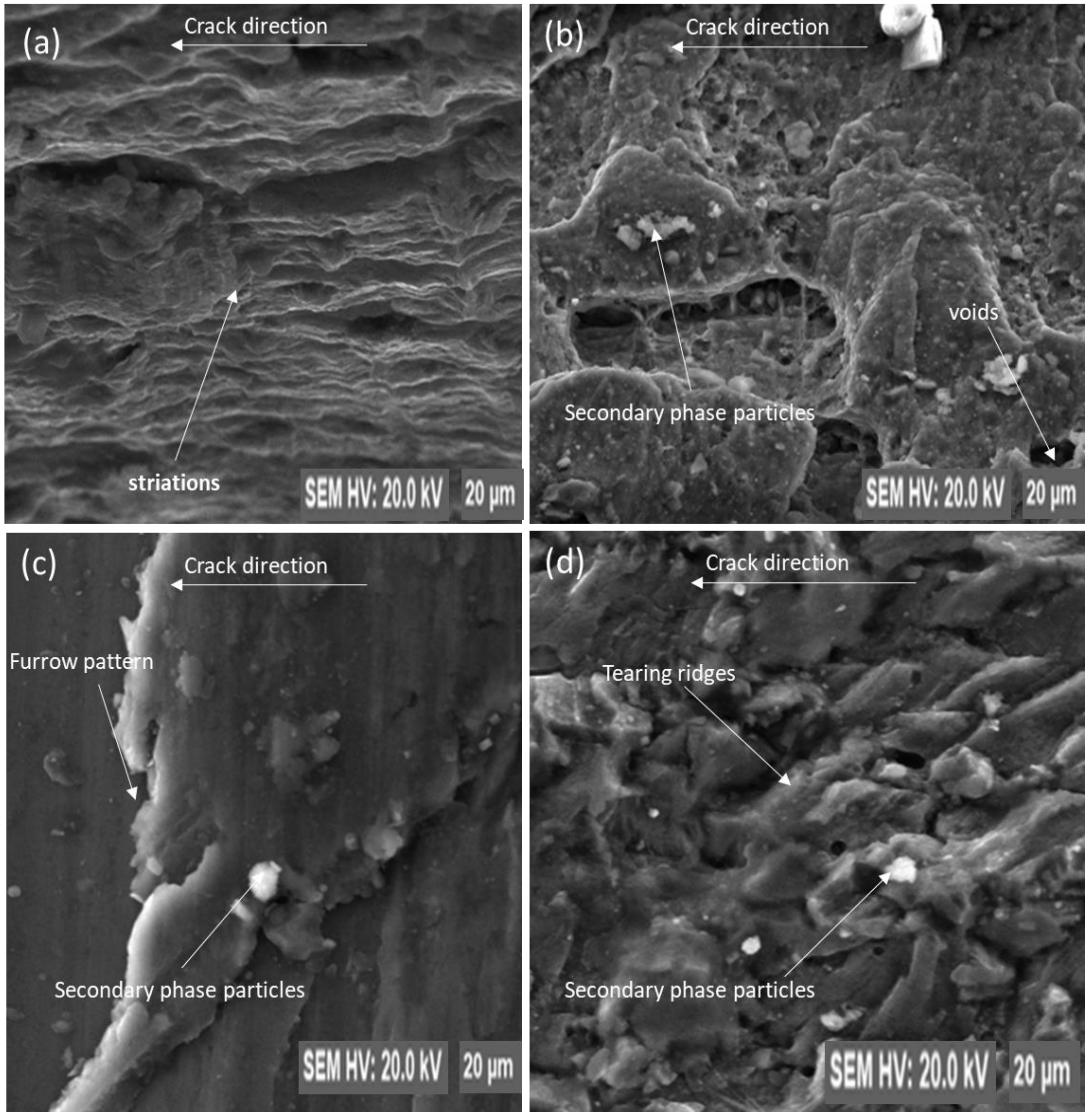

Figure 4.29: Final fatigue fracture morphology of Al alloy, (a)7075-O countersunk rivet hole,(b) 7075-O perpendicular rivet hole, (c)7075-T6 countersunk rivet hole, (d)7075-T6 perpendicular rivet hole.

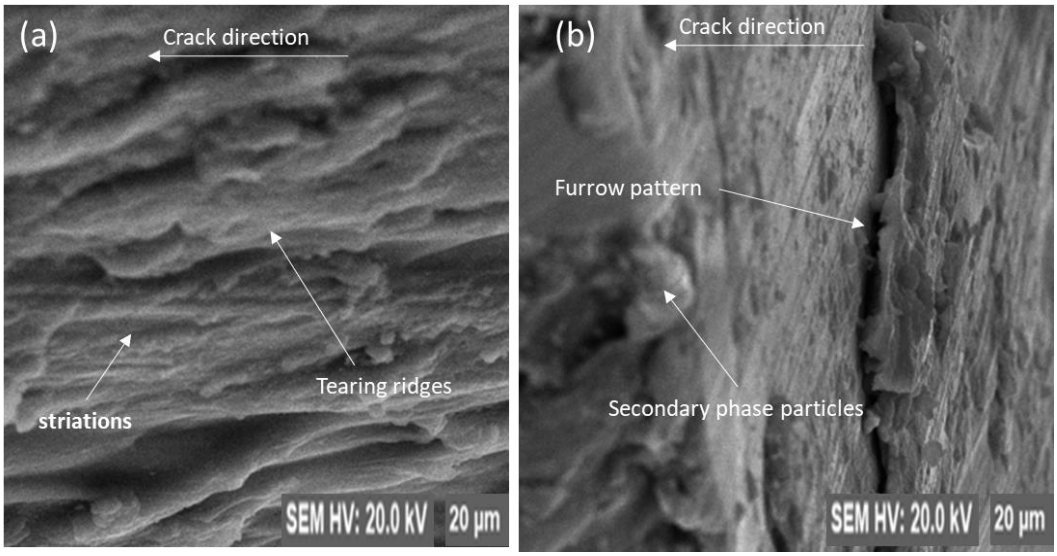

Figure 4.30: Final fatigue fracture morphology of Al alloy 7075-T7, (a) countersunk rivet hole, (b) perpendicular rivet hole.

A substantial contrast is visible in fractographic characteristics between the Al alloy 7075-O, 7075-T6, and 7075-T7 conditions and an insignificant difference between the countersunk and perpendicular rivet hole geometry for the same temper condition. The typical fractographs of the Al alloy 7075-O, 7075-T6, and 7075-T7 specimens of stress ratios 0.33 are shown for two different rivet hole geometry (countersunk and perpendicular). For crack initiation fatigue crack growth rates, slow crack propagation fatigue crack growth rates. Fast crack propagation fatigue cracks growth rates; final fatigue fracture fatigue cracks growth rates, in Figures 4.28 and 4.29. A faceted fatigue crack growth depicts the Al alloy 7075-O state. The facets are constituted on crystallographic planes, their direction transitions from grain to grain, and the crack surface is relatively rough. They agree with a predominantly planar slip mode, which transpires when the precipitates are shearable. The crack surface of the Al alloy 7075-T7 sample is somewhat flat, showing some regions without features, patches of murky striations, and dimples.

Similar to other aluminium alloys, the present results on metallurgy Al alloy 7075 demonstrate that Al alloy 7075-T7 microstructures have superior near-threshold fatigue crack propagation resistance to Al alloy 7075-T6 and Al alloy 7075-O microstructures (Fakioglu et al., 2013b, De et al., 2009).

4.5 Mitigating Considerations to Microstructural Crack Growth and Propagation of Al 7075-T6

The following considerations: (1) design considerations, (2) considerations during service that involve recording, inspections, alterations, and repair considerations, (3) pursuit of structural reliability, and (4) engineering viewpoints of safe life and fail-safe are paramount when considering mitigating actions to microstructural crack growth and propagation of Al 7075.

4.5.1 Design Considerations

Combating weariness in design can be difficult. Structural design alternatives can be broken down into categories like layout, design of fatigue essential notches in the structure, joints, material choice, surface treatments, and manufacturing factors. The operator of the structure, as well as external elements like air turbulence, sea waves, road roughness, and other usage situations, play a role in the load spectra during service conditions, which is another crucial part. During the design process, it is essential to think about how to address any potential tiredness issues.

The purpose of fatigue-resistant design is to achieve fatigue features that are deemed acceptable; however, adequate fatigue features may be defined differently depending on the type of structure being designed. There are three types of structures taken into account here:

I those where fatigue failures are unacceptable; (ii) those where fatigue cracks are possible, but the risk of complete failure must be maintained at a very low level; and (iii) those where crack initiation and growth until failure after a reasonable lifetime are acceptable.

Designing against fatigue includes avoiding high-stress concentrations and selecting fatigue-resistant materials, considering structural stiffness divergences load flow within the structure, preventing eccentricities, and applying surface treatments. Joints have their own unique set of difficulties. There is a lot of qualitative knowledge but not a lot of quantitative understanding concerning how fatigue cracks start and spread in metals. While it is possible to use quantitative and qualitative approaches to forecast fatigue parameters, it is recommended that experimental validations be undertaken to ensure accuracy.

Predictions of a structure's fatigue characteristics should be verified experimentally using service-simulation fatigue trials. The applied load history and fatigue-critical attributes of the structure must be realistic of the actual problem. Assessed load spectra, fatigue life forecasts, fatigue limit and crack growth, design stress levels, and supporting research stress levels can all benefit from applying safety factors. Premature fatigue failures' economic and safety effects should be considered while selecting safety criteria. Preventing corrosion is the primary difficulty in dealing with corrosive conditions. Safety concerns and realistic research should be explored if this is impossible.

Mechanisms for dealing with fatigue in structures are quite effective at present. The accuracy of FE analyses of stress and load distributions in a structure is high. The most difficult questions can be answered using experimental equipment for real-world fatigue tests.

In the end, load history measuring techniques can provide in-depth information about past load histories. Current worries about fatigue in design can be addressed using these methods.

Damage Accumulating over Time: Many experiments are conducted in the lab with constant stress (or strain) amplitude loading to learn more about materials and the effects of different design elements. While in service, most structural components will likely be subjected to more complex loading.

There are two possible solutions to the fundamental problem of handling this intricate issue. A "theory of cumulative damage" can be pursued, which will allow estimation (using S-N data gathered under simple laboratory tests) of the behaviour of the structural part under any given series of more complex variable amplitude loadings. In addition, it is possible to create a spectral loading model of service conditions and have all laboratory tests conducted under that load spectrum. The following categories of materials are vulnerable to cumulative fatigue damage: Materials Reaction (2). In the case of a crack, the crack will spread (3). Repercussions on the environment, and (4). They are transferring the load.

4.5.1.1 Factors in the Fatigue Behavior of Components

Since it is difficult to know whether the shape of the features in a component and the coupon being tested are the same, using design data gleaned from fatigue tests on small coupons is limiting.

This section elaborates on the material characteristics, fabrication factors, stress and environmental factors, and failure criteria that contribute to these unknowns. Considerations unique to the materials themselves: fatigue behaviour in metallurgical materials is highly nuanced and not usually immediately apparent, so even little changes can significantly affect

them. Although fatigue information may be available for a specific lot, traditional requirements do not ensure that the material purchased for a project will have the same level of fatigue resistance. Therefore, one should not consider the information contained in books entirely representative.

Factors affecting fatigue strength include the material's metallurgical structure, residual stresses, and surface state. These may have values that vary widely from those found in analyzed coupons, individually or across the board. In the absence of information about the nature and degree of differences, it is impossible to accurately predict a component's fatigue strength from data transmitted from coupon trials.

Complexity exists in the metallurgical properties used to create fatigue predictions for components using data collected from coupons. They exhibit varying degrees of variation from one alloy system to the next. What follows is possible for a large casting, forging, or extrusion to have varying metallurgical phases (grain size and direction, inclusions, and in homogeneities) in different areas. In some cases, evidence may be found by a thorough metallurgical analysis of a component. Such an analysis may be prohibitively expensive, time-consuming, or inconclusive in many other contexts. Therefore, it is recommended to check the actual component.

Residual stresses in a component might be caused by heat treatment or manufacture. Because coupons are sometimes free from residual pressures, this may provide additional differences between the element and a coupon. Coupons of the material undergo meticulous surface state management. The smoothness, working of surface layers, and residual stresses of surface finishes on different complicated items are rarely equal. Surface state identification of a component and a material examination coupon might be challenging or impossible

depending on the component's and material's nature. It has also been suggested that weariness is significantly affected by body size. Fatigue strength (especially in bending) of large monolithic constructions is drastically lower than that of smaller test coupons. A number of these questions might have statistical solutions. The effects of variations in surface quality and residual stress may be taken into account in some findings. This should always make us more wary of extrapolating from limited data to larger systems.

Factors in Fabrication: Shop fabrication of genuine parts typically involves elements that cannot be reproduced while creating material test coupons. Conscious machining and a high-quality final product are two examples. Careful attention and thorough investigation should be able to eliminate anomalies in theory. However, some details might be technically illogical or impossible to replicate. The fatigue strength of a product made via forging, extruding, punching, or any of a variety of similar processes may be affected by factors that are neither predictable nor amenable to quantitative assessment.

The fatigue strength of a given component made from a given material may be significantly affected by the specific procedures of a given production shop.

The heat treatment, grinding, rolling, shot peening, and surface (such as carburizing or nitriding for steels) processes, among others, can have a significant impact. Unfortunately, it is not always possible to link quantitatively relevant information on such aspects to a given circumstance. As a result, material histories rarely account for the cumulative effects of many production methods. The details of the joints in fabrication or assembly are crucial. Welded, bolted, riveted, and adhesive joints are used in aeroplane parts. These add variables to the fatigue equation that are not considered when testing material samples in a lab.

Despite extensive studies on the methods of stress investigation, it is still only possible to test a small sample of actual parts, leading to an estimate that is not precise enough for predicting fatigue behaviour. In contrast to the simple stress distribution planned in constructing a material examination coupon, significant genuine components feature several stress routes. Simple examples include a tensioned lap joint that has been riveted. It is accepted in engineering that the assumption that each rivet carries the same load is inaccurate. In addition to revealing the theoretically (but not numerically) expected more significant elevated stresses around certain edge rivets, stress coat procedures also show that these are the sites where fatigue cracks originate. Indeed, the results of an inquiry conducted using the well-established elastic-plastic techniques for stress evaluation at this stage could be unrealistic if not all relevant fabrication details are considered. Even if this is possible, the investigation's price tag might be too high compared to what a joint fatigue study would set you back.

Some examples of environmental influences include heat, humidity, fretting, and radiation. Fatigue tests on samples of the materials have helped to sketch out some of these consequences of aging. Quantitative evaluation of such problems is typically not possible in any significant aspect of complexity. Therefore, fatigue tests on material coupons can only provide a rough estimate of the environmental effects on components.

Fracture acceptance criterion: Fatigue tests on material samples have been performed up until recently. There has been a rise in fracture propagation research as of late. Overload on another component may be caused by excessive deformation or cracking; critical in spans of component working demands a slighter than complete fracture.

While it is true that there likely is not a single universal criterion for fatigue failure, the main point of this discussion is that it is not possible to reliably extrapolate from laboratory tests of material coupons to a component's catastrophic failure. Unlike the coupon, the part may have a different fracture initiation and growth timeline. Simple samples scarcely provide a good understanding of cumulative damage under loads of varied amplitude. There is evidence to suggest that in complex structures, stress dispersal may vary with load level to a span that is not obtained in a conventional coupon.

4.5.2 Considerations during Service

During an aircraft's service life, several concerns are appropriate to fatigue, including during different flight and ground handling situations, loads, and environmental parameters are recorded. Another deliberation is a routine inspection for possible developing fatigue damage. Yet another is a reassessment of fatigue resistance after modifications, either in the structure or in mission undertaking.

Fatigue deliberations during service have different likely goals. One is the ongoing appraisal of the reliability of a distinct aircraft, leading to a decision such as replacing a primary structural part or aircraft retirement. Inspection intervals and maintenance necessities can also be adjusted. The overall purpose is to get a service experience that will improve future design and fabrication techniques.

Engineers, maintenance crews, pilots, and operations staff are accountable for these various goals. On top of that, divergences in aircraft structural elements, performance specifications, and operational necessities need extensively distinct processes in recording, inspection, maintenance, and assessment of reliability against fatigue. Therefore, an account of all concerns appropriate to fatigue during service could need a collection of manuals per aircraft

type. The subsequent depicts some guidelines that have been carried out and some aspects to be evaluated.

4.5.2.1 Recording

This entails acquiring and examining an entire narrative of local strains at each fatigue critical site in each aircraft. Records created during service can be scrutinized in many forms and with various goals, such as (1) Determining any notable variations that might be noteworthy. (2) Acquiring data for a typical aircraft regarding load and stress allocation in response to different working circumstances. (3) Furnishing statistical information about the allocation of diverse load and stress situations throughout diverse kinds of service.

4.5.2.2 Inspection

A significant part of a regularly scheduled structural component inspection is noticing developing fatigue damage. This is essential to the fail-safe design strategy. The scheduling technique of inspections is fundamental in the deterrence of fatigue. Government agents that include the FAA for civil aircraft founded on multiple deliberations place the lowest inspection gaps.

4.5.2.3 Alterations and Repair Considerations

Modifications in Structure that entail transformations in structural parts can be made for multiple objectives that involve (1.) When a part is found unsatisfactory in service, this necessitates replacement by an improved design. (2). When there is a need to improve performance or capability for a change in assignment, thus replacement by a new design. (3). When some operational objective is added (4). When there is a need to improve fatigue resistance, it necessitates rework.

Consequences on the fatigue resistance of the part altered and of neighbouring parts that might incur additional loads should be regarded whenever a modification is completed. Similar reflection has not consistently been adequate in the past.

Existing techniques comprise, to an uneven extent, (1) the impact of the modification on fatigue resistance is computed. (2) Changed or added part undergoes Laboratory testing. (3) Aircraft with the alteration undergoes flight-testing. (4) Subsequent inspection techniques and programs are reviewed.

4.5.3 The Pursuit of Reliability

Engineering's overarching goal is to make planes more resilient to breakdowns (due to fatigue or any other cause) during their service lives, regardless of mission. Over the past decade, there has been a lot of focus on the dependability strategy of a system with several parts. Issues affecting the dependability of a complex system in a complex environment are presented in detail in recent articles discussed under the topic title "Aerospace Reliability and Maintainability."(Wang & Zhou, 2022)

4.5.4 Engineering Viewpoints

With the assumptions uncertainties, this type of calculation furnishes an estimation of the likely service lifetime. An opinion as to whether the wing is crucial for the low load levels or more elevated (but less often happening) loads is also recommended (by deliberation of the load level of the convergence). However, it does not furnish an opinion of dependability in the form of the potential of a wing on a specific aircraft holding lower fatigue strength than the "most probable" weight and facing loads of more rigour than moderate, therefore yielding shortly than others.

Some allowance for the number of sources of uncertainty with respect to dependability must be included in such an investigation. There are two relatively distinct strategies for this condition.

4.5.4.1.1 Safe-Life Evaluations and Scatter Factors

This requires a margin of safety between a component's calculated and/or tested lifetime and the planned service lifetime. This can be achieved by combining full-scale testing under a suitable load spectrum and computational lifetime evaluation. A "scatter factor" clause could be used to define this buffer, which requires the estimated lifespan to be significantly longer than the planned service lifetime. The procuring agent may specify the lowest acceptable dispersion factor.

Numerous distinct methods of investigating load events, calculating fatigue damage, and determining lifetime through full-scale tests. When taking the safe life strategy, you cannot forego the reliance on reliability. Scatter factor margin utilization, conservatively extreme inferences of load distribution, traditional fatigue allowance, product control to reduce variances among seemingly similar structures, and scatter factor margin utilization.

4.5.4.2 The Fail-Safe Approach

Once considered a viable alternative, this approach recognizes the possibility of fatigue cracking but aims to prevent catastrophic events by employing extensive inspection and designs that permit small fissures for safe flight between inspection junctures.

In failsafe design, probabilistic analyses can be performed on a variety of different factors:

1. The time before a crack is discovered is expected to vary depending on inspection accessibility, inspection techniques, inspection equipment, and inspection frequency.

The rate at which cracks expand varies not only with the loads experienced but also with the type of material used, the design (such as "crack stoppers"), and the production method.

3. Crack There is no fixed critical length since the cracked structure's residual strength and the loads encountered after cracking can change. As a result, there is a need for an evaluation of the critical fracture length values, which will inevitably result in some variation.

Even if approaches considering these likelihood components are being devised, current strategies are helpful in their own right. First, it is essential to ensure that a structure with a significant defect (such as a long artificial crack or the complete severance of one load path in a component of deliberate redundancy) can withstand the maximum possible load (or the considerable extreme possible load spectrum) until subsequent inspection and repair.

Regarding reliability against fatigue failure, these two approaches are not equivalent. With proper testing and scatter factor utilization, the uncertainty in safe-life computations is more than sufficient to warrant, for any structure designed on a safe-life base, the addition of any plausible criteria for fail-safe features. While inspection gaps and replacements must be managed in a way that is economically and logistically acceptable, fail-safe designs require suitable safe life features. In addition, a fail-safe design must allow for and depend upon inspection and maintenance to function. This has led to a situation in which modern engineering practices combine the two methods, with one being emphasized over the other depending on the nature of the structure, its required load, the frequency and nature of testing and maintenance, the requirements for acquiring materials, and the economic and logistical climate at the time.

CHAPTER FIVE: CONCLUSIONS AND RECOMMENDATIONS

5.1 Introduction

The chapter summarizes the significant research findings to bring conclusions from the study. Recommendations have also been proposed based on the research findings and conclusions. This will help in enhancing information provision. Suggestions on areas for further research have also been given.

5.2 Conclusions

Based on the study of microstructural cracking of riveted and heat-treated Al alloy 7075-T6 alloy used in aerospace stringer and frames under constant fatigue loading and identifying crack mitigation measures. The following determinations deduced at the end of the experimental study can be reached:

1. The stress intensity factor and maximum stress intensity factor of the Al alloy 7075-T7 were higher than those of the Al alloys 7075-O and T6, indicating that the alloy was more resistant to the formation of threshold fatigue cracks. The fatigue strength was found to change depending on the heat treatment applied to the specimen. The Al 7075-T7 condition-treated specimens showed the maximum fatigue strength, while the Al 7075-O samples showed the lowest.

   The fatigue performance of 7075 aluminium alloy has been enhanced by age treatment. The fatigue performances of aluminium alloy 7075 improve with increasing aging from O to T6 to T7, and the fatigue curves of aluminium alloy 7075 T6 are quite similar to those of aluminium alloy 7075 T7. The crack propagation rates of Al alloy 7075-T7 are less than those of Al alloy 7075-O for a given stress intensity factor, and the rates of Al alloy 7075-T6 are somewhere in the middle. The

Aging temper condition significantly impacts the high cycle fatigue performance. High-cycle fatigue lives are prolonged if heat treatment conditions are improved from O to T6 and T7.

2. Al alloy 7075 did not crack differently depending on the direction of the crack, as was predicted. Both countersunk and perpendicular rivet hole orientations produced identical fatigue performances in 7075 aluminium alloy under temper O. For the same orientations of rivet holes, the aging treatment enhances fatigue performance. For the same rivet hole orientation (100 degrees countersunk or perpendicular), the fatigue performances improve from O to T6 to T7 as the aging condition is increased. Compared to T6 and T7 aluminium, the 7075-aluminum alloy has a shorter lifespan after annealing when the rivet holes are oriented perpendicularly.
3. The specimen's fatigue strength changed after being heated. The Al alloy 7075-O specimens were found to have the weakest fatigue strength, while the Al alloy 7075-T7 specimens recorded the greatest. The fatigue threshold Kth values are more significant, the measured levels of crack closure are lower, and the tortuosity of the fracture path is reduced as the heat treatment progresses from -O to -T6 and -T7, respectively. It was clear from SEM analyses of fatigue-cracked surfaces that micro-cracks that induce fracturing originate in inclusion zones, coarse, secondary-stage particle regions, and micro-structural defect regions.

   a) The microstructure of the Al alloy 7075-O state displayed coherent shearable precipitates and a convoluted, faceted crack path. Microscopically, Al 7075-T7 and Al 7075-T6 exhibit a straight, practically parallel crack course and incoherent, non-shearable precipitates.

b) The threshold fatigue crack development resistance of the Al alloy 7075-O specimen was significantly increased due to the coherent shearable precipitates. In addition to facilitating fracture deflection and branching, these precipitates also decrease the effective stress intensity factor for fatigue crack propagation and slow its progression.

The crack propagation is a ductile-brittle mixed fracture, as evidenced by the fracture morphologies. The crack initiation is at the subsurface impurity particles (containing high silicon and rich iron metal compounds). The zone of quasi-cleavage planes and the breadth of fatigue strips both expand initially and subsequently contract with increasing heat treatment Temper from O to T6 and T7. Maximum values appear at Al alloy 7075-T7; final fracture zones feature dimple characteristics; dimensions get more extensive, and depth evolves deeper with increasing heat treatment Temper from O to T6 to T7.

4. After an acceptable lifetime, fatigue cracks can appear in some structural systems, although there should be little chance of total failure. There is also an interest in the crack initiation life, which must be long enough to ensure a satisfactory service life. A reliable inspection method is required if a total failure would be improper. This has several potential applications, but its primary use is in aeroplane structures. This means that the fracture initiation life and the crack development life are factors to consider.

5.3 Recommendations

5.3.1 Recommendations based on the Results.

1. The study recommends that heat-treated Al7075 be considered during design and repair where fatigue is critical, like aircraft stingers and frames. The study suggests Al7075-T7, with high purity and flawless installation process (without inclusions and flaws such as scratches), be used in aircraft frames and stingers design and repair.
2. The study recommends that aluminium alloys continue to operate over many decades with a high level of assurance when the effect of fatigue on rivet hole geometry and heat treatment on aircraft structures is fully understood via laboratory data.

5.3.2 Areas for future research/studies.

1. The results can be applied to other alloys, like Al-Mg or Al-Cu, based on what was learned about fatigue fracture initiation and propagation in Al alloy 7075 alloys. What role the inter-metallic phases generated play and how much the strength of the Al matrix influences the characteristics is of interest.
2. Consistent amplitude fatigue data from this analysis will be used in future studies to estimate the service life of the complex spectra loading generated and to investigate the effects of the order in which the loads occur.
3. Comparable experimental analyses will be applied to
    a. Other aluminium alloys and materials of interest in further studies.
    b. Various heat-treated and surface-treated alloys (surface roughness or residual surface stresses).
    c. Additional superimposed load sequences.
    d. Environmental effects on aluminium alloys will be studied more in the future.

4. Even laboratory air's water (vapour) content can have corrosive effects. In order to isolate the impact of fatigue life and crack formation from other factors, such as corrosion, a vacuum test is a valuable tool, especially in the highest high cycle fatigue regime.

REFERENCES

Albedah, A., Bouiadjra, B. B., Mohammed, S. M. A. K., & Benyahia, F. (2020a). Fractographic analysis of the overload effect on fatigue crack growth in 2024-T3 and 7075-T6 Al alloys. *International Journal of Minerals, Metallurgy and Materials*, *27*(1), 83–90. https://doi.org/10.1007/s12613-019-1896-4

Albedah, A., Bouiadjra, B. B., Mohammed, S. M. A. K., & Benyahia, F. (2020b). Fractographic analysis of the overload effect on fatigue crack growth in 2024-T3 and 7075-T6 Al alloys. *International Journal of Minerals, Metallurgy and Materials*, *27*(1), 83–90. https://doi.org/10.1007/s12613-019-1896-4

ASTM E647−13. (2014). Standard Test Method for Measurement of Fatigue Crack Growth Rates. *American Society for Testing and Materials*, 1–50. https://doi.org/10.1520/E0647-13A.2

ASTM E8. (2010). ASTM E8/E8M standard test methods for tension testing of metallic materials 1. *Annual Book of ASTM Standards 4*, *C*, 1–27. https://doi.org/10.1520/E0008

Benachour, M., Benachour, N., & Benguediab, M. (2013). *Fatigue Crack Initiation of Al-Alloys " Effect of Heat Treatment Condition ." 2*(11), 2270–2272.

Borrego, L. P., Costa, J. M., Antunes, F. V., & Ferreira, J. M. (2010). Fatigue crack growth in heat-treated aluminium alloys. *Engineering Failure Analysis*, *17*(1), 11–18. https://doi.org/10.1016/j.engfailanal.2008.11.007

Brahami, A., Bouchouicha, B., Zemri, M., & Fajoui, J. (2018). Fatigue crack growth rate, microstructure and mechanical properties of diverse range of aluminium alloy: A comparison. *Mechanics and Mechanical Engineering*, *22*(4), 1453–1462. https://doi.org/10.2478/mme-2018-0113

Cerny, I. (2012). Fatigue crack growth in a 7075 al-alloy with evaluation of overloading effects. *Komunikacie*, *14*(4), 99–105.

Chen, C., & Li, K. (2020). Design and Stress Analysis for Aircraft Structure Repair Beyond Specification. *Lecture Notes in Electrical Engineering*, *622*(2), 253–264. https://doi.org/10.1007/978-981-15-1773-0_19

Chen, S. Y., Chen, K. H., Dong, P. X., Ye, S. P., & Huang, L. P. (2014). Effect of heat treatment on stress corrosion cracking, fracture toughness and strength of 7085 aluminium alloy. *Transactions of Nonferrous Metals Society of China (English Edition)*, *24*(7), 2320–2325. https://doi.org/10.1016/S1003-6326(14)63351-3

Chen, Y. Q., Pan, S. P., Zhou, M. Z., Yi, D. Q., Xu, D. Z., & Xu, Y. F. (2013). Effects of inclusions, grain boundaries and grain orientations on the fatigue crack initiation and propagation behaviour of 2524-T3 Al alloy. *Materials Science and Engineering A*, *580*, 150–158. https://doi.org/10.1016/j.msea.2013.05.053

Cheraghi, S. H. (2008). Effect of variations in the riveting process on the quality of riveted joints. *International Journal of Advanced Manufacturing Technology*, *39*(11–12), 1144–1155. https://doi.org/10.1007/s00170-007-1291-6

Cicero, S., Alvarez, J. A., & Lacalle, R. (2020). *A. Basic Concepts*. 9–20. https://doi.org/10.1090/text/053/02

Cirik, E., & Genel, K. (2008). Effect of anodic oxidation on fatigue performance of 7075-T6 alloy. *Surface and Coatings Technology*, *202*(21), 5190–5201. https://doi.org/10.1016/j.surfcoat.2008.06.049

Clemens, H., Mayer, S., & Scheu, C. (2017). Microstructure and Properties of Engineering Materials. *Neutrons and Synchrotron Radiation in Engineering Materials Science: From Fundamentals to Applications: Second Edition*, 3–20. https://doi.org/10.1002/9783527684489.ch1

De, P. S., Mishra, R. S., & Smith, C. B. (2009). Effect of microstructure on fatigue life and fracture morphology in an aluminium alloy. *Scripta Materialia*, *60*(7), 500–503. https://doi.org/10.1016/j.scriptamat.2008.11.032

Dursun, T., & Soutis, C. (2014). Recent developments in advanced aircraft aluminium alloys. *Materials and Design*, *56*, 862–871. https://doi.org/10.1016/j.matdes.2013.12.002

Fakioglu, A., Özyürek, D., & Yilmaz, R. (2013a). Effects of different heat treatment conditions on fatigue behaviour of AA7075 alloy. *High Temperature Materials and Processes*, *32*(4), 345–351. https://doi.org/10.1515/htmp-2012-0146

Fakioglu, A., Özyürek, D., & Yilmaz, R. (2013b). Effects of different heat treatment conditions on fatigue behaviour of AA7075 alloy. *High Temperature Materials and Processes*, *32*(4), 345–351. https://doi.org/10.1515/htmp-2012-0146

Gasem, Z. M., & Gangloff, R. P. (2000). Effect of temper on environmental fatigue crack propagation in 7000-series aluminium alloys. *Materials Science Forum*, *331*, 1479–1488. https://doi.org/10.4028/www.scientific.net/msf.331-337.1479

Gloria, A., Montanari, R., Richetta, M., & Varone, A. (2019). Alloys for aeronautic applications: State of the art and perspectives. *Metals*, *9*(6), 1–26. https://doi.org/10.3390/met9060662

Hassanifard, S., Adibeig, M. R., Mohammadpour, M., & Varvani-Farahani, A. (2019). The fatigue life of axially loaded clamped rivet-nut joints: Experiments and analyses. *International Journal of Fatigue*, *129*, 105254. https://doi.org/https://doi.org/10.1016/j.ijfatigue.2019.105254

Huda, Z., & Edi, P. (2013). Materials selection in design of structures and engines of supersonic aircrafts: A review. *Materials and Design*, *46*, 552–560. https://doi.org/10.1016/j.matdes.2012.10.001

Imam, M. F. I. A., Rahman, M. S., & Khan, M. Z. H. (2015a). Influence of heat treatment on fatigue and fracture behaviour of aluminium alloy. *Journal of Engineering Science and Technology*, *10*(6), 730–742.

Imam, M. F. I. A., Rahman, M. S., & Khan, M. Z. H. (2015b). Influence of heat treatment on fatigue and fracture behaviour of aluminium alloy. *Journal of Engineering Science and Technology*, *10*(6), 730–742.

Kelly, T. P. M. F. (2020). 済無No Title No Title No Title. In *Angewandte Chemie International Edition, 6(11), 951–952.*

Leng, L., Zhang, Z. J., Duan, Q. Q., Zhang, P., & Zhang, Z. F. (2018). Improving the fatigue strength of 7075 alloy through aging. *Materials Science and Engineering A*, *738*, 24–30. https://doi.org/10.1016/j.msea.2018.09.047

Liu, C., Liu, Y., Ma, L., & Yi, J. (2017). Effects of solution treatment on microstructure and high-cycle fatigue properties of 7075 aluminium alloy. *Metals*, *7*(6). https://doi.org/10.3390/met7060193

Louthan, M. R. (2018). Optical Metallography. *Materials Characterization*, *10*, 299–308. https://doi.org/10.31399/asm.hb.v10.a0001754

Ma, X., Jin, S., Wu, R., Ji, Q., Hou, L., Krit, B., & Betsofen, S. (2022). Influence alloying elements of Al and Y in MgLi alloy on the corrosion behaviour and wear resistance of micro-arc oxidation coatings. *Surface and Coatings Technology*, *432*, 128042. https://doi.org/https://doi.org/10.1016/j.surfcoat.2021.128042

Meischel, M., Stanzl-Tschegg, S. E., Arcari, A., Iyyer, N., Apetre, N., & Phan, N. (2015). Constant and variable amplitude loading of aluminium alloy 7075 in the VHCF regime. *Procedia Engineering*, *101*(C), 501–508. https://doi.org/10.1016/j.proeng.2015.02.060

Merati, A., & Eastaugh, G. (2007). Determination of fatigue related discontinuity state of 7000 series of aerospace aluminium alloys. *Engineering Failure Analysis*, *14*(4), 673–685. https://doi.org/10.1016/j.engfailanal.2006.02.016

Pineau, A., McDowell, D. L., Busso, E. P., & Antolovich, S. D. (2016). Failure of metals II: Fatigue. *Acta Materialia*, *107*, 484–507. https://doi.org/10.1016/j.actamat.2015.05.050

Raghavender, G., & Sahoo, S. (2021). *Static and Fatigue Analysis on Repaired Fuselage Skin*. *11*(7), 45–52. https://doi.org/10.9790/9622-1107044552

Tang, K. K., Berto, F., & Wu, H. (2016). Fatigue crack growth in the micro to large scale of 7075-T6 Al sheets at different R ratios. *Theoretical and Applied Fracture Mechanics*, *83*, 93–104. https://doi.org/10.1016/j.tafmec.2016.02.009

Wang, H., Li, H., Zhao, Y., Liu, X., Peng, J., Liu, J., & Zhu, M. (2023). Fatigue behaviour analysis of aluminium alloy riveted single-shear lap joints. *International Journal of Fatigue*, *172*, 107610. https://doi.org/https://doi.org/10.1016/j.ijfatigue.2023.107610

WANG, J., & ZHOU, C. (2022). Analysis of crack initiation location and its influencing factors of fretting fatigue in aluminium alloy components. *Chinese Journal of Aeronautics*, *35*(6), 420–436. https://doi.org/https://doi.org/10.1016/j.cja.2021.12.011

Warren, A. S. (2004). Developments and challenges for aluminium - A boeing perspective. *Materials Forum*, *28*, 24–31.

Yang, D., Liu, Y., Li, S., Ma, L., Liu, C., & Yi, J. (2017a). Effects of aging temperature on microstructure and high cycle fatigue performance of 7075 aluminium alloy. *Journal Wuhan University of Technology, Materials Science Edition*, *32*(3), 677–684. https://doi.org/10.1007/s11595-017-1652-4

Yang, D., Liu, Y., Li, S., Ma, L., Liu, C., & Yi, J. (2017b). Effects of aging temperature on microstructure and high cycle fatigue performance of 7075 aluminium alloy. *Journal Wuhan University of Technology, Materials Science Edition*, *32*(3), 677–684. https://doi.org/10.1007/s11595-017-1652-4

Zeng, Y., Jiang, B., Li, R. H., & Liu, Y. H. (2012). Influences of alloying elements on the microstructure and properties of Mg-Li alloys. *Zhuzao/Foundry*, *61*(3), 275–279.

Zerbst, U., Madia, M., Klinger, C., Bettge, D., & Murakami, Y. (2019). Defects as a root cause of fatigue failure of metallic components. II: Non-metallic inclusions. *Engineering Failure Analysis*, *98*(January), 228–239. https://doi.org/10.1016/j.engfailanal.2019.01.054

Zhang, X., Chen, Y., & Hu, J. (2018). Recent advances in the development of aerospace materials. *Progress in Aerospace Sciences*, *97*(August 2017), 22–34. https://doi.org/10.1016/j.paerosci.2018.01.001

APPENDICES

Appendix A- SEM sampling.

Feature	Material	Identification number	Items to be viewed together
CI	7075-O	18	1
CP-S	7075-O	19	1
CP-F	7075-O	20,21,22	1
FF	7075-O	23	1
CI	7075-O,Countersunk rivet hole	29	2
CP-S	7075-O,Countersunk rivet hole	30	2
CP-F	7075-O,Countersunk rivet hole	31	2
FF	7075-O,Countersunk rivet hole	32	2
CI	7075-O,Perpendicular rivet hole	14	3
CP-S	7075-O,Perpendicular rivet hole	15	3
CP-F	7075-O,Perpendicular rivet hole	16	3
FF	7075-O,Perpendicular rivet hole	17	3
CI	7075-T6	24	4
CP-S	7075-T6	25	4
CP-F	7075-T6	26	4
FF	7075-T6	27,28	4
CI	7075-T6,Countersunk rivet hole	6	5
CP-S	7075-T6,Countersunk rivet hole	7	5
CP-F	7075-T6,Countersunk rivet hole	8	5
FF	7075-T6,Countersunk rivet hole	9	5
CI	7075-T6,Perpendicular rivet hole	37	6
CP-S	7075-T6,Perpendicular rivet hole	38	6
CP-F	7075-T6,Perpendicular rivet hole	39	6
FF	7075-T6,Perpendicular rivet hole	40	6
CI	7075-T7	1	7
CP-S	7075-T7	2	7
CP-F	7075-T7	3	7
FF	7075-T7	4,5	7
CI	7075-T7,Countersunk rivet hole	33	8
CP-S	7075-T7,Countersunk rivet hole	34	8
CP-F	7075-T7,Countersunk rivet hole	35	8
FF	7075-T7,Countersunk rivet hole	36	8
CI	7075-T7,Perpendicular rivet hole	10	9
CP-S	7075-T7,Perpendicular rivet hole	11	9
CP-F	7075-T7,Perpendicular rivet hole	12	9
FF	7075-T7,Perpendicular rivet hole	13	9

Key

CI	Crack Initiation
CP-S	Crack propagation -slow
CP-F	Crack propagation -fast
FF	Final fracture

Appendix B - Plagiarism Report

Designation: E647 – 13a

Standard Test Method for Measurement of Fatigue Crack Growth Rates[1]

This standard is issued under the fixed designation E647; the number immediately following the designation indicates the year of original adoption or, in the case of revision, the year of last revision. A number in parentheses indicates the year of last reapproval. A superscript epsilon (ε) indicates an editorial change since the last revision or reapproval.

1. Scope

1.1 This test method[2] covers the determination of fatigue crack growth rates from near-threshold to K_{max} controlled instability. Results are expressed in terms of the crack-tip stress-intensity factor range (ΔK), defined by the theory of linear elasticity.

1.2 Several different test procedures are provided, the optimum test procedure being primarily dependent on the magnitude of the fatigue crack growth rate to be measured.

1.3 Materials that can be tested by this test method are not limited by thickness or by strength so long as specimens are of sufficient thickness to preclude buckling and of sufficient planar size to remain predominantly elastic during testing.

1.4 A range of specimen sizes with proportional planar dimensions is provided, but size is variable to be adjusted for yield strength and applied force. Specimen thickness may be varied independent of planar size.

1.5 The details of the various specimens and test configurations are shown in Annex A1 – Annex A3. Specimen configurations other than those contained in this method may be used provided that well-established stress-intensity factor calibrations are available and that specimens are of sufficient planar size to remain predominantly elastic during testing.

1.6 Residual stress/crack closure may significantly influence the fatigue crack growth rate data, particularly at low stress-intensity factors and low stress ratios, although such variables are not incorporated into the computation of ΔK.

1.7 Values stated in SI units are to be regarded as the standard. Values given in parentheses are for information only.

1.8 This test method is divided into two main parts. The first part gives general information concerning the recommendations and requirements for fatigue crack growth rate testing. The second part is composed of annexes that describe the special requirements for various specimen configurations, special requirements for testing in aqueous environments, and procedures for non-visual crack size determination. In addition, there are appendices that cover techniques for calculating da/dN, determining fatigue crack opening force, and guidelines for measuring the growth of small fatigue cracks. General information and requirements common to all specimen types are listed as follows:

1.9 Special requirements for the various specimen configurations appear in the following order:

1.10 *This standard does not purport to address all of the safety concerns, if any, associated with its use. It is the responsibility of the user of this standard to establish appropriate safety and health practices and determine the applicability of regulatory limitations prior to use.*

2. Referenced Documents

2.1 *ASTM Standards:*[3]

E4 Practices for Force Verification of Testing Machines

[1] This test method is under the jurisdiction of ASTM Committee E08 on Fatigue and Fracture and is the direct responsibility of Subcommittee E08.06 on Crack Growth Behavior.

Current edition approved Oct. 15, 2013. Published February 2014. Originally approved in 1978. Last previous approved in 2013 as E647 – 13. DOI: 10.1520/E0647-13A.

[2] For additional information on this test method see RR: E24 – 1001. Available from ASTM Headquarters, 100 Barr Harbor Drive, West Conshohocken, PA 19428.

[3] For referenced ASTM standards, visit the ASTM website, www.astm.org, or contact ASTM Customer Service at service@astm.org. For *Annual Book of ASTM Standards* volume information, refer to the standard's Document Summary page on the ASTM website.

E6 Terminology Relating to Methods of Mechanical Testing
E8/E8M Test Methods for Tension Testing of Metallic Materials
E338 Test Method of Sharp-Notch Tension Testing of High-Strength Sheet Materials (Withdrawn 2010)[4]
E399 Test Method for Linear-Elastic Plane-Strain Fracture Toughness K_{Ic} of Metallic Materials
E467 Practice for Verification of Constant Amplitude Dynamic Forces in an Axial Fatigue Testing System
E561 Test Method for ***K-R*** Curve Determination
E1012 Practice for Verification of Testing Frame and Specimen Alignment Under Tensile and Compressive Axial Force Application
E1820 Test Method for Measurement of Fracture Toughness
E1823 Terminology Relating to Fatigue and Fracture Testing

3. Terminology

3.1 The terms used in this test method are given in Terminology E6, and Terminology E1823. Wherever these terms are not in agreement with one another, use the definitions given in Terminology E1823 which are applicable to this test method.

3.2 *Definitions:*

3.2.1 *crack size, a*[L], *n*—a linear measure of a principal planar dimension of a crack. This measure is commonly used in the calculation of quantities descriptive of the stress and displacement fields and is often also termed crack length or depth.

3.2.1.1 *Discussion*—In fatigue testing, crack length is the physical crack size. See *physical crack size* in Terminology E1823.

3.2.2 *cycle—in fatigue,* under constant amplitude loading, the force variation from the minimum to the maximum and then to the minimum force.

3.2.2.1 *Discussion*—In spectrum loading, the definition of cycle varies with the counting method used.

3.2.2.2 *Discussion*—In this test method, the symbol N is used to represent the number of cycles.

3.2.3 *fatigue-crack-growth rate, da/dN,* [*L/cycle*]—the rate of crack extension under fatigue loading, expressed in terms of crack extension per cycle .

3.2.4 *fatigue cycle*—See *cycle*.

3.2.5 *force cycle*—See *cycle.*

3.2.6 *force range,* ΔP [F]—*in fatigue*, the algebraic difference between the maximum and minimum forces in a cycle expressed as:

$$\Delta P = P_{max} - P_{min} \quad (1)$$

3.2.7 *force ratio (also called stress ratio), R—in fatigue*, the algebraic ratio of the minimum to maximum force (stress) in a cycle, that is, $R = P_{min}/P_{max}$.

3.2.8 *maximum force,* P_{max} [F]—*in fatigue*, the highest algebraic value of applied force in a cycle. Tensile forces are considered positive and compressive forces negative.

3.2.9 *maximum stress-intensity factor,* K_{max} [$FL^{-3/2}$]—*in fatigue*, the maximum value of the stress-intensity factor in a cycle. This value corresponds to P_{max}.

3.2.10 *minimum force,* P_{min} [F]—*in fatigue*, the lowest algebraic value of applied force in a cycle. Tensile forces are considered positive and compressive forces negative.

3.2.11 *minimum stress-intensity factor,* K_{min} [$FL^{-3/2}$]—*in fatigue*, the minimum value of the stress-intensity factor in a cycle. This value corresponds to P_{min} when $R > 0$ and is taken to be zero when $R \leq 0$.

3.2.12 *stress cycle*—See **cycle** in Terminology E1823.

3.2.13 *stress-intensity factor, K, K_1, K_2, K_3 [$FL^{-3/2}$]*—See Terminology E1823.

3.2.13.1 *Discussion*—In this test method, mode 1 is assumed and the subscript 1 is everywhere implied.

3.2.14 *stress-intensity factor range,* ΔK [$FL^{-3/2}$]—*in fatigue*, the variation in the stress-intensity factor in a cycle, that is

$$\Delta K = K_{max} - K_{min} \quad (2)$$

3.2.14.1 *Discussion*—The loading variables R, ΔK, and K_{max} are related in accordance with the following relationships:

$$\Delta K = (1 - R)K_{max} \text{ for } R \geq 0, \text{ and} \quad (3)$$

$$\Delta K = K_{max} \text{ for } R \leq 0.$$

3.2.14.2 *Discussion*—These operational stress-intensity factor definitions do not include local crack-tip effects; for example, crack closure, residual stress, and blunting.

3.2.14.3 *Discussion*—While the operational definition of ΔK states that ΔK does not change for a constant value of K_{max} when $R \leq 0$, increases in fatigue crack growth rates can be observed when R becomes more negative. Excluding the compressive forces in the calculation of ΔK does not influence the material's response since this response (da/dN) is independent of the operational definition of ΔK. For predicting crack-growth lives generated under various R conditions, the life prediction methodology must be consistent with the data reporting methodology.

3.2.14.4 *Discussion*—An alternative definition for the stress-intensity factor range, which utilizes the full range of R, is $\Delta K_{fr} = K_{max} - K_{min}$. (In this case, K_{min} is the minimum value of stress-intensity factor in a cycle, regardless of R.) If using this definition, in addition to the requirements of 10.1.13, the value of R for the test should also be tabulated. If comparing data developed under $R \leq 0$ conditions with data developed under $R > 0$ conditions, it may be beneficial to plot the da/dN data versus K_{max}.

3.3 *Definitions of Terms Specific to This Standard:*

3.3.1 *applied-K curve*—a curve (a fixed-force or fixed-displacement crack-extension-force curve) obtained from a fracture mechanics analysis for a specific specimen configuration. The curve relates the stress-intensity factor to crack size and either applied force or displacement.

3.3.1.1 *Discussion*—The resulting analytical expression is sometimes called a K calibration and is frequently available in handbooks for stress-intensity factors.

[4] The last approved version of this historical standard is referenced on www.astm.org.

3.3.2 *fatigue crack growth threshold,* ΔK_{th} [$FL^{-3/2}$]—that asymptotic value of ΔK at which d*a*/d*N* approaches zero. For most materials an *operational*, though arbitrary, definition of ΔK_{th} is given as that ΔK which corresponds to a fatigue crack growth rate of 10^{-10} m/cycle. The procedure for determining this *operational*ΔK_{th} is given in 9.4.

3.3.2.1 *Discussion*—The intent of this definition is not to define a true threshold, but rather to provide a practical means of characterizing a material's fatigue crack growth resistance in the near-threshold regime. Caution is required in extending this concept to design (see 5.1.5).

3.3.3 *fatigue crack growth rate, da/dN or* $\Delta a/\Delta N$*, [L]—in fatigue*, the rate of crack extension caused by fatigue loading and expressed in terms of average crack extension per cycle.

3.3.4 *normalized K-gradient, C = (1/K).* d*K*/d*a*[L^{-1}]—the fractional rate of change of *K* with increasing crack size.

3.3.4.1 *Discussion*—When *C* is held constant the percentage change in *K* is constant for equal increments of crack size. The following identity is true for the normalized *K*-gradient in a constant force ratio test:

$$\frac{1}{K}\cdot\frac{dK}{da}=\frac{1}{K_{max}}\cdot\frac{dK_{max}}{da}=\frac{1}{K_{min}}\cdot\frac{dK_{min}}{da}=\frac{1}{\Delta K}\cdot\frac{d\Delta K}{da} \quad (4)$$

3.3.5 *K-decreasing test*—a test in which the value of *C* is nominally negative. In this test method *K*-decreasing tests are conducted by shedding force, either continuously or by a series of decremental steps, as the crack grows.

3.3.6 *K-increasing test*—a test in which the value of *C* is nominally positive. For the standard specimens in this method the constant-force-amplitude test will result in a *K*-increasing test where the *C* value increases but is always positive.

4. Summary of Test Method

4.1 This test method involves cyclic loading of notched specimens which have been acceptably precracked in fatigue. Crack size is measured, either visually or by an equivalent method, as a function of elapsed fatigue cycles and these data are subjected to numerical analysis to establish the rate of crack growth. Crack growth rates are expressed as a function of the stress-intensity factor range, ΔK, which is calculated from expressions based on linear elastic stress analysis.

5. Significance and Use

5.1 Fatigue crack growth rate expressed as a function of crack-tip stress-intensity factor range, d *a*/d*N* versus ΔK, characterizes a material's resistance to stable crack extension under cyclic loading. Background information on the ration-ale for employing linear elastic fracture mechanics to analyze fatigue crack growth rate data is given in Refs (**1**)[5] and (**2**).

5.1.1 In innocuous (inert) environments fatigue crack growth rates are primarily a function of ΔK and force ratio, *R*, or K_{max} and *R* (Note 1). Temperature and aggressive environments can significantly affect d*a*/ d*N* versus ΔK, and in many cases accentuate *R*-effects and introduce effects of other loading variables such as cycle frequency and waveform. Attention needs to be given to the proper selection and control of these variables in research studies and in the generation of design data.

NOTE 1—ΔK, K_{max}, and *R* are not independent of each other. Specification of any two of these variables is sufficient to define the loading condition. It is customary to specify one of the stress-intensity parameters (ΔK or K_{max}) along with the force ratio, *R*.

5.1.2 Expressing d*a*/d*N* as a function of ΔK provides results that are independent of planar geometry, thus enabling exchange and comparison of data obtained from a variety of specimen configurations and loading conditions. Moreover, this feature enables d *a*/d*N* versus ΔK data to be utilized in the design and evaluation of engineering structures. The concept of similitude is assumed, which implies that cracks of differing lengths subjected to the same nominal ΔK will advance by equal increments of crack extension per cycle.

5.1.3 Fatigue crack growth rate data are not always geometry-independent in the strict sense since thickness effects sometimes occur. However, data on the influence of thickness on fatigue crack growth rate are mixed. Fatigue crack growth rates over a wide range of ΔK have been reported to either increase, decrease, or remain unaffected as specimen thickness is increased. Thickness effects can also interact with other variables such as environment and heat treatment. For example, materials may exhibit thickness effects over the terminal range of d*a*/ d*N* versus ΔK, which are associated with either nominal yielding (Note 2) or as K_{max} approaches the material fracture toughness. The potential influence of specimen thickness should be considered when generating data for research or design.

NOTE 2—This condition should be avoided in tests that conform to the specimen size requirements listed in the appropriate specimen annex.

5.1.4 Residual stresses can influence fatigue crack growth rates, the measurement of such growth rates and the predictability of fatigue crack growth performance. The effect can be significant when test specimens are removed from materials that embody residual stress fields; for example weldments or complex shape forged, extruded, cast or machined thick sections, where full stress relief is not possible, or worked parts having complex shape forged, extruded, cast or machined thick sections where full stress relief is not possible or worked parts having intentionally-induced residual stresses. Specimens taken from such products that contain residual stresses will likewise themselves contain residual stress. While extraction of the specimen and introduction of the crack starting slot in itself partially relieves and redistributes the pattern of residual stress, the remaining magnitude can still cause significant error in the ensuing test result. Residual stress is superimposed on the applied cyclic stress and results in actual crack-tip maximum and minimum stress-intensities that are different from those based solely on externally applied cyclic forces or displacements. For example, crack-clamping resulting from far-field 3D residual stresses may lead to partly compressive stress cycles, and exacerbate the crack closure effect, even when the specimen nominal applied stress range is wholly tensile. Machining distortion during specimen preparation, specimen location and configuration dependence, irregular crack growth during fatigue precracking (for example, unexpected slow or

[5] The boldface numbers in parentheses refer to the list of references at the end of this standard.

fast crack growth rate, excessive crack-front curvature or crack path deviation), and dramatic relaxation in crack closing forces (associated with specimen stress relief as the crack extends) will often indicate influential residual stress impact on the measured da/dN versus ΔK result. (3,4) Noticeable crack-mouth-opening displacement at zero applied force is indicative of residual stresses that can affect the subsequent fatigue crack growth property measurement.

5.1.5 The growth rate of small fatigue cracks can differ noticeably from that of long cracks at given ΔK values. Use of long crack data to analyze small crack growth often results in non-conservative life estimates. The small crack effect may be accentuated by environmental factors. Cracks are defined as being small when 1) their length is small compared to relevant microstructural dimension (a continuum mechanics limitation), 2) their length is small compared to the scale of local plasticity (a linear elastic fracture mechanics limitation), and 3) they are merely physically small (<1 mm). Near-threshold data established according to this method should be considered as representing the materials' steady-state fatigue crack growth rate response emanating from a long crack, one that is of sufficient length such that transition from the initiation to propagation stage of fatigue is complete. Steady-state near-threshold data, when applied to service loading histories, may result in non-conservative lifetime estimates, particularly for small cracks (5-7).

5.1.6 Crack closure can have a dominant influence on fatigue crack growth rate behavior, particularly in the near-threshold regime at low stress ratios. This implies that the conditions in the wake of the crack and prior loading history can have a bearing on the current propagation rates. The understanding of the role of the closure process is essential to such phenomena as the behavior of small cracks and the transient crack growth rate behavior during variable amplitude loading. Closure provides a mechanism whereby the cyclic stress intensity near the crack tip, ΔK_{eff}, differs from the nominally applied values, ΔK. This concept is of importance to the fracture mechanics interpretation of fatigue crack growth rate data since it implies a non-unique growth rate dependence in terms of ΔK, and R(8).[6]

NOTE 3—The characterization of small crack behavior may be more closely approximated in the near-threshold regime by testing at a high stress ratio where the anomalies due to crack closure are minimized.

5.2 This test method can serve the following purposes:

5.2.1 To establish the influence of fatigue crack growth on the life of components subjected to cyclic loading, provided data are generated under representative conditions and combined with appropriate fracture toughness data (for example, see Test Method E399), defect characterization data, and stress analysis information (9, 10).

NOTE 4—Fatigue crack growth can be significantly influenced by load history. During variable amplitude loading, crack growth rates can be either enhanced or retarded (relative to steady-state, constant-amplitude growth rates at a given ΔK) depending on the specific loading sequence. This complicating factor needs to be considered in using constant-amplitude growth rate data to analyze variable amplitude fatigue problems (11).

5.2.2 To establish material selection criteria and inspection requirements for damage tolerant applications.

5.2.3 To establish, in quantitative terms, the individual and combined effects of metallurgical, fabrication, environmental, and loading variables on fatigue crack growth.

6. Apparatus

6.1 *Grips and Fixtures*—Grips and fixturing required for the specimens outlined in this method are described in the appropriate specimen annex.

6.2 *Alignment of Grips*—It is important that attention be given to achieving good alignment in the force train through careful machining of all gripping fixtures. Misalignment can cause non-symmetric cracking, particularly for critical applications such as near-threshold testing, which in turn may lead to invalid data (see Sec. 8.3.4, 8.8.3). If non-symmetric cracking occurs, the use of a strain-gaged specimen to identify and minimize misalignment might prove useful. One method to identify bending under tensile loading conditions is described in Practice E1012. Another method which specifically addresses measurement of bending in pin-loaded specimen configurations is described in Ref (12). For tension-compression loading the length of the force train (including the hydraulic actuator) should be minimized, and rigid, non-rotating joints should be employed to reduce lateral motion in the force train.

NOTE 5—If compliance methods are used employing displacement gages similar to those described in Test Methods E399, E1820, or E561, knife edges can be integrally machined or rigidly affixed to the test sample (either fastened, bonded, or welded) and must be geometrically compatible with the displacement device such that line contact is maintained throughout the test.

7. Specimen Configuration, Size, and Preparation

7.1 *Standard Specimens*—Details of the test specimens outlined in this method are furnished as separate annexes to this method. Notch and precracking details for the specimens are given in Fig. 1.

7.1.1 For specimens removed from material for which complete stress relief is impractical (see 5.1.4), the effect of residual stresses on the crack propagation behavior can be minimized through the careful selection of specimen shape and size. By selecting a small ratio of specimen dimensions, B/W the effect of a through-the-thickness distribution of residual stresses acting perpendicular to the direction of crack growth can be reduced. This choice of specimen shape minimizes crack curvature or other crack front irregularities which confuse the calculation of both da/dN and ΔK. In addition, residual stresses acting parallel to the direction of crack growth can often produce clamping or opening moments about the crack-tip, which can also confound test results. This is particularly true for deep edge-notched specimens such as the C(T), which can display significant crack-mouth movement during machining of the crack starter notch. In these instances it is useful to augment both specimen preparation and subsequent testing with displacement measurements as has been recommended for

[6] Subcommittee E08.06 has initiated a study group activity on crack closure measurement and analysis. Reference (8) provides basic information on this subject.

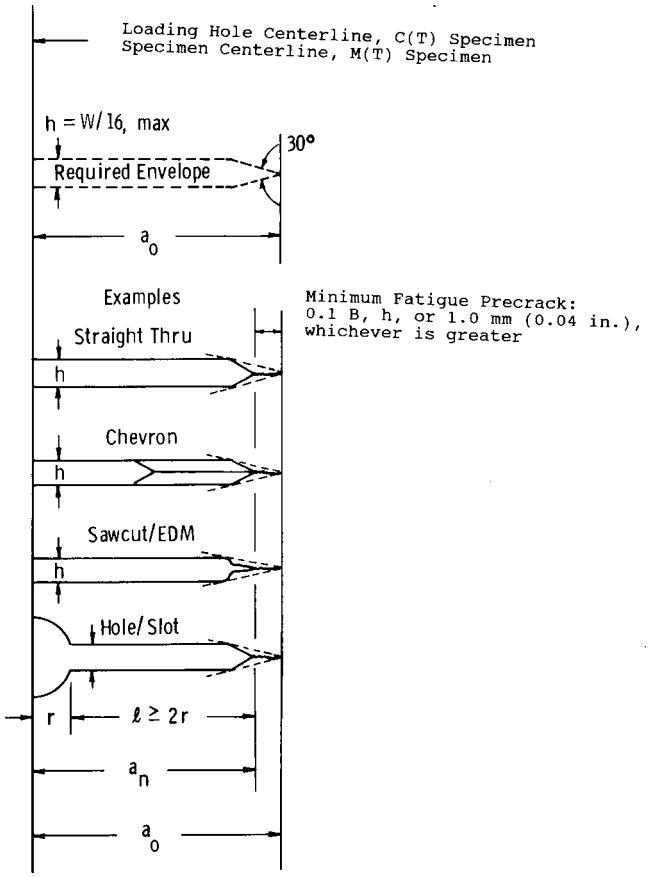

FIG. 1 Notch Details and Minimum Fatigue Precracking Requirements

fracture toughness determination in non-stress-relieved products. (**13**) In most, but not all, of these cases, the impact of residual-stress-induced clamping on crack growth property measurement can be minimized by selecting a symmetrical specimen configuration, that is, the M(T) specimen. Alternately, there can be situations where the specimen is too constrained to result in measurable post-machining movement after sharp-notch introduction. If this is so, and the crack is small enough to be wholly embedded in a field of tension or compression, then the cyclic stress ratio operating at the crack-tip will be different from that calculated from the applied cyclic loads. At this time the only recourse is to test an alternate specimen configuration or sample location to check for uniqueness of the d*a*/d*N*-Δ*K* relationship as a means to determine if residual stress is significantly biasing the measured result.

7.2 *Specimen Size*—In order for results to be valid according to this test method it is required that the specimen be predominantly elastic at all values of applied force. The minimum in-plane specimen sizes to meet this requirement are based primarily on empirical results and are specific to the specimen configuration as furnished in the appropriate specimen annex (**10**).

NOTE 6—The size requirements described in the various specimen annexes are appropriate for low-strain hardening materials ($\sigma_{ULT}/\sigma_{YS} \leq 1.3$) (**14**) and for high-strain hardening materials ($\sigma_{ULT}/\sigma_{YS} \geq 1.3$) under certain conditions of force ratio and temperature (**15**, **16**) (where σ_{ULT} is the ultimate tensile strength of the material). However, under other conditions of force ratio and temperature, the requirements listed in the annexes appear to be overly restrictive-that is, they require specimen sizes which are larger than necessary (**17**,**18**). Currently, the conditions giving rise to each of these two regimes of behavior are not clearly defined.

7.2.1 An alternative size requirement may be employed for high-strain hardening materials as follows. The uncracked ligament requirement listed for the specific specimen geometry may be relaxed by replacing σ_{YS} with a higher, effective yield strength which accounts for the material strain hardening capacity. For purposes of this test method, this *effective* yield strength, termed flow strength, is defined as follows:

$$\sigma_{FS} = (\sigma_{YS} + \sigma_{ULT})/2 \quad (5)$$

However, it should be noted that the use of this alternative size requirement allows mean plastic deflections to occur in the specimen. These mean deflections under certain conditions, as noted previously, can accelerate growth rates by as much as a factor of two. Although these data will generally add conservatism to design or structural reliability computations, they can also confound the effects of primary variables such as specimen thickness (if *B/W* is maintained constant), force ratio, and possibly environmental effects. Thus, when the alternative size requirement is utilized, it is important to clearly distinguish between data that meet the yield strength or flow strength criteria. In this way, data will be generated that can be used to formulate a specimen size requirement of general utility.

7.3 *Notch Preparation*—The machined notch for standard specimens may be made by electrical-discharge machining (EDM), milling, broaching, or sawcutting. The following notch preparation procedures are suggested to facilitate fatigue precracking in various materials:

7.3.1 *Electric Discharge Machining*—ρ < 0.25 mm (0.010 in.) (ρ = notch root radius), high-strength steels ($\sigma_{YS} \geq 1175$ MPa/170 ksi), titanium and aluminum alloys.

7.3.2 *Mill or Broach*—ρ ≤ 0.075 mm (0.003 in.), low or medium-strength steels ($\sigma_{YS} \leq 1175$ MPa/170 ksi), aluminum alloys.

7.3.3 *Grind*—ρ ≤ 0.25 mm (0.010 in.), low or medium-strength steels.

7.3.4 *Mill or Broach*—ρ ≤ 0.25 mm (0.010 in.), aluminum alloys.

7.3.5 *Sawcut*—Recommended only for aluminum alloys.

7.3.6 Examples of various machined-notch geometries and associated precracking requirements are given in Fig. 1 (see 8.3).

7.3.7 When residual stresses are suspected of being present (see 5.1.4), local displacement measurements made before and after machining the crack starter notch are useful for detecting the potential magnitude of the effect. A simple mechanical displacement gage can be used to measure distance between two hardness indentations at the mouth of the notch (**3**, **13**). Limited data obtained during preparation of aluminum alloy C(T) specimens with the specimen width, W, ranging from 50-100 mm (2-4 in.) has shown that fatigue crack growth rates can be impacted significantly when these mechanical displacement measurements change by more than 0.05 mm (0.002 in.).(**4**)

8. Procedure

8.1 *Number of Tests*—At crack growth rates greater than 10^{-8} m/cycle, the within-lot variability (neighboring specimens) of d*a*/d*N* at a given Δ*K* typically can cover about a factor of two (**19**). At rates below 10^{-8} m/cycle, the variability in d*a*/d*N* may increase to about a factor of five or more due to increased sensitivity of d*a*/d*N* to small variations in Δ*K*. This scatter may be increased further by variables such as microstructural differences, residual stresses, changes in crack tip geometry (crack branching) or near tip stresses as influenced for example by crack roughness or product wedging, force precision, environmental control, and data processing techniques. These variables can take on added significance in the low crack growth rate regime (d*a*/d*N* < 10^{-8} m/cycle). In view of the operational definition of the threshold stress-intensity (see 3.3.2 and 9.4), at or near threshold it is more meaningful to express variability in terms of Δ *K* rather than d*a*/d*N*. It is good practice to conduct replicate tests; when this is impractical, multiple tests should be planned such that regions of overlapping d*a*/d*N* versus Δ*K* data are obtained, particularly under both *K*-increasing and *K*-decreasing conditions. Since confidence in inferences drawn from the data increases with number of tests, the desired number of tests will depend on the end use of the data.

8.2 *Specimen Measurements*—The specimen dimensions shall be within the tolerances given in the appropriate specimen annex.

8.3 *Fatigue Precracking*—The importance of precracking is to provide a sharpened fatigue crack of adequate size and straightness (also symmetry for the M(T) specimen) which ensures that *1*) the effect of the machined starter notch is removed from the specimen *K*-calibration, and *2*) the effects on subsequent crack growth rate data caused by changing crack front shape or precrack load history are eliminated.

8.3.1 Conduct fatigue precracking with the specimen fully heat treated to the condition in which it is to be tested. The precracking equipment shall be such that the force distribution is symmetrical with respect to the machined notch and K_{max} during precracking is controlled to within ±5 %. Any convenient loading frequency that enables the required force accuracy to be achieved can be used for precracking. The machined notch plus the precrack must lie within the envelope, shown in Fig. 1, that has as its apex the end of the fatigue precrack. In addition the fatigue precrack shall not be less than 0.10*B*, *h*, or 1.0 mm (0.040 in.), whichever is greater (Fig. 1).

8.3.2 The final K_{max} during precracking shall not exceed the initial K_{max} for which test data are to be obtained. If necessary, forces corresponding to higher K_{max} values may be used to initiate cracking at the machined notch. In this event, the force range shall be stepped-down to meet the above requirement. Furthermore, it is suggested that reduction in P_{max} for any of these steps be no greater than 20 % and that measurable crack extension occur before proceeding to the next step. To avert transient effects in the test data, apply the force range in each step over a crack size increment of at least $(3/\pi)\ (K'_{max}/\sigma_{YS})^2$, where K'_{max} is the terminal value of K_{max} from the previous forcestep. If P_{min}/P_{max} during precracking differs from that used during testing, see the precautions described in 8.5.1.

8.3.3 For the *K*-decreasing test procedure, prior loading history may influence near-threshold growth rates despite the precautions of 8.3.2. It is good practice to initiate fatigue cracks at the lowest stress intensity possible. Precracking growth rates less than 10^{-8} m/cycle are suggested. A compressive force, less than or equal to the precracking force, may facilitate fatigue precracking and may diminish the influence of the *K*-decreasing test procedure on subsequent fatigue crack growth rate behavior.

8.3.4 Measure the crack sizes on the front and back surfaces of the specimen to within 0.10 mm (0.004 in.) or 0.002*W*, whichever is greater. For specimens where W > 127 mm (5 in.), measure crack size to within 0.25 mm (0.01 in.). If crack sizes measured on front and back surfaces differ by more than 0.25*B*, the pre-cracking operation is not suitable and subsequent testing would be invalid under this test method. In addition for the M(T) specimen, measurements referenced from the specimen centerline to the two cracks (for each crack use the average of measurements on front and back surfaces) shall not differ by more than 0.025*W*. If the fatigue crack departs more than the allowable limit from the plane of symmetry (see 8.8.3) the specimen is not suitable for subsequent testing. If the above requirements cannot be satisfied, check for potential problems in alignment of the loading system and details of the machined notch, or material-related problems such as residual stresses.

8.4 *Test Equipment*—The equipment for fatigue testing shall be such that the force distribution is symmetrical to the specimen notch.

8.4.1 Verify the force cell in the test machine in accordance with Practices E4 and E467. Conduct testing such that both Δ*P* and P_{max} are controlled to within ±2 % of the targeted values throughout the test.

8.4.2 An accurate digital device is required for counting elapsed cycles. A timer is a desirable supplement to the counter and provides a check on the counter. Multiplication factors (for example, ×10 or ×100) should not be used on counting devices when obtaining data at growth rates above 10^{-5} m/cycle since they can introduce significant errors in the growth rate determination.

8.5 *Constant-Force-Amplitude Test Procedure for da/dN > 10^{-8} m/cycle*—This test procedure is well suited for fatigue crack growth rates above 10^{-8} m/cycle. However, it becomes increasingly difficult to use as growth rates decrease below 10^{-8} m/cycle because of precracking considerations (see 8.3.3). (A *K*-decreasing test procedure which is better suited for rates below 10^{-8} m/cycle is provided in 8.6.) When using the constant-force-amplitude procedure it is preferred that each specimen be tested at a constant force range (Δ*P*) and a fixed set of loading variables (stress ratio and frequency). However, this may not be feasible when it is necessary to generate a wide range of information with a limited number of specimens. When loading variables are changed during a test, potential problems arise from several types of transient phenomenon (**20**). The following test procedures should be followed to minimize or eliminate transient effects while using this *K*-increasing test procedure.

8.5.1 If force range is to be incrementally varied it should be done such that P_{max} is increased rather than decreased to

preclude retardation of growth rates caused by overload effects; retardation being a more pronounced effect than accelerated crack growth associated with incremental increase in P_{max}. Transient growth rates are also known to result from changes in P_{min} or R. Sufficient crack extension should be allowed following changes in force to enable the growth rate to establish a steady-state value. The amount of crack growth that is required depends on the magnitude of force change and on the material. An incremental increase of 10 % or less will minimize these transient growth rates.

8.5.2 When environmental effects are present, changes in force level, test frequency, or waveform can result in transient growth rates. Sufficient crack extension should be allowed between changes in these loading variables to enable the growth rate to achieve a steady-state value.

8.5.3 Transient growth rates can also occur, in the absence of loading variable changes, due to long-duration test interruptions, for example, during work stoppages. In this case, data should be discarded if the growth rates following an interruption are less than those before the interruption.

8.6 *K-Decreasing Procedure for da/dN < 10^{-8} m/cycle*—This procedure is started by cycling at a ΔK and K_{max} level equal to or greater than the terminal precracking values. Subsequently, forces are decreased (shed) as the crack grows, and test data are recorded until the lowest ΔK or crack growth rate of interest is achieved. The test may then be continued at constant force limits to obtain comparison data under K-increasing conditions. The K-decreasing procedure is not recommended at fatigue crack growth rates above 10^{-8} m/cycle since prior loading history at such associated ΔK levels may influence the near-threshold fatigue crack growth rate behavior.

NOTE 7—ASTM Subcommittee E08.06 has initiated a task group (E08.06.06) that is investigating the procedures for the determination of fatigue crack growth rates at or near threshold. The outcome of this task group may influence the procedure outlined in this section. Recent research has indicated that the use of the force-reduction procedure, in some circumstances, may result in non-steady-state conditions, specimen-width effects (**21**), specimen-type effects (**22**), and non-conservative growth rates.

8.6.1 Force shedding during the K-decreasing test may be conducted as decreasing force steps at selected crack size intervals, as shown in Fig. 2. Alternatively, the force may be shed in a continuous manner by an automated technique (for example, by use of an analog computer or digital computer, or both) (**23**).

8.6.2 The rate of force shedding with increasing crack size shall be gradual enough to 1) preclude anomalous data resulting from reductions in the stress-intensity factor and concomitant transient growth rates, and 2) allow the establishment of about five da/dN, ΔK data points of approximately equal spacing per decade of crack growth rate. The above requirements can be met by limiting the normalized K-gradient, $C = 1/K \cdot dK/da$, to a value algebraically equal to or greater than -0.08 mm^{-1} (-2 in.$^{-1}$). That is:

$$C = \left(\frac{1}{K}\right)\cdot\left(\frac{dK}{da}\right) > -0.08\ \text{mm}^{-1}\ (-2\ \text{in.}^{-1}) \qquad (6)$$

When forces are incrementally shed, the requirements on C correspond to the nominal K-gradient depicted in Fig. 2.

NOTE 8—Acceptable values of C may depend on load ratio, test material, and environment. Values of C algebraically greater than that indicated above have been demonstrated as acceptable for use in decreasing K tests of several steel alloys and aluminum alloys tested in laboratory air over a wide range of force ratios (**14, 23**).

8.6.3 If the normalized K-gradient C is algebraically less than that prescribed in 8.6.2, the procedure shall consist of decreasing K to the lowest growth rate of interest followed by a K-increasing test at a constant ΔP (conducted in accordance with 8.5). Upon demonstrating that data obtained using

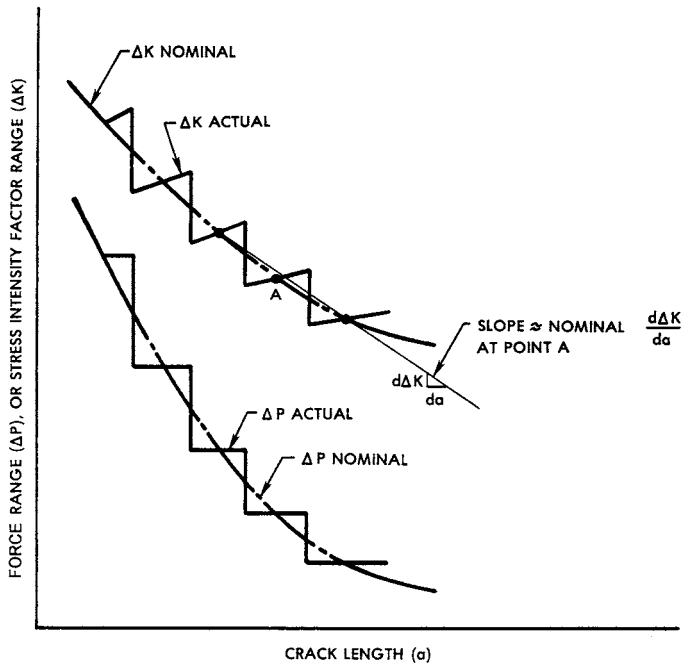

FIG. 2 Typical *K* Decreasing Test by Stepped Force Shedding

K-increasing and *K*-decreasing procedures are equivalent for a given set of test conditions, the *K*-increasing testing may be eliminated from all replicate testing under these same test conditions.

NOTE 9—It is good practice to have *K*-decreasing followed by *K*-increasing data for the first test of any single material regardless of the *C* value used.

8.6.4 It is recommended that the force ratio, *R*, and *C* be maintained constant during *K*-decreasing testing (see 8.7.1 for exceptions to this recommendation).

8.6.5 The relationships between *K* and crack size and between force and crack size for a constant-*C* test are given as follows:

8.6.5.1 $\Delta K = \Delta K_o \exp[C(a - a_o)]$, where ΔK_o is the initial ΔK at the start of the test, and a_o is the corresponding crack size. Because of the identities given in 5.1.1 (Note 1) and in the Definitions 3.2.14, the above relationship is also true for K_{max} and K_{min}.

8.6.5.2 The force histories for the standard specimens of this test method are obtained by substituting the appropriate *K*-calibrations given in the respective specimen annex into the above expression.

8.6.6 When employing step shedding of force, as in Fig. 2, the reduction in P_{max} of adjacent force steps shall not exceed 10 % of the previous P_{max}. Upon adjustment of maximum force from P_{max1} to a lower value, P_{max2}, a minimum crack extension of 0.50 mm (0.02 in.) is recommended.

8.6.7 When employing continuous shedding of force, the requirement of 8.6.6 is waived. Continuous force shedding is defined as $(P_{max1} - P_{max2})/P_{max1} \leq 0.02$.

8.7 *Alternative K-control test procedures*—Ideally, it is desirable to generate d*a*/d*N*, ΔK data at *K*-gradients independent of the specimen geometry **(24)**. Exercising control over this *K*-gradient allows much steeper gradients for small values of *a*/*W* without the undesirable feature of having too steep a *K*-gradient at the larger values of *a*/*W* associated with constant amplitude loading. Generating data at an appropriate *K*-gradient, using a constant and positive value of the *K*-gradient parameter, *C*, (see 8.6.2) provides numerous advantages: the test time is reduced; the d*a*/d *N*-ΔK data can be evenly distributed without using variable Δa increments; a wider range of data may be generated without incremental force increases; the *K*-gradient is independent of the specimen geometry.

8.7.1 Situations may arise where changing ΔK under conditions of constant K_{max} or constant K_{mean} may be more representative than under conditions of constant *R*. The application of the test data should be considered in choosing an appropriate mode of *K*-control. For example, a more conservative estimate of near-threshold behavior may be obtained by using this test method. This process effectively measures near-threshold data at a high stress ratio.

8.8 *Measurement of Crack Size*—Make fatigue crack size measurements as a function of elapsed cycles by means of a visual, or equivalent, technique capable of resolving crack extensions of 0.10 mm (0.004 in.), or 0.002*W*, whichever is greater. For visual measurements, polishing the test area of the specimen and using indirect lighting aid in the resolution of the crack-tip. It is suggested that, prior to testing, reference marks be applied to the test specimen at predetermined locations along the direction of cracking. Crack size can then be measured using a low power (20 to 50×) traveling microscope. Using the reference marks eliminates potential errors due to accidental movement of the traveling microscope. If precision photographic grids or polyester scales are attached to the specimen, crack size can be determined directly with any magnifying device that gives the required resolution. It is preferred that measurements be made without interrupting the test.

NOTE 10—Interruption of cyclic loading for the purpose of crack size measurement can be permitted providing strict care is taken to avoid introducing any significant extraneous damage (for example, creep deformation) or transient crack extension (for example, growth under static force). The interruption time should be minimized (less than 10 min.) and if a static force is maintained for the purpose of enhanced crack tip resolution, it should be carefully controlled. A static force equal to the fatigue mean force is probably acceptable (with high temperatures and corrosive environments, even mean levels should be questioned) but in no case should the static force exceed the maximum force applied during the fatigue test.

8.8.1 Make crack size measurements at intervals such that d*a*/d*N* data are nearly evenly distributed with respect to ΔK. Recommended intervals are given in the appropriate specimen annex.

8.8.1.1 A minimum Δa of 0.25 mm (0.01 in.) is recommended. However, situations may arise where the Δa needs to be reduced below 0.25 mm (0.01 in.). Such is the case for threshold testing where it is required that at least five d*a*/d*N*, ΔK data points in the near-threshold regime (see 9.4 3). In any case, the minimum Δa shall be ten times the crack size measurement precision.

NOTE 11—The crack size measurement precision is herein defined as the standard deviation on the mean value of crack size determined for a set of replicate measurements.

8.8.2 As a rule, crack size measurements should be made on both sides (front and back) of a specimen to ensure that the crack symmetry requirements of 8.8.3 are met. The average value of the measurements (two crack lengths for the C(T) specimen and four crack lengths for the M(T) specimen) should be used in all calculations of growth rate and K. If crack size measurements are not made on both sides at every crack size interval, the interval of both-side measurement must be reported. Measurement on only one side is permissible only if previous experience with a particular specimen configuration, test material, testing apparatus, and growth rate regime has shown that the crack symmetry requirements are met consistently.

8.8.3 If at any point in the test the crack deviates more than ±20° from the plane of symmetry over a distance of 0.1*W* or greater, the data are invalid according to this test method **(25)**. A deviation between ±10 and ±20° must be reported. (See Fig. 3) In addition, data are invalid if (1) crack sizes measured on front and back surfaces differ by more than 0.25*B*. Additional validity requirements may be included in the specimen annexes.

NOTE 12—The requirements on out-of-plane cracking are commonly

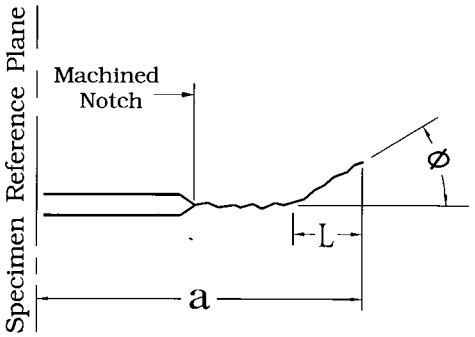

Valid if $\varnothing \leq 10^\circ$
Report if $10^\circ < \varnothing \leq 20^\circ$
Invalid if $\varnothing > 20^\circ$ for $L \geq 0.1W$

FIG. 3 Out-of-Plane Cracking Limits

violated for large-grained or single-crystal materials. In these instances, results from anisotropic, mixed-mode stress analyses may be needed to compute *K*; (for example, see Ref. (**26**)).

NOTE 13—Crack tip branching has been noted to occur. This characteristic is not incorporated into the computation of Δ*K*. As a result, crack branching, or bifurcating, may be a source of variability in measured fatigue crack growth rate data. Data recorded during branching must be noted as being for a branching crack.

8.8.3.1 If nonvisual methods for crack size measurement are used and nonsymmetric or angled cracking occurs, the nonvisual measurements derived during these periods shall be verified with visual techniques to ensure the requirements of 8.8.3 are satisfied.

9. Calculation and Interpretation of Results

9.1 *Crack Curvature Correction*—After completion of testing, examine the fracture surfaces, preferably at two locations (for example, at the precrack and terminal fatigue crack sizes), to determine the extent of through-thickness crack curvature (commonly termed *crack tunneling*). If a crack contour is visible, calculate a three-point, through-thickness average crack size in accordance with Test Method E399, sections on General Procedure related to Specimen Measurement; specifically the paragraph on crack size measurement. The difference between the average through-thickness crack size and the corresponding crack size recorded during the test (for example, if visual measurements were obtained this might be the average of the surface crack size measurements) is the crack curvature correction.

9.1.1 If the crack curvature correction results in a greater than 5 % difference in calculated stress-intensity factor at any crack size, then employ this correction when analyzing the recorded test data.

9.1.2 If the magnitude of the crack curvature correction either increases or decreases with crack size, use a linear interpolation to correct intermediate data points. Determine this linear correction from two distinct crack contours separated by a minimum spacing of 0.25*W* or *B*, whichever is greater. When there is no systematic variation of crack curvature with crack size, employ a uniform correction determined from an average of the crack contour measurements.

9.1.3 When employing a crack size monitoring technique other than visual, a crack curvature correction is generally incorporated in the calibration of the technique. However, since the magnitude of the correction will probably depend on specimen thickness, the preceding correction procedures may also be necessary.

9.2 *Determination of Crack Growth Rate*—The rate of fatigue crack growth is to be determined from the crack size versus elapsed cycles data (*a* versus *N*). Recommended approaches which utilize the secant or incremental polynomial methods are given in Appendix X1. Either method is suitable for the *K*-increasing, constant Δ*P* test. For the *K*-decreasing tests where force is shed in decremental steps, as in Fig. 2, the secant method is recommended. A crack growth rate determination shall not be made over any increment of crack extension that includes a force step. Where shedding of *K* is performed continuously with each cycle by automation, the incremental polynomial technique is applicable.

NOTE 14—Both recommended methods for processing *a* versus *N* data are known to give the same average d*a*/d*N* response. However, the secant method often results in increased scatter in d*a*/d*N* relative to the incremental polynomial method, since the latter numerically" smooths" the data (**19, 27**). This apparent difference in variability introduced by the two methods needs to be considered, especially in utilizing d*a*/d*N* versus Δ*K* data in design.

9.3 *Determination of Stress-Intensity Factor Range, Δ*K*—*Use the appropriate crack size values as described in the particular specimen annex to calculate the stress-intensity range corresponding to a given crack growth rate.

9.4 *Determination of a Fatigue Crack Growth Threshold*—The following procedure provides an operational definition of the threshold stress-intensity factor range for fatigue crack growth, ΔK_{th}, which is consistent with the general definition of 3.3.2.

9.4.1 Determine the best-fit straight line from a linear regression of log d*a*/d *N* versus log Δ*K* using a minimum of five d*a*/d*N*, Δ*K* data points of approximately equal spacing between growth rates of 10^{-9} and 10^{-10} m/cycle. Having specified the range of fit in terms of d*a*/d*N* requires that log Δ*K* be the dependent variable in establishing this straight line fit.

NOTE 15—Limitations of the linear regression approach of 9.4.1 are described in Ref (**28**). Alternative nonlinear approaches and their advantages are also given in Ref (**28**).

9.4.2 Calculate the Δ*K*-value that corresponds to a growth rate of 10^{-10} m/cycle using the above fitted line; this value of Δ*K* is defined as ΔK_{th} according to the operational definition of this test method.

NOTE 16—In the event that lower d*a*/d*N* data are generated, the above procedure can be used with the lowest decade of data. This alternative range of fit must then be specified according to 10.1.12.

10. Report

10.1 The report shall include the following information:

10.1.1 Specimen type, including thickness, *B*, and width, *W*. If the M(T) specimen is used, or if a specimen type not described in this test method is used, a figure of the specimen and grips shall be provided.

10.1.2 Description of the test machine and equipment used to measure crack size and the precision with which crack size measurements were made.

10.1.3 Test material characterization in terms of heat treatment, chemical composition, and mechanical properties (include at least the 0.2 % offset yield strength and either elongation or reduction in area measured in accordance with Test Methods E8/E8M). Product size and form (for example, sheet, plate, and forging) shall also be identified. Method of stress relief, if applicable, shall be reported. For thermal methods, details of time, temperature and atmosphere. For non-thermal methods, details of forces and frequencies.

10.1.4 The crack plane orientation according to the code given in Test Method E399. In addition, if the specimen is removed from a large product form, its location with respect to the parent product shall be given.

10.1.5 The terminal values of ΔK, R and crack size from fatigue precracking. If precrack forces were stepped-down, the procedure employed shall be stated and the amount of crack extension at the final force level shall be given.

10.1.6 Test loading variables, including ΔP, R, cyclic frequency, and cyclic waveform.

10.1.7 Environmental variables, including temperature, chemical composition, pH (for liquids), and pressure (for gases and vacuum). For tests in air, the relative humidity shall be reported. For tests in inert reference environments, such as dry argon, estimates of residual levels of water and oxygen in the test environment (generally this differs from the analysis of residual impurities in the gas supply cylinder) shall be given. Nominal values for all of the above environmental variables, as well as maximum deviations throughout the duration of testing, shall be reported. Also, the material employed in the chamber used to contain the environment and steps taken to eliminate chemical/electrochemical reactions between the specimen-environment system and the chamber shall be described.

10.1.8 Analysis methods applied to the data, including the technique used to convert a versus N to da/dN, specific procedure used to correct for crack curvature, and magnitude of crack curvature correction.

10.1.9 The specimen K-calibration and size criterion to ensure predominantly elastic behavior (for specimens not described in this test method).

10.1.10 da/dN as a function of ΔK shall be plotted. (It is recommended that ΔK be plotted on the abscissa and da/dN on the ordinate. Log-log coordinates are commonly used. For optimum data comparisons, the size of the ΔK-log cycles should be two or three times larger than da/dN-log cycles.) All data that violate the size requirements of the appropriate specimen annex shall be identified; state whether σ_{YS} or σ_{FS} was used to determine specimen size.

NOTE 17—The definition of σ_{FS} is provided in 7.2.1.

10.1.11 Description of any occurrences that appear to be related to anomalous data (for example, transients following test interruptions or changes in loading variables).

10.1.12 For K-decreasing tests, report C and initial values of K and a. Indicate whether or not the K-decreasing data were verified by K-increasing data. For near-threshold growth rates, report ΔK_{th}, the equation of the fitted line (see 9.4) used to establish ΔK_{th}, and any procedures used to establish ΔK_{th} which differ from the operational definition of 9.4. Also report the lowest growth rate used to establish ΔK_{th} using the operational definition of 9.4. It is recommended that these values be reported as $\Delta K_{th}(x)$ where x is the aforementioned lowest growth rate in m/cycle.

10.1.13 The following information shall be tabulated for each test: a, N, ΔK, da/dN, and, where applicable, the test variables of 10.1.3, 10.1.6, and 10.1.7. Also, all data determined from tests on specimens that violate the size requirements of the appropriate specimen annex shall be identified; state whether σ_{YS} or σ_{FS} was used to determine specimen size.

11. Precision and Bias

11.1 *Precision*—The precision of da/dN versus ΔK is a function of inherent material variability, as well as errors in measuring crack size and applied force. The required loading precision of 8.4.1 can be readily obtained with modern closed-loop electrohydraulic test equipment and results in a ±2 % variation in the applied ΔK; this translates to a ±4 % to ±10 % variation in da/dN, at a given ΔK, for growth rates above the near-threshold regime. However, in general, the crack size measurement error makes a more significant contribution to the variation in da/dN, although this contribution is difficult to isolate since it is coupled to the analysis procedure for converting a versus N to da/dN, and to the inherent material variability. Nevertheless, it is clear that the overall variation in da/dN is dependent on the ratio of crack size measurement interval to measurement error **(27, 29)**. Furthermore, an optimum crack size measurement interval exists due to the fact that the interval should be large compared to the measurement error (or precision), but small compared to the K-gradient of the test specimen. These considerations form the basis for the recommended measurement intervals as given in the appropriate specimen annex. Recommendations are specified relative to crack size measurement precision: a quantity that must be empirically established for the specific measurement technique being employed.

11.1.1 Although it is often impossible to separate the contributions from each of the above-mentioned sources of variability, an overall measure of variability in da/dN versus ΔK is available from results of an interlaboratory test program in which 14 laboratories participated **(19)**.[7] These data, obtained on a highly homogeneous 10 Ni steel, showed the repeatability in da/dN (within a laboratory) to average ±27 % and range from ±13 to ±50 %, depending on laboratory; the reproducibility (between laboratories) was ±32 %. Values cited are standard errors based on ±2 residual standard deviations about the mean response determined from regression analysis. In computing these statistics, abnormal results from two laboratories were not considered due to improper precracking and suspected errors in force calibration. Such problems would be avoided by complying with the current requirements of this test method as they have been upgraded since the interlaboratory test program was conducted. Because

[7] Supporting data have been filed at ASTM International Headquarters and may be obtained by requesting Research Report RR:E24-1001.

a highly homogeneous material was employed in this program, the cited variabilities in d*a*/d*N* are believed to have arisen primarily from random crack size measurement errors.

11.1.1.1 A more recent interlaboratory test program (**30**)[8] in which 18 laboratories participated (141 total fatigue crack growth rate tests) examined the variability obtained on three commonly used materials: 4130 steel (normalized and heat-treated) bar, 7075 T6 sheet, and 2024 T351 sheet. The data for the steel alloy showed the reproducibility in d*a*/d*N* to be ±31%, whereas an average of ±41% for the aluminum alloys. The repeatability (within a laboratory) was ±20% for the steel alloy and ±25% for the aluminum alloys. The reproducibility of a grouped population of all alloys tested ranged from a low of ±9% to typically ±43 to ±50%. This data suggests that there is little statistical change in variability between this and the previous (**19**) interlaboratory test program. However, the data suggests some effect of secondary variables on the variability levels. For instance, the influence of specimen geometry was noted with M(T) specimens exhibiting variability levels that are 30-40% less than similar C(T) specimens. A comparison between tests performed using DCPD and compliance as the continuous, non-visual crack size measurement suggests that variability levels are 20% less for DCPD when compared to compliance. Conversely, no discernable difference in variability level was noted between different load control methods (constant amplitude versus *K*-control).

11.1.2 For the near-threshold regime, a measure of the variability in ΔK_{th} is available from the results of an interlaboratory test program in which 15 laboratories participated (**31**).[9] These data, obtained on a homogeneous 2219 T851 aluminum alloy, show a repeatability in ΔK_{th} (within a laboratory) to average ±3 % with the reproducibility (between laboratories) of ±9 %. This observation is based on the 11 laboratories that provided valid near-threshold data. Because of the sensitivity of d*a*/d*N* to small changes in Δ*K*, growth rates in this near threshold regime often vary by an order of magnitude, or more, at a given Δ*K*(**31**).[7]

11.1.3 It is important to recognize that for purposes of design or reliability assessment, inherent material variability often becomes the primary source of variability in d*a*/d*N*. The variability associated with a given lot of material is caused by inhomogeneities in chemical composition, microstructure, or both. These same factors coupled with varying processing conditions give rise to further lot-to-lot variabilities. An assessment of inherent material variability, either within or between heats or lots, can only be determined by conducting a statistically planned test program on the material of interest. Thus, results cited above from the interlaboratory test programs on 10 Ni steel and 2219–T851 aluminum, materials selected to minimize material variability and therefore allow an assessment of measurement precision, are not generally applicable to questions regarding inherent variability in other materials.

11.2 *Bias*—There is no accepted "standard" value for d*a*/d*N* versus Δ*K* for any material. In the absence of such a true value, no meaningful statement can be made concerning bias of data.

12. Keywords

12.1 constant amplitude; crack size; fatigue crack growth rate; stress intensity factor range

[8] Supporting data have been filed at ASTM International Headquarters and may be obtained by requesting Research Report RR:E08-1007.

[9] Supporting data have been filed at ASTM International Headquarters and may be obtained by requesting Research Report RR:E24-1009.

ANNEXES

(Mandatory Information)

A1. THE COMPACT SPECIMEN

A1.1 Introduction

A1.1.1 The compact specimen, C(T), is a single edge-notch specimen loaded in tension.

A1.1.2 The C(T) specimen has the advantage over many other specimen types in that it requires the least amount of test material to evaluate crack growth behavior.

A1.1.3 The C(T) specimen is not recommended for tension-compression testing because of uncertainties introduced into the loading experienced at the crack tip.

A1.1.4 The C(T) specimen is not recommended for materials that utilize a whisker-type of discontinuous reinforcement and are anisotropic in nature; rather, the M(T) or ESE(T) specimens should be used.[10]

A1.2 Specimen

A1.2.1 The geometry of the standard C(T) specimen is given in Fig. A1.1.

[10] Subcommittee E08.09 has performed an interlaboratory test program on a material of this type. Reference (**32**) provided the results of this effort.

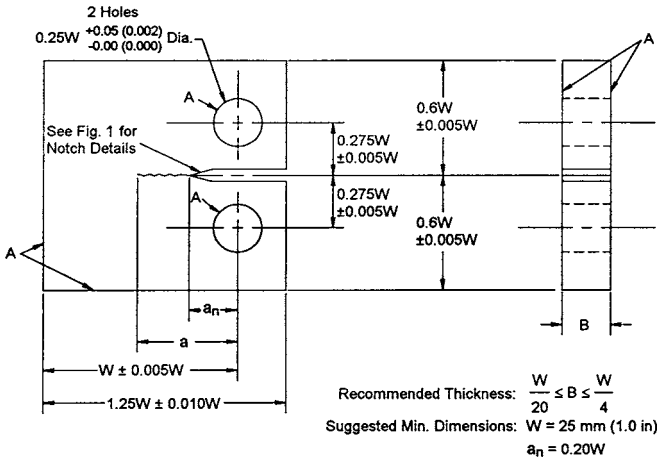

NOTE 1—Dimensions are in millimetres (inches).

NOTE 2—*A*-surfaces shall be perpendicular and parallel as applicable to within ±0.002 *W*, TIR.

NOTE 3—The intersection of the tips of the machined notch (a_n) with the specimen faces shall be equally distant from the top and bottom edges of the specimen to within 0.005 *W*.

NOTE 4—Surface finish, including holes, shall be 1.6 µm (63 µin.) or better. A surface finish of 0.8 µm (32 µin.) or better on the specimen faces may provide a better surface for making optical measurements of the crack.

FIG. A1.1 Standard Compact C(T) Specimen for Fatigue Crack Growth Rate Testing

A1.2.2 The thickness, *B*, and width, *W*, may be varied independently within the following limits, which are based on specimen buckling and through-thickness crack-curvature considerations:

A1.2.2.1 For C(T) specimens it is recommended that thickness be within the range $W/20 \le B \le W/4$. Specimens having thicknesses up to and including *W*/2 may also be employed; however, data from these specimens will often require through-thickness crack curvature corrections as listed in Section 9.1 of the main body of E647. In addition, difficulties may be encountered in meeting the through-thickness crack straightness requirements listed in Section 8 *Procedure* section of the main body of E647.

A1.2.3 In the C(T) specimen (Fig. A1.1), *a* is measured from the line connecting the bearing points of force application.

A1.2.4 It is required that the machined notch, a_n, in the C(T) specimen be at least 0.2*W* in length so that the *K*-calibration is not influenced by small variations in the location and dimensions of the loading-pin holes.

A1.2.5 Notch and precracking details for the C(T) specimen are given in Fig. 1 of the main body of E647.

A1.2.6 *Specimen Size*—In order for results to be valid according to this test method it is required that the specimen be predominantly elastic at all values of applied force. The minimum in-plane specimen sizes to meet this requirement are based primarily on empirical results and are specific to specimen configuration (**10**).

A1.2.6.1 For the C(T) specimen the following is required:

$$(W - a) \ge (4/\pi)(K\max/\sigma_{YS})^2 \qquad (A1.1)$$

where:

$(W - a)$ = specimen's uncracked ligament (Fig. A1.1), and

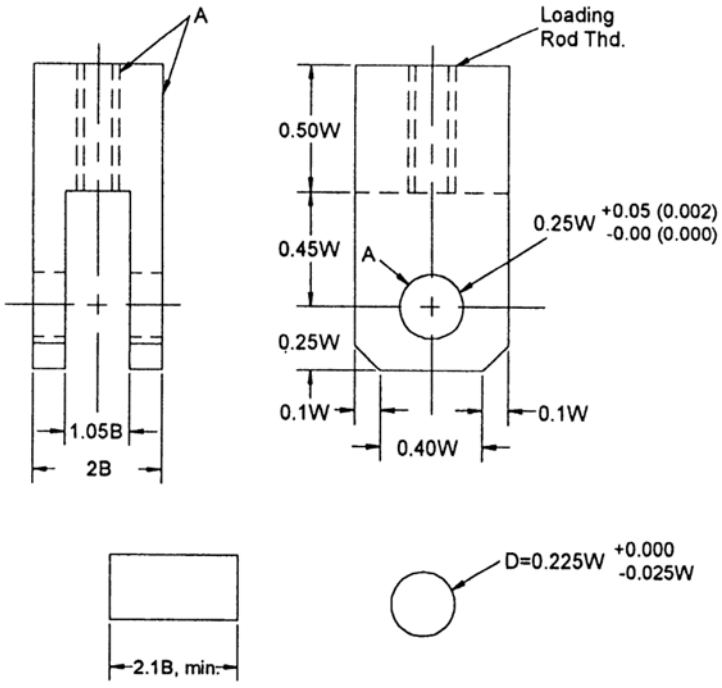

NOTE 1—Dimensions are in millimeters (inches).

A-surfaces shall be perpendicular and parallel as applicable to within ± 0.05 mm (0.002 in.) TIR.

Surface finish of holes and loading pins shall be 0.8 (32) or better.

FIG. A1.2 Clevis and Pin Assembly for Gripping C(T) Specimens

σ_{YS} = 0.2 % offset yield strength determined at the same temperature as used when measuring the fatigue crack growth rate data.

NOTE A1.1—For high-strain hardening materials, see Note 6 of the main body of E647.

A1.3 Apparatus

A1.3.1 *Grips and Fixtures for C(T) Specimens*—A clevis and pin assembly (Fig. A1.2) is used at both the top and bottom of the specimen to allow in-plane rotation as the specimen is loaded. This specimen and loading arrangement is to be used for tension-tension loading only.

A1.3.1.1 Suggested proportions and critical tolerances of the clevis and loading pin are given (Fig. A1.2) in terms of either the specimen width, *W*, or the specimen thickness, *B*, since these dimensions may be varied independently within certain limits.

A1.3.1.2 The pin-to-hole clearances illustrated in Fig. A1.2 are designed to reduce nonlinear force vs. displacement behavior caused by rotation of the specimen and pin (**33**). Using this arrangement to test materials with relatively low yield strength may cause plastic deformation of the specimen hole. Similarly, when testing high strength materials or when the clevis opening exceeds 1.05B (or both), a stiffer loading pin (that is, >0.225*W*) may be required. In these cases, a flat bottom clevis hole or bearings may be used with the appropriate loading pins (D = 0.24*W*) as indicated in Fig. A1.3. The use of high viscosity lubricants such as grease may introduce hysteresis in the force vs. displacement behavior and is not recommended.

A1.3.1.3 Using a 1000-MPa (150-ksi) yield-strength alloy (for example, AISI 4340 steel) for the clevis and pins provides adequate strength and resistance to galling and fatigue.

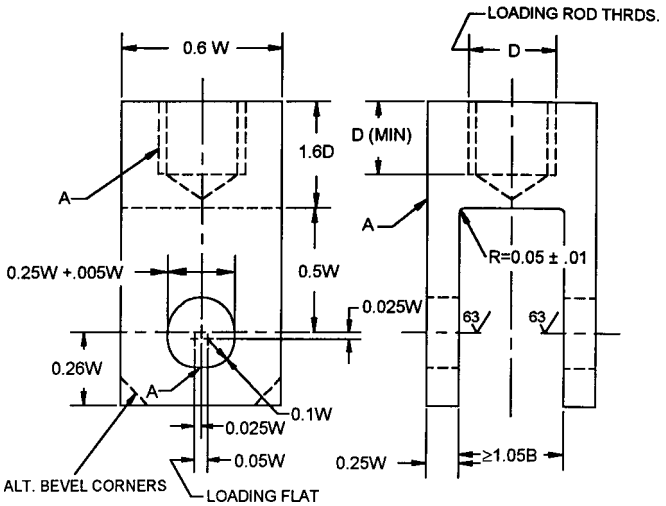

NOTE 1—Pin diameter = 0.24 W – 0.005 W.

NOTE 2—Flat bottom hole is a modified Test Method E399 design.

NOTE 3—Corners of clevis may be removed if necessary to accommodate clip gage.

A—surfaces must be flat, in-line, and perpendicular, as applicable, to within 0.05 mm.

FIG. A1.3 Two Suggested Clevis Designs for C(T) Specimen Testing

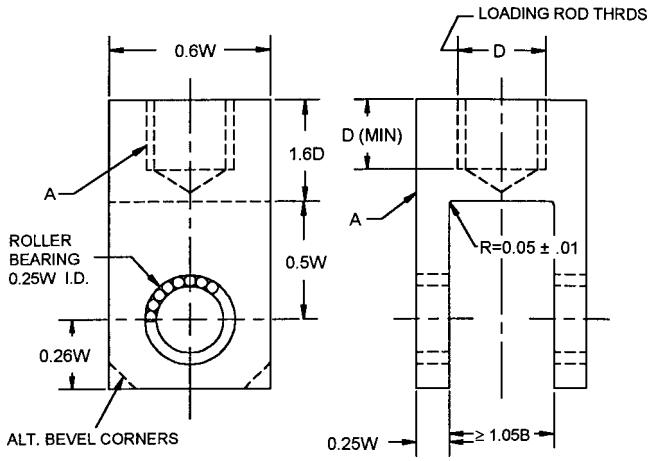

NOTE 1—Because of space requirements for the bearings, this grip is not practicable for small specimens.

A—surfaces must be flat, in-line, and perpendicular, as applicable, to within 0.05 mm.

FIG. A1.3 *(continued)*

A1.4 Procedure

A1.4.1 Make crack size measurements at intervals such that d*a*/d*N* data are nearly evenly distributed with respect to Δ*K*. For the C(T) specimen, the suggested intervals are:

$$\Delta a \le 0.04\ W \text{ for } 0.25 \le a/W \le 0.40 \qquad \text{(A1.2)}$$

$$\Delta a \le 0.02W \text{ for } 0.40 \le a/W \le 0.60$$

$$\Delta a \le 0.01\ W \text{ for } a/W \ge 0.60$$

If crack size is measured visually, the average value of the two surface crack lengths for the C(T) specimen should be used in all calculations of growth rate and *K* when using the *K* expression listed in A1.5.1.1. Further crack symmetry requirements are given in Section 8.3.4 of the main body of E647. Out-of-plane cracking limits are given in Section 8.8.3 of the main body of E647.

A1.5 Calculation and Interpretation of Results

A1.5.1 *Determination of Stress-Intensity Factor Range, ΔK*-Use the crack size values of Section 9.1 of the main body of E647 and Appendix X1 to calculate the stress-intensity range corresponding to a given crack growth rate from the following expressions:

A1.5.1.1 For the C(T) specimen calculate Δ*K* as follows:

$$\Delta K = \frac{\Delta P}{B\sqrt{W}} \frac{(2+\alpha)}{(1-\alpha)^{3/2}} (0.886 + 4.64\alpha - 13.32\alpha^2 + 14.72\alpha^3 - 5.6\alpha^4) \qquad \text{(A1.3)}$$

where α = *a*/*W*; expression valid for *a*/*W* ≥ 0.2 (**34**, **35**).

NOTE A1.2—Implicit in the above expression is the assumption that the test material is linear-elastic, isotropic, and homogeneous.

NOTE A1.3—The above operational definition does not include potential effects of residual stress or crack closure on the computed Δ*K* value. Autographic force versus crack mouth opening displacement traces are useful for detecting and correcting residual stress/crack closure influences (**3**).

A1.5.1.2 Check for compliance with the specimen size requirements of A1.2.6.

A1.5.2 *Determination of Crack Size by Compliance*—The crack size of a C(T) specimen can be determined by compliance procedures outlined in Annex A5.

A1.5.2.1 Theoretical compliance expressions for the specific measurement locations on the C(T) specimen are presented in Fig. A1.4 (**36**). Additional measurement locations are available through the use of rotation coefficients. This equation is for plane stress since this stress state is most applicable to measurements remote to the crack tip, regardless of the stress state local to the crack tip.

NOTE A1.4—For a C(T) specimen of $W = 40$ mm, a gage located at any of the four locations shown in Fig. A1.4 and calibrated to 50 μm/volt on a ±10 volt range will generally provide sufficient resolution.

A1.5.2.2 Gripping techniques for specimens that undergo bending, such as the C(T) specimen, have been observed to affect compliance readings. The C(T) specimen may be loaded with grips that have either flat bottom holes or needle bearings, as shown in Fig. A1.3, to circumvent such problems.

A1.5.3 *Determination of Crack Size by Electric Potential Difference (EPD)*—The crack size of a C(T) specimen can be determined by electric potential difference (EPD) procedures outlined in Annex A6.

A1.5.3.1 *C(T) Geometry Voltage versus Crack Size Relationships*—An example of a voltage versus crack size relationship for the C(T) specimen geometry is shown in Eq A1.4. The expression was developed by Hicks and Pickard from finite element analysis and was verified through both analogue and experimental techniques for a/W ranging from 0.24 to 0.7 (**38**). This equation has been employed in two multi-laboratory, international co-operative testing efforts (**39, 40**).

$$V/V_r = A_o + A_1(a/W) + A_2(a/W)^2 + A_3(a/W)^3 \qquad (A1.4)$$

$$\text{for } 0.24 \le a/W \le 0.7$$

where:

V = the measured EPD voltage,
V_r = the reference crack voltage corresponding to a/W = 0.241,
a = the crack size (as defined in Test Method E647),
W = the specimen width,
A_o = 0.5766,
A_1 = 1.9169,
A_2 = –1.0712, and
A_3 = 1.6898

or in reverse notation:

$$a/W = B_o + B_1(V/V_r) + B_2(V/V_r)^2 + B_3(V/V_r)^3 \qquad (A1.5)$$

$$\text{for } 0.24 \le a/W \le 0.7$$

where:

B_o = –0.5051,
B_1 = 0.8857,
B_2 = –0.1398,
B_3 = 0.0002398.

A1.5.3.2 Fig. A1.5 illustrates the C(T) geometry and specific wire placement locations for this solution. The relationship is valid only for the wire locations shown, which were determined by a compromise between sensitivity and reproducibility. If alternative wire placements (current or voltage) are used, the relationship shown is no longer valid and a new relationship must be developed.

A1.5.3.3 Note that the first form of the equation can be used to compute the constant V_r from any reference a/W and corresponding voltage measurement V. Computing V_r in this way accounts linearly for small changes in applied current, measured specimen dimensions, and slight errors in wire placement from specimen to specimen. The computed reference voltage can then be used with the second form of the equation to determine the crack size for all voltage values V.

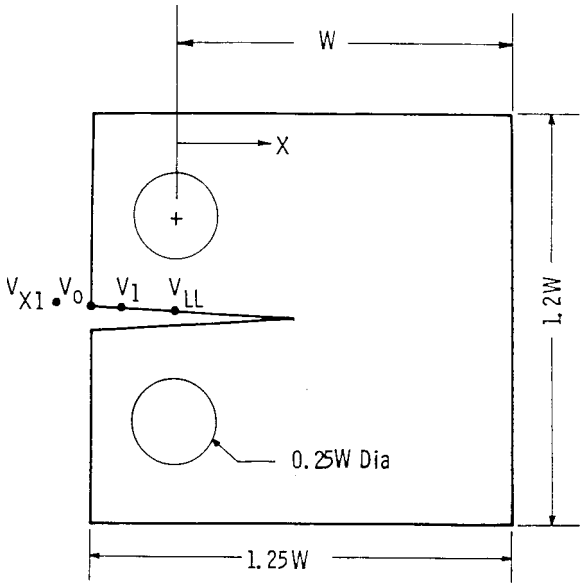

Meas. Location	*X/W*	C_0	C_1	C_2	C_3	C_4	C_5
			C(T) Specimen				
V_{X1}	−0.345	1.0012	−4.9165	23.057	−323.91	1798.3	−3513.2
V_0	−0.250	1.0010	−4.6695	18.460	−236.82	1214.9	−2143.6
V_1	−0.1576	1.0008	−4.4473	15.400	−180.55	870.92	−1411.3
V_{LL}	0	1.0002	−4.0632	11.242	−106.04	464.33	−650.68

$$\alpha = a/W = C_0 + C_1 u_X + C_2 u_X^2 + C_3 u_X^3 + C_4 u_X^4 + C_5 u_X^5$$

$$u_x = \left\{ \left[\frac{EvB}{P} \right]^{\frac{1}{2}} + 1 \right\}^{-1}$$

$$0.2 \leq a/W \leq 0.975$$

FIG. A1.4 Normalized Crack Size as a Function of Plane Stress Elastic Compliance for C(T) Specimens (37).

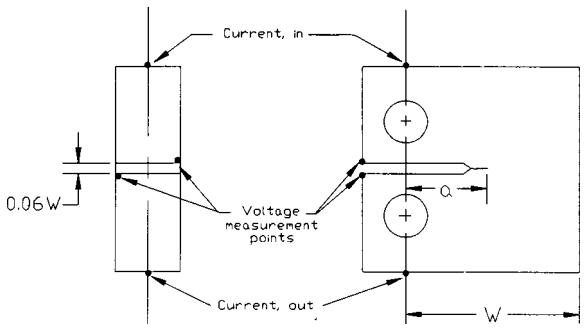

FIG. A1.5 C(T) Geometry and Electric Potential Wire Placement Locations for Eq A1.4 (41)

A2. THE MIDDLE TENSION SPECIMEN

A2.1 Introduction

A2.1.1 The middle tension, M(T), specimen is a center crack specimen that can be loaded in either tension-tension or tension-compression.

A2.1.2 The M(T) specimen has the advantage over many other specimen types in that it allows for fatigue loading under both positive and negative force ratios (R).

A2.1.3 In the near threshold regime (below 10^{-8} m/cycle), one can experience difficulty in meeting the crack symmetry requirements listed in this method when using the M(T) specimen; the C(T) or ESE(T) specimens may be appropriate alternatives, provided that R≥0.

A2.2 Specimen Configuration, Size, and Preparation

A2.2.1 The general geometry of the M(T) specimen is given in Fig. A2.1, however the specific geometry depends on the method of gripping as specified in A2.3.

A2.2.2 For the M(T) specimen, the thickness, *B*, and width, *W*, may be varied independently within the following limits, which are based on specimen buckling and through-thickness crack-curvature considerations.

A2.2.2.1 For M(T) specimens it is recommended that upper limit on thickness be within the range $W/8 \le B \le W/4$. The minimum thickness necessary to avoid excessive lateral deflections or buckling is sensitive to specimen gage length, grip alignment, and stress ratio, *R*. It is recommended that strain gage information be obtained for the particular specimen geometry and loading condition of interest and that bending strains not exceed 5 % of the nominal strain.

A2.2.3 In the M(T) specimen (Fig. A2.1), *a* is measured from the perpendicular bisector of the central crack.

A2.2.3.1 The machined notch, $2a_n$, in the M(T) specimen shall be centered with respect to the specimen centerline to within $\pm 0.001W$. The length of the machined notch in the M(T) specimen will be determined by practical machining considerations and is not restricted by limitations in the *K*-calibration.

A2.2.4 It is recommended that $2a_n$ be at least $0.2W$ when using the compliance method to monitor crack extension in the M(T) specimen so that accurate crack size determinations can be obtained.

A2.2.5 Notch and precracking details for the specimen are given in Fig. 1 of the main body of E647.

A2.2.6 *Specimen Size*—In order for results to be valid according to this test method it is required that the specimen be predominantly elastic at all values of applied force. The minimum in-plane specimen sizes to meet this requirement are based primarily on empirical results and are specific to specimen configuration (**10**).

A2.2.6.1 For the M(T) specimen the following is required:

$$(W - 2a) \ge 1.25\,P_{max}/(B\sigma_{YS}) \qquad (A2.1)$$

where:

$(W - 2a)$ = specimen's uncracked ligament (Fig. 2),
B = specimen thickness, and
σ_{YS} = 0.2 % offset yield strength determined at the same temperature as used when measuring the fatigue crack growth rate data.

NOTE A2.1—For high-strain hardening materials, see Note 6 of the main body of E647.

A2.3 Apparatus

A2.3.1 *Grips and Fixtures for M(T) Specimens*—The types of grips and fixtures to be used with the M(T) specimens will depend on the specimen width, *W*, (defined in Fig. A2.1), and the loading conditions (that is, either tension-tension or tension-compression loading). The minimum required specimen gage length varies with the type of gripping and is specified so that a uniform stress distribution is developed in the specimen gage length during testing. For testing of thin sheets, constraining plates may be necessary to minimize specimen buckling (see Practice E561 for recommendations on buckling constraints).

A2.3.1.1 For tension-tension loading of specimens with $W \le$ 75 mm (3 in.) a clevis and single pin arrangement is suitable for gripping provided that the specimen gage length (that is, the distance between loading pins) is at least $3W$ (Fig. A2.1). For this arrangement it is also helpful to either use brass shims between the pin and specimen or to lubricate the pin to prevent fretting-fatigue cracks from initiating at the specimen loading hole. Additional measures which may be taken to prevent cracking at the pinhole include attaching reinforcement plates to the specimen (for example, see Test Method E338) or employing a "dog bone" type specimen design. In either case, the gage length shall be defined as the uniform section and shall be at least $1.7W$.

A2.3.1.2 For tension-tension loading of specimens with $W \ge$ 75 mm (3 in.) a clevis with multiple bolts is recommended (for

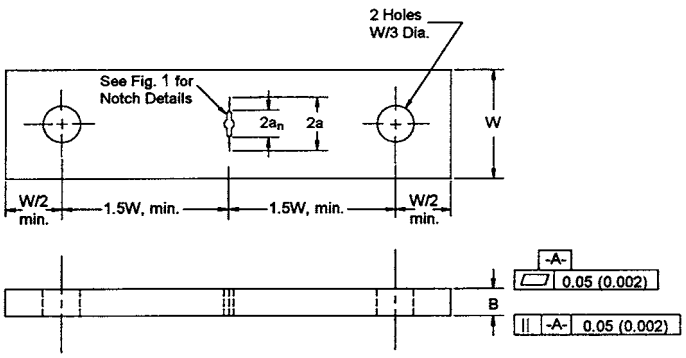

NOTE 1—Dimensions are in millimetres (inches).

NOTE 2—The machined notch ($2a_n$) shall be centered to within ± 0.001 *W*.

NOTE 3—For specimens with $W > 75$ mm (3 in.) a multiple pin gripping arrangement is recommended, similar to that described in Practice 561.

NOTE 4—Surface finish, including holes, shall be 0.8 (32) or better.

FIG. A2.1 Standard Middle-Tension M(T) Specimen for Fatigue Crack Growth Rate Testing when $W \le 75$ mm (3 in.)

example, see Practice E561). In this arrangement, the forces are applied more uniformly; thus, the minimum specimen gage length (that is, the distance between the innermost row of bolt holes) is relaxed to 1.5*W*.

A2.3.1.3 The M(T) specimen may also be gripped using a clamping device instead of the above arrangements. This type of gripping is necessary for tension-compression loading. An example of a specific bolt and keyway design for clamping M(T) specimens is given in Fig. A2.2, where the gage length (total free distance between the clamping elements) is 2L. In addition, various hydraulic and mechanical-wedge systems which supply adequate clamping force are commercially available and may be used. The minimum gage length requirement for clamped specimens for which the K-expression in A2.5.1.1 is valid is 2.0*W*(**42**).

A2.4 Procedure

A2.4.1 *Fatigue Precracking*—The importance of precracking is to provide a sharpened fatigue crack of adequate size, straightness, and symmetry for the M(T) specimen.

A2.4.1.1 In addition to the requirements listed in 8.3.4 of the main body, for the M(T) specimen, measurements referenced from the specimen centerline to the two cracks (for each crack use the average of measurements on front and back surfaces) shall not differ by more than 0.025W when using the K expression listed in A2.5.1.1.

A2.4.2 Make crack size measurements at intervals such that d*a*/d*N* data are nearly evenly distributed with respect to Δ*K*. For the M(T) specimen, the suggested intervals are:

$$\Delta a \le 0.03W \text{ for } 2a/W < 0.60 \qquad \text{(A2.2)}$$

$$\Delta a \le 0.02W \text{ for } 2a/W > 0.60$$

If crack size is measured visually, the average value of the four surface crack lengths for the M(T) specimen should be used in all calculations of growth rate and *K* when using the K expression listed in A2.5.1.1.

A2.4.3 In addition to the requirements listed in 8.8.3 of the main body, data are invalid if measurements referenced from the specimen centerline to the two cracks (for each crack, use the average of measurements on front and back surfaces) differ by more than 0.025*W* when using the K expression furnished in A2.5.1.1.

A2.5 Calculation and Interpretation of Results

A2.5.1 *Determination of Stress-Intensity Factor Range, ΔK*-Use the crack size values of 9.1 in the main body and Appendix X1 to calculate the stress-intensity range corresponding to a given crack growth rate from the following expression.

A2.5.1.1 For the M(T) specimen calculate Δ*K* consistent with the definitions of 3.2 in the main body; that is:

$$\Delta P = P\max - P\min \text{ for } R > 0 \qquad \text{(A2.3)}$$

$$\Delta P = P\max \text{ for } R \le 0$$

in the following expression (27):

$$\Delta K = \frac{\Delta P}{B}\sqrt{\frac{\pi\alpha}{2W}\sec\frac{\pi\alpha}{2}} \qquad \text{(A2.4)}$$

where $\alpha = 2a/W$; This expression is accurate to within 2% for $2a/W \le 0.9$ for the pin-loaded sample in Fig. A2.1. For the clamped-end case described in A2.3.1.3 and Fig. A2.2, the K expression is accurate to within 1% for $2a/W \le 0.8$.

NOTE A2.2—Implicit in the above expressions is the assumption that the test material is linear-elastic, isotropic, and homogeneous.

NOTE A2.3—The above operational definitions do not include potential effects of residual stress or crack closure on the computed Δ*K* value. Autographic force versus crack mouth opening displacement traces are useful for detecting and correcting residual stress/crack closure influences (**3**).

A2.5.1.2 Check for conformity with the specimen size requirements of A2.2.6.

A2.5.2 *Determination of Crack Size by Compliance*—The crack size of an M(T) specimen can be determined by compliance procedures outlined in Annex A5.

A2.5.2.1 An equation for the compliance measured on the centerline of the M(T) specimen is shown in Fig. A2.3 (**43**). This equation is for plane stress since this stress state is most applicable to measurements remote to the crack tip, regardless of the stress state local to the crack tip.

NOTE A2.4—An M(T) specimen of $W = 80$ mm and $2y/W \le 0.4$ will require a gage calibration of 15 μm/V on the same range. The increased resolution required for the M(T) specimen is caused by its greater stiffness which makes it less amenable to this form of nonvisual crack size monitoring. M(T) specimen compliance readings are also complicated by small, normally acceptable levels of bending.

A2.5.3 *Determination of Crack Size by Electric Potential Difference (EPD)*—The crack size of an M(T) specimen can be determined by electric potential difference (EPD) procedures outlined in Annex A6.

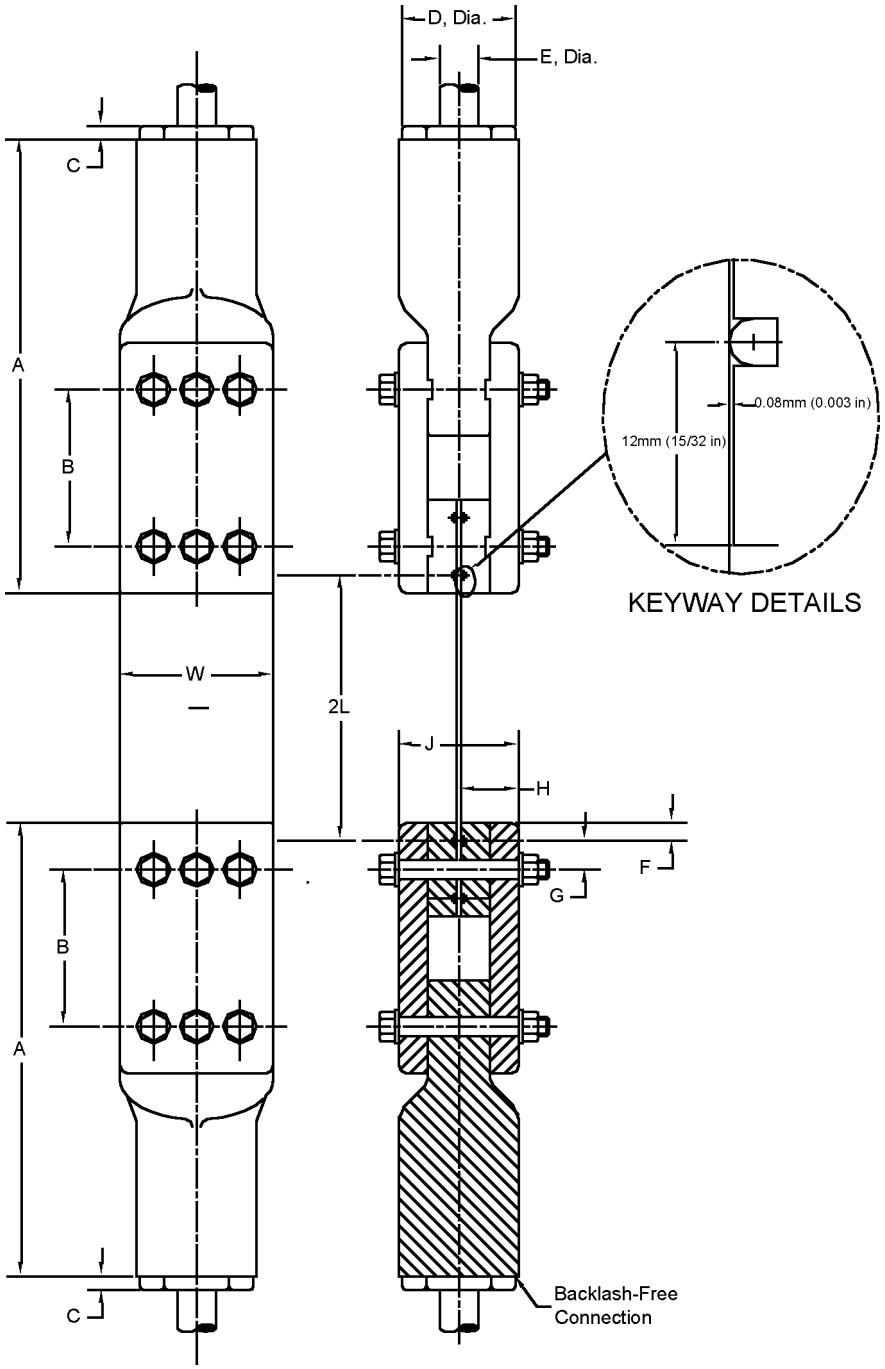

Table of Dimensions

	mm	in
A	326	12 27/32
B	104	4 3/32
C	19	3/4
D	76	3
E	38	1 1/2[A]
F	12	15/32
G	19	3/4
H	38	1 1/2
J	76	3
2L	200	8
W	100	4

[A] 12 NF, Class 2

FIG. A2.2 Example of Bolt and Keyway Assembly for Gripping 100-mm (4-in.) wide M(T) Specimen

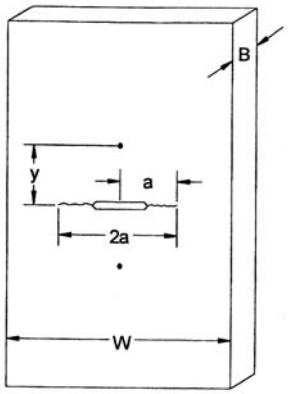

Middle-Tension, M(T) Specimen

a	=	crack length,
B	=	specimen thickness,
W	=	specimen width,
C	=	$^{v}/_{P}$ = compliance,
E	=	Young's modulus,
y	=	half gage length,
η	=	$^{2y}/_{W}$ = nondimensional gage length

$$^{2a}/_{W} = 1.06905x + 0.588106x^2 - 1.01885x^3 + 0.361691x^4$$

where:

$$x = 1 - e^{\left(\frac{-\sqrt{(EBC+\eta)(EBC-\eta+c_1\eta+c_2\eta^{c_3})}}{2.141}\right)}$$

NOTE 1—This expression is valid for (1) $0 \le 2y/W \le 1.0$, and (2) $0 \le 2a/W \le 1.0$. Values of c_1, c_2, and c_3 are dependent on loading conditions and are shown below for three examples.

FIG. A2.3 Plane Stress Compliance Expression for the M(T) Specimen (43).

Models of Laboratory Test Specimens

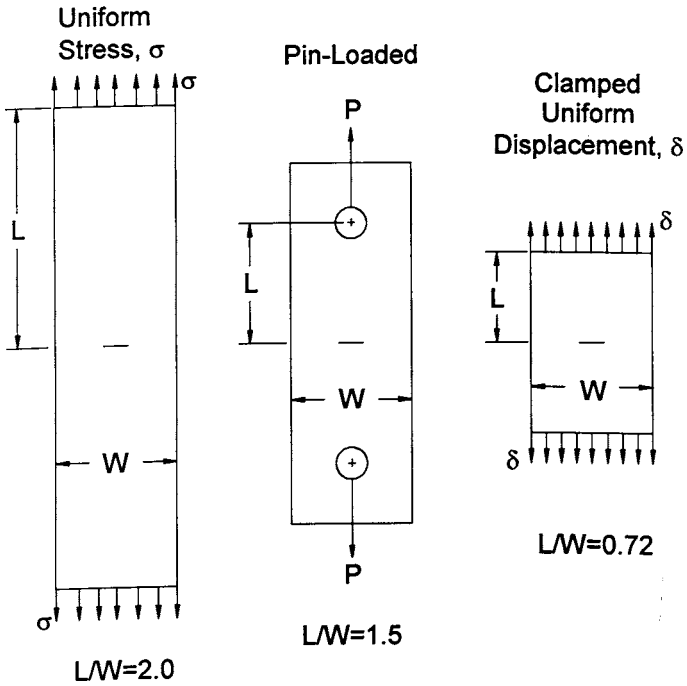

Modification to *x*(*EBC, 2y/W*) for Different Loading Conditions

Uniform Stress	Pin-Loaded	Clamped Uniform Displacement
$c_1 = 0.0$	$c_1 = 0.005$	$c_1 = -0.03$
$c_2 = 0.0$	$c_2 = 0.0184$	$c_2 = 0.013$
$c_3 = 0.0$	$c_3 = 3.0$	$c_3 = 4.0$

FIG. A2.3 *(continued)*

A2.5.3.1 *M(T) Geometry Voltage versus Crack Size Relationship*—A closed form analytical voltage versus crack size relationship for an infinitely long M(T) specimen (**44**) is shown below.

$$\frac{a}{} = \frac{W}{\pi} COS^{-1}\left[\frac{COSH\left(\frac{\pi}{W}\times Y_o\right)}{COSH\left[\frac{V}{V_r}\times COSH^{-1}\cdot\left[\frac{COSH\left(\frac{\pi}{W}\times Y_o\right)}{COS\left(\frac{\pi}{W}\times a_r\right)}\right]\right]}\right] \quad \text{(A2.5)}$$

$$\text{for } 0 \le \frac{2a}{W} \le 1$$

where:

a	=	the crack size (as defined in Test Method E647),
a_r	=	the reference crack size from some other method,
W	=	the specimen width,
V	=	the measured EPD voltage,
V_r	=	the measured voltage corresponding to a_r, and
Y_o	=	the voltage measurement lead spacing from the crack plane.

This relationship is valid only in cases where the current density is uniform at some cross section of the specimen remote from the crack plane and the voltage is measured on the centerline of the specimen across the crack plane. Fig. A2.4 illustrates the M(T) geometry and wire placement locations for this solution.

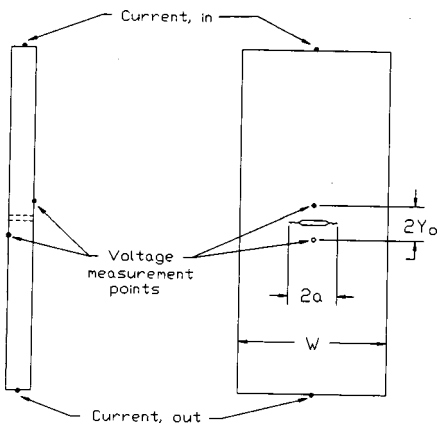

FIG. A2.4 M(T) Geometry and Electric Potential Wire Displacement Locations for Eq A2.5 (44)

The requirement that current density be uniform at some cross section remote from the crack plane can be easily met by introducing the current through the standard M(T) specimen ends, with a distance between current input locations of approximately three times the width. Shorter current lead spacing may also be used provided that the uniform current density requirement be demonstrated. The calibration constants a_o and V_o may be any crack size and corresponding voltage measurement where the crack size has been determined using an alternate method. Optical surface measurements may be used to determine a_o provided crack front curvature is not significant or is accounted for. If real time crack size measurements are not required during the test, post-test fracture surface measurements may be used to determine a_o.

A3. THE ECCENTRICALLY-LOADED SINGLE EDGE CRACK TENSION SPECIMEN

A3.1 Introduction

A3.1.1 The eccentrically-loaded single edge crack tension specimen ESE(T) is a single edge-cracked specimen similar to the C(T) specimen loaded in tension-tension. (**45-47**).

A3.1.2 The standard ESE(T) can exhibit advantages over other specimen types. The following paragraphs list possible advantages.

A3.1.2.1 The elongated (extended) design gives the experimenter additional working space compared to the standard compact C(T) specimen configuration. This configuration lends itself to attaching complex displacement or strain gage measurement systems and environmental cells (**48**).

A3.1.2.2 The specimen configuration requires lower applied forces for equivalent crack tip stress-intensity factor compared to other specimen configurations, such as the middle-crack tension M(T) specimen. This results in lower net section stress and reduces the likelihood of premature fracture of sheet materials tested in highly corrosive environments.

A3.1.2.3 The specimen design reduces the T-stress (stress parallel to crack surface) and crack fracture paths are more self-similar than in the standard C(T) specimen (**49**).

A3.1.2.4 The specimen design is compatible with common automated techniques for the measurement of through-the-thickness crack sizes.

A3.2 Specimen

A3.2.1 The general proportions of the ESE(T) specimen configuration are given in Fig. A3.1.

A3.2.2 It is recommended that the ESE(T) specimen thickness be in the range $W/20 \le B \le W/4$.

A3.2.3 *Specimen Size*—In order for results to be valid according to this test method it is required that the specimen be predominantly elastic at all values of applied force. For the ESE(T) specimen the following is required:

$$(W - a) \ge (4/\pi)(K\max/\sigma_{YS})^2 \qquad (A3.1)$$

where:

$(W - a)$ = specimen's uncracked ligament (Fig. A3.1), and
σ_{YS} = 0.2 % offset yield strength determined at the same temperature as used when measuring the fatigue crack growth rate data.

NOTE A3.1—For high-strain hardening materials, see Note 5 of the main body of E647.

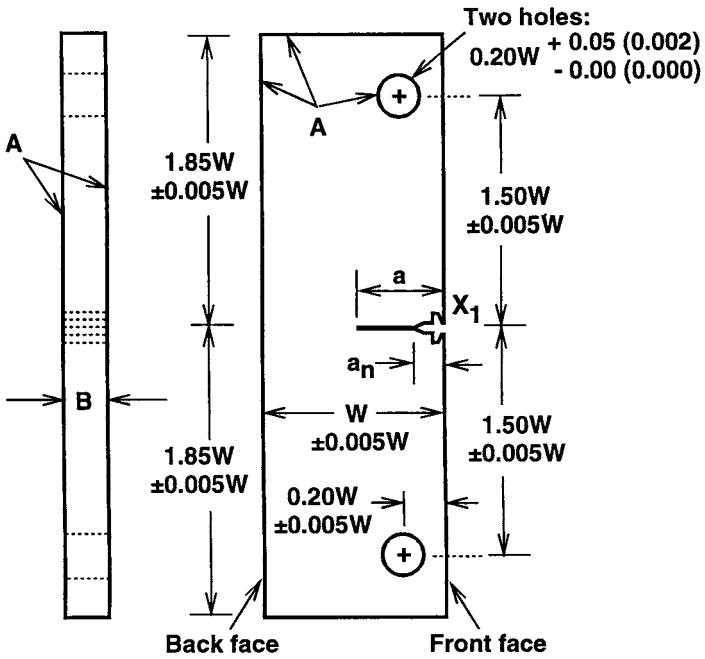

NOTE 1—Dimensions are in millimeters (inches).

NOTE 2—A-surfaces perpendicular and parallel (as applicable) to within ±0.002W, TIR.

NOTE 3—Intersection of the machined notch with the specimen face shall be equi-distant from top and bottom of the specimen to within 0.005W.

NOTE 4—Surface finish, including holes, shall be 0.8(32) or better.

FIG. A3.1 Standard Eccentrically-Loaded Single Edge Crack Tension Specimen.

A3.3 Apparatus

A3.3.1 Tension testing clevis and displacement gage apparatus are to be identical to that used by the C(T) specimen.

NOTE A3.2—The clevis pin is to be sized to 0.175W (+0.000, –0.025W).

A3.4 Procedure

A3.4.1 *Measurement*—Measure the width, *W*, and the crack size, *a*, from the specimen front face as shown in Fig. A3.1.

A3.4.2 ESE(T) *Specimen Testing*—All testing procedures are similar to the C(T) specimen.

A3.5 Calculations

A3.5.1 *Determination of Stress-Intensity Factor Range, ΔK*—For the ESE(T) specimen, calculate ΔK as follows (**46**).

$$\Delta K = [\Delta P/(B\sqrt{W})]\, F \quad \text{(A3.2)}$$

and

$$F = \alpha^{1/2}[1.4+\alpha][1-\alpha]^{-3/2}G \quad \text{(A3.3)}$$

where

$$G = 3.97 - 10.88\alpha + 26.25\alpha^2 - 38.9\alpha^3 + 30.15\alpha^4 - 9.27\alpha^5 \quad \text{(A3.4)}$$

$$\alpha = a/W$$

for $0 < \alpha < 1$.

A3.5.2 *Determination of Crack Size by Compliance*—The determination of crack size by the compliance methods outlined in Annex A5 can be conducted at the ESE(T) front-face and back-face locations.

A3.5.2.1 *Front-face compliance*—The following expressions were derived for monitoring crack size by measuring the displacement (v) at the front face. The term v_0 is the displacement at the front face knife edge location shown in Fig. A3.1 (**46, 50**).

$$a/W = M_0 + M_1 U + M_2 U^2 + M_3 U^3 + M_4 U^4 + M_5 U^5 \quad \text{(A3.5)}$$

where:

$U = [(EBv_0/P)^{1/2} + 1]^{-1}$
$M_0 = 1.00132$
$M_1 = -3.58451$
$M_2 = 6.599541$
$M_3 = -19.22577$
$M_4 = 41.54678$
$M_5 = -31.75871$

for $0.1 \le a/W \le 0.84$.

Normalized compliance in terms of crack size is given by

$$EBv_0/P = [15.52\ a/W - 26.38\ (a/W)^2 + 49.7\ (a/W)^3 - 40.74\ (a/W)^4 + 14.44\ (a/W)^5]/[1 - a/W]^2 \quad \text{(A3.6)}$$

for $0 < a/W < 1$.

A3.5.2.2 *Back-face compliance*—The following expression was derived for monitoring crack size by measuring strains at the back-face. Here, back-face strain, ε, is measured at a location along the crack plane similar to the C(T) specimen, shown in Fig. X2.1 of the standard.

$$a/W = N_0 + N_1(\log A) + N_2(\log A)^2 + N_3(\log A)^3 + N_4(\log A)^4 \quad \text{(A3.7)}$$

where:

$A = -(\varepsilon/P)BWE$
$N_0 = 0.09889$
$N_1 = 0.41967$
$N_2 = 0.06751$
$N_3 = -0.07018$
$N_4 = 0.01082$

for $0.1 \le a/W \le 0.84$.

A3.5.3 *Determination of Crack Size by Electrical Potential Difference*—The crack size of an ESE(T) specimen can be determined by electric potential difference (EPD) procedures outlined in Annex A6. Crack size determinations may be performed using the Johnson's equation (**44, 51**). Typical electrical potential wire placement locations are similar to the C(T) specimen, refer to Fig. A1.4 of the C(T) specimen annex.

NOTE A3.3—The Johnson equation, based on the electrostatic analysis of a finite width plate with an infinitesimally thin central slot, has been shown to give accurate results for M(T) specimens. Its use with the ESE(T) specimen configuration, however, must be experimentally verified.

A4. SPECIAL REQUIREMENTS FOR TESTING IN AQUEOUS ENVIRONMENTS

A4.1 Introduction

A4.1.1 Fatigue crack growth rates in metallic materials exposed to aqueous environments can vary widely as a function of mechanical, metallurgical, and electrochemical variables. Therefore, it is essential that test results accurately reflect the effects of specific variables under study. Test methods must be chosen to represent steady state fatigue crack growth behavior which neither accentuates nor suppresses the phenomena under investigation. Only then can data be compared from one laboratory investigation to another on a valid basis, or serve as valid basis for characterizing materials and assessing structural behavior.

A4.2 Scope

A4.2.1 This annex covers the determination of fatigue crack growth rates using the test specimens described in this test method under test conditions involving temperatures and pressures at, or near, ambient.

A4.3 Referenced Documents

A4.3.1 *ASTM Standards*[3]:

D1129 Terminology Relating to Water

E742 Definitions of Terms Relating to Fluid Aqueous and Chemical Environmentally Affected Fatigue Testing

G1 Practice for Preparing, Cleaning, and Evaluating Corrosion Test Specimens

G3 Practice for Conventions Applicable to Electrochemical Measurements in Corrosion Testing

G5 Reference Test Method for Making Potentiostatic and Potentiodynamic Anodic Polarization Measurements

G15 Terminology Relating to Corrosion and Corrosion Testing

A4.4 Terminology

A4.4.1 The terms used in this annex are defined in the main body of this test method. Additional terms more specific to testing in aqueous environments can be found in Terminologies D1129 and G15 and Definitions E742.

A4.5 Significance and Use

A4.5.1 In aqueous environments, fatigue crack growth rates are a complex function of many experimental variables. These include prior force history, stress-intensity range, force ratio, cyclic frequency, force-versus-time wave-form, specimen thickness, crack geometry and size, electrolyte species and concentration, exposure time, flow rate, temperature, pH, dissolved oxygen content, and potential (free corrosion or applied). Background information on these effects can be found in Refs. **(52-59)**.

A4.5.2 Specimens which undergo fatigue crack growth rate testing in aqueous environments are subject to various corrosive effects which can either hasten or retard crack growth rates (see Refs. **(60)** and **(61)**). Generation of fatigue crack growth rate data on metallic materials in aqueous environments requires judicious selection, monitoring, and control of mechanical, chemical, and electrochemical test variables in order to ensure that the data are applicable to the intended use. For example, data generated in a laboratory test at a cyclic frequency of 10 Hz may not be applicable for predicting crack growth rates in a structure which is cycled at 0.1 Hz.

A4.5.3 Fatigue crack growth which occurs in the presence of an aqueous environment may be the product of both mechanical and chemical driving forces. The chemical driving force can vary with crack size, crack shape, and the degree of crack opening. Thus, fatigue crack growth rates in the presence of an aqueous environment may exhibit non-uniqueness when characterized in terms of da/dN versus ΔK, Ref. **(59)**.

A4.6 Apparatus

A4.6.1 The environmental chamber shall enclose the entire portion of the test specimen over which crack extension occurs. A circulation system to provide replenishment and aeration of the test solution may be desirable. Nonmetallic materials are recommended for the entire environmental chamber and circulation system. The environmental chamber should be designed so as to prevent galvanic contact between dissimilar test specimen and grip assembly components. If a circulation system is employed, the environmental chamber should be of sufficient size, and inlet and outlet locations should be chosen, to ensure a flow of test solution around the portion of the test specimen where crack extension occurs. A circulation system should provide for continuous aeration and filtration of the test solution in order to remove corrosion products. Exceptions to the above may occur if a quiescent solution is specifically desired.

A4.7 Procedure

A4.7.1 *Specimen Preparation*—It is recommended that specimens be cleaned prior to precracking and testing in accordance with Practice G1.

A4.7.2 *Specimen Precracking*—Preliminary precracking may be conducted in an ambient laboratory air environment using a cyclic frequency and waveform which differ from the test conditions. However, a final 1.0-mm increment (0.040-in. increment) of precracking shall be conducted in the aqueous environment under full test conditions.

A4.7.3 *General Test Procedure*—Fatigue crack growth rate testing in aqueous environments provides a means of detecting and assessing the effects of localized corrosion processes involving metal surfaces at crack tips. Thus, the corrosive environment must physically reach the crack-tip region and time-dependent corrosion processes must have sufficient opportunity to proceed. If test techniques fail to adequately promote and maintain localized corrosion in crack-tip regions throughout the full test duration, nonsteady-state conditions can affect the da/dN versus ΔK data. Therefore, testing shall be conducted in a manner which seeks to eliminate or minimize transient or nonsteady-state effects, or both, on da/dN versus ΔK data. Nonsteady-state or transient effects are defined as time-dependent fluctuations in da/dN values which do not directly correspond to any concomitant changes in mechanical crack driving force parameters, Ref. **(20)**.

A4.7.3.1 It is recommended that specimens be immersed in the full test environment for a suitable period of time immediately prior to precracking or gathering crack growth rate data, or both. A minimum period of 24 h is recommended.

A4.7.3.2 It is recommended that specimens undergoing fatigue testing remain immersed in the test solution during brief periods of test interruption. If specimens are removed from the test solution for more than a brief period, it is recommended that fatigue data gathering shall not resume until the crack has extended by a 1.0-mm increment (0.040-in. increment) under test conditions.

A4.7.3.3 It is recommended that specimens be visually examined periodically during the course of testing for evidence of corrosive attack. Corrosion product accumulation which may inhibit access of the test solution to the crack-tip region may be removed. The crack-tip region of the specimen surface may also be cleaned periodically to aid in visual observation of crack size or crack-tip morphology, or both. Upon completion of fatigue testing, it is recommended that the specimen be loaded to fracture and receive a thorough visual post-mortem examination.

A4.7.3.4 It is necessary to carefully monitor tests for evidence of environmentally-induced phenomena which may affect steady state da/dN versus ΔK data. The presence of an aqueous environment may cause numerous environmentally-induced phenomena to occur in the course of fatigue crack growth rate testing of metallic materials. Some common examples are transient changes in da/dN versus ΔK data in response to changes or interruptions in cyclic loading, crack growth acceleration or retardation, crack arrest, crack branching, crack-front curvature or irregularity, out-of-plane cracking, or corrosion product build-up within cracks.

A4.7.3.5 Steady state fatigue crack growth rates in aqueous environments can be strongly affected by cyclic waveform or cyclic frequency, or both. Knowledge of these effects can be an important consideration in selecting test parameters. It is

especially important to note that certain frequencies or waveforms, or both, can act to suppress the influence of aqueous environments on fatigue crack growth in metallic materials. These effects generally relate to the rise time of the loading cycle, Refs. (**53**) and (**55**). For steels and high-strength aluminum alloys, crack growth rates in aqueous environments tend to vary directly with the rise time. However, exceptions to this trend have been observed in high strength titanium alloys under cyclic loading conditions where $K_{max} < K_{Iscc}$, Ref. (**56**).

A4.7.3.6 If significant transient behavior is apparent in d*a*/d*N* versus Δ*K* data for a particular test, it is recommended that the test be repeated. However, in assessing apparent transient behavior, particular care should be taken to ensure that the crack size measurement intervals used in the data reduction are in accordance with those recommended in 8.6.2. Improper selection of Δ*a* values for data reduction can greatly magnify apparent transients in d*a*/d*N* versus Δ*K* data.

A4.7.4 *Crack Size Measurement*—Since the presence of an environmental chamber containing an aqueous solution may tend to obscure the crack, a nonvisual technique is recommended as the primary method, Refs. (**37-63**). However, optical observation of the crack tip is recommended as an auxiliary method of crack size measurement and as a means of monitoring crack morphology, specifically crack branching or out-of-plane cracking which may render the test invalid. Fatigue crack surface features revealed in a post-mortem visual examination may provide useful reference marks for calibrating *in situ* crack size measurements. If the potential drop nonvisual technique is employed, it is recommended that care be taken to assure that electrochemical effects on the d*a*/d*N* versus Δ*K* data are not introduced. Electrochemical effects, if sustained in duration, can either accelerate or retard crack growth rates in aqueous environments (see Refs. (**54**) and (**61**)).

A4.7.5 *Environmental Monitoring and Control*—Environmental parameters can strongly influence the results of fatigue crack growth rate tests conducted in aqueous environments. Therefore, environmental monitoring and control are recommended.

A4.7.5.1 It is recommended that tests be initiated using unused solution which has not previously been in contact with other metallic test specimens. It is further recommended that replenishment of evaporated solution be conducted once every 24 h testing period, or more frequently if required, and the entire test solution be emptied and replaced not less than once a week.

A4.7.5.2 It is recommended that measurements of solution temperature and specimen corrosion potential be made and recorded not less than once every 8 h testing period. Potential measurements should be made in accordance with conventions and procedures set forth in Practices G3 and G5. It is further recommended that measurements be made and recorded of pH, conductivity, and dissolved oxygen at similar intervals. Control of environment temperature is also recommended.

A4.8 Report

A4.8.1 The following information shall be reported in addition to the requirements stated in Section 11.

A4.8.2 Descriptions of the environmental chamber and all equipment used for environmental monitoring or control, or both, shall be reported.

A4.8.3 Environmental variables shall be reported as follows: the bulk solution chemical composition and details of its application shall be described; procedures for environmental monitoring and control shall be described; environmental monitoring data for such parameters as pH, potential, or temperature shall be expressed in terms of the normal daily range experienced throughout the duration of the test; relevant trends or transients in environmental parameters data shall be reported.

A4.8.4 It is important to maintain a test log which records all test interruptions or force changes in terms of elapsed cycles, crack size, and time. All data shall be scrutinized for transients and anomalies. All anomalous behavior shall be reported and described in relation to recorded test events.

A5. GUIDELINES FOR USE OF COMPLIANCE TO DETERMINE CRACK SIZE

A5.1 The compliance method of crack size monitoring can be used during fatigue crack growth rate testing (**23**, **24**). The optimum procedure employs the use of high speed digital data acquisition and processing systems, but low-speed autographic equipment can also be used to record the force and displacement signals. Depending on the data acquisition equipment and cyclic force frequency, it may be necessary to lower the frequency during the period of data acquisition.

A5.2 The relationship between compliance (which is the reciprocal of the force-displacement slope normalized for elastic modulus and specimen thickness) and crack size has been analytically derived for a number of standard specimens (**36**). Such relationships are usually expressed in terms of the dimensionless quantities of compliance, $\frac{EvB}{P}$ (or ECB where C is $\frac{v}{P}$), and the normalized crack size, a/W, where E is the elastic modulus, v is the displacement between measurement points, B is specimen thickness, P is force, a is crack size, and W is the specimen width. All compliance-crack size relationships are applicable only for the measurement locations on the specimen for which they were developed. In lieu of an analytically derived compliance relationship, it is possible to empirically develop a compliance curve for any type of specimen used in fatigue crack growth rate testing. Such curves are not limited to displacement measurements alone and can involve strain related quantities.

A5.3 Specimens for fatigue crack growth rate testing covered in this standard are the compact, C(T), the middle tension, M(T), and the eccentrically-loaded single edge crack tension, ESE(T), specimens. Theoretical compliance expressions for these standard test specimens are presented in the respective test specimen annexes.

A5.4 Selection of displacement measurement gages, attachment points and methods of attachment are dependent on the test conditions such as frequency, environment, stress ratio, and temperature. Gages must be linear over the range of displacement measured, and must have sufficient resolution and frequency response. Insight into these issues can be obtained from Test Method E1820 and the relative Annex in Test Method E399. Smaller specimens generally require higher resolution gages. Attachment points must be accurately and repetitively placed on the specimen, and must not be susceptible to wearing during the fatigue cycling.

A5.5 Gripping techniques for specimens that undergo bending, such as the C(T) and ESE(T) specimens, have been observed to affect compliance readings. These specimens may be loaded with grips that have either flat bottom holes or needle bearings, as shown in the respective specimen annexes, to circumvent such problems.

A5.6 The force-displacement plot of one complete cycle of fatigue loading is generally not linear. The lower portion is usually nonlinear and the upper portion is linear. Compliance is calculated by fitting a straight line to the upper linear part of a force-displacement curve.

NOTE A5.1—When using a digital data acquisition system it is permissible to obtain data from a few consecutive cycles provided the growth rate is relatively small. During multiple cycle sampling the normalized crack size, a/W, cannot change by more than 0.001 ($\Delta a/W \leq 0.001$).

NOTE A5.2—There are indications that near the crack growth rate threshold, the upper linear portion of the curve may be very small making the compliance method unusable.

NOTE A5.3—It is usual practice to consistently fit to either the linear portion of the loading data or the unloading data.

NOTE A5.4—It is sometimes necessary to eliminate the data close to the top force reversal point because of rounding that occurs in this area. This is predominately true for data taken at low frequencies.

A5.7 At least one visual crack size reading must be taken either at the beginning or after the test. The visual reading must be adjusted for curvature to obtain the physical crack size using the procedures in the main section of this test method under Calculations and Interpretation of Results. Any difference between the physical and compliance crack size must be used to adjust all compliance crack sizes. Most often this is accomplished by calculating an elastic constraint modulus, E', and using this in the compliance equation to adjust all crack size calculations. If the elastic constraint modulus differs from the typical elastic modulus by more than 10 %, then the test equipment is improperly set-up and data generated from such records are to be considered invalid by this method.

NOTE A5.5—Usually $E \leq E' \leq E/(1-\mu^2)$, where μ is Poisson's ratio. E' might be thought of as being proportional to E, that is, $E' = \gamma E$, where γ is an adjustment factor that accounts for parameters not controllable or measurable during a test.

NOTE A5.6—It is recommended that periodic optical readings be taken for comparison purposes during the first series of tests that use this or any other nonvisual method of crack size measurement.

A6. GUIDELINES FOR ELECTRIC POTENTIAL DIFFERENCE DETERMINATION OF CRACK SIZE

A6.1 *Applications*—Electric potential difference (EPD) procedures for crack size determination are applicable to virtually any electrically conducting material in a wide range of testing environments. Non-conducting materials may also be tested using the electric potential method by firmly attaching a conducting foil or film and treating it as a replicate specimen. This method is acceptable provided that cracking in the film duplicates cracking in the test specimen, and the film does not alter the fatigue crack growth rate properties of the test specimen. This replicate film method may also be used with conducting specimens as well.

A6.1.1 Procedures discussed herein are those for which two-dimensional models can be used both for the specimen configuration and for the electric potential.

A6.2 *Principle*—Determining crack size from electric potential measurements relies on the principle that the electrical field in a cracked specimen with a current flowing through it is a function of the specimen geometry, and in particular the crack size. For a constant current flow, the electric potential or voltage drop across the crack plane will increase with increasing crack size due to modification of the electrical field and

associated perturbation of the current streamlines. The change in voltage can be related to crack size through analytical or experimental calibration relationships.

A6.3 *Basic Methods*—Both direct current (DC) and alternating current (AC) techniques have been used to measure crack size in test specimens(**64-70**). For the more common DC technique, a constant current is passed through the specimen resulting in a two-dimensional electrical field which is constant through the thickness at all points. For the AC technique, a constant amplitude (normally sinusoidal) current is passed through the specimen to generate the voltage drop across the crack tip. For relatively low frequencies (less than 100 Hz with common materials), the field is approximately two-dimensional as in the DC current case. For higher frequencies, however, a non-uniform current distribution occurs through the thickness, the degree of which is dependent on the AC frequency and magnetic permeability of the specimen. This phenomenon is commonly termed the "skin effect" because the current tends to be carried only near the surface of the specimen. For some materials, particularly ferromagnetic specimens, this skin effect can be significant at frequencies as low as 100 Hz, and below (**67, 68**). The AC methods can thus be subdivided into two groups: lower frequency methods where the skin effect is negligible and higher frequency methods where the skin effect must be taken into account.

A6.3.1 For many materials under test in oxidizing environments an oxide layer forms immediately upon the creation of a "fresh" fracture face, thereby insulating the two specimen halves. Under these conditions, the voltage drop across the fatigue crack should remain constant throughout a complete force cycle (assuming no crack extension). An insulating surface may not be created in a non-oxidizing environment or where high fracture surface closure forces tend to compromise such an oxide layer. In these cases, fracture surface shorting may occur at force levels above the minimum test force leading to an under-estimation of the physical fatigue crack size (**71, 72**). This effect is of particular concern when testing at near threshold conditions, when the force at which shorting occurs approaches the peak test force level.

A6.3.2 Unless it can be shown that electrical shorting does not occur during the entire force cycle, the voltage measurements should be taken at or near the peak tensile force. Depending on the frequency response of the AC or DC voltage measuring equipment, it may be necessary to reduce testing frequency or, in some extreme instances, even to stop the test during a voltage measurement to ensure that the measurement is taken only at peak force and without any signal attenuation. It should be noted that measurement of the electrical potential at maximum force does not always guarantee the absence of electrical shorting errors. Shorting errors can still be present at maximum force in cases where there is electrical contact between the fracture surfaces but no mechanical force is transferred. The fracture surface shorting effect can be accounted for after the test using post-test fracture surface crack size measurements. One approach is to compute offset and scaling factors to match the initial and final crack sizes from electric potential measurements and fracture surface measurements. A simple linear interpolation technique with the scaling factor as a function of a/W is then used to correct the intermediate electric potential values. This method may not be suitable for tests in which machine control parameters are derived from the crack size (such as a constant stress intensity test). In these cases, crack size measurement errors may cause unacceptable differences between the applied forces and the desired control force.

A6.3.3 Elastic and plastic deformation can in principle affect material resistivity and, for the case of AC potential difference measurement, magnetic permeability (**73**). While unlikely to be an important source of error for the stress intensities typical of fatigue crack growth under small scale yielding and Test Method E647, the user should document any force dependence of the potential for constant crack size without surface shorting and assess the importance of associated errors in calculated crack size. The correction method for shorting errors will generally account for deformation effects on the electrical and magnetic properties of the material.

A6.3.4 Changes in the specimen or instrumentation may result in proportional changes in the measured voltage. For example, a 1°C change in specimen temperature can result in a few μV change in EPD signal due to the change in the material's electrical resistivity. Also, some materials exhibit time-dependent conductivity changes while at elevated temperatures (**71**). Variations in the gain of amplifiers or calibration of voltmeters may also result in a proportional scaling of the measured voltages. To compensate for these effects, voltage measurements can be normalized using additional voltage measurements taken at a reference location. The reference location may be either on the test specimen or on an alternate specimen in the same environment, and powered by the same electrical current source as the test specimen. If the reference measurements are made directly on the test specimen, the location must be chosen so that the reference voltage is not affected by crack size. Since all material and instrument variations are also included in the reference measurements, the normalization process should eliminate them. Use of reference voltage measurements can significantly increase crack size resolution.

A6.3.5 *DC Current Method*—The DC method is an established technique which can be applied using equipment commonly found in most testing laboratories as shown in Fig. A6.1. The output voltages are typically in the 0.1 to 50.0 mV range for common current magnitudes (5 to 50 A), specimen dimensions, and materials. Precise measurements (typically ±0.1 %) of these relatively small output voltages must be made to obtain accurate crack size values. To obtain sufficient voltage resolution usually requires special care in eliminating electrical noise and drift (see A6.11). Generally, tradeoffs are made between measurement system response time and voltage resolution (see A6.5).

A6.3.5.1 The DC method is susceptible to thermoelectric effects (**74**) which produce DC potentials in addition to those due to the specimen electrical field. These thermoelectric voltages can be a substantial fraction of the total measured voltage. Since the thermoelectric effect is present even without the input current, it is possible to account for it by subtracting

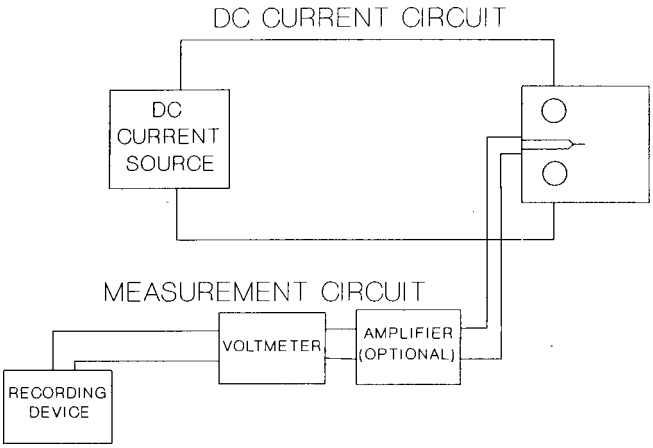

FIG. A6.1 Schematic Diagram of the DC Potential System

voltage measurements taken with the current off from the measurements made with the current on. An alternate method corrects for the thermoelectric effect by taking voltage measurements while reversing the direction of current flow. Corrected EPD measurements are then equal to one-half of the difference of the measured potential readings taken at each current polarity (**75**).

A6.3.6 *AC Current Method*—Both the low and high frequency AC methods require equipment similar to that shown in Fig. A6.2 (**67**). The AC equipment is more specialized than that for the DC approach (see A6.5.2). With the same specimen input current magnitude, this equipment can be used to obtain higher crack size resolution as compared to the DC method (**64**). This is due in part to the different amplification and filtering techniques used in the two methods in addition to the skin effect previously noted. The AC method is not influenced by thermoelectric effects which produce a DC voltage offset.

A6.3.6.1 *Low Frequency AC Current Method*—The low frequency AC method is similar to the DC current method except that as previously noted, different equipment is required to produce the drive current and measure the output voltage. One possible problem with this type of system is that if the test force frequency is an integral multiple of the AC potential

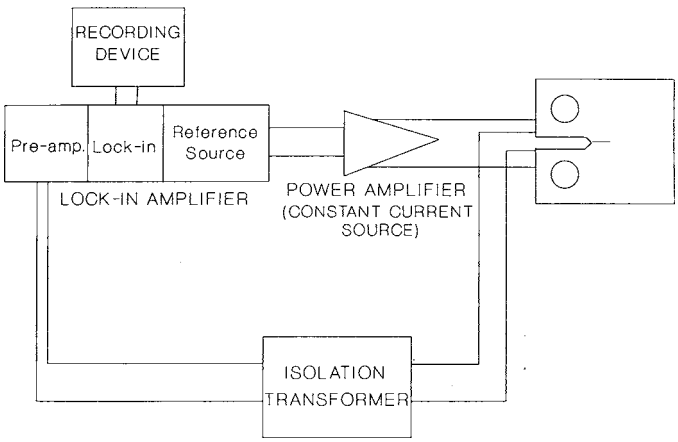

FIG. A6.2 Schematic Diagram of the AC Potential System (62)

frequency, fracture surface sorting (bridging) effects may produce unwanted signal components at the AC potential frequency.

A6.3.6.2 *High Frequency AC Current Method*—An advantage of this technique over the low frequency AC method is that better crack size resolution can typically be obtained using the same input current. This is due to the skin effect previously noted which effectively reduces the specimen thickness to the surface layers (**69**) and the fact that the output voltage is inversely proportional to the specimen thickness.

A6.3.6.3 At high frequencies where the skin effect becomes pronounced, only the near surface crack size will be obtained. This must be taken into account if through-the-thickness crack front curvature is significant. Other effects which may appear at high frequencies include induction and capacitance contributions from lead wires, specimen attachments, and the crack itself. These may be significant and may vary with crack size, causing difficulties in relating output voltage measurements to crack size unless precautions are taken (see A6.11.1).

A6.4 *Current Generating Equipment*—Any suitable constant current supply may be used which has sufficient short and long term stability. The required stability is a function of the resolution of the voltage measurement equipment (see A6.5) and the desired crack size resolution. For optimum conditions, the relative stability of the power supply should be equal to the effective resolution of the voltage measurements system; that is, if the voltage measurement system can effectively resolve one part in 10^3 of the output voltage from the specimen (including electrical noise, inherent inaccuracies such as nonlinearity, and so forth), then the power supply should be stable to one part in 10^3.

A6.4.1 For AC systems, the current should be generated using an amplifier to produce an output current proportional to an input reference signal. The use of an amplifier instead of a stand-alone current generator allows the use of lock-in detection in the voltage measurement circuit (see A6.5.2). The amplifier should have suitably high input impedance (>10 kΩ) and should be capable of generating an output current which is stable as per the preceding discussion.

A6.5 *Voltage Measurement Equipment*—Voltage measurements may be made with any equipment which has sufficient resolution, accuracy, and stability characteristics. The following subsections deal with measurement equipment particular to the different potential drop methods.

A6.5.1 *DC Voltage Measurement Equipment*—The DC method requires equipment capable of measuring small changes in DC voltage (that is, 0.05 to 0.5 μV) with relatively low DC signal to AC RMS noise ratios. Although there are a variety of ways to implement the voltage measurement system, three commonly used systems are: amplifier/autographic recorder, amplifier/microcomputer analog to digital converter, and digital voltmeter/microcomputer.

A6.5.1.1 Autographic recorders are commonly available with suitable sensitivity and can be used to record the output voltage directly from the specimen. A preamplifier can be used to boost the direct voltage output from the specimen before

recording. Another common technique uses a preamplifier to boost the direct output from the specimen to a level that can be digitized using a conventional analog to digital (A/D) converter and microcomputer. A third method makes use of a digital voltmeter with a digital output capability. The advantage of this type of system is that all of the sensitive analog circuits are contained within a single instrument. The response time of the voltage measurement system must be sufficient to resolve changes in EPD as a function of applied force if fracture surface shorting occurs.

A6.5.2 *AC Voltage Measurement Equipment*—Both low and high frequency AC systems make use of similar voltage measurement equipment as shown in Fig. A6.2. The voltage measurement circuit and the current amplifier (see A6.4) are interconnected through the lock-in amplifier. This specialized amplifier produces a reference output signal for the current amplifier and is able to discriminate against all input signals that are not at the reference signal frequency and phase. Thus, only signals produced as a result of the current amplifier output are amplified for measurement. This method is capable of amplifying only the desired AC voltage signal at very low signal-to-noise ratios and provides excellent noise rejection (**67**). Note that this type of system is insensitive to DC voltages which might be produced by thermoelectric effects.

A6.5.3 When selecting instrumentation for an AC system, care should be made to ensure proper impedance matching, since each component is designed for operation over a specific frequency domain. Input and output impedance should be matched. A check for frequency response to ensure operation in the "flat" region of the instruments' gain should also be performed.

A6.6 *Crack Size versus Potential Difference Relationships*—Closed form solutions for the relationship between potential difference versus crack size have been analytically derived for such specimen geometries as the M(T) specimen(**44**)and the part-through surface crack specimen(**76, 77**). Additional relationships are also available based on numerical solutions for a number of other specimen geometries (**38, 78 and 79**). Such relationships are usually expressed in terms of the normalized voltage (V/V_r) and some reference crack size (a_r) as shown in Eq A6.1.

$$a = f(V/V_r, a_r) \tag{A6.1}$$

where:

V = the measured voltage,
V_r = a reference crack voltage,
a = crack size, and
a_r = a reference crack or notch size associated with V_r.

Alternative formulations are also used when the crack size is normalized by an in-plane characteristic dimension such as the specimen width W. When written in this form, the solutions can be made independent of specimen thickness, in-plane specimen size, applied current, and material.

A6.6.1 In lieu of an analytically derived expression, it is possible to empirically develop relationships for virtually any type of specimen geometry used in fatigue crack growth rate testing. Such empirical relationships can be advantageous in instances when specimen geometries are complex, or wire placement must be altered. In any event, analytical or empirical relationships should be experimentally verified using alternative measurements at various crack sizes in the range of interest (optical surface measurements, compliance measurements, or post-test fracture surface measurements). Such measurements should be reported and may be used for correcting crack sizes inferred from equations of the type in Eq A6.1.

A6.6.2 Voltage wire placements are usually a compromise between good sensitivity to crack size changes and freedom from errors caused by minor variations in lead location from specimen to specimen. Near crack tip lead locations (or notch tip locations for uncracked specimens) yield better sensitivity to changes in crack size. The difficulty with this type of arrangement is that the electrical field is, in general, highly nonuniform in the near tip region. Thus, minor variations in lead placement from one specimen to the next may produce significant differences in measured voltage for the same crack size (**78**). In most cases those positions which give greatest sensitivity to crack size changes also have the greatest sensitivity to variations in lead wire positioning.

A6.7 *Specimen Geometries*—Specimen geometries for fatigue crack growth rate testing covered in this test method are the compact, C(T), the eccentrically-loaded single edge crack tension, ESE(T), and the middle tension, M(T). The equations listed in the respective specimen annexes are derived under DC conditions for sharp cracks in the respective specimen geometries. Errors in crack size measurements may arise if a blunt notch is used as the reference crack size(**44, 80**).

A6.7.1 One or more measurements of the crack size should be made during the test using an alternative technique such as optical measurements on the specimen surface. These values should be used for comparison to evaluate the progress of each test. This is particularly important where a parameter derived from the crack size (stress intensity, and so forth) is being controlled. If optical measurements cannot be made during the test, the final crack size, along with the initial starter crack size, should be compared to the crack sizes determined from electric potential measurements. If a difference is observed between the optical and EPD crack sizes, a linear correction factor, similar to that described for crack curvature correction in the main section (Calculation and Interpretation of Results), must be employed to "post-correct" the EPD crack size values (see also A6.3).

A6.7.2 Regardless of the EPD versus crack size expression used, the use of a reference probe is encouraged (see A6.3). This reference probe should be located on the test specimen (or another specimen at the identical test conditions) in a region unaffected by crack growth and should be equal to or greater in magnitude to the expected voltage levels measured across the crack. When employing such a reference probe, the EPD measurements made for crack size determination are divided by the ratio V_{ref}/V_{ref_0},

where:

V_{ref} = the reference probe voltage measured at the same time as the EPD crack voltage is measured, and

V_{ref_0} = the initial reference probe voltage.

A6.7.3 For AC potential systems, caution should be applied when using the referenced equations listed in the respective specimen annexes for crack size determination which were developed under the assumption that the measured potentials reflect only a resistive voltage component. With an AC potential system the measured EPD voltage across the crack contains both a resistive and a reactive voltage component. For materials with high conductivity at high AC frequencies the reactive component can be a substantial fraction of the measured voltage and can lead to significant errors if used with the equations cited above. If conditions are such that the reactive component is significant then a new relationship must be empirically developed for the particular test/specimen conditions.

A6.8 *Gripping Considerations*—The electric potential difference method of crack size determination relies on a current of constant magnitude passing through the specimen when the potential voltage is measured. During such potential measurements it is essential that no portion of the applied current be shunted in a parallel circuit through the test machine. For most commercially available test machines and grip assemblies the resistance through the test frame is considerably greater than that of the test specimen. However, in some situations an alternative path for the applied current may exist through the test frame. In such cases, additional steps to provide isolation between the specimen and test frame may be necessary. Users of the potential difference method should ensure that the electrical resistance measured between the grips (with no specimen in place) is several orders of magnitude higher than the resistance of the specimen between the current input locations. The specimen resistance should be determined for the range of crack sizes encountered during the test. A resistance ratio (test frame resistance divided by the specimen resistance) of 10^4 or greater is sufficient for most practical applications. Isolation of the specimen from the test frame is particularly important when using power supplies with non-isolated (ground referenced) outputs. Use of this type of power supply may require isolating both ends of the test specimen from the test frame to avoid ground loop problems.

A6.8.1 For specimens in which the current is introduced through the loading pins, care must be taken to ensure that good electrical contact is maintained between the pin and the specimen. Constant current power supplies can usually correct for small changes in the pin/specimen/grip resistance, however, abrupt or large changes in resistance due to oxidation or other effects may cause varying or erratic current levels, or both, during the force cycle. Poor loading pin contact may increase the percentage of an alternate current path and shunting errors.

A6.9 *Wire Selection and Attachment*—Careful selection and attachment of current input and voltage measurement wires can avoid many problems associated with the electric potential method. This is particularly important in aggressive test environments such as elevated temperature where the strength, melting point, and oxidation resistance of the wires must be taken into account. Aggressive test environments may require special lead wire materials or coatings, or both, to avoid loss of electrical continuity caused by corrosive attack.

A6.9.1 *Current Input Wires*—Selection of current input wire should be based on current carrying ability, and ease of attachment (weldability, connector compatibility). Wires must be of sufficient gage to carry the required current under test conditions and may be mechanically fastened or welded to the specimen or gripping apparatus.

A6.9.2 *Voltage Measurement Wires*—Voltage wires should be as fine as possible to allow precise location on the specimen and minimize stress on the wire during fatigue loading which could cause detachment. Ideally, the voltage sensing wires should be resistance welded to the specimen to ensure a reliable, consistent joint. Lead wires may be fastened using mechanical fasteners for materials of low weldability (for example, certain aluminum alloys), provided that the size of the fastener is accounted for when determining location of voltage sensing leads. Voltage sensing wire should be located diagonally across the starter notch or crack tip as shown in the respective specimen annexes to average measurements of non-uniform crack fronts.

A6.10 *Resolution of Electric Potential Systems*—The effective resolution of EPD measurements depends on a number of factors including voltmeter resolution (or amplifier gain, or both), current magnitude, specimen geometry, voltage measurement and current input wire locations, and electrical conductivity of the specimen material. Herein, effective resolution is defined as the smallest change in crack size which can be distinguished in actual test operation, not simply the best resolution of the recording equipment. For common laboratory specimens, a direct current in the range of 5 to 50 A and voltage resolution of about ±0.1 μ*V* or ±0.1 % of V_r will yield a resolution in crack size of better than 0.1 % of the specimen width (crack size resolution must be in accordance with 8.8). For highly conductive materials (that is, aluminum, copper) or lower current levels, or both, the resolution would decrease, while for materials with a lower conductivity (that is, titanium, nickel) resolutions of better than 0.01 % of the specimen width have been achieved. For a given specimen geometry, material, and instrumentation, crack size resolution shall be analyzed and reported.

NOTE A6.1—The following is an example of the magnitude of voltages as measured on a standard C(T) specimen for a direct current of 10 A:

Material	Approximate EPD Measured at 10A	Approximate Change in Crack Size for 1 μV Change in EPD
Aluminum	0.1 mV	300 μm
Steel	0.6 mV	50 μm
Titanium	3.5 mV	9 μm

Based on $a/W = 0.22$, $B = 7.7$ mm, and $W = 50$ mm.

A6.11 *Techniques to Reduce Voltage Measurement Scatter*—Because of the low level signals which must be measured with either the DC or AC current methods, a number of procedures should be followed to improve voltage measurement precision.

A6.11.1 *Induced EMF*—Voltage measurement lead wires should be as short as possible and should be twisted to reduce stray voltages induced by changing magnetic fields. Holding them rigid also helps reduce the stray voltages which can be generated by moving the wires through any static magnetic fields that may exist near the test frame. In addition, routing the voltage measurement leads away from the motors, transformers, or other devices which produce strong magnetic fields is recommended.

A6.11.1.1 For AC systems, care should be taken to keep the current wires away from the potential leads. If shielded voltage lead wire is used, the shield should be properly grounded at one end.

A6.11.2 *Electrical Groundings*—Proper grounding of all devices (current source, voltmeters, and so forth) should be made, avoiding ground loops. This is particularly important when DC procedures are used in conjunction with electrochemical polarization equipment relevant to corrosion fatigue.

A6.11.3 *Thermal Effects*—For DC systems thermal emf measurement and correction is critically important. A minimum number of connections should be used and maintained at a constant temperature to minimize thermoelectric effects (see A6.3.5.1).

A6.11.3.1 All measuring devices (amplifiers/preamplifiers, voltmeters, analog-to-digital converters) and the specimen itself should be maintained at a constant temperature. Enclosures to ensure constant temperatures throughout the test are generally beneficial.

A6.11.3.2 Some voltmeters for DC systems have built-in automatic correction for internal thermoelectric effects. These units may be of benefit in cases where it is not possible to control the laboratory environment.

A6.11.4 *Selection of Input Current Magnitude*—The choice of current magnitude is an important parameter: too low a value may not produce measurable output voltages; too high a value may cause excessive specimen heating or arcing (**69**).

A6.11.4.1 To minimize these problems, current densities should be kept to the minimum value which can be used to produce the required crack size resolution. The maximum current that can be used with a particular specimen can be determined by monitoring the specimen temperature while increasing the current in steps, allowing sufficient time for the specimen to thermally stabilize. Particular care should be exercised when testing in vacuum, as convection currents are not available to help maintain the specimen at ambient temperature.

A6.11.5 *DC Current Stabilization Period*—Allow a sufficient stabilization period after turning the DC electric potential current either on or off before making a voltage measurement. Most solid-state power sources can stabilize the output current within a period of 1 or 2 s for a step change in output, however, this should be verified for each particular specimen and experimental setup.

A6.12 *Precautions*—Care must be taken to demonstrate that the applied current does not affect crack tip damage processes and crack growth rates. For example, in corrosion fatigue, current leakage into the crack solution could alter electrochemical reaction rates and affect cracking. Results to date indicate that this is not a practical problem, presumably because of the high metal conductivity compared to even the most conductive of electrolytes (for example, NaCl). Current flow in the solution is not affected by the current in the specimen(**81**).

A6.12.1 Large-scale crack tip plasticity can increase measured electrical potentials due to resistivity increases without crack extension (**68**). Experience indicates that this potential source of error is not significant even when plastic deformation is greater than the small-scale yielding criteria of Test Method E647 (**65**).

APPENDIXES

(Nonmandatory Information)

X1. RECOMMENDED DATA REDUCTION TECHNIQUES

X1.1 Secant Method

X1.1.1 The secant or point-to-point technique for computing the crack growth rate simply involves calculating the slope of the straight line connecting two adjacent data points on the a versus N curve. It is more formally expressed as follows:

$$(da/dN)_{\bar{a}} = (a_{i+1} - a_i)/(N_{i+1} - N_i) \qquad (X1.1)$$

Since the computed da/dN is an average rate over the $(a_{i+1} - a_i)$ increment, the average crack size, $\bar{a} = \frac{1}{2}(a_{i+1} + a_i)$, is normally used to calculate ΔK.

X1.2 Incremental Polynomial Method

X1.2.1 This method for computing da/dN involves fitting a second-order polynomial (parabola) to sets of $(2n + 1)$ successive data points, where n is usually 1, 2, 3, or 4. The form of the equation for the local fit is as follows:

$$\hat{a}_i = b_0 + b_1\left(\frac{N_i - C_1}{C_2}\right) + b_2\left(\frac{N_i - C_1}{C_2}\right)^2 \qquad (X1.2)$$

where:

$$-1 \le \left(\frac{N_i - C_1}{C_2} \right) \le +1 \qquad \text{(X1.3)}$$

and b_0, b_1, and b_2 are the regression parameters that are determined by the least squares method (that is, minimization of the square of the deviations between observed and fitted values of crack size) over the range $a_{i-n} \le a \le a_{i+n}$. The value $\hat{a}_i$ is the fitted value of crack size at N_i. The parameters $C_1 = ½ (N_{i-n} + N_{i+n})$ and $C_2 = ½ (N_{i+n} - N_{i-n})$ are used to scale the input data, thus avoiding numerical difficulties in determining the regression parameters. The rate of crack growth at N_i is obtained from the derivative of the above parabola, which is given by the following expression:

$$(da/dN)_{\hat{a}_i} = (b_1)/(C_2) + 2b_2(N_i - C_1)/C_2^2 \qquad \text{(X1.4)}$$

The value of ΔK associated with this da/dN value is computed using the fitted crack size, $\hat{a}_i$, corresponding to N_i.

X1.2.2 A BASIC computer program that utilizes the above scheme for $n = 3$, that is, 7 successive data points, is given in Table X1.1 (see Eq X1.1). This program uses the specimen K-calibrations for the C(T) and M(T) geometries given in the respective specimen annexes and also checks the data against the size requirements listed in each annex.

X1.2.3 An example of the output from the program is given in Table X1.2. Information on the specimen, loading variables, and environment are listed in the output along with tabulated values of the raw data and processed data. A(Meas.) and A(Reg.) are values of total crack size obtained from measurement and from the regression equation (Eq X1.2), respectively. The goodness of fit of this equation is given by the multiple correlation coefficient, MCC (note that MCC = 1 represents a perfect fit). Values of Delta K (ΔK) and da/dN are given in the same units as the input variables (for the example problem these are ksi$\sqrt{in.}$ and in./cycle, respectively). Values of da/dN that violate the specimen size requirement appear with an asterisk and note as shown in Table X1.2 for the final 15 data points.

TABLE X1.1 BASIC Computer Program for Data Reduction by the Seven Point Incremental Polynomial Technique

```
'QuickBasic Computer Program for Data Reduction by the Seven Point Increment
'   Polynomial Technique

DIM a(200), n(200), bb(3), dadn(200), delk(200), id(7), aa(10), nn(10)

OPEN "example.DAT" FOR INPUT AS #1
OPEN "result.dat" FOR OUTPUT AS #2
'Input parameters as they should appear in input file:
'      ys: yield strength (ksi)
'      B:  thickness (inches)
'      W:  width (inches)
'      pmax: maximum load (kips)
'      pmin: minimum load (kips)
'      notch: notch length (inches)
'      freq: test frequency
'      type$: "ct" or "ccp"
'      temper$: temperature
'      labenviron$: lab environment
'      n(i), a(i): cycles, crack length (inches)- measured from notch tip

npts = 0
INPUT #1, ys, B, W, pmax, pmin, notch, freq, type$, temper$, labenviron$
DO UNTIL EOF(1)
  npts = npts + 1
  INPUT #1, n(npts), a(npts)
LOOP

k = 0
pi = 3.1416
deltap = pmax - pmin
Rratio = pmin / pmax

'Add notch length to measured crack length
FOR Inpt = 1 TO npts
  a(Inpt) = a(Inpt) + notch
NEXT Inpt

'Printing header information
PRINT #2, USING "&"; "Specimen No.: ", specnumber$;
PRINT #2, USING "&"; "   No. of Points: ", STR$(npts)
PRINT #2, USING "&"; "Specimen Type: ", type$, "    B= ", STR$(B);
PRINT #2, USING "&"; "    W= ", STR$(W), "    Ao= ", STR$(notch)
PRINT #2, USING "&"; "Pmin= ", STR$(pmin), "    Pmax= ", STR$(pmax);
PRINT #2, USING "&"; "    R= ", STR$(Rratio), "    Test Freq= ", STR$(freq)
PRINT #2, USING "&"; "Temperature= ", temper$;
PRINT #2, USING "&"; "    Environment: ", labenviron$
PRINT #2,
PRINT #2, USING "&"; "No.", " Cycles", "    A(Meas.)", " A(Reg.)";
PRINT #2, USING "&"; "   M.C.C.", "   Delta K", "    da/dN"
PRINT #2,

'First three data points are printed
FOR i = 1 TO 3
    PRINT #2, USING "##    "; i;
    PRINT #2, USING "######    "; n(i);
```

TABLE X1.1 *Continued*

```
   PRINT #2, USING "#.####   "; a(i)
NEXT i
npts = npts - 6
FOR Inpt = 1 TO npts
 l = 0
 k = k + 1
 k1 = k + 6
 FOR Iindex = k TO k1
  l = l + 1
  aa(l) = a(Iindex)
  nn(l) = n(Iindex)
 NEXT Iindex
 c1 = .5 * (nn(1) + nn(7))
 c2 = .5 * (nn(7) - nn(1))
 sx = 0
 sx2 = 0
 sx3 = 0
 sx4 = 0
 sy = 0
 syx = 0
 syx2 = 0
 FOR Inum = 1 TO 7
  x = (nn(Inum) - c1) / c2
  yy = aa(Inum)
  sx = sx + x
  sx2 = sx2 + x ^ 2
  sx3 = sx3 + x ^ 3
  sx4 = sx4 + x ^ 4
  sy = sy + yy
  syx = syx + x * yy
  syx2 = syx2 + yy * x ^ 2
 NEXT Inum
 Term1 = (sx2 * sx4 - sx3 ^ 2)
 Term2 = (sx * sx4 - sx2 * sx3)
 Term3 = (sx * sx3 - sx2 ^ 2)
 Denom = 7 * Term1 - sx * Term2 + sx2 * Term3
 Numer2 = sy * Term1 - syx * Term2 + syx2 * Term3
 bb(1) = Numer2 / Denom
 Term4 = syx * sx4 - syx2 * sx3
 Term5 = sy * sx4 - syx2 * sx2
 Term6 = sy * sx3 - syx * sx2
 Numer3 = 7 * Term4 - sx * Term5 + sx2 * Term6
 bb(2) = Numer3 / Denom
 Term7 = sx2 * syx2 - sx3 * syx
 Term8 = sx * syx2 - sx3 * sy
 Term9 = sx * syx - sx2 * sy
 Numer4 = 7 * Term7 - sx * Term8 + sx2 * Term9
 bb(3) = Numer4 / Denom
 yb = sy / 7
 rss = 0
 tss = 0
 FOR Inum = 1 TO 7
   x = (nn(Inum) - c1) / c2
yhat = bb(1) + bb(2) * x + bb(3) * x ^ 2
rss = rss + (aa(Inum) - yhat) ^ 2
   tss = tss + (aa(Inum) - yb) ^ 2
 NEXT Inum
```

TABLE X1.1 *Continued*

```
  r2 = 1 - rss / tss
  dadn(Inpt) = bb(2) / c2 + 2 * bb(3) * (nn(4) - c1) / c2 ^ 2
  x = (nn(4) - c1) / c2
  ar = bb(1) + bb(2) * x + bb(3) * x ^ 2
  s = 1E+10
  snet = 0
  qq = Inpt + 3
  IF (type$ = "ct") THEN
   t = ar / W
   num = (.886 + 4.64 * t - 13.32 * t ^ 2 + 14.72 * t ^ 3 - 5.6 * t ^ 4)
   den = (1 - t) ^ 1.5
   ft = ((2 + t) * num) / den
   s = ys * ((pi * W * (1 - t)) ^ .5) / 2
  ELSE
   t = 2 * ar / W
   sec = 1 / (COS(pi * t / 2))
   ft = (pi * t * sec / 2) ^ .5
   snet = pmax / (B * W * (1 - t))
  END IF
  delk(Inpt) = (ft * deltap) / (B * W ^ .5)
  ax = delk(Inpt) / (1 - Rratio)
  IF (ax >= s OR snet >= ys) THEN
   PRINT #2, USING "##   "; qq;
   PRINT #2, USING "###### "; n(qq);
   PRINT #2, USING "#.####  "; a(qq), ar, r2;
   PRINT #2, USING "  ##.##  "; delk(Inpt);
   PRINT #2, USING "#.####  "; dadn(Inpt);
   PRINT #2, " *"
  ELSE
   PRINT #2, USING "##   "; qq;
   PRINT #2, USING "###### "; n(qq);
   PRINT #2, USING "#.####  "; a(qq), ar, r2;
   PRINT #2, USING "  ##.##  "; delk(Inpt);
   PRINT #2, USING "#.####  "; dadn(Inpt)
  END IF
NEXT Inpt
j = npts + 4
k = npts + 6
FOR Iprnt = j TO k
  PRINT #2, USING "##   "; Iprnt;
  PRINT #2, USING "###### "; n(Iprnt);
  PRINT #2, USING "#.####  "; a(Iprnt)
NEXT Iprnt
PRINT #2, USING "&"; "* - Data violate specimen size requirements"

CLOSE #1
CLOSE #2
STOP
END
```

TABLE X1.2 Example Output from Incremental Polynomial Computer Program

```
Specimen No.:   No. of Points:  37
Specimen Type: ct   B=  .25   W=  2   Ao=  .5
Pmin=  4   Pmax=  5   R=  .8   Test Freq=  5
Temperature= 75 F   Environment: lab air

No. Cycles   A(Meas.) A(Reg.)  M.C.C.  Delta K   da/dN

 1        0   0.5990
 2    15480   0.6310
 3    22070   0.6560
 4    30240   0.6740  0.6772  0.9969    17.56    0.3233E-05
 5    36090   0.6980  0.6977  0.9963    18.03    0.3369E-05
 6    41370   0.7180  0.7156  0.9910    18.45    0.3189E-05
 7    46850   0.7350  0.7345  0.9925    18.90    0.3367E-05
 8    50090   0.7460  0.7439  0.9928    19.13    0.3404E-05
 9    54380   0.7530  0.7579  0.9956    19.48    0.3472E-05
10    60320   0.7810  0.7794  0.9965    20.04    0.3870E-05
11    65160   0.8010  0.7998  0.9965    20.58    0.4122E-05
12    70240   0.8210  0.8225  0.9990    21.21    0.4441E-05
13    74690   0.8430  0.8416  0.9995    21.77    0.4525E-05
14    80070   0.8650  0.8665  0.9994    22.51    0.4803E-05
15    83860   0.8860  0.8853  0.9993    23.11    0.4926E-05
16    88080   0.9060  0.9061  0.9992    23.79    0.5168E-05
17    91460   0.9250  0.9240  0.9991    24.41    0.5450E-05
18    95620   0.9450  0.9465  0.9995    25.21    0.5833E-05
19    99000   0.9670  0.9669  0.9992    25.99    0.6109E-05
20   102360   0.9880  0.9883  0.9985    26.84    0.6230E-05 *
21   105110   1.0080  1.0062  0.9971    27.58    0.6677E-05 *
22   108440   1.0280  1.0283  0.9973    28.55    0.6930E-05 *
23   111660   1.0470  1.0507  0.9973    29.60    0.7411E-05 *
24   113410   1.0670  1.0636  0.9976    30.23    0.7593E-05 *
25   116810   1.0900  1.0910  0.9969    31.65    0.8432E-05 *
26   118730   1.1080  1.1079  0.9959    32.59    0.8984E-05 *
27   121220   1.1280  1.1304  0.9986    33.91    0.1049E-04 *
28   121880   1.1380  1.1372  0.9986    34.32    0.1109E-04 *
29   122830   1.1480  1.1481  0.9981    35.00    0.1140E-04 *
30   124280   1.1660  1.1663  0.9993    36.20    0.1268E-04 *
31   125820   1.1870  1.1854  0.9992    37.54    0.1342E-04 *
32   127480   1.2070  1.2076  0.9930    39.20    0.1649E-04 *
33   128700   1.2260  1.2273  0.9946    40.79    0.2015E-04 *
34   129760   1.2450  1.2494  0.9776    42.69    0.2794E-04 *
35   130790   1.2770
36   131480   1.2980
37   131550   1.3230
* - Data violate specimen size requirements
```

X2. RECOMMENDED PRACTICE FOR DETERMINATION OF FATIGUE CRACK OPENING FORCE FROM COMPLIANCE

X2.1 Introduction

X2.1.1 The term *crack closure* refers to the phenomenon whereby the fracture surfaces of a fatigue crack come into contact during the unloading portion of a force cycle and force is transferred across the crack. In many materials, crack closure can occur while the force is above the minimum force in the cycle even when the minimum force is tensile. Upon reloading from minimum force, some increment of tensile loading must be applied before the crack is again fully open. Thus, crack closure provides a mechanism whereby the effective cyclic stress intensity factor range near the crack tip (ΔK_{eff}) differs from the nominally applied value (ΔK). Therefore, information on the magnitude of the crack closure effect is essential to understand and interpret observed crack growth behavior. An estimate of ΔK_{eff} can be obtained experimentally by determining the minimum force at which the crack is open (opening force, P_o) and, if $P_o > P_{min}$, using the effective force range ($\Delta P_{eff} = P_{max} - P_o$) in expressions for the stress intensity factor range instead of force range ($\Delta P = P_{max} - P_{min}$).

X2.1.2 Many experimental techniques have been used to determine the opening force. These techniques have included the use of ultrasonics, potential drop, eddy current, acoustic emission, high magnification photography, and strain or displacement versus force (compliance) measurements. Due

mainly to its experimental simplicity, the compliance technique has become the most widely used approach.

X2.2. Scope

X2.2.1 This appendix covers the experimental determination of fatigue crack opening force in tests of the specimens outlined in this test method, subjected to constant amplitude or slowly changing (similar to force shedding rates recommended in this test method for threshold tests at constant force ratio) loading.

X2.3 Terminology

X2.3.1 Definitions of terms specific to this appendix are given in this section. Other terms used in this appendix are defined in the main body of this test method.

X2.3.2 *Definitions:*

X2.3.2.1 *crack closure*—in fatigue, the phenomenon whereby the fracture surfaces of a fatigue crack come into contact during the unloading portion of a force cycle and force is transferred across the crack.

X2.3.2.2 *effective force range,* ΔP_{eff} $[F]$—in fatigue, that part of the increasing-force range of the cycle during which the crack is open. The effective force range is expressed as:

$$\Delta P_{\text{eff}} = P_{\max} - P_o \quad \text{if} \quad P_o > P_{\min}, \text{ and} \tag{X2.1}$$

$$\Delta P_{\text{eff}} = \Delta P = P_{\max} - P_{\min} \quad \text{if} \quad P_o < \text{or} = P_{\min} \tag{X2.2}$$

X2.3.2.3 *effective stress intensity factor range,* ΔK_{eff} $[FL^{-3/2}]$—in fatigue, the stress intensity factor range computed using the effective force range, ΔP_{eff}.

X2.3.2.4 *opening force,* P_o $[F]$—in fatigue, the minimum force at which the fatigue crack is open at the tip during the increasing-force part of a cycle.

X2.4. Significance and Use

X2.4.1 The method of determining crack opening force, and therefore of estimating ΔK_{eff} , presented in this appendix should be useful in assessing and comparing the effects of crack closure on the crack growth behavior of various materials. The method does not define the exact portion of the applied ΔK that is effective in growing the crack nor the exact values of the opening force at all points along the crack front, but does provide a well-defined operational approach that can be used to estimate the first-order effects of closure.

X2.4.2 Measurements of opening force made using this procedure can serve as reference or benchmark values that can be used in evaluating crack closure information from different sources and from other experimental techniques.

X2.5 Basis for Determination of Opening Force From Compliance

X2.5.1 The determination of opening force from compliance is based on the observation that when a cracked specimen is loaded up to the force at which the crack becomes fully open, the compliance (slope of the strain or displacement against force curve) attains a characteristic value and remains essentially constant upon further force increase until the force is increased enough to cause large-scale yielding near the crack tip. Upon unloading from the maximum force in a cycle, the compliance again has the characteristic value for the fully-open crack regardless of whether large-scale yielding occurred before maximum force was achieved. Conceptually, the experimental task is very simple—determine the force at which the strain or displacement against force curve becomes linear (analogous to the determination of proportional limit in a tensile test). However, in practice, this task is very difficult due to the gradual change in compliance as it approaches the open-crack value and to the nonlinearity and variability, or *noise*, in the compliance data. Nonlinearity and noise in the measurement system can cause significant variation in the estimates of opening force.

X2.5.2 One way to reduce scatter in opening force results due to noise and nonlinearity in the measurement system is to define opening force as the force corresponding to a compliance that is offset from (lower than) the fully-open-crack value rather than the force at which the compliance attains the fully-open value (that is, the point where the curve becomes linear). The scatter will be reduced because the offset compliance value corresponds to a position on the loading curve where a change in compliance is associated with a smaller change in force than would be the case for a position very near the start of the linear part of the curve. Of course, with the offset compliance approach, the opening forces determined will be somewhat lower than the force at which the crack becomes fully open. Selection of an appropriate compliance offset criterion then becomes a trade-off between achieving a reduction in scatter and minimizing the deviation of the compliance-offset opening force from the force at which the crack becomes fully open. Some information on this trade-off is given in Ref **(82)**.

X2.6. Apparatus

X2.6.1 The procedure requires a strain or displacement transducer which can be mounted on the specimen and a digital data acquisition and processing system capable of acquiring data from the testing machine force cell and the strain/displacement transducer.

X2.6.2 The requirements for the strain/displacement transducers and other experimental apparatus are, in general, the same as that specified in Annex A5 for using compliance to determine crack size. However, the requirement for high quality (good linearity and low noise) strain/displacement data is especially critical in measuring opening force using the compliance procedure. Accordingly, an accept/reject criterion for data quality is described in X2.8.

X2.6.3 The location of the strain or displacement measurement may be near the crack tip or remote from the tip. However, for tests within the scope of this appendix, remote measurements are recommended because they are experimentally simpler and are likely to be more repeatable than near-tip measurements. For the C(T) and ESE(T) specimens, the recommended measurements are: (*1*) displacement across the crack mouth, and (*2*) strain at the mid-height location on the back face. For the M(T) specimen, the recommended measurement is displacement across the crack on the longitudinal centerline (see Fig. X2.1).

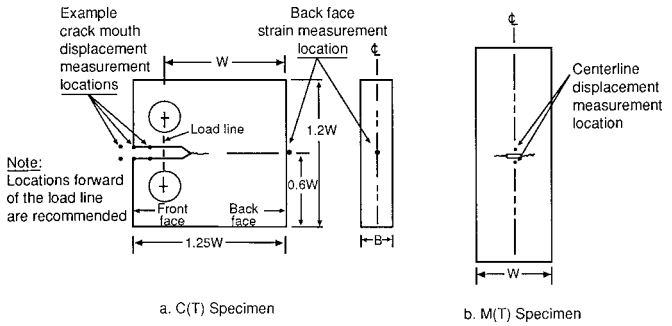

FIG. X2.1 Recommended Displacement and Strain Measurement Locations for Determination of Fatigue Crack Opening Load on C(T) and M(T) Specimens

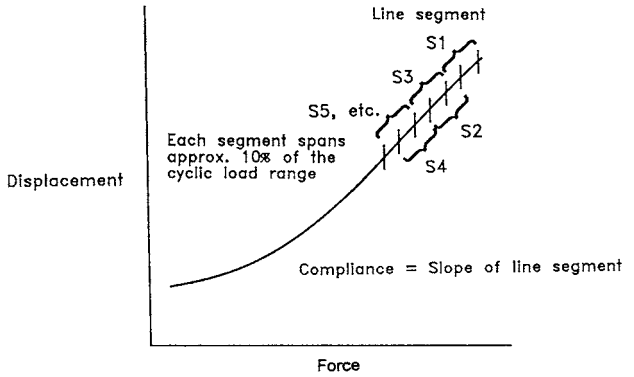

FIG. X2.2 Evaluation of the Variation of Compliance With Load for Use in Determination of Opening Force

X2.7. Recommended Procedure—Determination of Opening Force by the Compliance Offset Method

X2.7.1 Background information on the rationale for using this method can be found in Refs **(82)** and **(83)**. The step-by-step procedure for determining opening force from strain or displacement against force data is as follows:

X2.7.1.1 Collect digitized strain/displacement and force data for a complete force cycle. The data sampling rate should be high enough to ensure that at least one data pair (displacement and force) is taken in every 2 % interval of the cyclic force range for the entire cycle. (Different loading waveforms require different minimum sampling rates to ensure that one point is taken in every 2 % interval.)

X2.7.1.2 Starting just below maximum force (not less than 0.90 maximum force) on the unloading curve, fit a least-squares straight line to a segment of the curve that spans a range of approximately 25 % of the cyclic force range. The slope of this line is assumed to be the compliance value that corresponds to the fully-open crack configuration.

NOTE X2.1—**Warning:** For some materials and loading conditions that produce high opening forces, this assumption may not be correct. The opening force may actually lie within the fitted force range, and in that case, the computed open-crack compliance and the opening force from the analysis will be too low. The procedure in X2.7.1.6 provides a check on the reasonableness of the open-crack compliance assumption.

NOTE X2.2—**Warning:** Care must be taken to choose appropriate limits to calculate compliance offset. The limit should be low enough to allow a good fit to the data, but must be high enough to avoid crack closure affecting compliance offset. Results from a round-robin of R =0.10 testing in the Paris Regime suggest the upper 25% of the amplitude. However, the optimal range can be affected by factors such as stress ratio, stress intensity factor range, environment, material, and residual stresses.**(82)**

X2.7.1.3 Starting just below maximum force (not less than 0.95 maximum force) on the loading curve, fit least-squares straight lines to segments of the curve that span a range of approximately 10 % of the cyclic force range and that overlap each other by approximately 5 % of the cyclic force range (see Fig. X2.2). Determine the compliance (slope) and the corresponding mean force for each segment.

X2.7.1.4 Calculate the compliance offset for each segment as follows:

$$\text{Compliance offset} = \frac{[(\text{open} - \text{crack compliance}) - (\text{compliance})]\,(100)}{(\text{open} - \text{crack compliance})} \quad \text{(X2.3)}$$

where the *open-crack* value is taken from X2.7.1.2.

X2.7.1.5 Plot the (compliance offset, mean force) points from the segments and connect the points with straight lines (see Fig. X2.3). Determine the opening force (P_o) corresponding to the selected offset criterion as the lowest force at which a line connecting points has the value of compliance offset equal to the offset criterion.

NOTE X2.3—**Warning:** If more than one line connecting points crosses the offset criterion level (see Fig. X2.4), the variability of the compliance data is probably high enough to cause significant variation in the opening force results. Steps should be taken to reduce the variability. Variability can usually be reduced by electrically shielding the transducer wires and by appropriate electronic filtering of the signals before input into the data acquisition system. Matched filters must be used to prevent introduction of a phase shift between the force and displacement/strain signals.

X2.7.1.6 Check the reasonableness of the open-crack compliance value from X2.7.1.2 if an opening force above $0.50P_{max}$ was found in X2.7.1.5. To make the check, return to X2.7.1.2 and find the slopes of lines fit to several force ranges both larger and smaller than 25 %. Plot the resulting slopes against fitted-force-range and identify the largest range below which the slope remains constant. If the identified range is smaller than 25 %, the opening force analysis should be

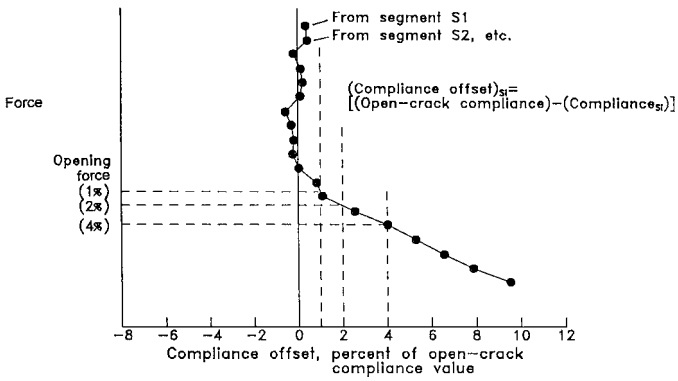

FIG. X2.3 Determination of Opening Force Using the Compliance Offset Method

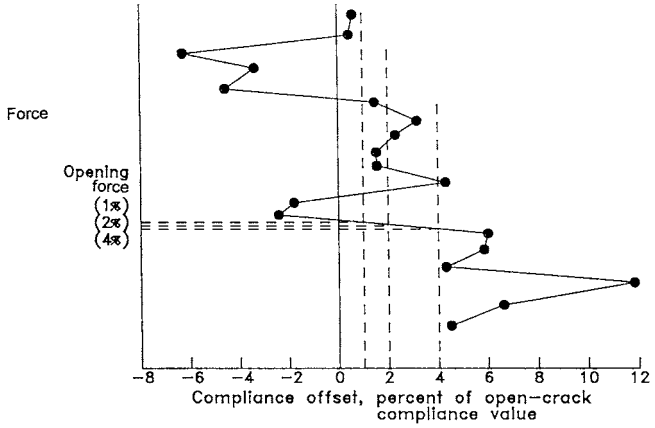

NOTE 1—Multiple crossings of the offset criteria levels is an indication that the variation is too high.

FIG. X2.4 Example of High Variability in Compliance Offset Data

performed again using the new, smaller-range slope value as the open-crack compliance.

X2.7.2 It is recommended that opening forces be determined and reported for offset criteria of 1, 2, and 4 % of the open-crack compliance value. As a minimum, the opening force defined by an offset criterion of 2 % of the open-crack compliance value should be reported.

X2.7.3 It is also recommended that multiple (as many as practicable) opening force determinations be made and that the mean value of the opening forces be reported. The cyclic force level must remain the same and the crack size, *a*, should not change more than 0.001 *W* during the multiple determinations.

X2.8 Data Quality Requirement

X2.8.1 The quality of the raw strain/displacement against force data can affect the value of the opening force determined using the compliance offset method. As used here, data quality is defined in terms of two attributes of the measurement system: (*1*) the linearity of the system, and (*2*) the noise or variability in the system. Both attributes can affect the opening force results. Therefore, it is recommended that the quality of the data be checked for each test specimen.

X2.8.2 To check the quality of data for each test specimen, strain/displacement against force data should be acquired on the notched specimen before a crack is generated in the specimen. Data should be acquired for a complete force cycle at the same loading rate at which data will be acquired during the test. Analyze the data for compliance offset using the same procedure as would be used for a cracked specimen as described in X2.7.1. Using the compliance offset values for the increasing force portion of the force cycle, compute the mean of the compliance offset values and the standard deviation of the offset values about the mean. For a perfectly linear noise-free measurement system, the mean and standard deviation of the offsets should be zero. If the absolute value of the mean of the measured offsets (expressed as percentages of the open-crack compliance) is greater than 1 % or the standard deviation of the offsets is greater than 2 %, the quality of the data is considered unacceptable for the determination of opening load using the compliance offset method. If data quality is not acceptable, the user should check for problems with transducer linearity (see A5.4), specimen flatness, force train alignment (see 6.2), gripping arrangement (see the appropriate specimen annex and A5.5), and noise on the transducer signals (see X2.7.1.5).

X2.9. Report

X2.9.1 The following information should be reported along with all reported measurements of opening force:

X2.9.1.1 The location of the strain or displacement measurement on the specimen and the transducer used to make the measurement.

X2.9.1.2 The value of the compliance offset criterion used in defining opening forces.

X2.9.1.3 The values of the mean and standard deviation of compliance offsets measured on the uncracked specimens.

X2.9.1.4 Typical plots of force against compliance offset for an uncracked specimen and a cracked specimen.

X2.9.1.5 Specimen thickness.

X2.9.1.6 A summary of the fatigue loading conditions prior to the opening force measurements.

X3. GUIDELINES FOR MEASURING THE GROWTH RATES OF SMALL FATIGUE CRACKS

X3.1 Introduction

X3.1.1 Fatigue cracks of relevance to many structural applications are often small or short for a significant fraction of the structural life. The growth rates of such cracks usually cannot be measured with the standard procedures described in the main body of Test Method E647, which emphasizes the use of large, traditional fracture mechanics specimen geometries. Of greater importance, the growth behavior of these small cracks is sometimes significantly different from what would be expected based on large-crack growth rate data and standard fatigue crack growth analysis techniques. Direct measurement of small-crack growth rates may be desirable in these situations.

X3.1.2 This appendix provides general guidelines for test methods and related data analysis techniques to measure the growth rates of small fatigue cracks. Complete, detailed test procedures are not prescribed. Instead, the appendix provides general guidance on the selection of appropriate experimental and analytical techniques and identifies aspects of the testing process that are of particular importance when fatigue cracks are small.

X3.1.3 Many of the principles and procedures described in the main body of Test Method E647 are applicable to small fatigue cracks, and their use is encouraged unless otherwise noted here. Several aspects of Test Method E647 that should be modified for small cracks are highlighted in this appendix.

X3.2 Scope

X3.2.1 This appendix describes the determination of fatigue crack growth rates in metallic materials for crack sizes that are too small to permit application of the standard methods described in the main body of Test Method E647. A variety of possible specimen geometries and crack size measurement techniques are introduced.

X3.3 Referenced Documents [3]

X3.3 E 4 Practices for Force Verification of Testing Machines

E 466 Practice for Conducting Constant Amplitude Axial Fatigue Tests of Metallic Materials

E 467 Practice for Verification of Constant Amplitude Dynamic Loads on Displacements in an Axial Load Fatigue Testing System

E 606 Practice for Strain-Controlled Fatigue Testing

E 1823 Terminology Relating to Fatigue and Fracture Testing

E 1351 Practice for Production and Evaluation of Field Metallographic Replicas

X3.4 Terminology

X3.4.1 The terms used in this appendix are given in the main body of Test Method E647 and in the other terminology documents referenced in X3.3.

X3.4.2 *Descriptions of Terms Specific to This Standard:*

X3.4.2.1 *small crack*—a crack is defined as being small when all physical dimensions (in particular, both length and depth of a surface crack) are small in comparison to a relevant microstructural scale, continuum mechanics scale, or physical size scale. The specific physical dimensions that define *small* vary with the particular material, geometric configuration, and loadings of interest.

X3.4.2.2 *short crack*—a crack is defined as being short when only one physical dimension (typically, the length of a through-crack) is small according to the description of X3.4.2.1.

NOTE X3.1—Historically, the distinction between *small* and *short* cracks delineated here has not always been observed. The two terms have sometimes been used interchangeably in the literature, and some authors (especially in Europe) employ the term *short crack* to denote the meaning given here to *small crack*.

X3.4.2.3 *surface-crack length*—see Terminology E1823. In this appendix, physical surface-crack length is represented as $2c$.

TABLE X3.1 Classification and Size Guidelines for Small Fatigue Cracks (adapted from 84)

NOTE 1—a here denotes a characteristic crack dimension (length or depth).
r_y is plastic zone size or plastic field of notch.
d_g is characteristic microstructural dimension, often grain size.

Type of Small Crack	Dimension
Mechanically-small	$a \sim \leq r_y$
Microstructurally-small	$a \sim \leq$ 5–10 d_g
Physically-small	$a \sim \leq$ 1 mm
Chemically-small	a up to ~10 mm

X3.4.2.4 *surface-crack depth*—see **crack depth** in Terminology E1823. In this appendix, the physical surface-crack depth is represented as a.

X3.5 Significance and Use

X3.5.1 *The Small-Crack Effect:*

X3.5.1.1 Small fatigue cracks can be particularly important in structural reliability because of the so-called *small-crack effect*, the observation that small cracks sometimes grow at rates that are faster than long fatigue cracks at the same nominal crack driving force (typically expressed as ΔK). The reasons for this effect, the circumstances under which it will occur, and the proper means of rationalizing it analytically have been studied and discussed extensively (**85-91**), although full consensus has not been reached on all major issues.

X3.5.1.2 The effect is most often observed when the crack size is on the order of a characteristic microstructural dimension, such as the grain size, or a characteristic continuum mechanics dimension, such as the crack-tip or notch plastic zone size. In the former case, enhanced or reduced crack growth rates arise from interactions with the local microstructure that do not occur when total crack sizes and crack-tip process zones are relatively large. In the latter case, the variation in growth rates may arise from a fundamental change (that is, an increase) in the crack driving force due to enhanced plastic deformation that is not reflected in the usual small-scale-yielding parameter ΔK. Small-crack effects can also arise from other phenomena, such as alterations in localized crack chemistry and the associated kinetics of environmentally-assisted fatigue crack growth.

X3.5.1.3 It is often of practical importance to estimate the crack size below which data from small- and large-crack tests tend to differ. Different criteria (**92**) have been proposed for this dimension depending on the particular type of small crack, as summarized in Table X3.1. A crack which satisfies any one (or more) of these dimensional criteria may exhibit small-crack behavior.

X3.5.1.4 Another approach to identification of the small-crack regime follows from the original work of Kitagawa and Takahashi (**93**) which showed that threshold crack growth rate data display a dependence on crack size that is related to the material's fatigue limit (ΔS_e) and ΔK_{th}. This idea, which combines fatigue crack initiation and propagation concepts, is illustrated schematically in Fig. X3.1. Considering crack initiation, and disregarding the possibility of a pre-existing crack, specimen failure should occur only if

$$\Delta S_{applied} > \Delta S_e \tag{X3.1}$$

Alternatively, considering a fracture mechanics approach, crack growth should occur only if

$$\Delta K_{applied} > \Delta K_{th} = F \Delta S \sqrt{\pi a} \tag{X3.2}$$

where F is a function of crack and specimen geometry and a is the crack length. Solving this equation for ΔS gives

$$\Delta S = \frac{\Delta K_{th}}{F\sqrt{\pi a}} \tag{X3.3}$$

indicating that crack propagation should only occur in the region above the line of slope equal to – 1/2. Thus, the utility

of ΔK_{th} as a *material property* appears to be limited to cracks of length greater than that given by the intersection of the two lines (a_0). For many materials, a_0 appears to give a rough approximation of the crack size below which microstructural small-crack effects become potentially significant (**94**). Note, however, that a_0 may underestimate the importance of small-crack effects when crack wake closure or localized chemistry dominates the geometry effect on crack growth rates. Further discussion of this construction and its limitations is available in (**95**).

X3.5.1.5 An important manifestation of the small-crack effect is that physically small cracks may grow at ΔK values below the measured large-crack threshold stress-intensity factor range, ΔK_{th}, even when the small cracks are large compared to the microstructure and small-scale-yielding parameters appear to adequately describe the crack driving force. It is not entirely clear if this phenomenon indicates anomalous small-crack behavior or anomalous large-crack behavior. These small-crack growth data are often consistent with the large-crack data if the near-threshold large-crack data are neglected and if large-crack data are determined so as to minimize the effects of crack closure. In any case, the phenomenon is significant because predictions of small-crack growth in engineering structures based on laboratory large-crack (near-threshold) data may be extremely nonconservative. It is not clear if a measurable threshold exists for the growth of small fatigue cracks, although small cracks are sometimes observed to become nonpropagating.

X3.5.1.6 Structural applications in which small fatigue cracks are significant may involve applied stresses that approach or exceed the yield strength of the material. Characterization of the material resistance to stable cyclic crack growth under these conditions may require laboratory testing at similar applied stresses. These tests are not valid by the criteria of the main body of Test Method E647 (see Specimen Configuration, Size, and Preparation), since the specimen is not predominantly elastic at all values of applied force. The basic techniques described in this appendix for performing the test, measuring crack length, and computing the crack growth rate are largely applicable, although a modified specimen design may be required. Alternative elastic-plastic formulations of the correlating parameter for fatigue crack growth rates, such as the range of the *J*-integral (ΔJ), may be required under these conditions (**96**). Changes in crack closure behavior, which may further influence the crack driving force, may also be significant at larger applied stresses.

X3.5.2 *Choice of a Test Method:*

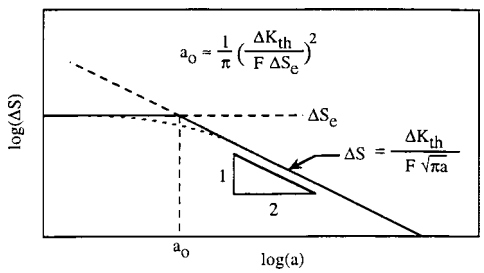

FIG. X3.1 Diagram for Estimating a_o

X3.5.2.1 Several well-established experimental techniques are available for measuring the growth rates of small fatigue cracks and for characterizing other important aspects of small-crack behavior. Some are more amenable than others for routine use, and some require significant expertise. Some require almost no financial investment, while others may require substantial expenditures. All are useful for measuring the growth of fatigue cracks sized on the order of 50 μm or greater, and some are applicable to even smaller cracks.

X3.5.2.2 It is not the purpose of this appendix to recommend one particular measurement technique to the exclusion of the others. Each technique has unique strengths and limitations, and different techniques are optimum for different circumstances. This appendix introduces the various methods available, highlights relative advantages and disadvantages, and discusses in more detail the procedural issues that are common to all methods.

X3.5.2.3 These techniques are described in detail in an ASTM Special Technical Publication, STP 1149 (**87**). That publication and related references should be consulted for further information before a specific testing program is devised. Descriptions of other small fatigue crack experimental and analytical investigations are available in (**88-91**).

X3.5.3 *Specific Test Methods Available:*

X3.5.3.1 *Replication* (**97**,**98**)—While fatigue cycling is interrupted and a static load (typically 50 to 75% of the maximum load) is applied to the specimen, a replica of the surface of the sample is made using a small piece of thin cellulose acetate sheet softened with acetone, a two-part silicon rubber material or a vinyl polysiloxane, gently applied to the specimen surface, and allowed to dry for a few minutes. These form a permanent record of the surface topography, including the crack mouth, and are subsequently viewed in an optical or (with appropriate replica processing) scanning electron microscope to measure surface crack length. See also Practice E1351.

X3.5.3.2 *Photomicroscopy* (**99**, **100**)—To implement photomicroscopy (PM), a camera is linked to a standard metallurgical microscope and interfaced with the fatigue test frame via a microcomputer. An extensive series of high magnification images of the small fatigue crack is obtained during brief interruptions of cycling. Following the test, the crack images are analyzed to determine the surface crack length. Additionally images can be collected at intervals during a load cycle to assess the crack opening behavior using digital image correlation (DIC) techniques.

X3.5.3.3 *Potential Difference* (**101**)—The direct current electric potential difference (DC-EPD) method for continuous in-situ monitoring of crack growth (see Annex A6 to Test Method E647) can be extended to small fatigue cracks. Closed-form analytical models are available to relate crack size to measured potential, as a function of crack shape and probe position locally spanning the crack mouth.

X3.5.3.4 *Scanning Electron Microscopy* (**102**)—A small specimen is cycled on a specialized fatigue loading stage located inside the scanning electron microscope (SEM), and appropriate images are taken as desired. Stereoimaging or

digital image correlation can be used to obtain high resolution displacement measurements on the specimen surface.

X3.5.3.5 *Constant K_{max}-Decreasing ΔK Method* (**103**)—The application of a constant K_{max}-decreasing ΔK load history to a standard (large-crack) FCG specimen has been proposed as a relatively rapid, simple means of minimizing the effects of crack closure. Based on the assumption that small cracks are distinguished from large cracks primarily in terms of reduced closure levels, it has been argued that the method generates an upper bound estimate to small-crack growth rates. This technique cannot address other aspects of the small-crack effect, such as microstructural interactions, extensive crack-tip plasticity, or near-surface residual stresses. This technique is addressed by the main body of Test Method E647.

X3.5.3.6 *Additional Techniques ((**104**),(**105**))*—There are additional techniques that have been used to measure small cracks that are less common than those discussed above. Surface acoustic waves, laser interferometry, ultrasonic, and eddy current techniques offer additional means to assess the size and shape of small cracks.

X3.5.4 *Comparative Remarks about Test Methods:*

X3.5.4.1 *Crack Location*—The replica technique is preferable when the location of crack initiation cannot be predicted with certainty. A chronological series of replicas can be used to track crack growth in reverse time from a large, easily found crack to its origins as a tiny, difficult-to-find microcrack. All other methods generally require a small crack to be located at an early stage of growth (perhaps by replication), or require the location of the crack to be fixed in advance with a micronotch.

X3.5.4.2 *Specimen and Crack Geometries*—The direct optical or imaging (PM, SEM) techniques require specimen surfaces that are either flat or gently curved. The replica and DC-EPD methods can be used on a wider variety of specimens, including cylindrical or notched geometries. Replica, PM, and SEM methods provide information on surface crack length only, while the DIC (if crack compliance can be measured), and DC-EPD measurements give information about crack depth or cracked area. All methods require independent confirmation of crack shape to complete a crack growth analysis. The DC-EPD information can be corrupted by the presence of multiple cracks.

X3.5.4.3 *Test Environments*—Replication is difficult to apply in any environment other than room temperature lab air unless the test is interrupted and the specimen is temporarily separated from the environment. Replication is easily applied to the room temperature laboratory air environment but can be used in other environments as long as test interruption and a temporary separation from the environment do not affect the subsequent crack growth behavior. Crack growth in high temperature or aggressive environments can be addressed by DC-EPD without test interuption. SEM, DIC, and PM can be used, in principle, at elevated temperatures, although additional specialized equipment may be required, and some limitations may remain. The replication process has been shown to influence crack growth rates artificially in some materials, perhaps related to environmental effects. Small-crack tests in the SEM must be performed in vacuum, which may influence crack behavior if ambient environmental effects are significant.

X3.5.4.4 *Resolution*—The SEM technique gives the highest resolution of surface crack length, followed by replication with a resolution on the order of 0.1 μm. Acetate and silicon have similar crack length resolution, but the acetate replica appears to provide microstructure or surface detail. The PM and DIC methods both claim resolutions on the order of 1 μm. The average crack depth resolution of DC-EPD is slightly lower. These are only general, comparative guidelines. The specific resolution attained can be influenced by the quality of the equipment, the experience of the investigators, and the material under investigation. The values given above are based on the work of specialists for each technique. Also note that "resolution" can have different meanings in different applications: for example, direct resolution of surface crack length vs. average resolution of crack depth from model calculations of some measured quantity.

X3.5.4.5 *Cost*—The replica technique involves minimal equipment cost but is extremely labor-intensive and time-consuming. The SEM and DIC approaches require expensive and highly specialized equipment and relatively highly trained operators. PM, DC-EPD techniques require some specialized but relatively inexpensive equipment and may be automated to reduce labor and clock time.

X3.6 Apparatus

X3.6.1 Specimens used to measure the growth rates of small fatigue cracks (X3.7.1) are usually different from standard geometries established for long fatigue crack testing or other fatigue and fracture studies addressed by ASTM standard practices. Because nonstandard specimens and test practices are employed, it is especially important to ensure that basic concerns about specimen fixturing and test frame preparation are given appropriate attention. Specimen fixtures should grip the ends securely, minimize backlash if negative stress ratios are imposed, transmit force to the specimen uniformly, and prevent crack formation at the grips. The test frame should be properly aligned and the force cell properly calibrated. Specific recommendations on some of these issues are contained in the main body of Test Method E647 and in Practices E4, E466, and E467.

X3.6.2 Some small-crack specimen geometries become asymmetric as the crack grows (for example, the corner crack specimen in X3.7.1.4), and the resulting bending moment imposed on the specimen depends on the nature and rigidity of the fixturing. Special caution should be taken to minimize and/or characterize the rotation of the fixturing.

X3.6.3 Nearly all small-crack size measurement techniques (X3.5.3) require additional specialized apparatus such as advanced electronic instrumentation, microscopes, or other devices. This apparatus must be recognized as the source of potential measurement error or artificial influence on crack growth rates. Careful attention must be given to appropriate equipment calibration and verification of proper operation before commencing small-crack testing. The sensitivity or precision of any equipment that directly influences the quantitative measurement of crack size should be determined and reported.

X3.7 Specimen Configuration and Preparation

X3.7.1 *Specimen Design:*

X3.7.1.1 The study of small fatigue cracks requires detection of crack initiation and growth while physical crack sizes are extremely small, and this requirement influences specimen design. Several different small- or short-crack test specimens have been developed to obtain fatigue crack growth rate data. Some of the early specimens were prepared by growing large cracks, interrupting the test, and machining away some of the specimen material to obtain a physically short crack. However, the preferred (and most widely used) specimens promote the initiation of naturally small surface or corner cracks. The early detection of these cracks can be facilitated by using specimens with very small machined starter notches or specimens with mild stress concentrations. Some recommended small-crack specimens are shown schematically in Fig. X3.2.

X3.7.1.2 The rectangular surface-crack specimen, Fig. X3.2(a), is subjected to either remote tension or bending forces. To localize the crack initiation site(s) for the convenience of crack monitoring, three-point bending can be used to confine the maximum outer fiber stress to a small region. Alternatively, a reduced section with a mild radius can be used to localize initiation sites under remote tension **(99)**. Note that although localization by either means is convenient, it may also influence the behavior of naturally initiated cracks due to sampling effects (for example, worst-case effects may not be observed due to biasing of the initiation location).

X3.7.1.3 The cylindrical surface-crack specimen, Fig. X3.2(b), may be identical to a traditional axial fatigue specimen or may be loaded in the rotating bend. This geometry may be particularly useful to avoid crack formation at specimen corners or for testing at large stress ranges. Cracks may be initiated naturally or from a small notch machined on the surface.

X3.7.1.4 The corner-crack specimen, Fig. X3.2(c), was developed to simulate geometries encountered in critical locations in engine discs **(39, 106)**. This specimen is subjected to remote tension forces. The small corner crack is introduced into the specimen by electrical-discharge machining a small corner notch into one edge. This specimen has the advantage that both crack length (c) and crack depth (a) can be monitored by either replication, visual or photographic means.

X3.7.1.5 The specimen with a surface or corner crack at a semi-circular edge notch, Fig. X3.2(d), was developed to produce naturally-occurring cracks at material defects and to propagate cracks through a three-dimensional stress field similar to that encountered at bolt holes in structures **(107)**. This specimen is subjected to either remote tension or bending forces.

X3.7.2 *Crack Initiation Sites:*

X3.7.2.1 Small artificial flaws can be introduced into a specimen through methods such as thin wafer cutoff wheels, electrical discharge machining, focused ion beam machining **(108)** or femtosecond laser ablation **(109)**. These methods may disturb the material ahead of the resulting notch, and require precracking past the distressed zone before the onset of data acquisition. In order to eliminate mechanical notch effects, the size of the precrack region, as measured from the notch root, should be at least two times the notch tip radius.

X3.7.2.2 The specimen geometries used for naturally occurring small fatigue cracks (X3.7.1.2) are designed to localize the crack initiation region within a small area, which allows for crack monitoring methods such as replication or microphotography to be used. These natural small cracks will typically initiate at inclusion particles, voids, scratches, or deformation bands. To ensure that cracks initiate in these intended regions, it is recommended that the corners of the specimens be rounded to suppress corner initiation. This type of specimen permits the acquisition of meaningful fatigue crack growth data immediately after first crack detection.

X3.7.3 *Surface Preparation:*

X3.7.3.1 Near-surface residual stresses and surface roughness induced by specimen machining can artificially influence small-crack growth behavior and should be eliminated prior to testing. However, it should be recognized that the growth rates of small surface cracks in engineering components may be influenced by residual stress fields arising from fabrication of the component, and this may have implications for the application of the laboratory small-crack data.

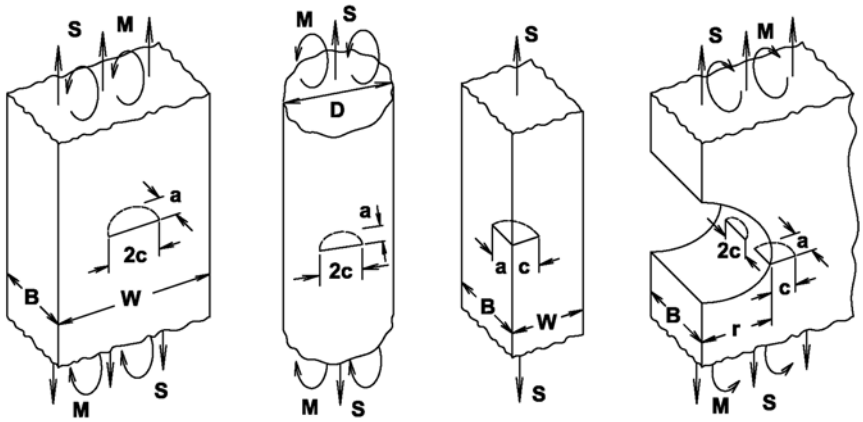

(a) Surface crack in plate (b) Surface crack in cylinder (c) Corner crack (d) Surface or corner crack at notch

FIG. X3.2 Schematic of Commonly Used Small Crack Specimens

X3.7.3.2 Electrical discharge machining and low stress grinding are the preferred machining methods since they have been found to produce significantly lower residual stresses than mechanical milling (**99**). If mechanical milling is employed, it should be followed by a low stress grinding operation.

X3.7.3.3 Surface polishing techniques are used to remove the residual stresses and surface roughness induced by the machining process, and to provide a reflective finish adequate for accurate surface crack size measurements if visual techniques are employed. The two recommended techniques for surface polishing are electropolishing and chemical polishing (**97, 99**). Both methods typically require a surface finish equivalent to 500 grit SiC or better before polishing is initiated. Hand polishing with abrasive media until a desired surface finish is achieved may also be used, but this procedure produces residual stresses and should be followed by either a chemical etching or electro-etching procedure to remove the affected material.

X3.7.3.4 Chemical or ion etching of the specimen surface prior to testing may facilitate identification of microstructural influences on crack behavior when optical or imaging methods are employed to measure the surface crack size. In some materials, however, an etch may confound clear identification of the crack tip location or even remove key microstructural features from which small cracks naturally initiate. Etching after a naturally-initiated crack has been located may be preferable in some cases, although chemical etching in this case may influence subsequent crack growth.The use of orientation imaging microscopy (**110**) before or after initiation of the crack may avoid these problems and still facilitate identification of important microstructural features that influence the crack growth.

X3.8 Procedure

X3.8.1 The detailed procedure for conducting small-crack experiments is test method-specific, and extended discussion of suggested practices for the methods discussed in X3.5.3 is found in (**87**). Procedural issues of general applicability are outlined below.

X3.8.2 *Crack Size and Geometry*—Because the initiation and growth of small fatigue cracks are often dominated by local microstructural and geometric features, it is important that small-crack test specimens simulate actual applications in terms of microstructure, heat treatment, surface finish, and residual stress state, as well as crack size and geometry. The range of crack sizes to be investigated and the crack geometry of interest may have a significant impact on the selection of a test method. For example, the smallest of cracks must be naturally initiated, which precludes the use of artificial crack starters that predetermine the point of crack initiation. Although the absolute minimum detectable crack size may be of scientific interest, data to be used in life predictions of engineering structures may have a practical minimum crack size that is dictated by the limits of available, or foreseeable, methods of nondestructive inspection. Crack sizes in this range tend to be more amenable to study by a variety of experimental techniques.

X3.8.3 *Stress Level and Stress Ratio*—Selection of the stress level and stress ratio for testing are important considerations, and have numerous ramifications, both experimentally and analytically. For many materials, nominal maximum stresses of the order of 0.6 times the material yield strength (σ_{YS}) will facilitate natural initiation of a small number of cracks in a relatively short time, and the nominally elastic stress state permits a traditional fracture mechanics analysis to be used. Maximum stress levels approaching or exceeding σ_{YS} tend to produce multiple cracks, and the associated analysis must deal with the accompanying extended plastic deformation. Moreover, the stress ratio chosen may dramatically influence the time required to naturally initiate cracks. Ultimately, decisions regarding stress level and stress ratio may be dictated by the intended application for the data.

X3.8.4 *Crack Size Measurements:*

X3.8.4.1 To document crack growth events adequately at the smallest crack sizes, it is desirable to measure crack size at frequent intervals. In addition, real-time assessment of crack size may not be practical using some techniques, requiring that frequent measurements be made to capture unexpected events. This is particularly true for the smallest crack sizes. Recommended analysis procedures for dealing with such data are discussed in X3.9.2.

X3.8.4.2 In addition to measurement of surface crack length ($2c$), calculations of crack driving force require knowledge of crack shape. Normally a semielliptical crack shape is assumed, but some measurement of crack depth (a) must be made. Given a knowledge of surface crack length, some measurement techniques provide approaches for deducing crack depth, but direct, nondestructive measurement of crack shape is not currently possible. For some materials, it is possible to use fractographic measurements to develop a relationship of crack aspect ratio as a function of crack size that is representative of all small cracks in the material (**97**). This relationship may then be used in crack driving force calculations.

X3.9 Calculation and Interpretation

X3.9.1 *Calculation of* ΔK*:*

X3.9.1.1 Many of the available small-crack test methods address cracks that are assumed to be approximately semielliptical in shape. Accepted stress intensity factor solutions for a variety of embedded, surface, and corner crack geometries in plates and rods are given in (**111-113**). The general form of these solutions is

$$\Delta K = F_j \Delta S_i \sqrt{\pi a/Q} \qquad \text{(X3.4)}$$

where ΔS_i is the remote uniform tensile stress range ($i = t$) or outer fiber bending stress range ($i = b$), Q is the elliptical crack shape factor, and F_j is the boundary-correction factor which accounts for the influence of the various free-boundary conditions. Note that F_j changes around the perimeter of the crack, and this dependence may influence the crack growth process. It is customary to characterize fatigue crack growth for a stable, semicircular crack shape on the basis of ΔK calculated at the deepest point of the crack. Note also that some K solutions in the literature are presented using notations that differ from the

notations in Fig. X3.2 (for example, plate half-width w versus full plate width $W = 2w$).

X3.9.1.2 For fine-grain, isotropic materials the assumption of a semielliptical shape appears reasonable. Although the shapes of very small cracks may be dramatically affected by local microstructural features, as the cracks grow they tend to assume a semielliptical shape and, in many instances, become nearly semicircular. Cracks in materials having coarse microstructures and/or exhibiting crystallographic texture and anisotropy may never assume a semielliptical shape. As stated in X3.8.4.2, crack shape must be documented for accurate calculation of ΔK. Simple approximation techniques have been presented to estimate the stress intensity factor for surface or corner cracks of non-elliptical shape (**114**). Typically, non-elliptical crack shapes depend on local microstructural features and, as such, their shapes tend to be inherently variable. Recognizing the stochastic nature of these cracks, it is often reasonable, or necessary, to approximate their shapes as semielliptical.

X3.9.1.3 Another problem involves the initiation of multiple cracks within a small region. These cracks may coalesce to form a single long, shallow surface crack. Criteria have been proposed (**97**) for defining the point at which the stress fields of closely spaced crack tips begin to interact.

X3.9.1.4 Under tension-compression loading, $R \leq 0$, it is conventional to use only the positive portion of the stress range to calculate the crack driving force; that is, $\Delta K = K_{max}$ (see Terminology in the main body of Test Method E647). When crack closure is considered, however, the issue becomes significantly more complex, and the conventional definition of $\Delta K = K_{max}$ may be inappropriate. Numerous investigators have demonstrated that the level of crack closure depends on many factors, including crack size (for example, see (**115**)). In particular, crack opening stresses are thought to be lower for small cracks, even opening at nominally compressive stresses under some conditions. This factor raises important questions regarding the applicability of large-crack data, particularly in the near-ΔK_{th} region, to the prediction of the growth of small cracks. Some of the crack size measurement techniques described in X3.5.3 also may be used to measure crack closure levels, particularly DIC and SEM.

X3.9.2 *Calculation of Crack Growth Rate:*

X3.9.2.1 Analysis of crack-size data to determine crack growth rates requires special consideration. The minimum interval between successive crack size measurements for large-crack tests (see Procedure in the main body of Test Method E647) is stipulated as ten times the measurement precision. This may require that crack growth data be acquired at specified intervals of crack length, or that the $a-N$ data be edited to remove data to achieve the desired interval, Δa. The inherent difficulty in this process is selecting the data points for removal. Small-crack measurement techniques often have measurement precision that is of the order of microstructural dimensions. As a result, discontinuities in the $a-N$ (or $2c-N$) data arise due to crack interactions with microstructure, as well as from inherent errors in the measurements. If a minimum level of Δa is used as a criterion for editing the data, then the selected data points will often be the first point after the crack has broken through a local microstructural obstacle, and the data exhibiting the crack retardation in the microstructure will be lost. While the large-crack measurement intervals are recommended where possible, some uses of small-crack data may require smaller measurement intervals in order to capture key microstructural effects.

X3.9.2.2 Much of the small-crack growth rate data in the literature has not been reduced following the above guidance, and in many cases the da/dN calculations appear to demonstrate variability that is significantly influenced by measurement error. The basic problem may be outlined as follows. As the crack size interval, Δa, between successive measurements decreases, the relative contribution of the measurement error to the calculated value of da/dN increases. For example, assume that a single crack size measurement is given by $\hat{a} = a + \varepsilon$, where $\hat{a}$ is the measured crack size, a is the true crack size, and ε is the error inherent in the crack size measurement, normally distributed about zero. A direct-secant calculation of crack growth rate between two successive crack size measurements (a_1 and a_2) is given by

$$\frac{\Delta \hat{a}}{\Delta N} = \frac{(a_2+\varepsilon_2) - (a_1+\varepsilon_1)}{\Delta N} = \frac{\Delta a}{\Delta N} + \frac{\Delta \varepsilon}{\Delta N} \qquad \text{(X3.5)}$$

Thus, as $\Delta a/\Delta N$ approaches zero, the error term $\Delta\varepsilon/\Delta N$ dominates the calculated value of $\Delta\hat{a}/\Delta N$. Since small-crack data are often acquired at low growth rates, the crack extension between successive measurements tends to be small, and the growth rate data may exhibit an unusually large variability due to measurement error. It is recommended that the small-crack data be edited to remove this variability, or one may use a modified version (for example, (**99**)) of the standard incremental polynomial regression used for large cracks. The reader is cautioned that different data analysis procedures can also significantly influence the apparent scatter in growth rate (**116**).

X3.10 Reporting

X3.10.1 The reporting guidelines prescribed in the main body of Test Method E647 apply to the suggested procedure for small-crack tests. In addition, it is often useful to provide a record of the degree of crack deflection and tortuosity, the degree of asymmetric crack growth, and the crack shape for use in calculations of crack driving force. It is customary to report crack size in terms of its projection on a plane normal to the axis of loading, but significant deviations of the crack path from this plane should be noted in the report. Since the method of crack initiation can have a significant influence on subsequent crack growth, the test conditions and number of cycles required for crack initiation should be reported, along with the measured size of the crack at this number of cycles. The estimated resolution of the crack size measurement technique, the specific data analysis method used to calculate crack growth rates, and the specific K solution employed should also be recorded.

X4. RECOMMENDED PRACTICE FOR DETERMINATION OF ACR-BASED STRESS-INTENSITY FACTOR RANGE

X4.1 Introduction

X4.1.1 This appendix describes the Adjusted Compliance Ratio (ACR) method to estimate the effects of remote closure. Remote closure refers to crack tip shielding as a result of contact in the crack wake away from the crack tip (**117**). This is in contrast to other shielding mechanisms near to the crack tip such as plasticity. The ACR method is based on the same measurement signals that are used for the opening force method in Appendix X2, which describes a method to estimate the 2% crack opening force.

X4.2 Scope

X4.2.1 This appendix covers the experimental determination of the ACR-based crack driving force during tests of the specimens outlined in this test method, subjected to constant amplitude or K-control methods, and based on procedures recommended in this standard. The ACR method builds on the opening force method of closure determination as well as compliance method of crack size determination, so familiarity and conformity with Appendix X2 and Annex A5 of this standard are assumed.

X4.3 Terminology

X4.3.1 *Definitions*—Definitions of terms specific to this appendix are given in this section. Other terms used in this appendix are defined in the main body of this test method.

X4.3.1.1 *open-crack compliance, C_o $[LF^{-1}]$*—the open-crack compliance for the specimen at a given crack size.

X4.3.1.1.1 *Discussion*—for the purposes of this appendix, all compliance values may be expressed as either *EvB/P* or *v/P*, where *E* is elastic modulus, *v* is displacement between two points, *B* is specimen thickness, and *P* is force. The former is dimensionless, while the latter has dimensions of LF^{-1}. For consistency with Appendix X2, all compliances in this appendix are assumed to be calculated as $C = v/P$.

X4.3.1.2 *secant compliance, C_s $[LF^{-1}]$*—the secant compliance for the specimen at a given crack size as defined by the secant of the unloading compliance curve between the maximum force and minimum force.

X4.3.1.3 *initial open-crack compliance, C_{oi} $[LF^{-1}]$*—the notch open-crack compliance before a crack has formed.

X4.3.1.4 *initial secant compliance, C_{si} $[LF^{-1}]$*—the notch secant compliance before a crack has formed.

X4.3.1.5 *adjusted compliance ratio, UACR* —a dimensionless parameter representing the ratio of secant to open-crack compliances, both adjusted by the initial compliance.

X4.3.1.6 *stress-intensity factor range based on adjusted compliance ratio, ΔK_{ACR} $[FL^{-3/2}]$*—in fatigue, the stress-intensity factor range computed using the Adjusted Compliance Ratio method.

X4.4 Significance and Use

X4.4.1 The method of determining ΔK_{ACR} presented in this appendix provides an engineering approximation that has been used in various ways to predict crack growth (**118**, **119**) and compare material performance (**120**, **121**, **122**). The method has been used for removing remote closure effects associated with microstructure or residual stress (**120**, **121**) and has been used in conjunction with a power law equation to collapse data to a unique curve (**123**, **122**), which can then be transformed into design curves (**122**).

NOTE X4.1—Some materials and loading situations may exhibit strong near-tip closure effects (that is, due to oxide formation, etc). In this case the ACR method may not be suitable.

X4.5 Basis for Determination of Driving Force by the ACR Method

X4.5.1 The ACR method has been shown to be independent of measurement location for experimental measurements along the crack plane behind the crack tip (**118**) and for an analytical evaluation along the load line (**124**), which provides a foundation for using the same algorithm for front-face clip-gage and back-face strain-gage. Additional research was performed to investigate a relationship between remote crack wake interference and the crack-tip cyclic strain (**125**). An interlaboratory round robin was performed as part of the second round robin on closure measurement (**126**) based on the measured force-displacement traces collected in the second round robin on closure measurement.

X4.5.2 The ACR method focuses on the displacement or strain range between maximum and minimum force due to crack closure rather than the point of deviation in linearity of the force versus displacement/strain curve. Although the opening force, P_{op}, is not used directly in the calculation of ACR values, accurately determining the opening force is essential to guarantee that the linear slope of the fully open crack is achieved. The same precautions regarding apparatus and data quality given in the opening force method are equally applicable to the ACR method. Therefore, adherence to the procedures specified in sections X2.5 through X2.8 of Appendix X2 are necessary for the proper determination of ACR.

X4.6 Apparatus

X4.6.1 The procedure requires no new hardware beyond what is necessary to evaluate P_{op} in Appendix X2 of this standard. However, the apparatus should be capable of recording the secant compliance as outlined below in addition to the open crack compliance and other quantities specified in Test Method E647.

X4.7 Recommended Procedure-Determination of Driving Force by the ACR Method

X4.7.1 *Data Collection:*

X4.7.1.1 The ACR method is intended to be implemented in the context of a computer monitored or controlled fatigue crack growth rate test that meets the requirements of this test method. In a typical implementation, a digital data acquisition system is used to collect the cyclic force and associated frontface clip gage displacement data on a periodic basis. These data are tabulated and used to determine the open-crack compliance,

crack size, and stress-intensity factor as a function of elapsed cycle count; then these data are subjected to numerical analysis to determine the crack growth rate as a function of stress-intensity factor. In the ACR method, an additional quantity is saved. Each time that the open-crack compliance and other quantities are calculated, the secant compliance must also be calculated using the end points of the force-displacement data. Fig. X4.1 contains a schematic of two force-displacement curves – one for the notch before the crack forms and one for a current crack configuration after the crack has formed and grown. For the current crack, Fig. X4.1 indicates the opening force, P_{op}, which defines the lower bound for the linear portion of the force-displacement curve, and the open-crack compliance, C_o, which is calculated by fitting a straight line to the upper linear part of a force-displacement curve. The secant compliance, C_s, is the slope drawn between the upper and lower coordinates of the force versus displacement curve for a given loading cycle, as shown in Fig. X4.1, and is computed from maximum and minimum values of force and displacement as follows:

$$C_s = \frac{\upsilon_{max} - \upsilon_{min}}{P_{max} - P_{min}} \quad \text{(X4.1)}$$

where:

P_{max} = maximum value of applied force,
P_{min} = minimum value of applied force,
υ_{max} = value of crack opening displacement at P_{max},
υ_{min} = value of crack opening displacement at P_{min}.

X4.7.1.2 When back-face strain is used, the secant compliance can be defined as:

$$C_s = \frac{\varepsilon_{max} - \varepsilon_{min}}{P_{max} - P_{min}} \quad \text{(X4.2)}$$

where:

ε_{max} = value of back surface strain at P_{max},
ε_{min} = value of back surface strain at P_{min}.

X4.7.1.3 The ACR method adds one new quantity, the secant compliance, to the table of data that will be subjected to numerical analysis.

X4.7.2 *Results Calculation:*

X4.7.2.1 After data collection the ACR method values are calculated as follows:

X4.7.2.2 The initial values of open-crack compliance, C_{oi}, and secant compliance, C_{si}, must be calculated. These are the respective average values associated with the notch before crack formation. The number of cycles necessary for averaging may be dependent on the magnitude and range of the signals as well as signal quality. One approach is to review the respective compliance values, for instance as a plot of compliance versus cycles or compliance versus crack length. Then identify an initial range for each that represents average response for cycles applied before crack growth has occurred. In addition, Note A5.1 contains guidance for averaging data in terms of crack length increment that may be useful for averaging the initial values of open-crack and secant compliances here.

X4.7.2.3 For each recorded value of the open-crack and secant compliances the U_{ACR} value is calculated as follows:

$$U_{ACR} = \frac{C_{oi}}{C_{si}} \cdot \frac{C_s - C_{oi}}{C_g - C_{gi}} \quad \text{(X4.3)}$$

where the ratio of C_{oi}/C_{si} compensates for a possible bias in the secant or open-crack compliances because of signal conditioning noise or nonlinearity.

NOTE X4.2—Experience has shown that, under most circumstances, the difference between C_{oi} and C_{si} is less than 0.5%. An analysis of error limits for typical clip-gage displacement and force indicates that a nearly

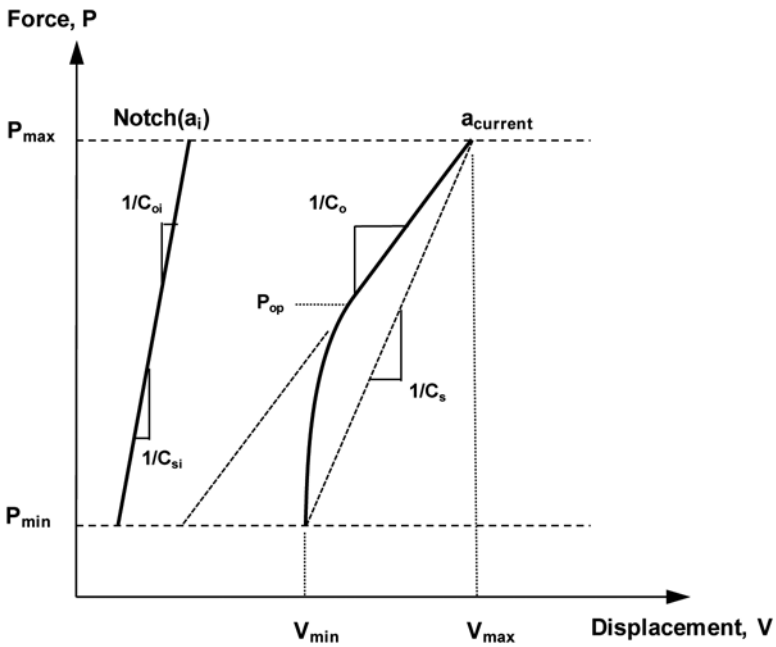

FIG. X4.1 Schematic of Force Displacement Records showing Critical Parameters for the ACR Method.

1% difference between the compliances may be possible when the force and displacement errors are combined. Thus, a ratio of C_{oi}/C_{si} outside the range $0.99 \le C_{oi}/C_{si} \le 1.01$ may indicate poor data quality or excessive nonlinearity in one or both of the transducer signals that should be investigated. Note that frequency effects, such as nonlinearity as a result of electronic filtering effects or increased noise caused by resonant frequencies can influence the quality of ACR data.

NOTE X4.3—The value of U_{ACR} is theoretically undefined until crack advance occurs because C_s, C_o, and C_{oi} will initially be nominally equal to each other. In practice, for high-speed digital systems, enough data collection and testing variability occur for this not to create difficulties numerically. However, the recommended practice is to use the crack formation period to calculate the initial values of the open crack and secant compliances and use the crack growth period to calculate the U_{ACR} and ΔK_{ACR} values.

X4.7.2.4 The driving force, ΔK_{ACR}, is calculated as follows:

$$\Delta K_{ACR} = U_{ACR} \cdot \Delta K_{fr} \quad \text{(X4.4)}$$

where ΔK_{fr} is the full range stress-intensity factor as calculated for each data point and as discussed in Section 3, Terminology.

X4.8 Data Quality Requirement

X4.8.1 The procedure has no new data quality or hardware requirements beyond what are necessary to evaluate P_{op} in Appendix X2 of this standard.

X4.9 Report

X4.9.1 The following information should be reported:

X4.9.1.1 All items in section X2.9 of Appendix X2.

X4.9.1.2 The initial open-crack compliance before a crack has formed, C_{oi}.

X4.9.1.3 The initial secant compliance before a crack has formed, C_{si}.

X4.9.1.4 All calculated values of the open-crack compliance, C_o.

X4.9.1.5 All calculated values of the secant compliance, C_s.

X4.9.1.6 All calculated values of the adjusted compliance ratio, U_{ACR}.

X4.9.1.7 All calculated values of the ACR stress-intensity factor range, ΔK_{ACR}.

REFERENCES

(1) Hudak, Jr., S. J., and Bucci, R. J., *Fatigue Crack Growth Measurement and Data Analysis, ASTM STP 738*, ASTM, 1981.

(2) Paris, P. C., "The Fracture Mechanics Approach to Fatigue," *Proceedings of the Tenth Sagamore Army Materials Research Conference*, Syracuse University Press, 1964, pp. 107–132.

(3) Bucci, R. J., "Effect of Residual Stress on Fatigue Crack Growth Rate Measurement," *Fracture Mechanics (13th Conference), ASTM STP 743*, 1981, pp. 28–47.

(4) Bush, R.W., Bucci, R.J., Magnusen, P.E., and Kuhlman, G.W., "Fatigue Crack Growth Rate Measurements in Aluminum Alloy Forgings: Effects of Residual Stress and Grain Flow," Fracture Mechanics: Twenty Third Symposium, ASTM STP 1189, Ravinder Chona, Ed., American Society for Testing and Materials, Philadelphia, 1993, pp. 568-589.

(5) Suresh, S., and Ritchie, R. O.," Propagation of Short Fatigue Cracks," *International Metals Review*, Vol 29, #6, December 1984, pp. 445 –476.

(6) Hudak, Jr., S. J., "Small Crack Behavior and the Prediction of Fatigue Life," *Journal of Engineering Materials and Technology*, Vol 103, Jan. 1981, pp. 26–35.

(7) Herman, W. A., Hertzberg, R. W., and Jaccard, R., "A Simplified Laboratory Approach for the Prediction of Short Crack Behavior in Engineering Structures," Fatigue and Fracture of Engineering Materials and Structures, Vol II, No. 4, 1988.

(8) Suresh, S., and Ritchie, R. O., "Near-Threshold Fatigue Crack Propagation: A Perspective on the Role of Crack Closure," *Fatigue Crack Growth Threshold Concepts* TMS-AIME D. L. Davidson, S. Suresh, editors; Warrendale, PA, 1984, pp. 227–261.

(9) Clark, Jr., W. G., "Fracture Mechanics in Fatigue," *Experimental Mechanics*, September 1971, pp. 1–8.

(10) Hoeppner, D. W., and Krupp, W. E., "Prediction of Component Life by Application of Fatigue Crack Growth Knowledge," *Engineering Fracture Mechanics*, Vol 6, 1974, pp. 47–70.

(11) *Fatigue Crack Growth Under Spectrum Loads, ASTM STP 595*, ASTM, 1976.

(12) Scavone, D. W., "Development of an Instrumented Device to Measure Fixture-Induced Bending in Pin-Loaded Specimen Trains," *Factors That Affect the Precision of Mechanical Test, ASTM STP 1025*, Papirno, R. and Weiss, H. C. Eds., ASTM, 1989, pp. 160–173.

(13) ASTM B909-00: Standard Guide for Plane Strain Fracture Toughness Testing of Non-Stress Relieved Aluminum Products, Annual Book of Standards, Section 2 – Nonferrous Metal Products, Vol. 02.02, Aluminum and Magnesium Alloys, ASTM, West Conshohocken, PA, 2001, pp. 614-617.

(14) Hudak, Jr., S. J., Saxena, A., Bucci, R. J., and Malcolm, R. C., "Development of Standard Methods of Testing and Analyzing Fatigue Crack Growth Rate Data—Final Report," *AFML TR 78-40*, Air Force Materials Laboratory, Wright Patterson Air Force Base, OH, 1978.

(15) Brose, W. R., and Dowling, N. E., "Size Effects on the Fatigue Crack Growth Rate of Type 304 Stainless Steel," *Elastic-Plastic Fracture, ASTM STP 668*, 1979, pp. 720–735.

(16) Hudak, Jr., S. J., "Defining the Limits of Linear Elastic Fracture Mechanics in Fatigue Crack Growth," *Fatigue Crack Growth Measurement and Data Analysis, ASTM STP 738*, ASTM, Oct. 29–30, 1980.

(17) Dowling, N. E., "Fatigue Crack Growth Rate Testing at High Stress Intensities," *Flaw Growth and Fracture, ASTM STP 631*, ASTM, 1977, pp. 139–158.

(18) James, L. A., "Specimen Size Considerations in Fatigue-Crack Growth Rate Testing," *Fatigue Crack Growth Measurement and Data Analysis, ASTM STP 738*, ASTM, 1981, pp. 45–57.

(19) Clark, Jr., W. G., and Hudak, Jr., S. J., "Variability in Fatigue Crack Growth Rate Testing," *Journal of Testing and Evaluation*, Vol 3, No. 6, 1975, pp. 454–476.

(20) Hudak, Jr., S. J., and Wei, R. P., "Consideration of Nonsteady State Crack Growth in Materials Evaluation and Design," *International Journal of Pressure Vessels and Piping*, Vol 9, 1981, pp. 63–74.

(21) Garr, K. R. and Hresko, G. C., "A Size Effect on the Fatigue Crack Growth Rate Threshold of Alloy 718", Fatigue Crack Growth Thresholds, Endurance Limits, and Design, ASTM STP 1372, J.

Newman, Jr. and R. Piascik, eds., American Society for Testing and Materials, West Conshohocken, PA, 2000.
(22) Forth, S.C., Newman, J.C., Jr., and Forman, R.G. "Anomalous Fatigue Crack Growth Data Generated using the ASTM Standards," 35th NSFFM, Reno, NV, May 2005 .
(23) Saxena, A., Hudak, Jr., S. J., Donald, J. K., and Schmidt, D. W., "Computer-Controlled Decreasing Stress Intensity Technique for Low Rate Fatigue Crack Growth Testing," *Journal of Testing and Evaluation*, Vol 6, No. 3, 1978, pp. 167–174.
(24) Donald, J. K., and Schmidt, D. W., "Computer-Controlled Stress Intensity Gradient Technique for High Rate Fatigue Crack Growth Testing," *Journal of Testing and Evaluation*, Vol 8, No. 1, Jan. 1980, pp. 19–24.
(25) Donald, J. K., "The Effect of Out-of-Plane Cracking on FCGR Behavior," ASTM Research Report #E8-1001, December 12, 1995.
(26) Chan, K. S., and Cruse, T. A., "Stress Intensity Factors for Anisotropic Compact Tension Specimens With Inclined Cracks," Engineering Fracture Mechanics, Vol 23, No. 5, pp. 863–874.
(27) Clark, Jr., W. G., and Hudak, Jr., S. J., "The Analysis of Fatigue Crack Growth Rate Data," *Application of Fracture Mechanics to Design*, Burke, J. J. and Weiss, V., Eds, Vol 22, Plenum, 1979, pp. 67–81.
(28) Bucci, R. J., in *Fatigue Crack Growth Measurement and Data Analysis, ASTM STP 738*, ASTM, 1981, pp. 5–28.
(29) Wei, R. P., Wei, W., and Miller, G. A., "Effect of Measurement Precision and Data-Processing Procedure on Variability in Fatigue Crack Growth-Rate Data," *Journal of Testing and Evaluation*, Vol 7, No. 2, March 1979, pp. 90–95.
(30) McKeighan, P.C., Feiger, J.H. amd McKnight, D.H., "Round Robin Test Program and Results for Fatigue Crack Growth Measurement in Support of ASTM Standard E647," Final Report, Southwest Research Institute, February 2008.
(31) Donald, J. K.," Preliminary Results of the ASTM E24.04.03 Round-Robin Test Program on Low Delta-*K* Fatigue Crack Growth Rates," ASTM E24.04.03 Task Group Document, December 1982.
(32) Saliver, G.C. and Goree, J.G., "The Applicability of ASTM Standard Test Specimens to Fracture and Fatigue Crack Growth of Discontinuous-Fiber Composites," *Journal of Testing and Evaluation*, JTEVA, Vol. 26, No. 4, July 1998, pp. 336-345.
(33) Hartman, G. A., and Ashbaugh, N. E., "Load Pin Size Effects in the C(T) Geometry," ASTM Research Report RR:E24-1016, Oct 1991.
(34) Newman, Jr., J. C.," Stress Analysis of the Compact Specimen Including the Effects of Pin Loading" *Fracture Analysis (8th Conference), ASTM STP 560*, ASTM, 1974, pp. 105–121.
(35) Srawley, J. E., "Wide Range Stress Intensity Factor Expressions for ASTM Method E399 Standard Fracture Toughness Specimens," *International Journal of Fracture*, Vol 12 , June 1976, pp. 475–476.
(36) Saxena, A., and Hudak, Jr., S. J., "Review and Extension of Compliance Information for Common Crack Growth Specimens," International Journal of Fracture, Vol 14, No. 5, Oct 1978.
(37) Yoder, G. R., Cooley, L. A., and Crooker, T. W., "Procedures for Precision Measurement of Fatigue Crack Growth Rate Using Crack-Opening Displacement Techniques," *Fatigue Crack Growth Measurements and Data Analysis, ASTM STP 738*, ASTM, 1981, pp. 85–102.
(38) Hicks, M. A., and Pickard, A. C., "A Comparison of Theoretical and Experimental Methods of Calibrating the Electrical Potential Drop Technique for Crack Length Determination," *Int. Journal of Fracture*, No. 20, 1982, pp. 91–101.
(39) Mom, A., and Raizenne, M. D.," AGARD Engine Disk Cooperative Test Programme," AGARD report number 766, Aug., 1988.
(40) Raizenne, M. D., "AGARD TX114 Test Procedures for Supplemental Engine Disc Test Programme," National Research Council Canada, LTR-ST-1671, June 1988.
(41) Metals Handbook, Vol 8, Published under the direction of the American Society for Metals, 9th Edition, Metals Park, OH, 1987, pp. 386–391.
(42) Newman, J.C., Jr., Haines, M.J., "Verification of Stress-Intensity Factors for Various Middle-Crack Tension Test Specimens," Engineering Fracture Mechanics – Technical Note, August 2004.
(43) Ashbaugh, N. E., and Johnson, D. A.," Determination of Crack Length as a Function of Compliance and Gage Length for an M(T) Specimen," ASTM Research Report (RR: E24–1017, April 1992).
(44) Johnson, H. H., "Calibrating the Electric Potential Method for Studying Slow Crack Growth," *Materials Research and Standards*, Vol 5, No. 9, Sept. 1965, pp. 442–445.
(45) Sullivan, A.M., "New Specimen Design for Plane-Strain Fracture Toughness Tests," *Materials Research and Standard*, Vol. 4, No. 1, 1964, pp. 20–24.
(46) Piascik, R.S., Newman, J.C., Jr., and Underwood, J.H., "The Extended Compact Tension Specimen," *Fatigue and Fract. Engng. Mater. Struct.,* Vol. 20, No. 4, 1997, pp. 559–563.
(47) John, R., "Stress Intensity Factor and Compliance Solutions for an Eccentrically Loaded Single Edge Cracked Geometry," *Engineering Fracture Mechanics*, Vol. 58, No. 1/2, 1997, pp. 87–96.
(48) Piascik, R. S. and Willard, S. A, "The Growth of Small Corrosion Fatigue Cracks in Alloy 2024," *Fatigue Fract. Engng. Mater. Struct.*, Vol. 17, No. 11, 1994, pp. 1247–1259.
(49) Richardson, D. E. and Goree, J. G., "Experimental Verification of a New Two-Parameter Fracture Model," *ASTM STP 1189*, R. Chona, ed., 1993, pp. 738–750.
(50) Piascik, R.S. and Newman, J.C., Jr., "An Extended Compact Tension Specimen for Fatigue Crack Growth and Fracture Testing," *International Journal of Fracture*, Vol. 76, No. 3, 1995, pp. R43-R48.
(51) Schwalbe, K. H. and Hellmann, "Applications of the Electrical Potential Method to Crack Length Measurements Using Johnson's Formula," *Journal of Testing and Evaluation*, Vol. 9 , No. 3, 1981, pp. 218–221.
(52) Wei, R. P., and Shim, G., "Fracture Mechanics and Corrosion Fatigue," *Corrosion Fatigue: Mechanics, Metallurgy, Electrochemistry and Engineering, ASTM STP 801*, ASTM, 1983, pp. 5–25.
(53) Barsom, J. M., "Effects of Cyclic Stress Form on Corrosion Fatigue Crack Propagation Below K_{Iscc} in a High Yield Strength Steel," *Corrosion Fatigue: Chemistry, Mechanics and Microstructure*, NACE-2, National Association of Corrosion Engineers, 1972 , pp. 424–433.
(54) Vosikovsky, O., "Effects of Mechanical and Environmental Variables on Fatigue Crack Growth Rates in Steel. A Summary of Work Done At CANMET," *Canadian Metallurgical Quarterly*, Vol 19, 1980, pp. 87–97.
(55) Selines, R. J., and Pelloux, R. M., "Effect of Cyclic Stress Wave Form on Corrosion Fatigue Crack Propagation in Al-Zn-Mg Alloys," *Metallurgical Transactions*, Vol 3, 1972, pp. 2525–2531.
(56) Dawson, D. B., and Pelloux, R. M., "Corrosion Fatigue Crack Growth in Titanium Alloys in Aqueous Environments." *Metallurgical Transactions*, Vol 5, 1974, pp. 723–731.
(57) Bogar, F. D., and Crooker, T. W., "The Influence of Bulk-Solution-Chemistry Conditions on Marine Corrosion Fatigue Crack Growth Rate," *Journal of Testing and Evaluation*, Vol 7, 1979, pp. 155–159.
(58) Vosikovsky, O., Neill, W. R., Carlyle, D. A., and Rivard, A., "The Effect of Sea Water Temperature on Corrosion Fatigue Crack Growth in Structural Steels," *CANMET Physical Metallurgy Research Laboratories Report* ERP/PMRL 83-27 (OP-J), Ottawa, Canada, April 1983.
(59) Gangloff, R. P., "The Criticality of Crack Size in Aqueous Corrosion Fatigue," *Res Mechanica Letters*, Vol 1, 1981, pp. 299–306.
(60) van der Velden, R., Ewalds, H. L., Schultze, W. A., and Punter, A., "Anomalous Fatigue Crack Growth Retardation in Steels for Offshore Applications," *Corrosion Fatigue: Mechanics, Metallurgy, Electrochemistry and Engineering, ASTM STP 180*, ASTM, 1983, pp. 64–80.
(61) Bogar, F. D., and Crooker, T. W., "Effects of Natural Seawater and Electrochemical Potential on Fatigue-Crack Growth in 5086 and

5456 Aluminum Alloys," *NRL Report 8153*, Naval Research Laboratory, Washington, DC, October 7, 1977.

(62) Wei, R. P., and Brazill, R. L., "An Assessment of A-C and D-C Potential Systems for Monitoring Fatigue Crack Growth," *Fatigue Crack Growth Measurement and Data Analysis, ASTM STP 738*, ASTM, 1981, pp. 103–119.

(63) Liaw, P. K., Hartmann, H. R., and Helm, E. J., "Corrosion Fatigue Crack Propagation Testing with the KRAK-GAGE® in Salt Water," *Engineering Fracture Mechanics*, Vol 18, 1983, pp. 121–131.

(64) Watt, K. R., "Consideration of an a.c. Potential Drop Method for Crack Length Measurement," from *The Measurement of Crack Length and Shape During Fracture and Fatigue*, Beevers, C. J., Ed., EMAS, Cradley Heath, UK, 1980, pp. 202 –201.

(65) Bakker, A., "A DC Drop Procedure for Crack Initiation and R-Curve Measurements During Fracture Tests," *Elastic-Plastic Fracture Test Methods: The User Experience, ASTM STP 856*, Wessel, E. T. and Loss, F. J., Eds., ASTM, 1985, pp. 394–410.

(66) Richards, C. E., "Some Guidelines to the Selection of Techniques," *The Measurement of Crack Length and Shape During Fracture and Fatigue*, Beevers, C. J., Ed., EMAS, Cradley Heath, UK, 1980, pp. 461–468.

(67) Wei, R. P., and Brazill, R. L., "An a.c. Potential System for Crack Length Measurement" from *The Measurement of Crack Length and Shape During Fracture and Fatigue*, Beevers, C. J., Ed., EMAS, Cradley Heath, UK, 1980, pp. 190 –201.

(68) Wilkowski, G. M., and Maxey, W. A.," Review and Applications of the Electric Potential Method for Measuring Crack Growth in Specimens, Flawed Pipes, and Pressure Vessels," *Fracture Mechanics: Fourteenth Symposium-Volume II: Testing and Applications, ASTM STP 791*, Lewis, J. C. and Sines, G., Eds., ASTM, 1983, pp. II-266–II-294.

(69) Dover, W. D., et al.," a.c. Field Measurement—Theory and Practice," from *The Measurement of Crack Length and Shape During Fracture and Fatigue*, Beevers, C. J., Ed., EMAS, Cradley Heath, UK, 1980, pp. 222 –260.

(70) Gangloff, R. P., "Electrical Potential Monitoring of the Formation and Growth of Small Fatigue Cracks in Embrittling Environments," from *Advances in Crack Length Measurement*, Beevers, C. J., Ed., EMAS, Cradley Heath, UK, 1982, pp. 175–229.

(71) Hartman, G. A., and Johnson, D. A.," D-C Electric Potential Method Applied to Thermal/Mechanical Fatigue Crack Growth," *Experimental Mechanics*, March 1987, pp. 106–112.

(72) Bachman, V., and Munz, D., "Fatigue Crack Closure Evaluation with the Potential Method," *Engineering Fracture Mechanics*, Vol 11, No. 1, 1979, pp. 61–71.

(73) Okumra, N., Venkatasubramanian, T. V., Unvala, B. A., and Baker, T. J., "Application of the AC Potential Drop Technique to the Determination of R-Curves of Tough Ferritic Steels," *Engineering Fracture Mechanics*, Vol 14, 1981, pp. 617–625.

(74) Pollock, D. D., "Thermoelectricity, Theory, Thermometry, Tool," *ASTM STP 852*, ASTM, 1985.

(75) Catlin, W. R., Lord, D. C., Prater, T. A., and Coffin, L. F., "The Reversing D-C Electrical Potential Method," *Automated Test Methods for Fracture and Fatigue Crack Growth, ASTM STP 877*, Cullen, W. H., Landgraf, R. W., Kaisand, L. R., and Underwood, J. H., Eds., ASTM, 1985, pp. 67–85.

(76) Van Stone, R. H., and Richardson, T. L., "Potential Drop Monitoring of Cracks in Surface Flawed Specimens," *Automated Test Methods for Fracture and Fatigue Crack Growth, ASTM STP 877*, W. H. Cullen, R. W. Landgraf, L. R. Kaisand, and J. H. Underwood, Eds., ASTM, 1985, pp. 148 –166.

(77) Gangloff, R. P., "Electrical Potential Monitoring of Crack Formation and Subcritical Growth from Small Defects," *Fatigue of Engineering Materials and Structures*, Vol 4, 1981, pp. 15–33.

(78) Aronson, G. H., and Ritchie, R. O., "Optimization of the Electrical Potential Technique for Crack Monitoring in Compact Test Pieces Using Finite Element Analysis," *Journal of Testing and Evaluation, JTEVA*, Vol 7, No. 4, July 1979, pp. 208–215.

(79) Ritchie, R. O., and Bathe, K. J., "On the Calibration of the Electrical Potential Technique for Monitoring Crack Growth Using Finite Element Methods," *International Journal of Fracture*, Vol 15 , No. 1, February 1979, pp. 47–55.

(80) Li, Che-Yu, and Wei, R. P., "Calibrating the Electrical Potential Method for Studying Slow Crack Growth," *Materials Research & Standards*, Vol 6, No. 8, August 1966, pp. 392–394.

(81) Piascik, R. S.," Mechanisms of Intrinsic Damage Localization During Corrosion Fatigue: Al-Li-Cu System," Ph.D. Dissertation, University of Virginia, 1989.

(82) Phillips, Edward P., "Results of the Second Round Robin on Opening-Load Measurement Conducted by ASTM Task Group E24.04.04 on Crack Closure Measurement and Analysis," NASA Technical Memorandum 109032, November 1993.

(83) Donald, J. Keith," A Procedure for Standardizing Crack Closure Levels," *Mechanics of Fatigue Crack Closure, ASTM STP 982*, ASTM, 1988, pp. 222–229.

(84) *Short Fatigue Cracks, ESIS 13*, Miller, K. J., and de los Rios, E. R., Eds., Mechanical Engineering Publications, London, 1992.

(85) Suresh, S., and Ritchie, R. O., "Propagation of Short Fatigue Cracks," *International Metals Review*, Vol 29, 1984, pp. 445–476.

(86) Hudak, S. J., Jr., "Small Crack Behavior and the Prediction of Fatigue Life," *ASME Journal of Engineering Materials and Technology*, Vol 103, 1981, pp. 26–35.

(87) *Small-Crack Test Methods, ASTM STP 1149*, Larsen, J. M., and Allison, J. E., Eds., ASTM, 1992.

(88) *Current Research on Fatigue Cracks*, Tanaka, T., Jono, M., and Komai, K., Eds., The Society of Materials Science, Japan, 1985.

(89) *Small Fatigue Cracks*, Ritchie, R. O., and Lankford, J., Eds., The Metallurgical Society, Warrendale, PA, 1986.

(90) *The Behaviour of Short Fatigue Cracks, EGF 1*, Miller, K. J., and de los Rios, E. R., Eds., Mechanical Engineering Publications, London, 1986.

(91) *Small Fatigue Cracks, Mechanics, Mechanisms and Applications*, K.S. Ravichandran, R.O. Ritchie, and Y. Murakami, Eds, Elsevier, Oxford, 1999.

(92) Ritchie, R. O., and Lankford, J., "Overview of the Small Crack Problem," *Small Fatigue Cracks*, Ritchie, R. O., and Lankford, J., Eds., The Metallurgical Society, Warrendale, PA, 1986 , pp. 1–5.

(93) Kitagawa, H., and Takahashi, S.," Applicability of Fracture Mechanics to Very Small Cracks or the Cracks in the Early Stage," Proc. Second International Conference on Mechanical Behavior of Materials, Boston, MA, 1976, pp. 627–631.

(94) Tanaka, K., Nakai, Y., and Yamashita, M., "Fatigue Growth Threshold of Small Cracks," *International Journal of Fracture*, Vol 17 , 1981, pp. 519–533.

(95) Miller, K. J., "Materials Science Perspective of Metal Fatigue Resistance," *Materials Science and Technology*, Vol 9, 1993, pp. 453–462.

(96) McClung, R. C., and Sehitoglu, H., "Characterization of Fatigue Crack Growth in Intermediate and Large Scale Yielding," *ASME Journal of Engineering Materials and Technology*, Vol 113, 1991, pp. 15–22.

(97) Swain, M. H., "Monitoring Small-Crack Growth by the Replication Method," *ASTM STP 1149*, ASTM, pp. 34–56.

(98) Newman, J.A., Willard, S.A., Smith, S.W., and Piascik, R.S., "Replica-Based Crack Inspection", *Engineering Fracture Mechanics*, 76, 2009, pp 898-910.

(99) Larsen, J. M., Jira, J. R., and Ravichandran, K. S., "Measurement of Small Cracks by Photomicroscopy: Experiments and Analysis," *ASTM STP 1149*, ASTM, pp. 57–80.

(100) *Image Correlation for Shape, Motion and Deformation Measurements*, M.A. Sutton, J.-J. Orteu, H.W. Schreier, Eds, Springer, New York, 2009.

(101) Gangloff, R. P., Slavik, D. C., Piascik, R. S., and Van Stone, R. H., "Direct Current Electrical Potential Measurement of the Growth of Small Cracks," *ASTM STP 1149*, ASTM, pp. 116–168.

(102) Davidson, D. L., "The Experimental Mechanics of Microcracks," *ASTM STP 1149*, ASTM, pp. 81–91.

(103) Hertzberg, R., Herman, W. A., Clark, T., and Jaccard, R., "Simulation of Short Crack and Other Low Closure Loading Conditions Utilizing Constant K_{max} ΔK-Decreasing Fatigue Crack Growth Procedures," *ASTM STP 1149*, ASTM, pp. 197–220.

(104) Resch, M. T., and Nelson, D. V., "An Ultrasonic Method for Measurement of Size and Opening Behavior of Small Fatigue Cracks," *ASTM STP 1149*, ASTM, pp. 169–196.

(105) Sharpe, W. N., Jr., Jira, J. R., and Larsen, J. M., "Real-Time Measurement of Small-Crack Opening Behavior Using an Interferometric Strain/Displacement Gage," *ASTM STP 1149*, ASTM, pp. 92–115.

(106) Pickard, A. C., Brown, C. W., and Hicks, M. A., "The Development of Advanced Specimen Testing and Analysis Techniques Applied to Fracture Mechanics Lifting of Gas Turbine Components," *Advances in Life Prediction Methods*, Woodford, D. A. and Whitehead, J. R., Eds., ASME, New York, 1983, pp. 173–178.

(107) Newman, J. C., Jr., and Edwards, P. R., "Short-Crack Growth Behaviour in an Aluminum Alloy—an AGARD Cooperative Test Programme," AGARD Report No. 732, 1988 (available NTIS).

(108) Caton, M.J. and Jha, S.K. "Small Fatigue Crack Growth and Failure Mode Transition in a Ni-Base Superalloy at Elevated Temperature", *International Journal of Fatigue*, 32(9), 2010, 1461-1472.

(109) Feng, Q., Picard, Y.N., Liu, H., Yalisove, S.M., Mourou, G., and Pollock, T.M., " Femtosecond Laser Micromachining of a Single-Crystal Superalloy," *Scripta Materialia*, 53(5) 2005, pp 511-516

(110) Porter, W.J. III, Li, K., Caton, M.J., Jha, S., Bartha, B.B., and Larsen, J.M., " Microstructrual Conditions Contributing to Fatigue Variability in P/M Nickel-Base Superalloys," *Superalloys* 2008, R.C. Reed, et al., Eds, TMS, 2008, pp. 541- 548.

(111) Newman, J. C., Jr., and Raju, I. S., "Stress-Intensity Factor Equations for Cracks in Three-Dimensional Finite Bodies," *Fracture Mechanics: Fourteenth Symposium—Volume I: Theory and Analysis, ASTM STP 791*, Lewis, J. C. and Sines, G., Eds., ASTM, 1983, pp. I-238–I-265.

(112) Raju, I. S., and Newman, J. C., Jr., "Stress-Intensity Factors for Circumferential Surface Cracks in Pipes and Rods under Tension and Bending Loads," *Fracture Mechanics: Seventeenth Volume, ASTM STP 905*, Underwood, J. H., Chait, R., Smith, C. W., Wilhem, D. P., Andrews, W. A., and Newman, J. C., Jr., Eds., ASTM, 1986, pp. 789–805.

(113) Newman, J. C., Jr., "Fracture Mechanics Parameters for Small Fatigue Cracks," *ASTM STP 1149*, ASTM, pp. 6–33.

(114) Tada, H., and Paris, P., "Discussion on Stress-Intensity Factors for Cracks," *Part-Through Crack Fatigue Life Prediction, ASTM STP 687*, Chang, J. B., Ed., ASTM, 1979, pp. 43–46.

(115) *Mechanics of Fatigue Crack Closure, ASTM STP 982*, Newman, J. C., Jr., and Elber, W., Eds., ASTM, 1988.

(116) Kendall, J. M., and King, J. E.," Short Fatigue Crack Growth Behaviour: Data Analysis Effects," *International Journal of Fatigue*, Vol 10, 1988, pp. 163–170.

(117) Ritchie, R. O., " *Crack Tip Shielding in Fatigue*," Fifth International Conference on Mechanical Behavior, China, 1987.

(118) Brockenbrough, J. R. and Bray, G. H., "Prediction of S-N Fatigue Curves Using Various Long-Crack Derived ΔKeff Fatigue Crack Growth Curves and a Small Crack Life Prediction Model", *Fatigue and Fracture Mechanics*, 30th Volume, ASTM STP 1360, P. C. Paris and K. L. Jerina, Eds., ASTM International, West Conshohocken, PA, West Conshohocken, PA, 1999, pp. 388–402.

(119) Zonker H. R., G. H. Bray, K. George, and M. D. Garratt , "Use of ACR Method to Estimate Closure and Residual Stress Free Small Crack Growth Data", Journal of ASTM International, July/August 2005, Vol. 2, No. 7.

(120) Lados, Diana A., Apelian, Diran , Paris, Paul C., J., Donald Keith, "Closure mechanisms in Al–Si–Mg cast alloys and long-crack to small-crack corrections," *International Journal of Fatigue* 27 (2005) 1463–1472.

(121) Donald, J. Keith and Lados, Diana A., "An integrated methodology for separating closure and residual stress effects from fatigue crack growth rate data," *Fatigue Fract Engng Mater Struct* 30, 223-230, 2006.

(122) Ball, D. L., " The Influence of Residual Stress on the Design of Aircraft Primary Structure" Seventh International ASTM/ESIS Symposium on Fatigue and Fracture Mechanics, R.W. Neu, K.R.W. Wallin, S.R. Thompson, Eds., ASTM International, West Conshohocken, PA, 2007.

(123) Donald, J. K., Bray, G. H., Bush, R. W., "An Evaluation of the Adjusted Compliance Ratio Technique for Determining the Effective Stress Intensity Factor," 29th National Symposium on Fatigue and Fracture Mechanics, ASTM STP 1332, T. L. Panontin, S. D. Sheppard, Eds., American Society for Testing and Materials 1998.

(124) Lados, Diana A., Apelian, Diran , and Donald, J. Keith , "Fracture mechanics analysis for residual stress and crack closure corrections", *International Journal of Fatigue* 29 (2007) 687–694.

(125) Donald, J. K., Connelly, G. M., Paris, P. C., and Tada, H., "Crack Wake Influence Theory and Elastic Crack Closure Measurement," *Fatigue and Fracture Mechanics*: 30th Volume, ASTM STP 1360, P. C. Paris and K. L. Jerina, Eds., American Society for Testing and Materials, West Conshohocken, PA, 2000, pp. 185-200.

(126) Donald, J. K. and Phillips, E. P., "Analysis of the Second ASTM Round Robin Program on Opening Load Measurement Using the Adjusted Compliance Ratio Technique," *Advances in Fatigue Crack Closure Measurement and Analysis*: Second Volume, ASTM STP 1343, R. C. McClung, J. C. Newman, Jr., Eds., American Society for Testing and Materials, 1997.

(127) Beevers, C. J., *The Measurement of Crack Length and Shape During Fracture and Fatigue*, Engineering Materials Advisory Services LTD, West Middlelands, U.K., 1981.

(128) Jira, J. R., Nagy, D., and Nicholas, T., "Influences of Crack Closure and Load History on Near-Threshold Crack Growth Behavior in Surface Flaws," *Surface-Crack Growth: Models, Experiments, and Structures, ASTM STP 1060*, Reuter, W. G., Underwood, J. H., and Newman, J. C., Jr., Eds., ASTM, 1990, pp. 303–314.

Designation: E8/E8M – 13a Standard Test Methods for Tension Testing of Metallic Materials 1

Method · April 2019

DOI: 10.1520/E0008_E0008M-13A

1 author:

Zainab Raheem
Baghdad University College of Science
133 PUBLICATIONS **186** CITATIONS

SEE PROFILE

Designation: E8/E8M – 13a

American Association State
Highway and Transportation Officials Standard
AASHTO No.: T68
An American National Standard

Standard Test Methods for Tension Testing of Metallic Materials[1]

This standard is issued under the fixed designation E8/E8M; the number immediately following the designation indicates the year of original adoption or, in the case of revision, the year of last revision. A number in parentheses indicates the year of last reapproval. A superscript epsilon (ε) indicates an editorial change since the last revision or reapproval.

This standard has been approved for use by agencies of the Department of Defense.

1. Scope*

1.1 These test methods cover the tension testing of metallic materials in any form at room temperature, specifically, the methods of determination of yield strength, yield point elongation, tensile strength, elongation, and reduction of area.

1.2 The gauge lengths for most round specimens are required to be 4D for E8 and 5D for E8M. The gauge length is the most significant difference between E8 and E8M test specimens. Test specimens made from powder metallurgy (P/M) materials are exempt from this requirement by industry-wide agreement to keep the pressing of the material to a specific projected area and density.

1.3 Exceptions to the provisions of these test methods may need to be made in individual specifications or test methods for a particular material. For examples, see Test Methods and Definitions A370 and Test Methods B557, and B557M.

1.4 Room temperature shall be considered to be 10 to 38°C [50 to 100°F] unless otherwise specified.

1.5 The values stated in SI units are to be regarded as separate from inch/pound units. The values stated in each system are not exact equivalents; therefore each system must be used independently of the other. Combining values from the two systems may result in non-conformance with the standard.

1.6 *This standard does not purport to address all of the safety concerns, if any, associated with its use. It is the responsibility of the user of this standard to establish appropriate safety and health practices and determine the applicability of regulatory limitations prior to use.*

2. Referenced Documents

2.1 *ASTM Standards:*[2]

A356/A356M Specification for Steel Castings, Carbon, Low Alloy, and Stainless Steel, Heavy-Walled for Steam Turbines

A370 Test Methods and Definitions for Mechanical Testing of Steel Products

B557 Test Methods for Tension Testing Wrought and Cast Aluminum- and Magnesium-Alloy Products

B557M Test Methods for Tension Testing Wrought and Cast Aluminum- and Magnesium-Alloy Products (Metric)

E4 Practices for Force Verification of Testing Machines

E6 Terminology Relating to Methods of Mechanical Testing

E29 Practice for Using Significant Digits in Test Data to Determine Conformance with Specifications

E83 Practice for Verification and Classification of Extensometer Systems

E345 Test Methods of Tension Testing of Metallic Foil

E691 Practice for Conducting an Interlaboratory Study to Determine the Precision of a Test Method

E1012 Practice for Verification of Testing Frame and Specimen Alignment Under Tensile and Compressive Axial Force Application

D1566 Terminology Relating to Rubber

E1856 Guide for Evaluating Computerized Data Acquisition Systems Used to Acquire Data from Universal Testing Machines

3. Terminology

3.1 *Definitions of Terms Common to Mechanical Testing*—

3.1.1 The definitions of mechanical testing terms that appear in the Terminology E6 apply to this test method.

[1] These test methods are under the jurisdiction of ASTM Committee E28 on Mechanical Testing and are the direct responsibility of Subcommittee E28.04 on Uniaxial Testing.

Current edition approved July 1, 2013. Published August 2013. Originally approved in 1924. Last previous edition approved 2013 as E8/E8M – 13. DOI: 10.1520/E0008_E0008M-13A.

[2] For referenced ASTM standards, visit the ASTM website, www.astm.org, or contact ASTM Customer Service at service@astm.org. For *Annual Book of ASTM Standards* volume information, refer to the standard's Document Summary page on the ASTM website.

***A Summary of Changes section appears at the end of this standard**

3.1.1.1 These terms include bending strain, constraint, elongation, extensometer, force, gauge length, necking, reduced section, stress-strain diagram, testing machine, and modulus of elasticity.

3.1.2 In addition, the following common terms from Terminology E6 are defined:

3.1.3 *discontinuous yielding, n—in a uniaxial test*, a hesitation or fluctuation of force observed at the onset of plastic deformation, due to localized yielding.

3.1.3.1 *Discussion*—The stress-strain curve need not appear to be discontinuous.

3.1.4 *elongation after fracture, n*—the elongation measured by fitting the two halves of the broken specimen together.

3.1.5 *elongation at fracture, n*—the elongation measured just prior to the sudden decrease in force associated with fracture.

3.1.6 *lower yield strength, LYS [FL^{-2}]—in a uniaxial test*, the minimum stress recorded during discontinuous yielding, ignoring transient effects.

3.1.7 *reduction of area, n*—the difference between the original cross-sectional area of a tension test specimen and the area of its smallest cross section.

3.1.7.1 *Discussion*—The reduction of area is usually expressed as a percentage of the original cross-sectional area of the specimen.

3.1.7.2 *Discussion*—The smallest cross section may be measured at or after fracture as specified for the material under test.

3.1.7.3 *Discussion*—The term reduction of area when applied to metals generally means measurement after fracture; when applied to plastics and elastomers, measurement at fracture. Such interpretation is usually applicable to values for reduction of area reported in the literature when no further qualification is given. **(E28.04)**

3.1.8 *tensile strength, S_u* [FL^{-2}], *n*—the maximum tensile stress that a material is capable of sustaining.

3.1.8.1 *Discussion*—Tensile strength is calculated from the maximum force during a tension test carried to rupture and the original cross-sectional area of the specimen.

3.1.9 *uniform elongation, El_u, [%]*—the elongation determined at the maximum force sustained by the test piece just prior to necking or fracture, or both.

3.1.9.1 *Discussion*—Uniform elongation includes both elastic and plastic elongation.

3.1.10 *upper yield strength, UYS [FL^{-2}]—in a uniaxial test*, the first stress maximum (stress at first zero slope) associated with discontinuous yielding at or near the onset of plastic deformation.

3.1.11 *yield point elongation, YPE, n—in a uniaxial test*, the strain (expressed in percent) separating the stress-strain curve's first point of zero slope from the point of transition from discontinuous yielding to uniform strain hardening.

3.1.11.1 *Discussion*— If the transition occurs over a range of strain, the YPE end point is the intersection between *(a)* a horizontal line drawn tangent to the curve at the last zero slope and *(b)* a line drawn tangent to the strain hardening portion of the stress-strain curve at the point of inflection. If there is no point at or near the onset of yielding at which the slope reaches zero, the material has 0 % YPE.

3.1.12 *yield strength, YS* or S_y [FL^{-2}], *n*—the engineering stress at which, by convention, it is considered that plastic elongation of the material has commenced.

3.1.12.1 *Discussion*—This stress may be specified in terms of (*a*) a specified deviation from a linear stress-strain relationship, (*b*) a specified total extension attained, or (*c*) maximum or minimum engineering stresses measured during discontinuous yielding.

3.2 *Definitions of Terms Specific to This Standard:*

3.2.1 *referee test, n*—test made to settle a disagreement as to the conformance to specified requirements, or conducted by a third party to arbitrate between conflicting results. **D1566, D11.08**

4. Significance and Use

4.1 Tension tests provide information on the strength and ductility of materials under uniaxial tensile stresses. This information may be useful in comparisons of materials, alloy development, quality control, and design under certain circumstances.

4.2 The results of tension tests of specimens machined to standardized dimensions from selected portions of a part or material may not totally represent the strength and ductility properties of the entire end product or its in-service behavior in different environments.

4.3 These test methods are considered satisfactory for acceptance testing of commercial shipments. The test methods have been used extensively in the trade for this purpose.

5. Apparatus

5.1 *Testing Machines*—Machines used for tension testing shall conform to the requirements of Practices E4. The forces used in determining tensile strength and yield strength shall be within the verified force application range of the testing machine as defined in Practices E4.

5.2 *Gripping Devices:*

5.2.1 *General*—Various types of gripping devices may be used to transmit the measured force applied by the testing machine to the test specimens. To ensure axial tensile stress within the gauge length, the axis of the test specimen should coincide with the center line of the heads of the testing machine. Any departure from this requirement may introduce bending stresses that are not included in the usual stress computation (force divided by cross-sectional area).

NOTE 1—The effect of this eccentric force application may be illustrated by calculating the bending moment and stress thus added. For a standard 12.5-mm [0.500-in.] diameter specimen, the stress increase is 1.5 percentage points for each 0.025 mm [0.001 in.] of eccentricity. This error increases to 2.5 percentage points/ 0.025 mm [0.001 in.] for a 9 mm [0.350-in.] diameter specimen and to 3.2 percentage points/ 0.025 mm [0.001 in.] for a 6-mm [0.250-in.] diameter specimen.

NOTE 2—Alignment methods are given in Practice E1012.

5.2.2 *Wedge Grips*—Testing machines usually are equipped with wedge grips. These wedge grips generally furnish a satisfactory means of gripping long specimens of ductile metal

and flat plate test specimens such as those shown in Fig. 1. If, however, for any reason, one grip of a pair advances farther than the other as the grips tighten, an undesirable bending stress may be introduced. When liners are used behind the wedges, they must be of the same thickness and their faces must be flat and parallel. For best results, the wedges should be supported over their entire lengths by the heads of the testing machine. This requires that liners of several thicknesses be available to cover the range of specimen thickness. For proper gripping, it is desirable that the entire length of the serrated face of each wedge be in contact with the specimen. Proper alignment of wedge grips and liners is illustrated in Fig. 2. For short specimens and for specimens of many materials it is generally necessary to use machined test specimens and to use a special means of gripping to ensure that the specimens, when under load, shall be as nearly as possible in uniformly distributed pure axial tension (see 5.2.3, 5.2.4, and 5.2.5).

5.2.3 *Grips for Threaded and Shouldered Specimens and Brittle Materials*—A schematic diagram of a gripping device for threaded-end specimens is shown in Fig. 3, while Fig. 4 shows a device for gripping specimens with shouldered ends. Both of these gripping devices should be attached to the heads of the testing machine through properly lubricated spherical-seated bearings. The distance between spherical bearings should be as great as feasible.

5.2.4 *Grips for Sheet Materials*—The self-adjusting grips shown in Fig. 5 have proven satisfactory for testing sheet materials that cannot be tested satisfactorily in the usual type of wedge grips.

5.2.5 *Grips for Wire*—Grips of either the wedge or snubbing types as shown in Fig. 5 and Fig. 6 or flat wedge grips may be used.

5.3 *Dimension-Measuring Devices*—Micrometers and other devices used for measuring linear dimensions shall be accurate and precise to at least one half the smallest unit to which the individual dimension is required to be measured.

5.4 *Extensometers*—Extensometers used in tension testing shall conform to the requirements of Practice E83 for the classifications specified by the procedure section of this test method. Extensometers shall be used and verified to include the strains corresponding to the yield strength and elongation at fracture (if determined).

5.4.1 Extensometers with gauge lengths equal to or shorter than the nominal gauge length of the specimen (dimension shown as "*G*-Gauge Length" in the accompanying figures) may be used to determine the yield behavior. For specimens without a reduced section (for example, full cross sectional area specimens of wire, rod, or bar), the extensometer gauge length for the determination of yield behavior shall not exceed 80 % of the distance between grips. For measuring elongation at fracture with an appropriate extensometer, the gauge length of the extensometer shall be equal to the nominal gauge length required for the specimen being tested.

6. Test Specimens

6.1 *General:*

6.1.1 *Specimen Size*—Test specimens shall be either substantially full size or machined, as prescribed in the product specifications for the material being tested.

6.1.2 *Location*—Unless otherwise specified, the axis of the test specimen shall be located within the parent material as follows:

6.1.2.1 At the center for products 40 mm [1.500 in.] or less in thickness, diameter, or distance between flats.

6.1.2.2 Midway from the center to the surface for products over 40 mm [1.500 in.] in thickness, diameter, or distance between flats.

6.1.3 *Specimen Machining*—Improperly prepared test specimens often are the reason for unsatisfactory and incorrect test results. It is important, therefore, that care be exercised in the preparation of specimens, particularly in the machining, to maximize precision and minimize bias in test results.

6.1.3.1 The reduced sections of prepared specimens should be free of cold work, notches, chatter marks, grooves, gouges, burrs, rough surfaces or edges, overheating, or any other condition which can deleteriously affect the properties to be measured.

NOTE 3—Punching or blanking of the reduced section may produce significant cold work or shear burrs, or both, along the edges which should be removed by machining.

6.1.3.2 Within the reduced section of rectangular specimens, edges or corners should not be ground or abraded in a manner which could cause the actual cross-sectional area of the specimen to be significantly different from the calculated area.

6.1.3.3 For brittle materials, large radius fillets at the ends of the gauge length should be used.

6.1.3.4 The cross-sectional area of the specimen should be smallest at the center of the reduced section to ensure fracture within the gauge length. For this reason, a small taper is permitted in the reduced section of each of the specimens described in the following sections.

6.1.4 *Specimen Surface Finish*—When materials are tested with surface conditions other than as manufactured, the surface finish of the test specimens should be as provided in the applicable product specifications.

NOTE 4—Particular attention should be given to the uniformity and quality of surface finish of specimens for high strength and very low ductility materials since this has been shown to be a factor in the variability of test results.

6.2 *Plate-Type Specimens*—The standard plate-type test specimen is shown in Fig. 1. This specimen is used for testing metallic materials in the form of plate, shapes, and flat material having a nominal thickness of 5 mm [0.188 in.] or over. When product specifications so permit, other types of specimens may be used, as provided in 6.3, 6.4, and 6.5.

6.3 *Sheet-Type Specimens:*

6.3.1 The standard sheet-type test specimen is shown in Fig. 1. This specimen is used for testing metallic materials in the form of sheet, plate, flat wire, strip, band, hoop, rectangles, and shapes ranging in nominal thickness from 0.13 to 19 mm [0.005 to 0.750 in.]. When product specifications so permit, other types of specimens may be used, as provided in 6.2, 6.4, and 6.5.

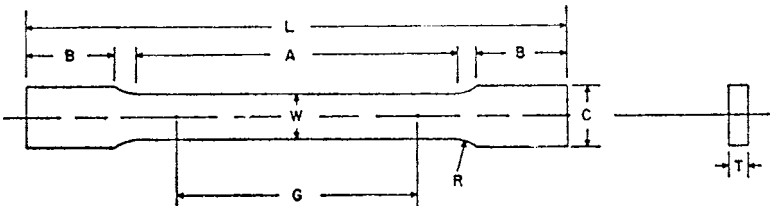

	Dimensions		
	Standard Specimens		Subsize Specimen
	Plate-Type, 40 mm [1.500 in.] Wide	Sheet-Type, 12.5 mm [0.500 in.] Wide	6 mm [0.250 in.] Wide
	mm [in.]	mm [in.]	mm [in.]
G—Gauge length (Note 1 and Note 2)	200.0 ± 0.2 [8.00 ± 0.01]	50.0 ± 0.1 [2.000 ± 0.005]	25.0 ± 0.1 [1.000 ± 0.003]
W—Width (Note 3 and Note 4)	40.0 ± 2.0 [1.500 ± 0.125, -0.250]	12.5 ± 0.2 [0.500 ± 0.010]	6.0 ± 0.1 [0.250 ± 0.005]
T—Thickness (Note 5)		thickness of material	
R—Radius of fillet, min (Note 6)	25 [1]	12.5 [0.500]	6 [0.250]
L—Overall length, min (Note 2, Note 7, and Note 8)	450 [18]	200 [8]	100 [4]
A—Length of reduced section, min	225 [9]	57 [2.25]	32 [1.25]
B—Length of grip section, min (Note 9)	75 [3]	50 [2]	30 [1.25]
C—Width of grip section, approximate (Note 4 and Note 9)	50 [2]	20 [0.750]	10 [0.375]

NOTE 1—For the 40 mm [1.500 in.] wide specimen, punch marks for measuring elongation after fracture shall be made on the flat or on the edge of the specimen and within the reduced section. Either a set of nine or more punch marks 25 mm [1 in.] apart, or one or more pairs of punch marks 200 mm [8 in.] apart may be used.

NOTE 2—When elongation measurements of 40 mm [1.500 in.] wide specimens are not required, a minimum length of reduced section (*A*) of 75 mm [2.25 in.] may be used with all other dimensions similar to those of the plate-type specimen.

NOTE 3—For the three sizes of specimens, the ends of the reduced section shall not differ in width by more than 0.10, 0.05 or 0.02 mm [0.004, 0.002 or 0.001 in.], respectively. Also, there may be a gradual decrease in width from the ends to the center, but the width at each end shall not be more than 1 % larger than the width at the center.

NOTE 4—For each of the three sizes of specimens, narrower widths (*W* and *C*) may be used when necessary. In such cases the width of the reduced section should be as large as the width of the material being tested permits; however, unless stated specifically, the requirements for elongation in a product specification shall not apply when these narrower specimens are used.

NOTE 5—The dimension *T* is the thickness of the test specimen as provided for in the applicable material specifications. Minimum thickness of 40 mm [1.500 in.] wide specimens shall be 5 mm [0.188 in.]. Maximum thickness of 12.5 and 6 mm [0.500 and 0.250 in.] wide specimens shall be 19 and 6 mm [0.750 and 0.250 in.], respectively.

NOTE 6—For the 40 mm [1.500 in.] wide specimen, a 13 mm [0.500 in.] minimum radius at the ends of the reduced section is permitted for steel specimens under 690 MPa [100 000 psi] in tensile strength when a profile cutter is used to machine the reduced section.

NOTE 7—The dimension shown is suggested as a minimum. In determining the minimum length, the grips must not extend in to the transition section between Dimensions *A* and *B*, see Note 9.

NOTE 8—To aid in obtaining axial force application during testing of 6-mm [0.250-in.] wide specimens, the overall length should be as large as the material will permit, up to 200 mm [8.00 in.].

NOTE 9—It is desirable, if possible, to make the length of the grip section large enough to allow the specimen to extend into the grips a distance equal to two thirds or more of the length of the grips. If the thickness of 12.5 mm [0.500-in.] wide specimens is over 10 mm [0.375 in.], longer grips and correspondingly longer grip sections of the specimen may be necessary to prevent failure in the grip section.

NOTE 10—For the three sizes of specimens, the ends of the specimen shall be symmetrical in width with the center line of the reduced section within 2.5, 1.25 and 0.13 mm [0.10, 0.05 and 0.005 in.], respectively. However, for referee testing and when required by product specifications, the ends of the 12.5 mm [0.500 in.] wide specimen shall be symmetrical within 0.2 mm [0.01 in.].

NOTE 11—For each specimen type, the radii of all fillets shall be equal to each other within a tolerance of 1.25 mm [0.05 in.], and the centers of curvature of the two fillets at a particular end shall be located across from each other (on a line perpendicular to the centerline) within a tolerance of 2.5 mm [0.10 in.].

NOTE 12—Specimens with sides parallel throughout their length are permitted, except for referee testing, provided: *(a)* the above tolerances are used; *(b)* an adequate number of marks are provided for determination of elongation; and *(c)* when yield strength is determined, a suitable extensometer is used. If the fracture occurs at a distance of less than 2 W from the edge of the gripping device, the tensile properties determined may not be representative of the material. In acceptance testing, if the properties meet the minimum requirements specified, no further testing is required, but if they are less than the minimum requirements, discard the test and retest.

FIG. 1 Rectangular Tension Test Specimens

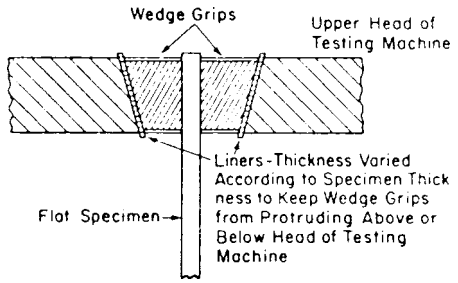

FIG. 2 Wedge Grips with Liners for Flat Specimens

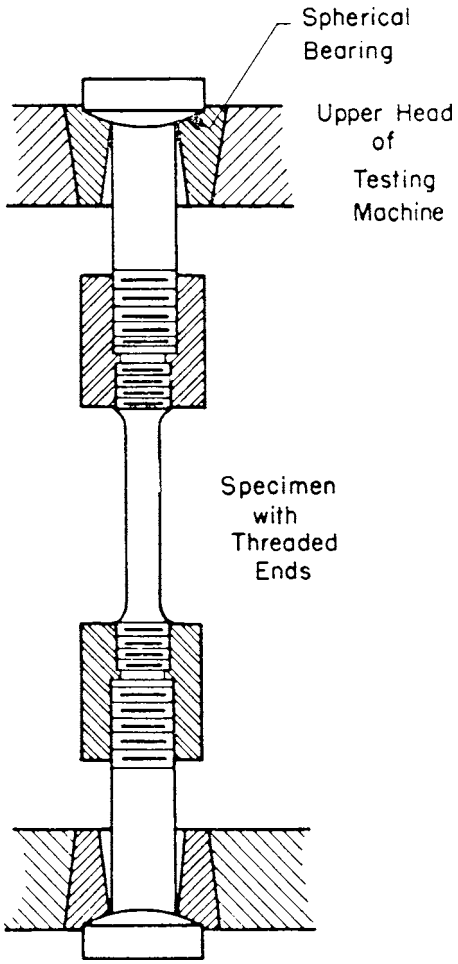

FIG. 3 Gripping Device for Threaded-End Specimens

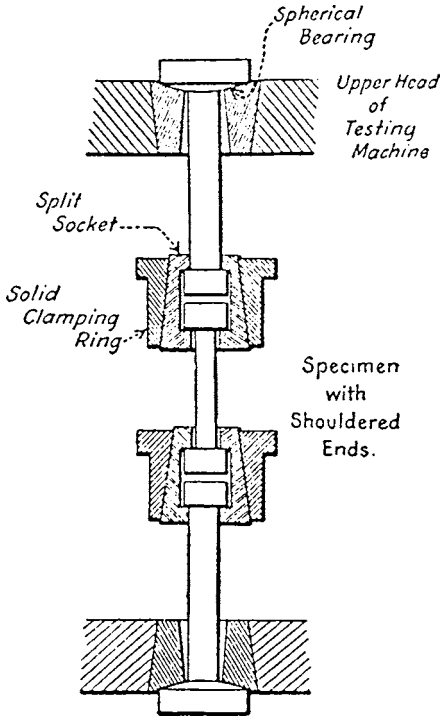

FIG. 4 Gripping Device for Shouldered-End Specimens

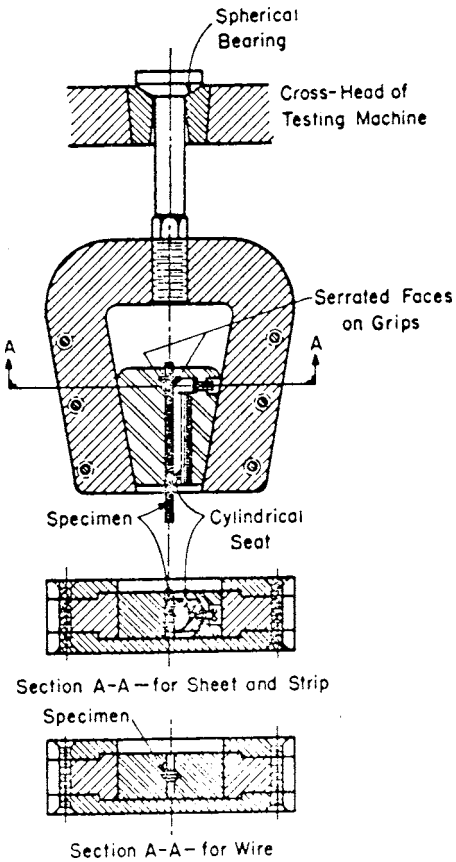

FIG. 5 Gripping Devices for Sheet and Wire Specimens

NOTE 5—Test Methods E345 may be used for tension testing of materials in thicknesses up to 0.15 mm [0.0059 in.].

6.3.2 Pin ends as shown in Fig. 7 may be used. In order to avoid buckling in tests of thin and high-strength materials, it may be necessary to use stiffening plates at the grip ends.

6.4 *Round Specimens:*

6.4.1 The standard 12.5-mm [0.500-in.] diameter round test specimen shown in Fig. 8 is used quite generally for testing metallic materials, both cast and wrought.

6.4.2 Fig. 8 also shows small-size specimens proportional to the standard specimen. These may be used when it is necessary to test material from which the standard specimen or specimens shown in Fig. 1 cannot be prepared. Other sizes of small round specimens may be used. In any such small-size specimen it is important that the gauge length for measurement of elongation

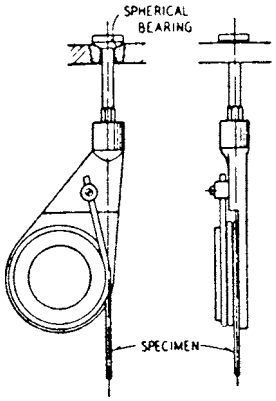

FIG. 6 Snubbing Device for Testing Wire

be four times the diameter of the specimen when following E8 and five times the diameter of the specimen when following E8M.

6.4.3 The shape of the ends of the specimen outside of the gauge length shall be suitable to the material and of a shape to fit the holders or grips of the testing machine so that the forces may be applied axially. Fig. 9 shows specimens with various types of ends that have given satisfactory results.

6.5 *Specimens for Sheet, Strip, Flat Wire, and Plate*—In testing sheet, strip, flat wire, and plate, use a specimen type appropriate for the nominal thickness of the material, as described in the following:

6.5.1 For material with a nominal thickness of 0.13 to 5 mm [0.005 to 0.1875 in.], use the sheet-type specimen described in 6.3.

6.5.2 For material with a nominal thickness of 5 to 12.5 mm [0.1875 to 0.500 in.], use either the sheet-type specimen of 6.3 or the plate-type specimen of 6.2.

6.5.3 For material with a nominal thickness of 12.5 to 19 mm [0.500 to 0.750 in.], use either the sheet-type specimen of 6.3, the plate-type specimen of 6.2, or the largest practical size of round specimen described in 6.4.

6.5.4 For material with a nominal thickness of 19 mm [0.750 in.], or greater, use the plate-type specimen of 6.2 or the largest practical size of round specimen described in 6.4.

6.5.4.1 If the product specifications permit, material of a thickness of 19 mm [0.750 in.], or greater may be tested using a modified sheet-type specimen conforming to the configuration shown by Fig. 1. The thickness of this modified specimen must be machined to 10 ± 0.5 mm [0.400 ± 0.020 in.], and must be uniform within 0.1 mm [0.004 in.] throughout the reduced section. In the event of disagreement, a round specimen shall be used as the referee test (comparison) specimen.

6.6 *Specimens for Wire, Rod, and Bar:*

6.6.1 For round wire, rod, and bar, test specimens having the full cross-sectional area of the wire, rod, or bar shall be used wherever practicable. The gauge length for the measurement of elongation of wire less than 4 mm [0.125 in.] in diameter shall be as prescribed in product specifications. When testing wire, rod, or bar having a diameter of 4 mm [0.125 in.] or larger, a gauge length equal to four times the diameter shall be used when following E8 and a gauge length equal to five times the diameter shall be used when following E8M unless otherwise specified. The total length of the specimens shall be at least equal to the gauge length plus the length of material required for the full use of the grips employed.

6.6.2 For wire of octagonal, hexagonal, or square cross section, for rod or bar of round cross section where the specimen required in 6.6.1 is not practicable, and for rod or bar of octagonal, hexagonal, or square cross section, one of the following types of specimens shall be used:

6.6.2.1 *Full Cross Section* (Note 6)—It is permissible to reduce the test section slightly with abrasive cloth or paper, or machine it sufficiently to ensure fracture within the gauge marks. For material not exceeding 5 mm [0.188 in.] in diameter or distance between flats, the cross-sectional area may be reduced to not less than 90 % of the original area without changing the shape of the cross section. For material over 5 mm [0.188 in.] in diameter or distance between flats, the diameter or distance between flats may be reduced by not more than 0.25 mm [0.010 in.] without changing the shape of the cross section. Square, hexagonal, or octagonal wire or rod not exceeding 5 mm [0.188 in.] between flats may be turned to a round having a cross-sectional area not smaller than 90 % of the area of the maximum inscribed circle. Fillets, preferably with a radius of 10 mm [0.375 in.], but not less than 3 mm [0.125 in.], shall be used at the ends of the reduced sections. Square, hexagonal, or octagonal rod over 5 mm [0.188 in.] between flats may be turned to a round having a diameter no smaller than 0.25 mm [0.010 in.] less than the original distance between flats.

NOTE 6—The ends of copper or copper alloy specimens may be flattened 10 to 50 % from the original dimension in a jig similar to that shown in Fig. 10, to facilitate fracture within the gauge marks. In flattening the opposite ends of the test specimen, care shall be taken to ensure that the four flattened surfaces are parallel and that the two parallel surfaces on the same side of the axis of the test specimen lie in the same plane.

6.6.2.2 For rod and bar, the largest practical size of round specimen as described in 6.4 may be used in place of a test specimen of full cross section. Unless otherwise specified in the product specification, specimens shall be parallel to the direction of rolling or extrusion.

6.7 *Specimens for Rectangular Bar*—In testing rectangular bar one of the following types of specimens shall be used:

6.7.1 *Full Cross Section*—It is permissible to reduce the width of the specimen throughout the test section with abrasive cloth or paper, or by machining sufficiently to facilitate fracture within the gauge marks, but in no case shall the reduced width be less than 90 % of the original. The edges of the midlength of the reduced section not less than 20 mm [¾ in.] in length shall be parallel to each other and to the longitudinal axis of the specimen within 0.05 mm [0.002 in.]. Fillets, preferably with a radius of 10 mm [⅜ in.] but not less than 3 mm [⅛ in.] shall be used at the ends of the reduced sections.

6.7.2 Rectangular bar of thickness small enough to fit the grips of the testing machine but of too great width may be reduced in width by cutting to fit the grips, after which the cut surfaces shall be machined or cut and smoothed to ensure failure within the desired section. The reduced width shall not

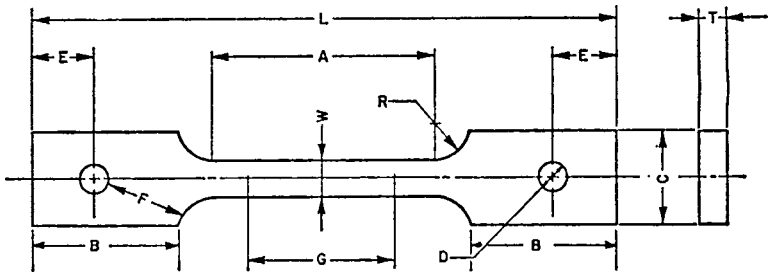

Dimensions, mm [in.]	
G—Gauge length	50.0 ± 0.1 [2.000 ± 0.005]
W—Width (Note 1)	12.5 ± 0.2 [0.500 ± 0.010]
T—Thickness, max (Note 2)	16 [0.625]
R—Radius of fillet, min (Note 3)	13 [0.5]
L—Overall length, min	200 [8]
A—Length of reduced section, min	57 [2.25]
B—Length of grip section, min	50 [2]
C—Width of grip section, approximate	50 [2]
D—Diameter of hole for pin, min (Note 4)	13 [0.5]
E—Edge distance from pin, approximate	40 [1.5]
F—Distance from hole to fillet, min	13 [0.5]

NOTE 1—The ends of the reduced section shall differ in width by not more than 0.1 mm [0.002 in.]. There may be a gradual taper in width from the ends to the center, but the width at each end shall be not more than 1 % greater than the width at the center.

NOTE 2—The dimension *T* is the thickness of the test specimen as stated in the applicable product specifications.

NOTE 3—For some materials, a fillet radius *R* larger than 13 mm [0.500 in.] may be needed.

NOTE 4—Holes must be on center line of reduced section within ± 0.05mm [0.002 in].

NOTE 5—Variations of dimensions *C*, *D*, *E*, *F*, and *L* may be used that will permit failure within the gauge length.

FIG. 7 Pin-Loaded Tension Test Specimen with 50-mm [2-in.] Gauge Length

be less than the original bar thickness. Also, one of the types of specimens described in 6.2, 6.3, and 6.4 may be used.

6.8 *Shapes, Structural and Other*—In testing shapes other than those covered by the preceding sections, one of the types of specimens described in 6.2, 6.3, and 6.4 shall be used.

6.9 *Specimens for Pipe and Tube* (Note 7):

6.9.1 For all small tube (Note 7), particularly sizes 25 mm [1 in.] and under in nominal outside diameter, and frequently for larger sizes, except as limited by the testing equipment, it is standard practice to use tension test specimens of full-size tubular sections. Snug-fitting metal plugs shall be inserted far enough into the ends of such tubular specimens to permit the testing machine jaws to grip the specimens properly. The plugs shall not extend into that part of the specimen on which the elongation is measured. Elongation is measured over a length of four times the diameter when following E8 or five times the diameter when following E8M unless otherwise stated in the product specification. Fig. 11 shows a suitable form of plug, the location of the plugs in the specimen, and the location of the specimen in the grips of the testing machine.

NOTE 7—The term "tube" is used to indicate tubular products in general, and includes pipe, tube, and tubing.

6.9.2 For large-diameter tube that cannot be tested in full section, longitudinal tension test specimens shall be cut as indicated in Fig. 12. Specimens from welded tube shall be located approximately 90° from the weld. If the tube-wall thickness is under 20 mm [0.750 in.], either a specimen of the form and dimensions shown in Fig. 13 or one of the small-size specimens proportional to the standard 12.5-mm [0.500-in.] specimen, as mentioned in 6.4.2 and shown in Fig. 8, shall be used. Specimens of the type shown in Fig. 13 may be tested with grips having a surface contour corresponding to the curvature of the tube. When grips with curved faces are not available, the ends of the specimens may be flattened without heating. If the tube-wall thickness is 20 mm [0.750 in.] or over, the standard specimen shown in Fig. 8 shall be used.

NOTE 8—In clamping of specimens from pipe and tube (as may be done during machining) or in flattening specimen ends (for gripping), care must be taken so as not to subject the reduced section to any deformation or cold work, as this would alter the mechanical properties.

6.9.3 Transverse tension test specimens for tube may be taken from rings cut from the ends of the tube as shown in Fig. 14. Flattening of the specimen may be either after separating as in *A*, or before separating as in *B*. Transverse tension test specimens for large tube under 20 mm [0.750 in.] in wall thickness shall be either of the small-size specimens shown in Fig. 8 or of the form and dimensions shown for Specimen 2 in Fig. 13. When using the latter specimen, either or both surfaces of the specimen may be machined to secure a uniform thickness, provided not more than 15 % of the normal wall thickness is removed from each surface. For large tube 20 mm [0.750 in.] and over in wall thickness, the standard specimen shown in Fig. 8 shall be used for transverse tension tests. Specimens for transverse tension tests on large welded tube to determine the strength of welds shall be located perpendicular to the welded seams, with the welds at about the middle of their lengths.

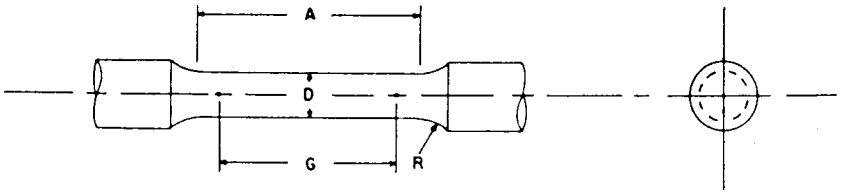

Dimensions, mm [in.]

For Test Specimens with Gauge Length Four times the Diameter [E8]

	Standard Specimen	Small-Size Specimens Proportional to Standard			
	Specimen 1	Specimen 2	Specimen 3	Specimen 4	Specimen 5
G—Gauge length	50.0 ± 0.1 [2.000 ± 0.005]	36.0 ± 0.1 [1.400 ± 0.005]	24.0 ± 0.1 [1.000 ± 0.005]	16.0 ± 0.1 [0.640 ± 0.005]	10.0 ±0.1 [0.450 ± 0.005]
D—Diameter (Note 1)	12.5 ± 0.2 [0.500 ± 0.010]	9.0 ±0.1 [0.350 ± 0.007]	6.0 ± 0.1 [0.250 ± 0.005]	4.0 ± 0.1 [0.160 ± 0.003]	2.5 ± 0.1 [0.113 ± 0.002]
R—Radius of fillet, min	10 [0.375]	8 [0.25]	6 [0.188]	4 [0.156]	2 [0.094]
A—Length of reduced section, min (Note 2)	56 [2.25]	45 [1.75]	30 [1.25]	20 [0.75]	16 [0.625]

Dimensions, mm [in.]

For Test Specimens with Gauge Length Five times the Diameter [E8M]

	Standard Specimen	Small-Size Specimens Proportional to Standard			
	Specimen 1	Specimen 2	Specimen 3	Specimen 4	Specimen 5
G—Gauge length	62.5 ± 0.1 [2.500 ± 0.005]	45.0 ± 0.1 [1.750 ± 0.005]	30.0 ± 0.1 [1.250 ± 0.005]	20.0 ± 0.1 [0.800 ± 0.005]	12.5 ± 0.1 [0.565 ± 0.005]
D—Diameter (Note 1)	12.5 ± 0.2 [0.500 ± 0.010]	9.0 ± 0.1 [0.350 ± 0.007]	6.0 ± 0.1 [0.250 ± 0.005]	4.0 ± 0.1 [0.160 ± 0.003]	2.5 ± 0.1 [0.113 ± 0.002]
R—Radius of fillet, min	10 [0.375]	8 [0.25]	6 [0.188]	4 [0.156]	2 [0.094]
A—Length of reduced section, min (Note 2)	75 [3.0]	54 [2.0]	36 [1.4]	24 [1.0]	20 [0.75]

NOTE 1—The reduced section may have a gradual taper from the ends toward the center, with the ends not more than 1 % larger in diameter than the center (controlling dimension).

NOTE 2—If desired, the length of the reduced section may be increased to accommodate an extensometer of any convenient gauge length. Reference marks for the measurement of elongation should, nevertheless, be spaced at the indicated gauge length.

NOTE 3—The gauge length and fillets may be as shown, but the ends may be of any form to fit the holders of the testing machine in such a way that the force shall be axial (see Fig. 9). If the ends are to be held in wedge grips it is desirable, if possible, to make the length of the grip section great enough to allow the specimen to extend into the grips a distance equal to two thirds or more of the length of the grips.

NOTE 4—On the round specimens in Figs. 8 and 9, the gauge lengths are equal to four [E8] or five times [E8M] the nominal diameter. In some product specifications other specimens may be provided for, but unless the 4-to-1 [E8] or 5-to-1 [E8M] ratio is maintained within dimensional tolerances, the elongation values may not be comparable with those obtained from the standard test specimen.

NOTE 5—The use of specimens smaller than 6-mm [0.250-in.] diameter shall be restricted to cases when the material to be tested is of insufficient size to obtain larger specimens or when all parties agree to their use for acceptance testing. Smaller specimens require suitable equipment and greater skill in both machining and testing.

NOTE 6—For inch/pound units only: Five sizes of specimens often used have diameters of approximately 0.505, 0.357, 0.252, 0.160, and 0.113 in., the reason being to permit easy calculations of stress from loads, since the corresponding cross-sectional areas are equal or close to 0.200, 0.100, 0.0500, 0.0200, and 0.0100 in.^{2}, respectively. Thus, when the actual diameters agree with these values, the stresses (or strengths) may be computed using the simple multiplying factors 5, 10, 20, 50, and 100, respectively. (The metric equivalents of these five diameters do not result in correspondingly convenient cross-sectional areas and multiplying factors.)

FIG. 8 Standard 12.5-mm [0.500-in.] Round Tension Test Specimen and Examples of Small-Size Specimens Proportional to the Standard Specimen

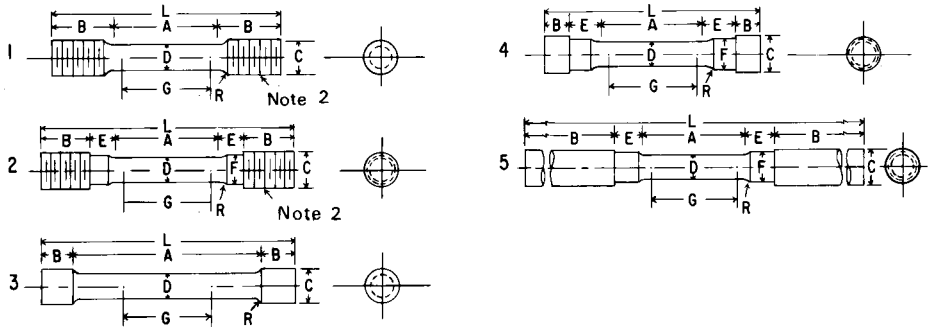

Dimensions, mm [in.]

For Test Specimens with Gauge Length Four times the Diameter [E8]

	Specimen 1	Specimen 2	Specimen 3	Specimen 4	Specimen 5
G—Gauge length	50 ± 0.1 [2.000 ± 0.005]	50 ± 0.1 [2.000 ± 0.005]	50 ± 0.1 [2.000 ± 0.005]	50 ± 0.1 [2.000 ± 0.005]	50 ± 0.1 [2.000 ± 0.005]
D—Diameter (Note 1)	12.5 ± 0.2 [0.500 ± 0.010]	12.5 ± 0.2 [0.500 ± 0.010]	12.5 ± 0.2 [0.500 ± 0.010]	12.5 ± 0.2 [0.500 ± 0.010]	12.5 ± 0.2 [0.500 ± 0.010]
R—Radius of fillet, min	10 [0.375]	10 [0.375]	2 [0.0625]	10 [0.375]	10 [0.375]
A—Length of reduced section	56 [2.25] min	56 [2.25] min	100 [4] approximate	56 [2.25] min	56 [2.25] min
L—Overall length, approximate	145 [5]	155 [5.5]	155 [5.5]	140 [4.75]	255 [9.5]
B—Length of end section (Note 3)	35 [1.375] approximate	25 [1] approximate	20 [0.75] approximate	15 [0.5] approximate	75 [3] min
C—Diameter of end section	20 [0.75]	20 [0.75]	20 [0.75]	22 [0.875]	20 [0.75]
E—Length of shoulder and fillet section, approximate		15 [0.625]		20 [0.75]	15 [0.625]
F—Diameter of shoulder		15 [0.625]		15 [0.625]	15 [0.625]

Dimensions, mm [in.]

For Test Specimens with Gauge Length Five times the Diameter [E8M]

	Specimen 1	Specimen 2	Specimen 3	Specimen 4	Specimen 5
G—Gauge length	62.5 ± 0.1 [2.500 ± 0.005]	62.5 ± 0.1 [2.500 ± 0.005]	62.5 ± 0.1 [2.500 ± 0.005]	62.5 ± 0.1 [2.500 ± 0.005]	62.5 ± 0.1 [2.500 ± 0.005]
D—Diameter (Note 1)	12.5 ± 0.2 [0.500 ± 0.010]	12.5 ± 0.2 [0.500 ± 0.010]	12.5 ± 0.2 [0.500 ± 0.010]	12.5 ± 0.2 [0.500 ± 0.010]	12.5 ± 0.2 [0.500 ± 0.010]
R—Radius of fillet, min	10 [0.375]	10 [0.375]	2 [0.0625]	10 [0.375]	10 [0.375]
A—Length of reduced section	75 [3] min	75 [3] min	75 [3] approximate	75 [3] min	75 [3] min
L—Overall length, approximate	145 [5]	155 [5.5]	155 [5.5]	140 [4.75]	255 [9.5]
B—Length of end section (Note 3)	35 [1.375] approximate	25 [1] approximate	20 [0.75] approximate	15 [0.5] approximate	75 [3] min
C—Diameter of end section	20 [0.75]	20 [0.75]	20 [0.75]	22 [0.875]	20 [0.75]
E—Length of shoulder and fillet section, approximate		15 [0.625]		20 [0.75]	15 [0.625]
F—Diameter of shoulder		15 [0.625]		15 [0.625]	15 [0.625]

NOTE 1—The reduced section may have a gradual taper from the ends toward the center with the ends not more than 1 %. larger in diameter than the center.

NOTE 2—On Specimens 1 and 2, any standard thread is permissible that provides for proper alignment and aids in assuring that the specimen will break within the reduced section.

NOTE 3—On Specimen 5 it is desirable, if possible, to make the length of the grip section great enough to allow the specimen to extend into the grips a distance equal to two thirds or more of the length of the grips.

NOTE 4—The values stated in SI units in the table for Fig. 9 are to be regarded as separate from the inch/pound units. The values stated in each system are not exact equivalents; therefore each system must be used independently of the other.

FIG. 9 Various Types of Ends for Standard Round Tension Test Specimens

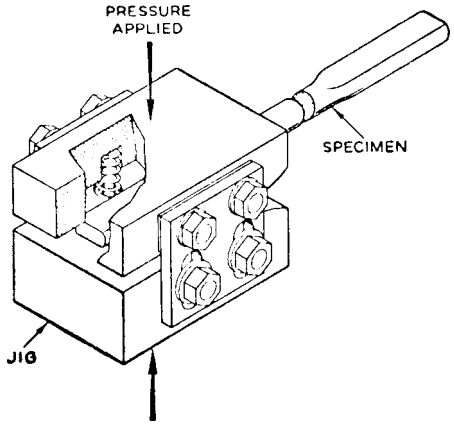

FIG. 10 Squeezing Jig for Flattening Ends of Full-Size Tension Test Specimens

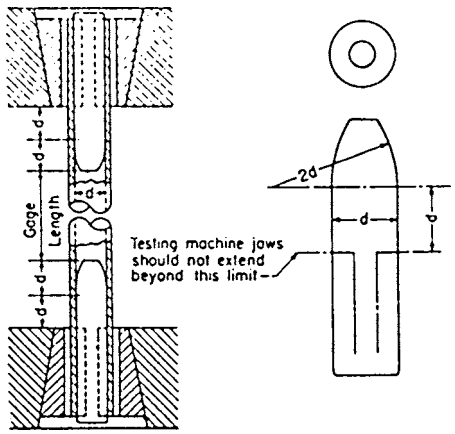

NOTE 1—The diameter of the plug shall have a slight taper from the line limiting the test machine jaws to the curved section.

FIG. 11 Metal Plugs for Testing Tubular Specimens, Proper Location of Plugs in Specimen and of Specimen in Heads of Testing Machine

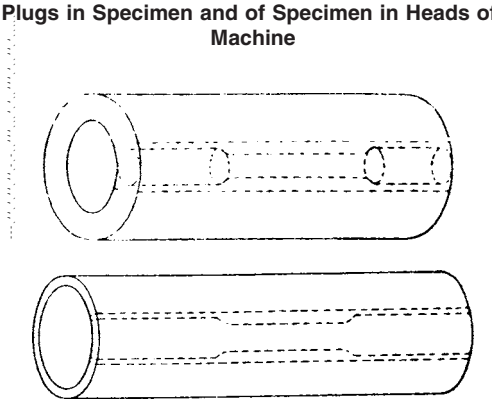

NOTE 1—The edges of the blank for the specimen shall be cut parallel to each other.

FIG. 12 Location from Which Longitudinal Tension Test Specimens Are to be Cut from Large-Diameter Tube

6.10 *Specimens for Forgings*—For testing forgings, the largest round specimen described in 6.4 shall be used. If round specimens are not feasible, then the largest specimen described in 6.5 shall be used.

6.10.1 For forgings, specimens shall be taken as provided in the applicable product specifications, either from the predominant or thickest part of the forging from which a coupon can be obtained, or from a prolongation of the forging, or from separately forged coupons representative of the forging. When not otherwise specified, the axis of the specimen shall be parallel to the direction of grain flow.

6.11 *Specimens for Castings*—In testing castings either the standard specimen shown in Fig. 8 or the specimen shown in Fig. 15 shall be used unless otherwise provided in the product specifications.

6.11.1 Test coupons for castings shall be made as shown in Fig. 16 and Table 1.

6.12 *Specimen for Malleable Iron*—For testing malleable iron the test specimen shown in Fig. 17 shall be used, unless otherwise provided in the product specifications.

6.13 *Specimen for Die Castings*—For testing die castings the test specimen shown in Fig. 18 shall be used unless otherwise provided in the product specifications.

6.14 *Specimens for Powder Metallurgy (P/M) Materials*—For testing powder metallurgy (P/M) materials the test specimens shown in Figs. 19 and 20 shall be used, unless otherwise provided in the product specifications. When making test specimens in accordance with Fig. 19, shallow transverse grooves, or ridges, may be pressed in the ends to allow gripping by jaws machined to fit the grooves or ridges. Because of shape and other factors, the flat unmachined tensile test specimen (Fig. 19) in the heat treated condition will have an ultimate tensile strength of 50 % to 85 % of that determined in a machined round tensile test specimen (Fig. 20) of like composition and processing.

7. Procedures

7.1 *Preparation of the Test Machine*—Upon startup, or following a prolonged period of machine inactivity, the test machine should be exercised or warmed up to normal operating temperatures to minimize errors that may result from transient conditions.

7.2 *Measurement of Dimensions of Test Specimens:*

7.2.1 To determine the cross-sectional area of a test specimen, measure the dimensions of the cross section at the center of the reduced section. For referee testing of specimens less than 5 mm [0.188 in.] in their least dimension, measure the dimensions where the least cross-sectional area is found. Measure and record the cross-sectional dimensions of tension test specimens as follows:

(1) Specimen dimension ≥ 5 mm [0.200 in.] to the nearest 0.02 mm [0.001 in.].

(2) 2.5 mm [0.100 in.] ≤ Specimen dimension < 5 mm [0.200 in.] to the nearest 0.01 mm [0.0005 in.].

(3) 0.5 mm [0.020 in.] ≤ specimen dimension < 2.5 mm [0.100 in.] to the nearest 0.002 mm [0.0001 in.].

(4) Specimen dimensions < 0.5 mm [0.020 in.], to at least the nearest 1 % when practical but in all cases to at least the nearest 0.002 mm [0.0001 in.].

NOTE 9—Accurate and precise measurement of specimen dimensions can be one of the most critical aspects of tension testing, depending on specimen geometry. See Appendix X2 for additional information.

NOTE 10—Rough surfaces due to the manufacturing process such as hot rolling, metallic coating, etc., may lead to inaccuracy of the computed

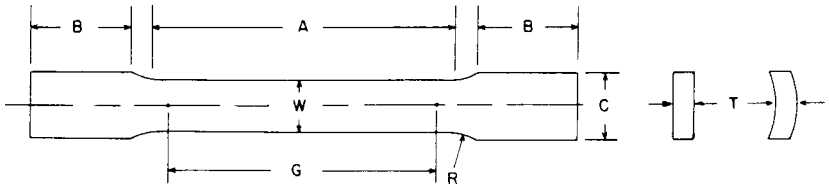

	Dimensions						
	Specimen 1	Specimen 2	Specimen 3	Specimen 4	Specimen 5	Specimen 6	Specimen 7
	mm [in.]	mm [in.]	mm [in.]	mm [in.]	mm [in.]	mm [in.]	mm [in.]
G—Gauge length	50.0 ± 0.1 [2.000 ± 0.005]	50.0 ± 0.1 [2.000 ± 0.005]	200.0 ± 0.2 [8.00 ± 0.01]	50.0 ± 0.1 [2.000 ± 0.005]	100.0 ± 0.1 [4.000 ± 0.005]	50.0 ± 0.1 [2.000 ± 0.005]	100.0 ± 0.1 [4.000 ± 0.005]
W—Width (Note 1)	12.5 ± 0.2 [0.500 ± 0.010]	40.0 ± 2.0 [1.5 ± 0.125-0.25]	40.0 ± 0.2 [1.5 ± 0.125,-0.25]	20.0 ± 0.7 [0.750 ± 0.031]	20.0 ± 0.7 [0.750 ± 0.031]	25.0 ± 1.5 [1.000 ± 0.062]	25.0 ± 1.5 [1.000 ± 0.062]
T—Thickness	measured thickness of specimen						
R—Radius of fillet, min	12.5 [0.5]	25 [1]	25 [1]	25 [1]	25 [1]	25 [1]	25 [1]
A—Length of reduced section, min	60 [2.25]	60 [2.25]	230 [9]	60 [2.25]	120 [4.5]	60 [2.25]	120 [4.5]
B—Length of grip section, min (Note 2)	75 [3]	75 [3]	75 [3]	75 [3]	75 [3]	75 [3]	75 [3]
C—Width of grip section, approximate (Note 3)	20 [0.75]	50 [2]	50 [2]	25 [1]	25 [1]	40 [1.5]	40 [1.5]

NOTE 1—The ends of the reduced section shall differ from each other in width by not more than 0.5 %. There may be a gradual taper in width from the ends to the center, but the width at each end shall be not more than 1 % greater than the width at the center.

NOTE 2—It is desirable, if possible, to make the length of the grip section great enough to allow the specimen to extend into the grips a distance equal to two thirds or more of the length of the grips.

NOTE 3—The ends of the specimen shall be symmetrical with the center line of the reduced section within 1 mm [0.05 in.] for specimens 1, 4, and 5, and 2.5 mm [0.10 in.] for specimens 2, 3, 6, and 7.

NOTE 4—For each specimen type, the radii of all fillets shall be equal to each other within a tolerance of 1.25 mm [0.05 in.], and the centers of curvature of the two fillets at a particular end shall be located across from each other (on a line perpendicular to the centerline) within a tolerance of 2.5 mm [0.10 in.].

NOTE 5—For circular segments, the cross-sectional area may be calculated by multiplying *W* and *T*. If the ratio of the dimension *W* to the diameter of the tubular section is larger than about ⅙, the error in using this method to calculate the cross-sectional area may be appreciable. In this case, the exact equation (see 7.2.3) must be used to determine the area.

NOTE 6—Specimens with *G/W* less than 4 should not be used for determination of elongation.

NOTE 7—Specimens with sides parallel throughout their length are permitted, except for referee testing, provided: *(a)* the above tolerances are used; *(b)* an adequate number of marks are provided for determination of elongation; and *(c)* when yield strength is determined, a suitable extensometer is used. If the fracture occurs at a distance of less than 2 W from the edge of the gripping device, the tensile properties determined may not be representative of the material. If the properties meet the minimum requirements specified, no further testing is required, but if they are less than the minimum requirements, discard the test and retest.

FIG. 13 Tension Test Specimens for Large-Diameter Tubular Products

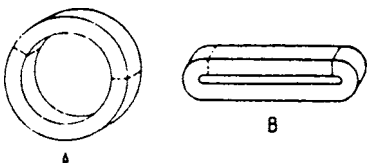

FIG. 14 Location of Transverse Tension Test Specimen in Ring Cut from Tubular Products

areas greater than the measured dimensions would indicate. Therefore, cross-sectional dimensions of test specimens with rough surfaces due to processing may be measured and recorded to the nearest 0.02 mm [0.001 in.]

NOTE 11—See X2.9 for cautionary information on measurements taken from coated metal products.

7.2.2 Determine the cross-sectional area of a full-size test specimen of uniform but nonsymmetrical cross section by determining the mass of a length not less than 20 times longer than the largest cross-sectional dimension.

7.2.2.1 Determine the weight to the nearest 0.5 % or less.

7.2.2.2 The cross-sectional area is equal to the mass of the specimen divided by the length and divided by the density of the material.

7.2.3 When using specimens of the type shown in Fig. 13 taken from tubes, the cross-sectional area shall be determined as follows:

If $D/W \leq 6$:

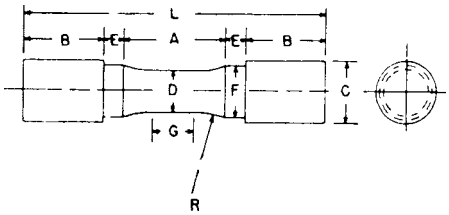

Dimensions			
	Specimen 1	Specimen 2	Specimen 3
	mm [in.]	mm [in.]	mm [in.]
G—Length of parallel section	Shall be equal to or greater than diameter *D*		
D—Diameter	12.5 ± 0.2 [0.500 ± 0.010]	20 ± 0.4 [0.750 ± 0.015]	36.0 ± 0.6 [1.25 ± 0.02]
R—Radius of fillet, min	25 [1]	25 [1]	50 [2]
A—Length of reduced section, min	32 [1.25]	38 [1.5]	60 [2.25]
L—Overall length, min	95 [3.75]	100 [4]	160 [6.375]
B—Length of end section, approximate	25 [1]	25 [1]	45 [1.75]
C—Diameter of end section, approximate	20 [0.75]	30 [1.125]	48 [1.875]
E—Length of shoulder, min	6 [0.25]	6 [0.25]	8 [0.312]
F—Diameter of shoulder	16.0 ± 0.4 [0.625 ± 0.016]	24.0 ± 0.4 [0.94 ± 0.016]	36.5 ± 0.4 [1.438 ± 0.016]

NOTE 1—The reduced section and shoulders (dimensions *A*, *D*, *E*, *F*, *G*, and *R*) shall be as shown, but the ends may be of any form to fit the holders of the testing machine in such a way that the force can be axial. Commonly the ends are threaded and have the dimensions *B* and *C* given above.

FIG. 15 Standard Tension Test Specimen for Cast Iron

$$A = \left[\left(\frac{W}{4}\right) \times \sqrt{(D^2 - W^2)}\right] + \left[\left(\frac{D^2}{4}\right) \times \arcsin\left(\frac{W}{D}\right)\right] - \left[\left(\frac{W}{4}\right) \times \sqrt{(D - 2T)^2 - W^2}\right] - \left[\left(\frac{D - 2T}{2}\right)^2 \times \arcsin\left(\frac{W}{D - 2T}\right)\right] \quad (1)$$

where:

A = exact cross-sectional area, mm^2 [in.^{2}],
W = width of the specimen in the reduced section, mm [in.],
D = measured outside diameter of the tube, mm [in.], and
T = measured wall thickness of the specimen, mm [in.].

arcsin values to be in radians

If $D/W > 6$, the exact equation or the following equation may be used:

$$A = W \times T \quad (2)$$

where:

A = approximate cross-sectional area, mm^2 [in.^{2}],
W = width of the specimen in the reduced section, mm [in.], and
T = measured wall thickness of the specimen, mm [in.].

NOTE 12—See X2.8 for cautionary information on measurements and calculations for specimens taken from large-diameter tubing.

7.3 *Gauge Length Marking of Test Specimens:*

7.3.1 The gauge length for the determination of elongation shall be in accordance with the product specifications for the material being tested. Gauge marks shall be stamped lightly with a punch, scribed lightly with dividers or drawn with ink as preferred. For material that is sensitive to the effect of slight notches and for small specimens, the use of layout ink will aid in locating the original gauge marks after fracture.

7.3.2 For materials where the specified elongation is 3 % or less, measure the original gauge length to the nearest 0.05 mm [0.002 in.] prior to testing.

7.4 *Zeroing of the Testing Machine:*

7.4.1 The testing machine shall be set up in such a manner that zero force indication signifies a state of zero force on the specimen. Any force (or preload) imparted by the gripping of the specimen (see Note 13) must be indicated by the force measuring system unless the preload is physically removed prior to testing. Artificial methods of removing the preload on the specimen, such as taring it out by a zero adjust pot or removing it mathematically by software, are prohibited because these would affect the accuracy of the test results.

NOTE 13—Preloads generated by gripping of specimens may be either tensile or compressive in nature and may be the result of such things as:
— grip design
— malfunction of gripping apparatus (sticking, binding, etc.)
— excessive gripping force
— sensitivity of the control loop

NOTE 14—It is the operator's responsibility to verify that an observed preload is acceptable and to ensure that grips operate in a smooth manner. Unless otherwise specified, it is recommended that momentary (dynamic) forces due to gripping not exceed 20 % of the material's nominal yield strength and that static preloads not exceed 10 % of the material's nominal yield strength.

7.5 *Gripping of the Test Specimen:*

7.5.1 For specimens with reduced sections, gripping of the specimen shall be restricted to the grip section, because gripping in the reduced section or in the fillet can significantly affect test results.

7.6 *Speed of Testing:*

7.6.1 Speed of testing may be defined in terms of *(a)* rate of straining of the specimen, *(b)* rate of stressing of the specimen, *(c)* crosshead speed, *(d)* the elapsed time for completing part or all of the test, or *(e)* free-running crosshead speed (rate of movement of the crosshead of the testing machine when not under load).

7.6.2 Specifying suitable numerical limits for speed and selection of the method are the responsibilities of the product committees. Suitable limits for speed of testing should be specified for materials for which the differences resulting from the use of different speeds are of such magnitude that the test results are unsatisfactory for determining the acceptability of the material. In such instances, depending upon the material and the use for which the test results are intended, one or more of the methods described in the following paragraphs is recommended for specifying speed of testing.

NOTE 15—Speed of testing can affect test values because of the rate sensitivity of materials and the temperature-time effects.

7.6.2.1 *Rate of Straining*—The allowable limits for rate of straining shall be specified in mm/mm/min [in./in./min]. Some testing machines are equipped with pacing or indicating devices for the measurement and control of rate of straining,

TABLE 1 Details of Test Coupon Design for Castings (see Fig. 16)

NOTE 1—*Test Coupons for Large and Heavy Steel Castings:* The test coupons in Fig. 16A and B are to be used for large and heavy steel castings. However, at the option of the foundry the cross-sectional area and length of the standard coupon may be increased as desired. This provision does not apply to Specification A356/A356M.

NOTE 2—*Bend Bar:* If a bend bar is required, an alternate design (as shown by dotted lines in Fig. 16) is indicated.

Leg Design, 125 mm [5 in.]		Riser Design	
1. *L* (length)	A 125mm [5-in.] minimum length will be used. This length may be increased at the option of the foundry to accommodate additional test bars (see Note 1).	1. *L* (length)	The length of the riser at the base will be the same as the top length of the leg. The length of the riser at the top therefore depends on the amount of taper added to the riser.
2. End taper	Use of and size of end taper is at the option of the foundry.	2. Width	The width of the riser at the base of a multiple-leg coupon shall be *n* (57 mm) – 16 mm [*n* (2.25 in.) – 0.625 in.] where n equals the number of legs attached to the coupon. The width of the riser at the top is therefore dependent on the amount of taper added to the riser.
3. Height	32 mm [1.25 in.]		
4. Width (at top)	32 mm [1.25 in.] (see Note 1)		
5. Radius (at bottom)	13 mm [0.5 in.] max		
6. Spacing between legs	A 13 mm [0.5 in.] radius will be used between the legs.		
7. Location of test bars	The tensile, bend, and impact bars will be taken from the lower portion of the leg (see Note 2).		
8. Number of legs	The number of legs attached to the coupon is at the option of the foundry providing they are equispaced according to Item 6.	3. *T* (riser taper) Height	Use of and size is at the option of the foundry. The minimum height of the riser shall be 51 mm [2 in.]. The maximum height is at the option of the foundry for the following reasons: *(a)* many risers are cast open, *(b)* different compositions may require variation in risering for soundness, or *(c)* different pouring temperatures may require variation in risering for soundness.
9. R_x	Radius from 0 to approximately 2 mm [0.062 in.]		

but in the absence of such a device the average rate of straining can be determined with a timing device by observing the time required to effect a known increment of strain.

7.6.2.2 *Rate of Stressing*—The allowable limits for rate of stressing shall be specified in megapascals per second [pounds per square inch per minute]. Many testing machines are equipped with pacing or indicating devices for the measurement and control of the rate of stressing, but in the absence of such a device the average rate of stressing can be determined with a timing device by observing the time required to apply a known increment of stress.

7.6.2.3 *Crosshead Speed*—The allowable limits for crosshead speed, during a test, may be specified in mm/min [in./min]; in this case, the limits for the crosshead speed should be further qualified by specifying different limits for various types and sizes of specimens. In cases where different length specimens may be used, it is often more practical to specify the crosshead speed in terms of mm [in.] per mm [in.] of length of the original reduced section of the specimen (or distance between grips for specimens not having reduced sections) per minute. Many testing machines are equipped with pacing or indicating devices for the measurement and control of the crosshead speed during a test, but in the absence of such devices the average crosshead speed can be experimentally determined by using suitable length-measuring and timing devices.

NOTE 16—This method of specifying speed of testing, "Crosshead Speed", was previously called "Rate of Separation of Heads During Tests."

NOTE 17—For machines not having crossheads or having stationary crossheads, the phrase "crosshead speed" may be interpreted to mean the rate of grip separation.

7.6.2.4 *Elapsed Time*—The allowable limits for the elapsed time from the beginning of force application (or from some specified stress) to the instant of fracture, to the maximum force, or to some other stated stress, shall be specified in minutes or seconds. The elapsed time can be determined with a timing device.

7.6.2.5 *Free-Running Crosshead Speed*—The allowable limits for the rate of movement of the crosshead of the testing machine, with no force applied by the testing machine, shall be specified in mm per mm [inches per inch] of length of reduced section (or distance between grips for specimens not having reduced sections) per second [minute]. The limits for the crosshead speed may be further qualified by specifying different limits for various types and sizes of specimens. The average crosshead speed can be experimentally determined by using suitable length-measuring and timing devices.

NOTE 18—For machines not having crossheads or having stationary crossheads, the phrase "free-running crosshead speed" may be interpreted to mean the free-running rate of grip separation.

7.6.3 *Speed of Testing When Determining Yield Properties*—Unless otherwise specified, any convenient speed of testing may be used up to one half the specified minimum yield strength or up to one quarter of the specified minimum tensile strength, whichever is smaller. The speed above this point shall be within the specified limits. If different speed limitations are required for use in determining yield strength, yield point elongation, tensile strength, elongation, and reduction of area,

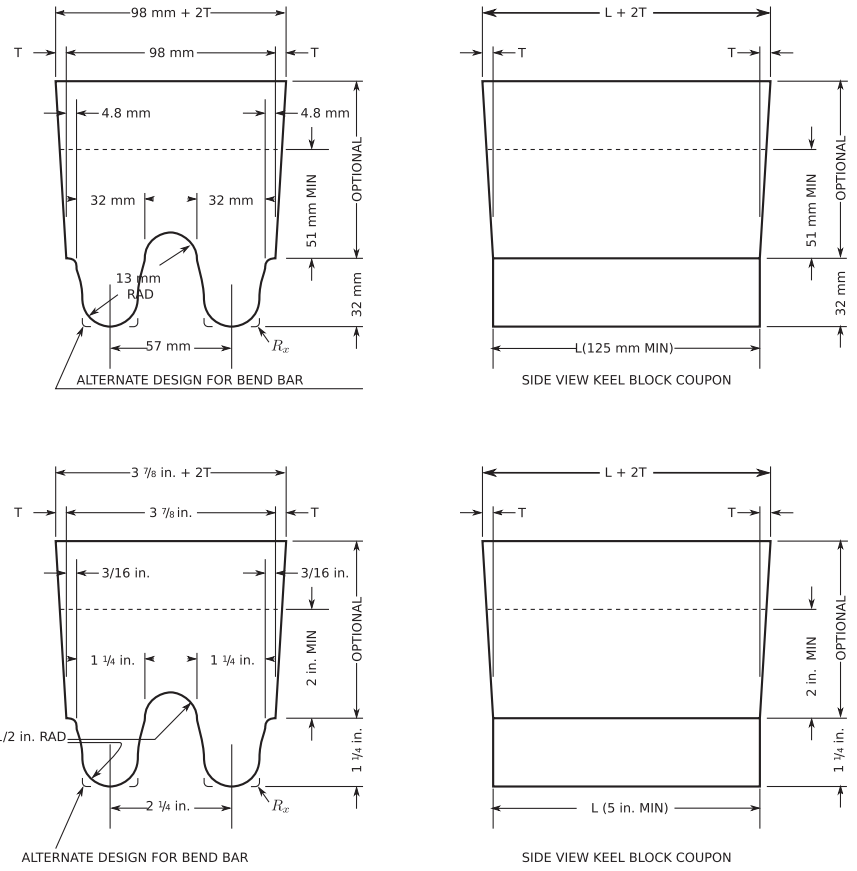

Design for Double Keel Block Coupon

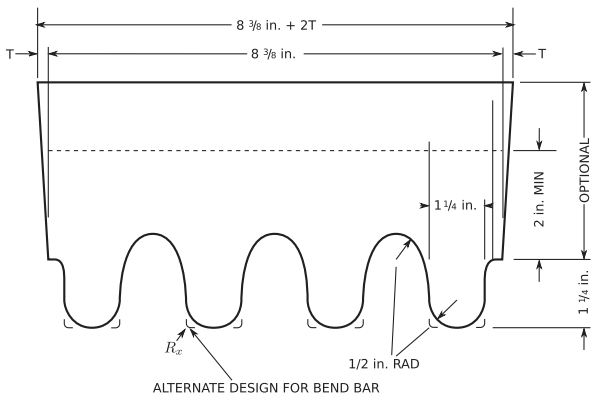

Design for Multiple Keel Block Coupon (4 legs)

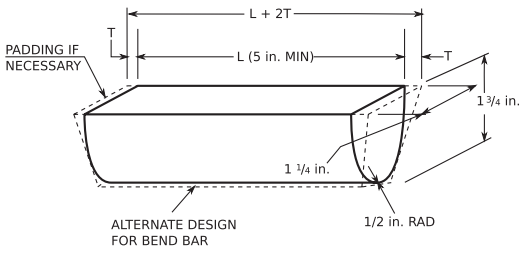

Design for "Attached" Coupon

FIG. 16 Test Coupons for Castings

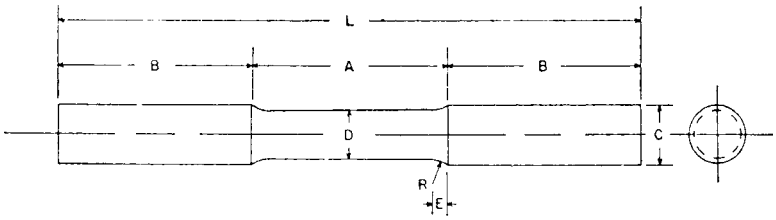

Dimensions, mm [in.]	
D—Diameter	16 [0.625]
R—Radius of fillet	8 [0.312]
A—Length of reduced section	64 [2.5]
L—Overall length	190 [7.5]
B—Length of end section	64 [2.5]
C—Diameter of end section	20 [0.75]
E—Length of fillet	5 [0.188]

FIG. 17 Standard Tension Test Specimen for Malleable Iron

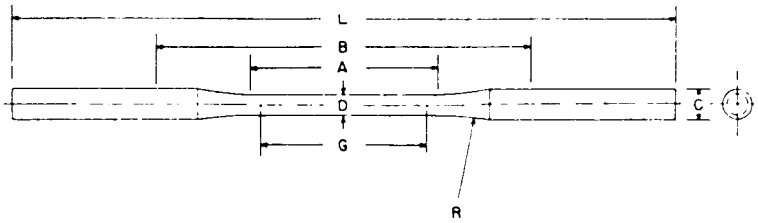

Dimensions, mm [in.]	
G—Gauge length	50 ± 0.1 [2.000 ± 0.005]
D—Diameter (see Note)	6.4 ± 0.1 [0.250 ± 0.005]
R—Radius of fillet, min	75 [3]
A—Length of reduced section, min	60 [2.25]
L—Overall length, min	230 [9]
B—Distance between grips, min	115 [4.5]
C—Diameter of end section, approximate	10 [0.375]

NOTE 1—The reduced section may have a gradual taper from the end toward the center, with the ends not more than 0.1 mm [0.005 in.] larger in diameter than the center.

FIG. 18 Standard Tension Test Specimens for Die Castings

they should be stated in the product specifications. In all cases, the speed of testing shall be such that the forces and strains used in obtaining the test results are accurately indicated. Determination of mechanical properties for comparison of product properties against a specification value should be run using the same control method and rate used to determine the specification value unless it can be shown that another method yields equivalent or conservative results. In the absence of any specified limitations, one of the following control methods shall be used. Appendix X4 provides additional guidance on selecting the control method.

NOTE 19—In the previous and following paragraphs, the yield properties referred to include yield strength, yield point, and yield point elongation.

7.6.3.1 *Control Method A—Rate of Stressing Method for Determining Yield Properties* - In this method, the testing machine shall be operated such that the rate of stress application in the linear elastic region is between 1.15 and 11.5 MPa/s [10 000 and 100 000 psi/min]. The speed of the testing machine shall not be increased in order to maintain a stressing rate when the specimen begins to yield. It is not recommended that the testing machine be operated in closed-loop control using the force signal through yield; however closed-loop control of the force signal can be used in the linear-elastic portion of the test.

NOTE 20—It is not the intent of this method to maintain constant stress rate or to control stress rate with closed loop force control while determining yield properties, but only to set the crosshead speed to achieve the target stress rate in the elastic region. When a specimen being tested begins to yield, the stressing rate decreases and may even become negative in the case of a specimen with discontinuous yielding. To maintain a constant stressing rate through the yielding process requires the testing machine to operate at extremely high speeds and, in most cases, this is neither practical nor desirable. In practice, it is simpler to use either a strain rate, crosshead speed, or a free-running crosshead speed that approximates the desired stressing rate in the linear-elastic portion of the test. As an example, use a strain rate that is between 1.15 and 11.5 MPa/s divided by the nominal Young's Modulus of the material being tested. As another example, find a crosshead speed through experimentation that approximates the desired stressing rate prior to the onset of yielding, and maintain that crosshead speed through the region that yield properties are determined. While both of these methods will provide similar rates of stressing and straining prior to the onset of yielding, the rates of stressing and straining are generally quite different in the region where yield properties are determined.

NOTE 21—This method has been the default method for many years for

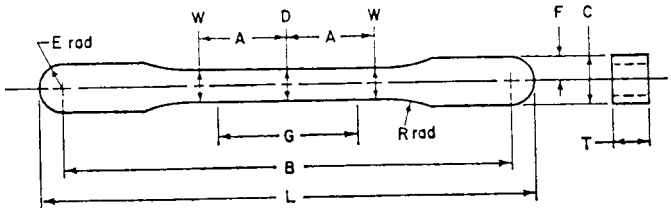

Pressing Area = 645 mm^2 [1.00 in.^{2}]

Dimensions, mm [in.]	
G—Gauge length	25.4 ± 0.08 [1.000 ± 0.003]
D—Width at center	5.72 ± 0.03 [0.225 ± 0.001]
W—Width at end of reduced section	5.97 ± 0.03 [0.235 ± 0.001]
T—Compact to this thickness	3.56 to 6.35 [0.140 to 0.250]
R—Radius of fillet	25.4 [1]
A—Half-length of reduced section	15.9 [0.625]
B—Grip length	80.95 ± 0.03 [3.187 ± 0.001]
L—Overall length	89.64 ± 0.03 [3.529 ± 0.001]
C—Width of grip section	8.71 ± 0.03 [0.343 ± 0.001]
F—Half-width of grip section	4.34 ± 0.03 [0.171 ± 0.001]
E—End radius	4.34 ± 0.03 [0.171 ± 0.001]

NOTE 1—Dimensions Specified, except *G* and *T*, are those of the die.

FIG. 19 Standard Flat Unmachined Tension Test Specimens for Powder Metallurgy (P/M) Products

testing materials that exhibit low strain rate sensitivity such as some steels and aluminum.

7.6.3.2 *Control Method B - Rate of Straining Control Method for Determining Yield Properties*—In this method, the testing machine shall be operated in closed-loop control using the extensometer signal. The rate of straining shall be set and maintained at 0.015 ± 0.006 mm/mm/min [in./in./min].

NOTE 22—Proper precautions must be observed when operating a machine in closed-loop strain control because unexpected crosshead movement may occur if the control parameters are not set properly, if proper safety limits are not set, or if the extensometer slips.

NOTE 23—A Rate of Straining at 0.005 mm/mm/min [in./in./min] is often required for aerospace, high-temperature alloys, and titanium applications and when specified, must be followed rather than the requirement above.

7.6.3.3 *Control Method C—-Crosshead Speed Control Method for Determining Yield Properties*–The testing machine shall be set to a crosshead speed equal to 0.015 ± 0.003 mm/mm/min [in./in./min] of the original reduced section (dimension A in Fig. 1, Fig. 7, Fig. 8, Fig. 9, Fig. 13, Fig. 15, Fig. 17, Fig. 18, and Fig. 20, and 2 times dimension A in Fig. 19) or distance between grips for specimens without reduced sections.

NOTE 24—It is recommended that crosshead speed be used for control in regions of discontinuous yielding.

NOTE 25—Using different Control Methods may produce different yield results especially if the material being tested is strain-rate sensitive. To achieve the best reproducibility in cases where the material may be strain-rate sensitive, the same control method should be used. Methods described in 7.6.3.2 or 7.6.3.3 will tend to give similar results in the case of a strain-rate sensitive material. The control method described in 7.6.3.1 should be avoided for strain rate sensitive materials if it is desirable to reproduce similar test results on other testing machines or in other laboratories.

7.6.4 *Speed of Testing When Determining Tensile Strength*—In the absence of any specified limitations on speed

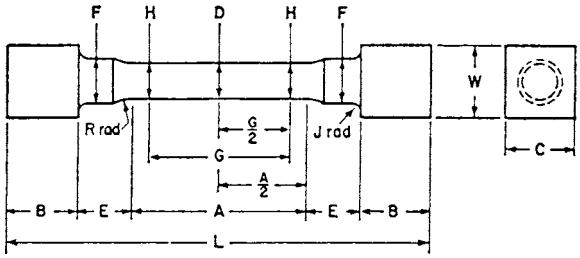

Approximate Pressing Area of Unmachined Compact = 752 mm^2 [1.166 in.^{2}] Machining Recommendations

1. Rough machine reduced section to 6.35-mm [0.25-in.] diameter
2. Finish turn 4.75/4.85-mm [0.187/0.191-in.] diameter with radii and taper
3. Polish with 00 emery cloth
4. Lap with crocus cloth

Dimensions, mm [in.]	
G—Gauge length	25.4 ± 0.08 [1.000 ± 0.003]
D—Diameter at center of reduced section	4.75 ± 0.03 [0.187± 0.001]
H—Diameter at ends of gauge length	4.85 ± 0.03 [0.191 ± 0.001]
R—Radius of gauge fillet	6.35 ± 0.13 [0.250 ± 0.005]
A—Length of reduced section	47.63 ± 0.13 [1.875 ± 0.003]
L—Overall length (die cavity length)	75 [3], nominal
B—Length of end section	7.88 ± 0.13 [0.310 ± 0.005]
C—Compact to this end thickness	10.03 ± 0.13 [0.395 ± 0.005]
W—Die cavity width	10.03 ± 0.08 [0.395 ± 0.003]
E—Length of shoulder	6.35 ± 0.13 [0.250 ± 0.005]
F—Diameter of shoulder	7.88 ± 0.03 [0.310 ± 0.001]
J—End fillet radius	1.27 ± 0.13 [0.050 ± 0.005]

NOTE 1—The gauge length and fillets of the specimen shall be as shown. The ends as shown are designed to provide a practical minimum pressing area. Other end designs are acceptable, and in some cases are required for high-strength sintered materials.

NOTE 2—It is recommended that the test specimen be gripped with a split collet and supported under the shoulders. The radius of the collet support circular edge is to be not less than the end fillet radius of the test specimen.

NOTE 3—Diameters *D* and *H* are to be concentric within 0.03 mm [0.001 in.] total indicator runout (T.I.R.), and free of scratches and tool marks.

FIG. 20 Standard Round Machined Tension Test Specimen for Powder Metallurgy (P/M) Products

of testing, the following general rules shall apply for materials with expected elongations greater than 5 %. When determining only the tensile strength, or after the yield behavior has been recorded, the speed of the testing machine shall be set between 0.05 and 0.5 mm/mm [or in./in.] of the length of the reduced section (or distance between the grips for specimens not having a reduced section) per minute. Alternatively, an extensometer and strain rate indicator may be used to set the strain rate between 0.05 and 0.5 mm/mm/min [or in./in./min].

NOTE 26—For materials with expected elongations less than or equal to 5 %, the speed of the testing machine may be maintained throughout the test at the speed used to determine yield properties.

NOTE 27—Tensile strength and elongation are sensitive to test speed for many materials (see Appendix X1) to the extent that variations within the range of test speeds given above can significantly affect results.

7.7 *Determination of Yield Strength*—Determine yield strength by any of the methods described in 7.7.1 to 7.7.4.

Where extensometers are employed, use only those that are verified over a strain range in which the yield strength will be determined (see 5.4).

NOTE 28—For example, a verified strain range of 0.2 % to 2.0 % is appropriate for use in determining the yield strengths of many metals.

NOTE 29—Determination of yield behavior on materials which cannot support an appropriate extensometer (thin wire, for example) is problematic and outside the scope of this standard.

7.7.1 *Offset Method*—To determine the yield strength by the offset method, it is necessary to secure data (autographic or numerical) from which a stress-strain diagram may be drawn. Then on the stress-strain diagram (Fig. 21) lay off *Om* equal to the specified value of the offset, draw *mn* parallel to *OA*, and thus locate *r*, the intersection of mn with the stress-strain diagram (Note 36). In reporting values of yield strength obtained by this method, the specified value of offset used should be stated in parentheses after the term yield strength. Thus:

$$\text{Yield strength}\,(\text{offset} = 0.2\,\%) = 360\ \text{MPa}\,[52\,000\ \text{psi}] \qquad (3)$$

In using this method, a Class B2 or better extensometer (see Practice E83) shall be used.

NOTE 30—There are two general types of extensometers, averaging and non-averaging, the use of which is dependent on the product tested. For most machined specimens, there are minimal differences. However, for some forgings and tube sections, significant differences in measured yield strength can occur. For these cases, it is recommended that the averaging type be used.

NOTE 31—When there is a disagreement over yield properties, the offset method for determining yield strength is recommended as the referee test method.

NOTE 32—In practice, for a number of reasons, the straight-line portion of the stress-strain curve (line *OA* shown in Fig. 21) may not go through the origin of the stress-strain diagram. In these cases, Point *O* in Figs. 21-27is not the origin of the stress-strain diagram, but rather where the straight-line portion of the stress-strain curve, *OA*, intersects the strain axis, see Fig. 26 and Fig. 27. All offsets and extensions are calculated from the intersection of the straight-line portion of the stress-strain curve, *OA*, with the strain axis, and not necessarily from the origin of the stress-strain diagram.

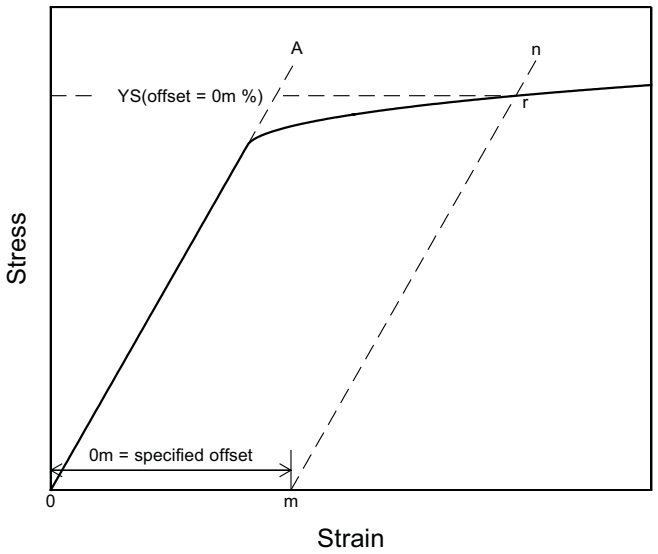

FIG. 21 Stress-Strain Diagram for Determination of Yield Strength by the Offset Method

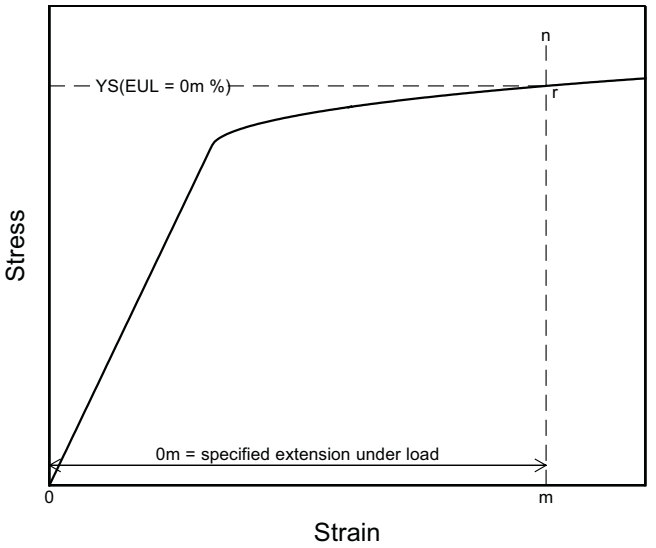

FIG. 22 Stress-Strain Diagram for Determination of Yield Strength by the Extension-Under-Load Method

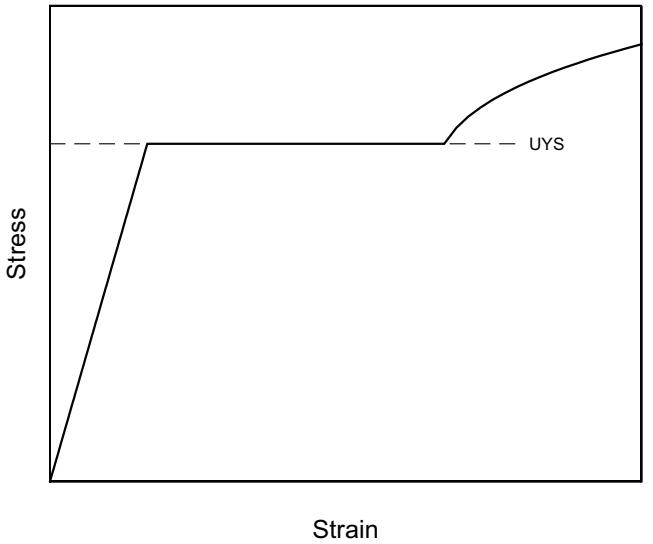

FIG. 23 Stress-Strain Diagram Showing Upper Yield Strength Corresponding with Top of Knee

7.7.2 *Extension-Under-Load (EUL) Method*—Yield strength by the extension-under-load method may be determined by: *(1)* using autographic or numerical devices to secure stress-strain data, and then analyzing this data (graphically or using automated methods) to determine the stress value at the specified value of extension, or *(2)* using devices that indicate when the specified extension occurs, so that the stress then occurring may be ascertained (Note 34). Any of these devices may be automatic. This method is illustrated in Fig. 22. The stress at the specified extension shall be reported as follows:

$$\text{Yield strength}\,(\text{EUL} = 0.5\,\%) = 52\,000\ \text{psi} \qquad (4)$$

Extensometers and other devices used in determination of the extension shall meet or exceed Class B2 requirements (see Practice E83) at the strain of interest, except where use of low-magnification Class C devices is helpful, such as in

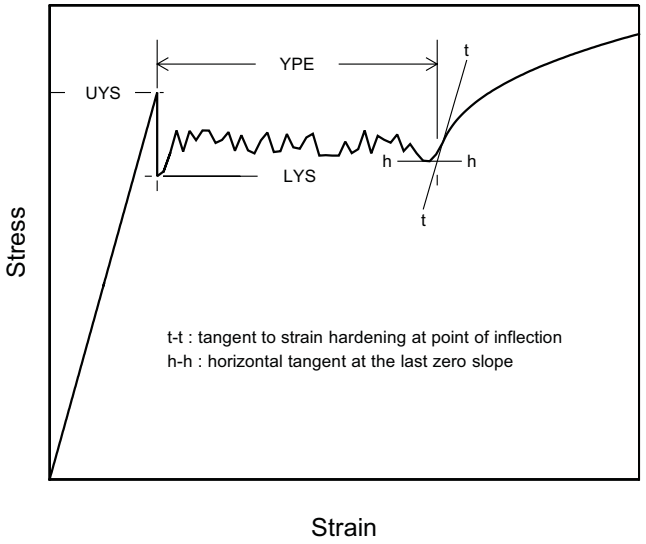

FIG. 24 Stress-Strain Diagram Showing Yield Point Elongation (YPE) and Upper (UYS) and Lower (LYS) Yield Strengths

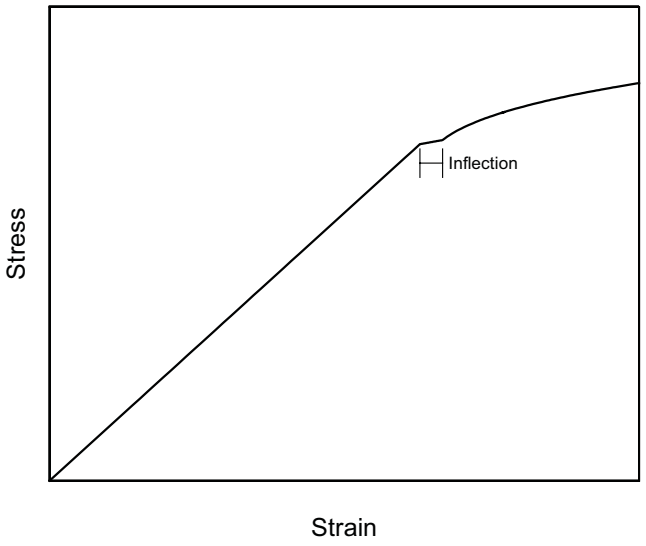

FIG. 25 Stress-Strain Diagram With an Inflection, But No YPE

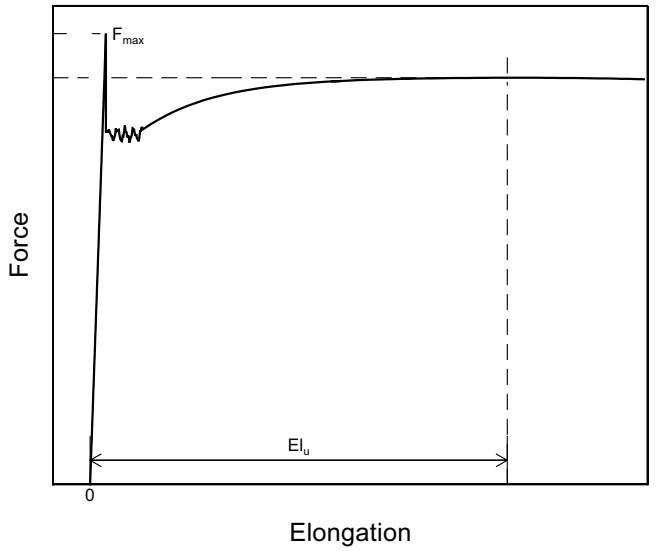

FIG. 26 Stress-Strain Diagram in Which the Upper Yield Strength is the Maximum Stress Recorded Method

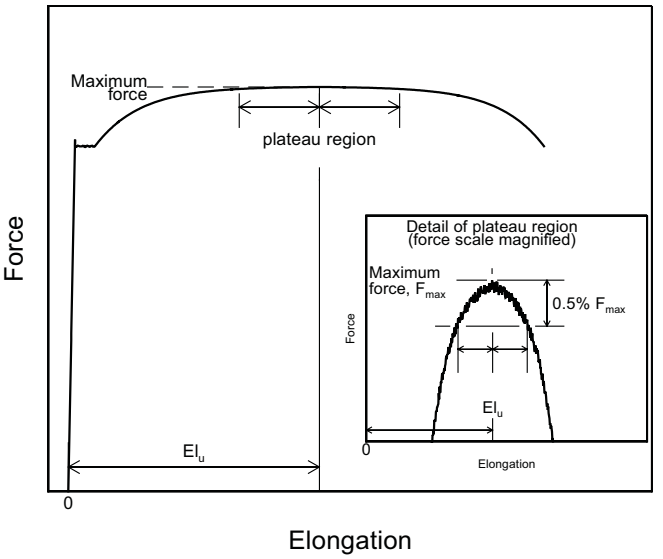

FIG. 27 Force-Elongation Diagram for Determination of Uniform Elongation of Steel Sheet Materials Exhibiting a Plateau at Maximum Force

facilitating measurement of YPE, if observed. If Class C devices are used, this must be reported along with the results.

NOTE 33—The appropriate value of the total extension must be specified. For steels with nominal yield strengths of less than 550 MPa [80 000 psi], an appropriate value is 0.005 mm/mm [or in./in.] (0.5 %) of the gauge length. For higher strength steels, a greater extension or the offset method should be used.

NOTE 34—When no other means of measuring elongation are available, a pair of dividers or similar device can be used to determine a point of detectable elongation between two gauge marks on the specimen. The gauge length shall be 50 mm [2 in.]. The stress corresponding to the load at the instant of detectable elongation may be recorded as the approximate extension-under-load yield strength.

7.7.3 *Autographic Diagram Method (for materials exhibiting discontinuous yielding)*—Obtain stress-strain (or force-elongation) data or construct a stress-strain (or force-elongation) diagram using an autographic device. Determine the upper or lower yield strength as follows:

7.7.3.1 Record the stress corresponding to the maximum force at the onset of discontinuous yielding as the upper yield strength. This is illustrated in Figs. 23 and 24.

NOTE 35—If multiple peaks are observed at the onset of discontinuous yielding, the first is considered the upper yield strength. (See Fig. 24.)

7.7.3.2 Record the minimum stress observed during discontinuous yielding (ignoring transient effects) as the lower yield strength. This is illustrated in Fig. 24.

NOTE 36—Yield properties of materials exhibiting yield point elongation are often less repeatable and less reproducible than those of similar materials having no YPE. Offset and EUL yield strengths may be significantly affected by stress fluctuations occurring in the region where the offset or extension intersects the stress-strain curve. Determination of upper or lower yield strengths (or both) may therefore be preferable for such materials, although these properties are dependent on variables such

as test machine stiffness and alignment. Speed of testing may also have a significant effect, regardless of the method employed.

NOTE 37—Where low-magnification autographic recordings are needed to facilitate measurement of yield point elongation for materials which may exhibit discontinuous yielding, Class C extensometers may be employed. When this is done but the material exhibits no discontinuous yielding, the extension-under-load yield strength may be determined instead, using the autographic recording (see Extension-Under-Load Method).

7.7.4 *Halt-of-the-Force Method (for materials exhibiting discontinuous yielding)*—Apply an increasing force to the specimen at a uniform deformation rate. When the force hesitates, record the corresponding stress as the upper yield strength.

NOTE 38—The Halt-of-the-Force Method was formerly known as the Halt-of-the-Pointer Method, the Drop-of-the-Beam Method, and the Halt-of-the-Load Method.

7.8 *Yield Point Elongation*—Calculate the yield point elongation from the stress-strain diagram or data by determining the difference in strain between the upper yield strength (first zero slope) and the onset of uniform strain hardening (see definition of YPE in Terminology E6 and Fig. 24).

NOTE 39—The stress-strain curve of a material exhibiting only a hint of the behavior causing YPE may have an inflection at the onset of yielding with no point where the slope reaches zero (Fig. 25). Such a material has no YPE, but may be characterized as exhibiting an inflection. Materials exhibiting inflections, like those with measurable YPE, may in certain applications acquire an unacceptable surface appearance during forming.

7.9 *Uniform Elongation (if required):*

7.9.1 Uniform elongation shall include both plastic and elastic elongation.

7.9.2 Uniform elongation shall be determined using autographic methods with extensometers conforming to Practice E83. Use a class B2 or better extensometer for materials having a uniform elongation less than 5 %. Use a class C or better extensometer for materials having a uniform elongation greater than or equal to 5 % but less than 50 %. Use a class D or better extensometer for materials having a uniform elongation of 50 % or greater.

7.9.3 Determine the uniform elongation as the elongation at the point of maximum force from the force elongation data collected during a test.

7.9.3.1 Some materials exhibit a yield point followed by considerable elongation where the yield point is the maximum force achieved during the test. In this case, uniform elongation is not determined at the yield point, but instead at the highest force occurring just prior to necking (see Fig. 26).

7.9.3.2 Stress-strain curves for some materials exhibit a lengthy, plateau-like region in the vicinity of the maximum force. For such materials, determine the uniform elongation at the center of the plateau as indicated in Fig. 27 (see also Note 40 below).

NOTE 40—When uniform elongation is being determined digitally, noise in the stress-strain data generally causes many small, local peaks and valleys to be recorded in the plateau region. To accommodate this, the following procedure is recommended:

— Determine the maximum force recorded (after discontinuous yielding).

— Evaluate the sequence of force values recorded before and after the maximum force.

— Digitally define the "plateau" as consisting of all consecutive data points wherein the force value is within 0.5 % of the magnitude of the peak force value.

— Determine the uniform elongation as the strain at the mid-point of the "plateau."

7.9.3.3 *Discussion*—The 0.5 % value of Note 40 has been selected arbitrarily. In actual practice, the value should be selected so as to be the minimum figure that is large enough to effectively define the force plateau. This may require that the percentage be about five times the amplitude of the force fluctuations occurring due to noise. Values ranging from 0.1 % to 1.0 % may be found to work acceptably.

7.10 *Tensile Strength (also known as Ultimate Tensile Strength)*—Calculate the tensile strength by dividing the maximum force carried by the specimen during the tension test by the original cross-sectional area of the specimen.

NOTE 41—If the upper yield strength is the maximum stress recorded, and if the stress-strain curve resembles that of Fig. 26, it is recommended that the maximum stress after discontinuous yielding be reported as the tensile strength. Where this may occur, determination of the tensile strength should be in accordance with the agreement between the parties involved.

7.11 *Elongation:*

7.11.1 In reporting values of elongation, give both the original gauge length and the percentage increase. If any device other than an extensometer is placed in contact with the specimen's reduced section during the test, this also shall be noted.

$$\textit{Example}\text{: Elongation} = 30\,\%\ \text{increase}\ (50\ -\ \text{mm}\,[2\ -\ \text{in.}]\ \text{gauge length}) \quad (5)$$

NOTE 42—Elongation results are very sensitive to variables such as: *(a)* speed of testing, *(b)* specimen geometry (gauge length, diameter, width, and thickness), *(c)* heat dissipation (through grips, extensometers, or other devices in contact with the reduced section), *(d)* surface finish in reduced section (especially burrs or notches), *(e)* alignment, and *(f)* fillets and tapers. Parties involved in comparison or conformance testing should standardize the above items, and it is recommended that use of ancillary devices (such as extensometer supports) which may remove heat from specimens be avoided. See Appendix X1 for additional information on the effects of these variables.

7.11.2 When the specified elongation is greater than 3 %, fit ends of the fractured specimen together carefully and measure the distance between the gage marks to the nearest 0.25 mm [0.01 in.] for gauge lengths of 50 mm [2 in.] and under, and to at least the nearest 0.5 % of the gauge length for gauge lengths over 50 mm [2 in.]. A percentage scale reading to 0.5 % of the gauge length may be used.

7.11.3 When the *specified* elongation is 3 % or less, determine the elongation of the specimen using the following procedure, except that the procedure given in 7.11.2 may be used instead when the *measured* elongation is greater than 3 %.

7.11.3.1 Prior to testing, measure the original gauge length of the specimen to the nearest 0.05 mm [0.002 in.].

7.11.3.2 Remove partly torn fragments that will interfere with fitting together the ends of the fractured specimen or with making the final measurement.

7.11.3.3 Fit the fractured ends together with matched surfaces and apply a force along the axis of the specimen sufficient to close the fractured ends together. If desired, this force may then be removed carefully, provided the specimen remains intact.

NOTE 43—The use of a force generating a stress of approximately 15 MPa [2000 psi] has been found to give satisfactory results on test specimens of aluminum alloy.

7.11.3.4 Measure the final gauge length to the nearest 0.05 mm [0.002 in.] and report the elongation to the nearest 0.2 %.

7.11.4 Elongation measured per paragraph 7.11.2 or 7.11.3 may be affected by location of the fracture, relative to the marked gauge length. If any part of the fracture occurs outside the gauge marks or is located less than 25 % of the elongated gauge length from either gauge mark, the elongation value obtained using that pair of gauge marks may be abnormally low and non-representative of the material. If such an elongation measure is obtained in acceptance testing involving only a minimum requirement and meets the requirement, no further testing need be done. Otherwise, discard the test and retest the material.

7.11.5 *Elongation at Fracture:*

7.11.5.1 Elongation at fracture shall include elastic and plastic elongation and may be determined with autographic or automated methods using extensometers verified over the strain range of interest (see 5.4). Use a class B2 or better extensometer for materials having less than 5 % elongation, a class C or better extensometer for materials having elongation greater than or equal to 5 % but less than 50 %, and a class D or better extensometer for materials having 50 % or greater elongation. In all cases, the extensometer gauge length shall be the nominal gauge length required for the specimen being tested. Due to the lack of precision in fitting fractured ends together, the elongation after fracture using the manual methods of the preceding paragraphs may differ from the elongation at fracture determined with extensometers.

7.11.5.2 Percent elongation at fracture may be calculated directly from elongation at fracture data and be reported instead of percent elongation as calculated in 7.11.2 to 7.11.3. However, these two parameters are not interchangeable. Use of the elongation at fracture method generally provides more repeatable results.

NOTE 44—When disagreements arise over the percent elongation results, agreement must be reached on which method to use to obtain the results.

7.12 *Reduction of Area:*

7.12.1 The reduced area used to calculate reduction of area (see 7.11.2 and 7.11.3) shall be the minimum cross section at the location of fracture.

7.12.2 *Specimens with Originally Circular Cross Sections*—Fit the ends of the fractured specimen together and measure the reduced diameter to the same accuracy as the original measurement.

NOTE 45—Because of anisotropy, circular cross sections often do not remain circular during straining in tension. The shape is usually elliptical, thus, the area may be calculated by $\pi \cdot d_1 \cdot d_2/4$, where d_1 and d_2 are the major and minor diameters, respectively.

7.12.3 *Specimens with Original Rectangular Cross Sections*—Fit the ends of the fractured specimen together and measure the thickness and width at the minimum cross section to the same accuracy as the original measurements.

NOTE 46—Because of the constraint to deformation that occurs at the corners of rectangular specimens, the dimensions at the center of the original flat surfaces are less than those at the corners. The shapes of these surfaces are often assumed to be parabolic. When this assumption is made, an effective thickness, t_e, may be calculated as follows: $(t_1 + 4t_2 + t_3)/6$, where t_1 and t_3 are the thicknesses at the corners, and t_2 is the thickness at mid-width. An effective width may be similarly calculated.

7.12.4 Calculate the reduced area based upon the dimensions determined in 7.12.2 or 7.12.3. The difference between the area thus found and the area of the original cross section expressed as a percentage of the original area is the reduction of area.

7.12.5 If any part of the fracture takes place outside the middle half of the reduced section or in a punched or scribed gauge mark within the reduced section, the reduction of area value obtained may not be representative of the material. In acceptance testing, if the reduction of area so calculated meets the minimum requirements specified, no further testing is required, but if the reduction of area is less than the minimum requirements, discard the test results and retest.

7.12.6 Results of measurements of reduction of area shall be rounded using the procedures of Practice E29 and any specific procedures in the product specifications. In the absence of a specified procedure, it is recommended that reduction of area test values in the range from 0 to 10 % be rounded to the nearest 0.5 % and test values of 10 % and greater to the nearest 1 %.

7.13 *Rounding Reported Test Data for Yield Strength and Tensile Strength*—Test data should be rounded using the procedures of Practice E29 and the specific procedures in the product specifications. In the absence of a specified procedure for rounding the test data, one of the procedures described in the following paragraphs is recommended.

7.13.1 For test values up to 500 MPa [50 000 psi], round to the nearest 1 MPa [100 psi]; for test values of 500 MPa [50 000 psi] and up to 1000 MPa [100 000 psi], round to the nearest 5 MPa [500 psi]; for test values of 1000 MPa [100 000 psi] and greater, round to the nearest 10 MPa [1000 psi].

NOTE 47—For steel products, see Test Methods and Definitions A370.

7.13.2 For all test values, round to the nearest 1 MPa [100 psi].

NOTE 48—For aluminum- and magnesium-alloy products, see Methods B557.

7.13.3 For all test values, round to the nearest 5 MPa [500 psi].

7.14 *Replacement of Specimens*—A test specimen may be discarded and a replacement specimen selected from the same lot of material in the following cases:

7.14.1 The original specimen had a poorly machined surface,

7.14.2 The original specimen had the wrong dimensions,

7.14.3 The specimen's properties were changed because of poor machining practice,

7.14.4 The test procedure was incorrect,

7.14.5 The fracture was outside the gauge length,

7.14.6 For elongation determinations, the fracture was outside the middle half of the gauge length, or

7.14.7 There was a malfunction of the testing equipment.

NOTE 49—The tension specimen is inappropriate for assessing some types of imperfections in a material. Other methods and specimens employing ultrasonics, dye penetrants, radiography, etc., may be considered when flaws such as cracks, flakes, porosity, etc., are revealed during a test and soundness is a condition of acceptance.

8. Report

8.1 Test information on materials not covered by a product specification should be reported in accordance with 8.2 or both 8.2 and 8.3.

8.2 Test information to be reported shall include the following when applicable:

8.2.1 Reference to the standard used, i.e. E8 or E8M.

8.2.2 Material and sample identification.

8.2.3 Specimen type (see Section 6).

8.2.4 Yield strength and the method used to determine yield strength (see 7.7).

8.2.5 Yield point elongation (see 7.8).

8.2.6 Tensile Strength (also known as Ultimate Tensile Strength) (see 7.10).

8.2.7 Elongation (report original gauge length, percentage increase, and method used to determine elongation; i.e. at fracture or after fracture) (see 7.11).

8.2.8 Uniform Elongation, if required (see 7.9).

8.2.9 Reduction of area, if required (see 7.12).

8.3 Test information to be available on request shall include:

8.3.1 Specimen test section dimension(s).

8.3.2 Equation used to calculate cross-sectional area of rectangular specimens taken from large-diameter tubular products.

8.3.3 Speed and method used to determine speed of testing (see 7.6).

8.3.4 Method used for rounding of test results (see 7.13).

8.3.5 Reasons for replacement specimens (see 7.14).

9. Precision and Bias

9.1 *Precision*—An interlaboratory test program[3] gave the following values for coefficients of variation for the most commonly measured tensile properties:

Coefficient of Variation, %

	Tensile Strength	Yield Strength Offset = 0.02 %	Yield Strength Offset = 0.2 %	Elongation Gauge Length = 4 Diameter	Reduction of Area
CV $\%_r$	0.9	2.7	1.4	2.8	2.8
CV $\%_R$	1.3	4.5	2.3	5.4	4.6

CV $\%_r$ = repeatability coefficient of variation in percent within a laboratory
CV $\%_R$ = repeatability coefficient of variation in percent between laboratories

9.1.1 The values shown are the averages from tests on six frequently tested metals, selected to include most of the normal range for each property listed above. When these materials are compared, a large difference in coefficient of variation is found. Therefore, the values above should not be used to judge whether the difference between duplicate tests of a specific material is larger than expected. The values are provided to allow potential users of this test method to assess, in general terms, its usefulness for a proposed application.

9.2 *Bias*—The procedures in Test Methods E8/E8M for measuring tensile properties have no bias because these properties can be defined only in terms of a test method.

10. Keywords

10.1 accuracy; bending stress; discontinuous yielding; drop-of-the-beam; eccentric force application; elastic extension; elongation; extension-under-load; extensometer; force; free-running crosshead speed; gauge length; halt-of-the force; percent elongation; plastic extension; preload; rate of stressing; rate of straining; reduced section; reduction of area; sensitivity; strain; stress; taring; tensile strength; tension testing; yield point elongation; yield strength

[3] Supporting data can be found in Appendix X1 and additional data are available from ASTM Headquarters. Request RR:E28-1004.

APPENDIXES

(Nonmandatory Information)

X1. FACTORS AFFECTING TENSION TEST RESULTS

X1.1 The precision and bias of tension test strength and ductility measurements depend on strict adherence to the stated test procedure and are influenced by instrumental and material factors, specimen preparation, and measurement/testing errors.

X1.2 The consistency of agreement for repeated tests of the same material is dependent on the homogeneity of the material, and the repeatability of specimen preparation, test conditions, and measurements of the tension test parameters.

X1.3 Instrumental factors that can affect test results include: the stiffness, damping capacity, natural frequency, and mass of moving parts of the tensile test machine; accuracy of force indication and use of forces within the verified range of the machine; rate of force application, alignment of the test specimen with the applied force, parallelness of the grips, grip pressure, nature of the force control used, appropriateness and calibration of extensometers, heat dissipation (by grips, extensometers, or ancillary devices), and so forth.

X1.4 Material factors that can affect test results include: representativeness and homogeneity of the test material, sampling scheme, and specimen preparation (surface finish, dimensional accuracy, fillets at the ends of the gauge length, taper in the gauge length, bent specimens, thread quality, and so forth).

X1.4.1 Some materials are very sensitive to the quality of the surface finish of the test specimen (see Note 4) and must be ground to a fine finish, or polished to obtain correct results.

X1.4.2 Test results for specimens with as-cast, as-rolled, as-forged, or other non-machined surface conditions can be affected by the nature of the surface (see Note 10).

X1.4.3 Test specimens taken from appendages to the part or component, such as prolongs or risers, or from separately produced castings (for example, keel blocks) may produce test results that are not representative of the part or component.

X1.4.4 Test specimen dimensions can influence test results. For cylindrical or rectangular specimens, changing the test specimen size generally has a negligible effect on the yield and tensile strength but may influence the upper yield strength, if one is present, and elongation and reduction of area values. Comparison of elongation values determined using different specimens requires that the following ratio be controlled:

$$L_o/(A_o)^{1/2} \qquad \text{(X1.1)}$$

where:

L_o = original gauge length of specimen, and
A_o = original cross-sectional area of specimen.

X1.4.4.1 Specimens with smaller $L_o/(A_o)^{1/2}$ ratios generally give greater elongation and reduction in area values. This is the case for example, when the width or thickness of a rectangular tensile test specimen is increased.

X1.4.4.2 Holding the $L_o/(A_o)^{1/2}$ ratio constant minimizes, but does not necessarily eliminate, differences. Depending on material and test conditions, increasing the size of the proportional specimen of Fig. 8 may be found to increase or decrease elongation and reduction in area values somewhat.

X1.4.5 Use of a taper in the gauge length, up to the allowed 1 % limit, can result in lower elongation values. Reductions of as much as 15 % have been reported for a 1 % taper.

X1.4.6 Changes in the strain rate can affect the yield strength, tensile strength, and elongation values, especially for materials which are highly strain rate sensitive. In general, the yield strength and tensile strength will increase with increasing strain rate, although the effect on tensile strength is generally less pronounced. Elongation values generally decrease as the strain rate increases.

X1.4.7 Brittle materials require careful specimen preparation, high quality surface finishes, large fillets at the ends of the gauge length, oversize threaded grip sections, and cannot tolerate punch or scribe marks as gauge length indicators.

X1.4.8 Flattening of tubular products to permit testing does alter the material properties, generally nonuniformly, in the flattened region which may affect test results.

X1.5 Measurement errors that can affect test results include: verification of the test force, extensometers, micrometers, dividers, and other measurement devices, alignment and zeroing of chart recording devices, and so forth.

X1.5.1 Measurement of the dimensions of as-cast, as-rolled, as-forged, and other test specimens with non-machined surfaces may be imprecise due to the irregularity of the surface flatness.

X1.5.2 Materials with anisotropic flow characteristics may exhibit non-circular cross sections after fracture and measurement precision may be affected, as a result (see Note 41).

X1.5.3 The corners of rectangular test specimens are subject to constraint during deformation and the originally flat surfaces may be parabolic in shape after testing which will affect the precision of final cross-sectional area measurements (see Note 46).

X1.5.4 If any portion of the fracture occurs outside of the middle of the gauge length, or in a punch or scribe mark within the gauge length, the elongation and reduction of area values may not be representative of the material. Wire specimens that break at or within the grips may not produce test results representative of the material.

X1.5.5 Use of specimens with shouldered ends (“button-head” tensiles) will produce lower 0.02 % offset yield strength values than threaded specimens.

X1.6 Because standard reference materials with certified tensile property values are not available, it is not possible to rigorously define the bias of tension tests. However, by the use of carefully designed and controlled interlaboratory studies, a reasonable definition of the precision of tension test results can be obtained.

X1.6.1 An interlaboratory test program[3] was conducted in which six specimens each, of six different materials were prepared and tested by each of six different laboratories. Tables X1.1-X1.6 present the precision statistics, as defined in Practice E691, for: tensile strength, 0.02 % yield strength, 0.2 % yield strength, % elongation in 4D, % elongation in 5D, and % reduction in area. In each table, the first column lists the six materials tested, the second column lists the average of the average results obtained by the laboratories, the third and fifth columns list the repeatability and reproducibility standard deviations, the fourth and sixth columns list the coefficients of variation for these standard deviations, and the seventh and eighth columns list the 95 % repeatability and reproducibility limits.

X1.6.2 The averages (below columns four and six in each table) of the coefficients of variation permit a relative comparison of the repeatability (within-laboratory precision) and reproducibility (between-laboratory precision) of the tension test parameters. This shows that the ductility measurements exhibit less repeatability and reproducibility than the strength measurements. The overall ranking from the least to the most repeatable and reproducible is: % elongation in 4*D*, % elongation in 5*D*, % reduction in area, 0.02 % offset yield strength, 0.2 % offset yield strength, and tensile strength. Note that the rankings are in the same order for the repeatability and reproducibility average coefficients of variation and that the

reproducibility (between-laboratory precision) is poorer than the repeatability (within-laboratory precision) as would be expected.

X1.6.3 No comments about bias can be made for the interlaboratory study due to the lack of certified test results for these specimens. However, examination of the test results showed that one laboratory consistently exhibited higher than average strength values and lower than average ductility values for most of the specimens. One other laboratory had consistently lower than average tensile strength results for all specimens.

TABLE X1.1 Precision Statistics—Tensile Strength, MPa [ksi]

NOTE 1—X is the average of the cell averages, that is, the grand mean for the test parameter,
s_r is the repeatability standard deviation (within-laboratory precision) in MPa [ksi],
s_r/X is the coefficient of variation in %,
s_R is the reproducibility standard deviation (between-laboratory precision) in MPa [ksi],
s_R/X is the coefficient of variation, %,
r is the 95 % repeatability limits in MPa [ksi],
R is the 95 % reproducibility limits in MPa [ksi].

Material	X	s_r	s_r/X, %	s_R	s_R/X, %	r	R
EC-H19	176.9 [25.66]	4.3 [0.63]	2.45	4.3 [0.63]	2.45	12.1 [1.76]	12.1 [1.76]
2024-T351	491.3 [71.26]	6.1 [0.88]	1.24	6.6 [0.96]	1.34	17.0 [2.47]	18.5 [2.68]
ASTM A105	596.9 [86.57]	4.1 [0.60]	0.69	8.7 [1.27]	1.47	11.6 [1.68]	24.5 [3.55]
AISI 316	694.6 [100.75]	2.7 [0.39]	0.39	8.4 [1.22]	1.21	7.5 [1.09]	23.4 [3.39]
Inconel 600	685.9 [99.48]	2.9 [0.42]	0.43	5.0 [0.72]	0.72	8.2 [1.19]	13.9 [2.02]
SAE 51410	1253.0 [181.73]	0.25 [0.46]	0.25	7.9 [1.14]	0.63	8.9 [1.29]	22.1 [3.20]
		Averages:	0.91		1.30		

TABLE X1.2 Precision Statistics—0.02 % Yield Strength, MPa [ksi]

Material	X	s_r	s_r/X, %	s_R	s_R/X, %	r	R
EC-H19	111.4 [16.16]	4.5 [0.65]	4.00	8.2 [1.19]	7.37	12.5 [1.81]	23.0 [3.33]
2024-T351	354.2 [51.38]	5.8 [0.84]	1.64	6.1 [0.89]	1.73	16.3 [2.36]	17.2 [2.49]
ASTM A105	411.1 [59.66]	8.3 [1.20]	2.02	13.1 [1.90]	3.18	23.2 [3.37]	36.6 [5.31]
AISI 316	336.1 [48.75]	16.7 [2.42]	4.97	31.9 [4.63]	9.49	46.1 [6.68]	89.0 [12.91]
Inconel 600	267.1 [38.74]	3.2 [0.46]	1.18	5.2 [0.76]	1.96	8.8 [1.28]	14.7 [2.13]
SAE 51410	723.2 [104.90]	16.6 [2.40]	2.29	21.9 [3.17]	3.02	46.4 [6.73]	61.2 [8.88]
		Averages:	2.68		4.46		

TABLE X1.3 Precision Statistics—0.2 % Yield Strength, MPa [ksi]

Material	X	s_r	s_r/X, %	s_R	s_R/X, %	r	R
EC-H19	158.4 [22.98]	3.3 [0.47]	2.06	3.3 [0.48]	2.07	9.2 [1.33]	9.2 [1.33]
2024-T351	362.9 [52.64]	5.1 [0.74]	1.41	5.4 [0.79]	1.49	14.3 [2.08]	15.2 [2.20]
ASTM A105	402.4 [58.36]	5.7 [0.83]	1.42	9.9 [1.44]	2.47	15.9 [2.31]	27.8 [4.03]
AISI 316	481.1 [69.78]	6.6 [0.95]	1.36	19.5 [2.83]	4.06	18.1 [2.63]	54.7 [7.93]
Inconel 600	268.3 [38.91]	2.5 [0.36]	0.93	5.8 [0.85]	2.17	7.0 [1.01]	16.3 [2.37]
SAE 51410	967.5 [140.33]	8.9 [1.29]	0.92	15.9 [2.30]	1.64	24.8 [3.60]	44.5 [6.45]
		Averages:	1.35		2.32		

TABLE X1.4 Precision Statistics—% Elongation in 4D for E8 Specimens

NOTE 1—Length of reduced section = 6D.

Material	X	s_r	s_r/X, %	s_R	s_R/X, %	r	R
EC-H19	17.42	0.64	3.69	0.92	5.30	1.80	2.59
2024-T351	19.76	0.58	2.94	1.58	7.99	1.65	4.43
ASTM A105	29.10	0.76	2.62	0.98	3.38	2.13	2.76
AISI 316	40.07	1.10	2.75	2.14	5.35	3.09	6.00
Inconel 600	44.28	0.66	1.50	1.54	3.48	1.86	4.31
SAE 51410	14.48	0.48	3.29	0.99	6.83	1.34	2.77
		Averages:	2.80		5.39		

TABLE X1.5 Precision Statistics—% Elongation in 5D for E8M Specimens

NOTE 1—Length of reduced section = 6D.

Material	X	s_r	s_r/X, %	s_R	s_R/X, %	r	R
EC-H19	14.60	0.59	4.07	0.66	4.54	1.65	1.85
2024-T351	17.99	0.63	3.48	1.71	9.51	1.81	4.81
ASTM A105	25.63	0.77	2.99	1.30	5.06	2.15	3.63
AISI 316	35.93	0.71	1.98	2.68	7.45	2.00	7.49
Inconel 600	41.58	0.67	1.61	1.60	3.86	1.88	4.49
SAE 51410	13.39	0.45	3.61	0.96	7.75	1.25	2.89
		Averages:	2.96		6.36		

X2. MEASUREMENT OF SPECIMEN DIMENSIONS

TABLE X1.6 Precision Statistics—% Reduction in Area

Material	X	s_r	s_r/X, %	s_R	s_R/X, %	r	R
EC-H19	79.15	1.93	2.43	2.01	2.54	5.44	5.67
2024-T351	30.41	2.09	6.87	3.59	11.79	5.79	10.01
ASTM A105	65.59	0.84	1.28	1.26	1.92	2.35	3.53
AISI 316	71.49	0.99	1.39	1.60	2.25	2.78	4.50
Inconel 600	59.34	0.67	1.14	0.70	1.18	1.89	1.97
SAE 51410	50.49	1.86	3.69	3.95	7.81	5.21	11.05
		Averages:	2.80		4.58		

X2.1 Measurement of specimen dimensions is critical in tension testing, and it becomes more critical with decreasing specimen size, as a given absolute error becomes a larger relative (percent) error. Measuring devices and procedures should be selected carefully, so as to minimize measurement error and provide good repeatability and reproducibility.

X2.2 Relative measurement error should be kept at or below 1 %, where possible. Ideally, this 1 % error should include not only the resolution of the measuring device but also the variability commonly referred to as repeatability and reproducibility. (Repeatability is the ability of any operator to obtain similar measurements in repeated trials. Reproducibility is the ability of multiple operators to obtain similar measurements.)

X2.3 Formal evaluation of gage repeatability and reproducibility (GR and R) by way of a GR and R study is highly recommended. A GR and R study involves having multiple operators each take two or three measurements of a number of parts—in this case, test specimens. Analysis, usually done by computer, involves comparing the observed measurement variations to a tolerance the procedure is to determine conformance to. High GR and R percentages (more than 20 %) indicate much variability relative to the tolerance, whereas low percentages (10 % or lower) indicate the opposite. The analysis also estimates, independently, the repeatability and reproducibility.

X2.4 GR and R studies in which nontechnical personnel used different brands and models of hand-held micrometers have given results varying from about 10 % (excellent) to nearly 100 % (essentially useless), relative to a dimensional tolerance of 0.075 mm [0.003 in.]. The user is therefore advised to be very careful in selecting devices, setting up measurement procedures, and training personnel.

X2.5 With a 0.075 mm [0.003 in.] tolerance, a 10 % GR and R result (exceptionally good, even for digital hand-held micrometers reading to 0.001 mm [0.00005 in.]) indicates that the total variation due to repeatability and reproducibility is around 0.0075 [0.0003 in.]. This is less than or equal to 1 % only if all dimensions to be measured are greater than or equal to 0.75 mm [0.03 in.]. The relative error in using this device to measure thickness of a 0.25 mm [0.01 in.] flat tensile specimen would be 3 %—which is considerably more than that allowed for force or strain measurement.

X2.6 Dimensional measurement errors can be identified as the cause of many *out-of-control* signals, as indicated by statistical process control (SPC) charts used to monitor tension testing procedures. This has been the experience of a production laboratory employing SPC methodology and the best hand-held micrometers available (from a GR and R standpoint) in testing of 0.45 to 6.35 mm [0.018 to 0.25 in.] flat rolled steel products.

X2.7 Factors which affect GR and R, sometimes dramatically, and which should be considered in the selection and evaluation of hardware and procedures include:

X2.7.1 Resolution,

X2.7.2 Verification,

X2.7.3 Zeroing,

X2.7.4 Type of anvil (flat, rounded, or pointed),

X2.7.5 Cleanliness of part and anvil surfaces,

X2.7.6 User-friendliness of measuring device,

X2.7.7 Stability/temperature variations,

X2.7.8 Coating removal,

X2.7.9 Operator technique, and

X2.7.10 Ratchets or other features used to regulate the clamping force.

X2.8 Flat anvils are generally preferred for measuring the dimensions of round or flat specimens which have relatively smooth surfaces. One exception is that rounded or pointed anvils must be used in measuring the thickness of curved specimens taken from large-diameter tubing (see Fig. 13), to prevent overstating the thickness. (Another concern for these curved specimens is the error that can be introduced through use of the equation $A = W \times T$; see 7.2.3.)

X2.9 Heavy coatings should generally be removed from at least one grip end of flat specimens taken from coated products to permit accurate measurement of base metal thickness, assuming *(a)* the base metal properties are what are desired, *(b)* the coating does not contribute significantly to the strength of the product, and *(c)* coating removal can be easily accomplished (some coatings may be easily removed by chemical stripping). Otherwise, it may be advisable to leave the coating intact and determine the base metal thickness by an alternate method. Where this issue may arise, all parties involved in comparison or conformance testing should agree as to whether or not coatings are to be removed before measurement.

X2.10 As an example of how the considerations identified above affect dimensional measurement procedures, consider the case of measuring the thickness of 0.40 mm [0.015 in.) painted, flat rolled steel specimens. The paint should be removed prior to measurement, if possible. The measurement device used should have flat anvils, must read to 0.0025 mm [0.0001 in.] or better, and must have excellent repeatability and reproducibility. Since GR and R is a significant concern, it will be best to use a device which has a feature for regulating the clamping force used, and devices without digital displays should be avoided to prevent reading errors. Before use of the device, and periodically during use, the anvils should be cleaned, and the device should be verified or zeroed (if an electronic display is used) or both. Finally, personnel should be trained and audited periodically to ensure that the measuring device is being used correctly and consistently by all.

X3. SUGGESTED ACCREDITATION CRITERIA FOR LABORATORIES PERFORMING TENSILE TESTS

X3.1 Scope

X3.1.1 The following are specific features that an assessor may check to assess a laboratory's technical competence, if the laboratory is performing tests in accordance with Test Methods E8/E8M.

X3.2 Preparation

X3.2.1 The laboratory should follow documented procedures to ensure that machining or other preparation generates specimens conforming to applicable tolerances and requirements of Test Methods E8/E8M. Particularly important are those requirements that pertain to the dimensions and finish of reduced sections, as found in the text and in applicable figures.

X3.2.2 Where gauge marks are used, the laboratory should employ documented gauge marking procedures to ensure that the marks and gauge lengths comply with the tolerances and guidelines of Test Methods E8/E8M.

X3.2.2.1 The gauge marking procedure used should not deleteriously affect the test results.

NOTE X3.1—Frequent occurrence of fracturing at the gauge marks may indicate that gage marks have excessive depth or sharpness and may be affecting test results.

X3.3 Test Equipment

X3.3.1 As specified in the Apparatus sections of Test Methods E8/E8M, the axis of the test specimen should coincide with the center line of the heads of the testing machine, in order to minimize bending stresses which could affect the results.

X3.3.2 Equipment verification requirements of Practices E4 and E83 shall be met. Documentation showing the verification work to have been thorough and technically correct should be available.

X3.3.2.1 Verification reports shall demonstrate that force and extension readings have been taken at the prescribed intervals and that the prescribed runs have been completed.

X3.3.3 Extensometers used shall meet all requirements of Test Methods E8/E8M as to the classification of device to be used for the results determined. For example, an extensometer not meeting the Class B2 requirements of Practice E83 may not be used in determination of offset yield strengths.

X3.3.4 Before computerized or automated test equipment is put into routine service, or following a software revision, it is recommended that measures be taken to verify proper operation and result interpretation. Guide E1856 addresses this concern.

X3.3.5 Micrometers and other devices used in measurement of specimen dimensions should be selected, maintained and used in such a manner as to comply with the appendixes of Test Methods E8/E8M on measurement. Traceability to national standards should be established for these devices, and reasonable effort should be employed to prevent errors greater than 1 % from being generated as a result of measurement error, resolution, and rounding practice.

X3.4 Procedures

X3.4.1 The test machine shall be set up and zeroed in such a manner that zero force indication signifies a state of zero force on the specimen, as indicated in the Zeroing of the Test Machine sections of Test Methods E8/E8M.

NOTE X3.2—Provisions should be made to ensure that zero readings are properly maintained, from test to test. These may include, for example, zeroing after a predetermined number of tests or each time, under zero force conditions, the indicator exceeds a predetermined value.

X3.4.2 Upon request, the laboratory should be capable of demonstrating (perhaps through time, force, displacement or extensometer measurements, or both) that the test speeds used conform to the requirements of Test Methods E8/E8M, or other standards which take precedence.

X3.4.3 Upon request, the laboratory should be capable of demonstrating that the offsets and extensions used in determining yield strengths conform to the requirements of Test Methods E8/E8M and are constructed so as to indicate the forces corresponding to the desired offset strain or total strain.

NOTE X3.3—Use caution when performing calculations with extensometer magnification, because the manufacturer may report strain magnification, which relates the strain (not the elongation) to the x-axis displacement on the stress strain diagram. A user or assessor interested in an extensometer's magnification may use calibration equipment to determine the ratio between elongation and chart travel or may verify a reported magnification by calculating the Young's modulus from tests of specimens of a known nominal modulus.

X3.4.4 Measurement of elongation shall conform to requirements of Test Methods E8/E8M.

NOTE X3.4—Test Methods E8/E8M permit the measurement and reporting of elongation at fracture in place of elongation, as is often done in automated testing.

X3.4.5 Reduction of area, when required, shall be determined in accordance with the requirements of Test Methods E8/E8M.

X3.4.6 Procedures for recording, calculating, and reporting data and test results shall conform to all applicable requirements of Test Methods E8/E8M. In addition, wherever practical, the procedures should also be in accordance with widely accepted provisions of good laboratory practice, such as those detailed below.

X3.4.6.1 When recording data, personnel should record all figures that are definite, plus the best estimate of the first figure which is uncertain. (If a result is known to be approximately midway between 26 and 27, 26.5 should be the result recorded (not 26, 27, or 26.475).

X3.4.6.2 When performing calculations, personnel should avoid compounding of rounding errors. This may be accomplished by performing one large calculation, rather than several calculations using individual results. Alternatively, if multistep calculations are done, intermediate results should not be rounded before use in subsequent calculations.

X3.4.6.3 In rounding, no final result should retain more significant figures than the least-significant-figure measurement or data point used in the calculation.

X3.5 Retention

X3.5.1 A retention program appropriate for the nature and frequency of testing done in the laboratory should be maintained. Items that may warrant retention for defined time periods include:

X3.5.1.1 Raw data and forms,

X3.5.1.2 Force-elongation or stress-strain charts,

X3.5.1.3 Computer printouts of curves and test results,

X3.5.1.4 Data and results stored on computer discs or hard drives,

X3.5.1.5 Broken specimens,

X3.5.1.6 Excess material,

X3.5.1.7 Test reports, and

X3.5.1.8 Verification reports and certifications.

X3.6 Environment

X3.6.1 All test equipment should be located and connected to power sources in such a manner as to minimize the effects of vibrations and electrical disturbances on raw data collected, stress-strain charts, and operation of equipment.

X3.7 Controls

X3.7.1 Controlled procedures and work instructions should cover all aspects of specimen preparation, tensile testing, and result reporting. These documents should be readily available to all involved in the documented tasks.

X3.7.2 Clear, concise, operating instructions should be maintained for equipment used in specimen preparation and tensile testing. These instructions should be readily available to all qualified operators.

X3.7.3 All applicable verification requirements shall be met, as detailed in X3.3.2.

X3.7.4 It is recommended that special studies and programs be employed to monitor and control tensile testing, because tensile test results are easily affected by operators, measuring devices, and test equipment. Examples of such programs include but are not limited to:

X3.7.4.1 Round-robin studies, proficiency tests, or other cross-checks,

X3.7.4.2 Repeatability and reproducibility (R and R) studies,

X3.7.4.3 Control charting, and

X3.7.4.4 Determination of typical lab uncertainties for each result typically reported.

NOTE X3.5—For nondestructive testing, repeatability and reproducibility are often measured by conducting gage R and R studies, as discussed in Appendix X2 of Test Methods E8/E8M. These studies involve repeated determination of a test result, using a single part or specimen, so gage R and Rs are not directly applicable to mechanical properties, which are obtained through destructive testing. (True differences between even the best duplicate specimens manifest themselves in the form of poorer R and R results than would be obtained for perfect duplicates.) Nevertheless, quasi-R and R studies conducted with these limitations taken into consideration may be helpful in analyzing sources of error and improving reliability of test results.

X4. ADDITIONAL INFORMATION ON SPEED OF TESTING AND EXAMPLES

X4.1 Many materials are strain-rate sensitive that is, the yield strength or tensile strength of the material is a function of the rate at which the material is being deformed. The yield strength of some materials can change by more than ten percent when tested with the slowest and then the highest speeds permitted by Test Methods E8/E8M. In order to reproduce yield test results, for strain-rate sensitive materials, it is important that strain rates during the determination of yield are similar.

X4.2 The following paragraphs further explain the various Control Methods required to be used by Test Methods E8/E8M when other guidance is not given. When other test speed requirements are specified, those speeds must be followed to comply with this test method. For example, aerospace specifications often require a test speed when determining yield strength to be a strain rate equal to 0.005 ± 0.002 mm/mm/min [in./in./min]; when specified, that speed must be followed in order to comply with this standard.

X4.2.1 *Control Method A - Rate of Stressing Method for Determining Yield Properties* – This method has been the default method of control in Test Methods E8/E8M for many years. In this method, the crosshead speed of the machine is adjusted during the linear elastic portion of the curve to achieve the desired stress rate (or the speed is set to a predetermined value known to achieve the desired stress rate). The crosshead speed is not adjusted when the material begins to yield. The advantage of this control method is that it does not require any transducers other than the load indicator itself, although, load pacers and stress-rate indicators can be helpful. This method of control has a limitation in that the strain rate of the specimen at yield depends on the slope of the stress-strain curve (tangent modulus) and the testing machine stiffness. Because of this, the strain rate of the specimen when yield is determined can be different for different specimen sizes, different specimen configurations, different gripping configurations, and different testing machines. This difference in strain rate can affect the reproducibility of yield strength in strain-rate-sensitive materials.

X4.2.1.1 It is not the intent of this method to run the testing machine in closed-loop force control, because as the material begins to yield the testing machine will speed up, possibly to its maximum speed. However, using closed-loop force control during the elastic region of the test and switching to an equivalent crosshead speed prior to yield is an acceptable method.

X4.2.2 *Control Method B —Rate of Straining Control Method for Determining Yield Properties* - This method is usually performed with a testing machine that has a closed-loop control system that uses feedback from an extensometer to automatically adjust the speed of the testing machine. However, some skilled operators can monitor a strain rate indicator attached to the extensometer and adjust the speed of the testing machine manually to maintain the required strain rate test speed. To maintain constant strain rate control during a test, the crosshead speed of the testing machine must slow down drastically when the specimen begins to yield. This method has three advantages. *(1)* The time to achieve yield results is short (about 20 to 40 s). *(2)* The reproducibility of yield strength test results from machine to machine and laboratory to laboratory is good. *(3)* The agreement with the results of Control Method C is good, because the strain rates are similar when the specimen's yield strength is determined. This method has three disadvantages. *(1)* The testing equipment is generally more expensive. *(2)* Proper control and safety depend on the control parameters to be properly set and that the extensometer integrity be maintained (accidental slippage of the extensometer can result in unexpected movement of the crosshead). Proper safety limits must be set to ensure safety of personnel and equipment. *(3)* When materials have yield points or yield discontinuously, a machine under closed-loop strain-rate control can behave erratically. This control method is not recommended for materials that yield discontinuously.

X4.2.3 *Control Method C - Crosshead Speed Control Method for Determining Yield Properties*—This method can be performed on any testing machine that has reasonably good crosshead speed control. This method has three advantages. *(1)* The reproducibility from machine to machine and laboratory to laboratory is good. *(2)* The agreement with Control Method B is good, because the strain rates are similar when the specimen's yield strength is determined. *(3)* This method of controlling a testing machine is excellent for materials that yield discontinuously. The disadvantage of this method of control is that the test time to yield can be more than three minutes, depending on the material being tested and the compliance of the testing machine including its grip assemblies.

X4.2.3.1 *An example using SI metric units of how to apply Control Method C* to testing Specimen 1 in Fig. 13 is as follows. The length of the reduced section, that is, dimension *A* in Fig. 13, is equal to 60 mm. The crosshead speed is determined per Control Method C by multiplying 60 mm by 0.015 mm/mm/min to arrive at a crosshead speed of 0.9 mm/min.

X4.2.3.2 *An example using U.S. customary units of how to apply Control Method C* to testing Specimen 1 in Fig. 13 is as follows. The length of the reduced section, that is, dimension *A* in Fig. 13 is equal to 2.25 in. The crosshead speed is determined per Control Method C by multiplying 2.25 in. by 0.015 in./in./min to arrive at a crosshead speed of 0.034 in./min.

SUMMARY OF CHANGES

Committee E28 has identified the location of selected changes to this standard since the last issue (E8/E8M-13) that may impact the use of this standard. (Approved July 1, 2013.)

(1) 3.1.4 was revised.

(2) 3.1.5 was added.

Committee E28 has identified the location of selected changes to this standard since the last issue (E8/E8M-11) that may impact the use of this standard. (Approved June. 1, 2013.)

(1) Replaced 3.1.
(2) Added 3.1.2.
(3) Reformatted 3.1.3.
(4) Reformatted 3.1.4.
(5) Added 3.1.7, 3.1.8, and 3.1.12.
(6) Reformatted 3.1.11.
(7) Added 3.2.1.
(8) Added Note 32.

Cover Page

Standard: BAC5602 Rev: (AH) 16-Nov-2020

WARNING - The Export Control or Intellectual Property language on this page takes precedence over any such language that may appear on subsequent pages of this document.

EXPORT CONTROLLED - This technology or software is subject to the U.S. Export Administration Regulations (EAR), (15 C.F.R. Parts 730-774). No authorization from the U.S. Department of Commerce is required for export, re-export, in-country transfer, or access EXCEPT to country group E:1 or E:2 countries/persons per Supp.1 to Part 740 of the EAR. ECCN EAR99

Boeing Proprietary, Distribution limited to Boeing employees and others covered by applicable proprietary information or nondisclosure agreements.

Product Standards requirements are binding for all Boeing and non-Boeing production facilities and must be implemented in accordance with the following: Part Standards: D-590-PREFACE, Material Specifications: BMS0-PREF, Process Specifications: BAC001PREF, and Support Standards: BSS001PREF.

1 SCOPE

NOTE: Incorporated Departures: None
Cancelled Departures: None

a. This specification establishes the requirements for heat treatment of aluminum alloys. Annealing, solution treatment, precipitation treatment and stress relief requirements are included.

b. This specification is applicable whenever referenced by Boeing Engineering Drawings or specifications with the following exceptions:

(1) When heat treating mill products (forgings, rough machined forgings, sheet, extrusions, plate, et cetera) for conformance to wrought material specifications, producers or their independent heat treaters may use AMS2772 except acceptance criteria must be in accordance with the referencing specification. When specific requirements are not provided by the referencing specification (drawing, process specification, et cetera), acceptance criteria must be in accordance with BAC5602. Mill products furnished to a user, which are subsequently returned to the mill for heat treatment, must be processed in accordance with to BAC5602.

(2) Heat treatment of castings may be in accordance with AMS2771.

c. Heat treatment of 7175 aluminum forgings to the -T74 (-T736) temper within The Boeing Company must be accomplished in accordance with an internal reference document for Heat Treatment of 7175-T74 (formerly T736) Aluminum Die Forgings. For contractors outside of Boeing, 7175-01 die forgings and hand forgings must be returned to the supplier of those forgings or an independent heat treater authorized by the supplier for heat treatment to the T74 condition.

d. Refer to BAC001PREF for guidance on use of Boeing process specifications and Boeing process specification departures.

WARNING

WARNINGs may be included throughout this specification. Do not take these WARNINGs to be all inclusive, nor to completely describe hazards or precautionary measures applicable to specific procedures or operating environments.

Non-Boeing personnel must refer to their employer's safety instructions for information concerning hazards which may occur during operations described in this specification.

2 CLASSIFICATION

Not applicable to this specification.

3 REFERENCES

The current issue of the following standards must be considered a part of this specification to the extent herein indicated. See Section 5 for material references.

3 REFERENCES (Continued)

AA H35.1/H35.1M	-	American National Standard Alloy and Temper Designation Systems for Aluminum
AMS2750	-	Pyrometry
AMS2771	-	Heat Treatment of Aluminum Alloy Castings
AMS2772	-	Heat Treatment of Aluminum Alloy Raw Materials
ASTM A919	-	Standard Terminology Relating to Heat Treatment of Metals
ASTM B557	-	Standard Test Methods for Tension Testing Wrought and Cast Alluminum-and Magnesium-Alloy Products
ASTM D445	-	Standard Test Method for Kinematic Viscosity of Transparent and Opaque Liquids (and Calculation of Dynamic Viscosity)
ASTM G34	-	Standard Test Method for Exfoliation Corrosion Susceptibility in 2XXX and 7XXX Series Aluminum Alloys (EXCO Test)
BAC5001-12	-	Forming and Straightening of Ducts
BAC5034	-	Temporary Protection of Production Materials, Parts and Assemblies
BAC5300-2	-	Metal Part Forming, Straightening, and Fitting
BAC5408	-	Vapor Degreasing
BAC5621	-	Temperature Control for Processing of Materials
BAC5650	-	Hardness Testing
BAC5651	-	Eddy Current Electrical Conductivity Inspection
BAC5748	-	Abrasive Cleaning, Deburring, and Finishing
BAC5750	-	Solvent Cleaning
BAC5763	-	Emulsion Cleaning and Aqueous Degreasing
BAC5765	-	Cleaning and Deoxidizing Aluminum Alloys
BAC5772	-	Chemical Milling Aluminum Alloys
BAC5941	-	Aluminum Brazing
BAC5946	-	Temper Inspection of Aluminum Alloys
BPS-R-131	-	Rivets, Solid

4 **CONTENTS**

4 **CONTENTS (Continued)**

4 **CONTENTS (Continued)**

4 **CONTENTS (Continued)**

LIST OF FIGURES

LIST OF TABLES

4 **CONTENTS (Continued)**

5 MATERIALS CONTROL

5.1 PROCUREMENT REQUIREMENTS

Use the materials in the following list. The use of alternative materials requires approval from the Boeing Company. Contact Boeing Research and Technology (BR&T) for approval.

a. Salts, Heat Treating, premixed or as individual salts for mixing in accordance with Section 9.1.

(1) Sodium Nitrate Salt

(2) Sodium Nitrite Salt

(3) Potassium Nitrate Salt

(4) AMS2821, Class 2

b. Ammonium Fluoborate (NH_4BF_4) (minimum 95 percent purity)

c. Sodium Fluoborate ($NaBF_4$) (minimum 95 percent purity)

d. AMS3025 Type I Glycol Quenchants, as follows:

(1) Ucon A Quenchant - The Dow Chemical Company

(2) Jo-Quench P-52 - Dynamation Research Inc.

(3) Aqua Quench 260 - Houghton International

(4) Aquatensid D-Hard Castle- Petrofer PVT.LTD

e. AMS3025 Type II Glycol Quenchants, as follows:

(1) Aqua Quench 251 - Houghton International

(2) Aqua Quench 364 - Houghton International

(3) Aquatensid BW/RB - Petrofer Industrial Oils and Chemicals

f. Turco Aquasorb - Henkel

g. Alcohol, Isopropyl or Denatured, Commercial Grade

6 FACILITIES CONTROL

6.1 FURNACES

6.1.1 GENERAL REQUIREMENTS

a. Air furnaces, molten salt baths, oil baths or fluidized beds are permitted for heating aluminum alloys. Superheated steam can be used as a heat source for furnaces used for precipitation heat treatment. The steam must not touch the material.

6.1.1 GENERAL REQUIREMENTS (Continued)

b. Gas-fired furnaces in which the by-products of combustion come in contact with the charge can be used for heat treatment. Alloys that are processed in these furnaces must be tested in accordance with Section 12.4. These alloys must be free from high temperature oxidization.

c. Shield electrical heating elements and radiant tubes in air furnaces to prevent direct radiation from striking parts in the furnace charge.

d. Construct racks and fixtures to be used for solution treatment to prevent quenchant entrapment on racks or parts. If necessary, use drain holes on racks and fixtures.

6.1.2 FACILITIES CERTIFICATION

a. Certification for all furnaces must be in accordance with BAC5621.

b. Table I describes the minimum equipment class and instrumentation types that are necessary for specific heat treating operations in accordance with BAC5621.

TABLE I - MINIMUM EQUIPMENT CLASS AND INSTRUMENTATION TYPE

PROCESS	BAC5621	
	EQUIPMENT CLASS, MINIMUM	INSTRUMENTATION TYPE
All solution heat treating and artificial aging.	II (± 10 F) or (± 6 C)	B
Annealing (full or partial)		
30 F (16 C) temperature range	III (± 15 F) or (± 8 C)	B
50 F (28 C) temperature range or use where no temperature range is identified.	IV (± 25 F) or (± 14 C)	B
Heated units for accelerated "natural" aging below 125 F (52 C).	VI (Maximum Temperature)	I

6.1.3 FURNACE RECOVERY RATE FOR SOLUTION HEAT TREATING AND ANNEALING OF CLAD ALUMINUM MATERIAL

After the load insertion, the furnace recovery time must be in these limits:

a. 30 minutes for part thickness up to 0.10 inch (2.5 mm)

b. 60 minutes for part thickness greater than 0.10 inch (2.5 mm) and above.

6.2 QUENCHING TANKS

a. Quench tanks must have agitation, heating, and cooling of the quench media to meet the requirements of Section 8.2.4. With air agitation, air bubbles must not touch the parts.

b. Each quenching tank must have a temperature indicator or recorder with an instrument accuracy of ± 5 F (± 3 C).

6.2 QUENCHING TANKS (Continued)

c. While water quenching from a salt bath, the quench tank must have a continuous in-flow of clean water. This prevents dissolved salt concentrations and temperatures from rising above the specified limits. After quenching, salt residue on dry part surfaces is not permitted.

d. Clean tanks, as necessary, to remove accumulated debris.

e. Adjustments to glycol quench solutions must be made in accordance with the glycol supplier/manufacturer recommendations. Glycol/water solution concentrations must be in accordance with Section 8.

6.3 RINSE FACILITY

Use fresh water rinse tanks or sprays to remove all visible indications of glycol quenchants or salts. Use agitation, as necessary. It is permitted to use quench tanks to rinse parts if there is no visible glycol or salt residue remaining on the parts.

6.4 COLD STORAGE UNITS

a. Cold storage units for rivets must keep temperatures at -10 F (-23 C) or below.

b. Cold storage units for rivets must have a temperature indicator or recorder with a temperature tolerance of ± 5 F (± 3 C).

c. It is permitted to use portable equipment to transfer rivets to cold storage without temperature recorders or indicators. This portable equipment must keep the rivets at -10 F (-23 C) for the time necessary to complete the transfer. Proof of such capability must be available to Boeing Company representatives.

d. See BAC5300-2 for cold storage of products other than rivets. See BAC5001-12 for cold storage of ducts.

6.5 HEAT TREATING CONTAINERS FOR RIVETS AND OTHER SMALL PARTS

Containers for rivets can also be used for nuts and similar small parts.

a. Use containers for heat treating rivets that permit the center of the charge to get to the minimum of the specified temperature range in 50 minutes from insertion into the furnace.

(1) Rivet containers for air furnaces must be made from wire mesh or fully perforated sheet metal. The design must let the furnace atmosphere circulate through the charge.

(2) 2024 rivets heat treated in salt must be in containers that prevent the rivets from touching the salt. The length of the containers must be so the bath surface is:

(a) 6 inches or more above the top of the rivets and

(b) 6 inches or more below the top of the container.

(3) For rivets other than 2024, it is permitted to use wire mesh baskets for solution heat treatment in a fluidized bed or salt bath.

6.5 HEAT TREATING CONTAINERS FOR RIVETS AND OTHER SMALL PARTS (Continued)

b. Qualify each container design with the tests given in this section. Qualify each container design for each applicable furnace. For salt baths, qualification of a container design in one salt bath will qualify for all other salt baths.

(1) Fill the container with the maximum permitted charge of the smallest diameter rivets for the heat treatment. Put a thermocouple approximately in the center of the charge.

(2) Solution heat treat in accordance with Section 8.2.10. Heating can be stopped when the thermocouple is at the specified temperature range.

(3) Record the heat up time. Heat up time is the actual time from the start of the holding period (Section 8.2.10.1.d.) to the time when the thermocouple is at the minimum of the specified temperature range specified in Table XVI. The container design is satisfactory if the heat up time is less than 50 minutes. See Section 8.2.10.1.d. for application of the heat up time. Post the time at the furnace facility for each qualified container design.

(4) Select a minimum of three rivets from the periphery of the charge. If there was more than one thermocouple monitoring the temperature, examine the rivets from the periphery adjacent to the hottest thermocouple. Do eutectic melting and high temperature oxidation tests in accordance with Section 12.4. Rivets must be free of eutectic melting.

7 DEFINITIONS

The following definitions apply to terms that are uncommon or have special meaning as used in this specification.

Aborted Load - A solution heat treat load for which the soak period is interrupted. For example, the soak temperature falls below the minimum solution treat temperature, or the solution treatment is not in the specified temperature range.

Aging - The process that strengthens alloys, also known as precipitation hardening. It forms a relatively even distribution of microscopic particles (the precipitate) through the material. The material is first prepared by solution treatment (see definition below). Reheating the material (aging) permits formation of the precipitate. The rate at which precipitation occurs is dependent on the alloy and precipitation temperature. It occurs relatively slowly at room temperature (natural aging) and more quickly at elevated temperatures (artificial aging).

Blisters - Raised spots on the surface of the metal caused by expansion of gas in a subsurface zone during thermal treatment.

Charge - See Heat Treat Load.

7 DEFINITIONS (Continued)

Engineering Drawing	-	The collection of product definition data used to disclose, directly or by reference, through pictorial or textual presentations, or combinations of both, the physical and functional end product requirements and configuration of an item. The term may be used regardless of the actual medium or method used for its depiction. A drawing may be computer-aided, manually produced, digitally defined within a dataset and plotted, or digitally defined within a dataset and not plotted.
Eutectic Melting	-	Partial melting of an aluminum alloy caused by heat treating above the normal solution heat treatment temperature.
Full Anneal	-	Thermal treatments to decrease strengths to the lowest levels and give best formability (Condition -O).
Furnace Controller	-	Instruments that control and/or adjust the furnace temperature received from temperature sensor signals.
Furnace Recovery Time	-	The time necessary for the furnace to go back to the minimum of the specified temperature range. Also, the time between insertion of a load and the start of the soaking period.
Hardness Test Scales	-	Designated test scales to get a degree of hardness. HB - Hardness, Brinell, HRB - Hardness, Rockwell B Scale, HRE - Hardness, Rockwell E Scale, HR15T - Hardness, Rockwell scale R15T
Heat Treat Load	-	One or more lots of parts in the furnace during heat treatment.
Heat Treat Lot	-	All parts of the same part number, processed in the same processing equipment (furnace, oven) at the same time.
High Temperature Oxidation	-	Damage to heat treated material caused by contaminants (usually water or sulfur compounds) in the furnace atmosphere or on the parts. Damage is usually in the form of blisters or subsurface voids. Also known as hydrogen induced porosity (HTO).
Interruption	-	The period during which any furnace instrumentation show temperatures below the specified range.
Load	-	See Heat Treat Load.
Load Thermocouple	-	Thermocouples in contact with individual parts or multiple parts in a container in a furnace load to supply temperature data to recording instrumentation. As an alternative, thermocouples imbedded in blocks representative of the thickest section in the load.
Partial Anneal	-	Thermal treatments applied to cold worked material to decrease strength to a controlled level (This is condition -O only if performed on material originally in the -O condition, with or without cold work).

7 **DEFINITIONS (Continued)**

Precipitation Treatment	-	See Aging.
Process Thermocouple	-	Thermocouple installed in processing equipment to supply temperature data to the process control or recording instrumentation specified by the instrumentation Type.
Room Temperature	-	The ambient temperature of the room or area that contains the heat treating equipment.
Small Parts	-	Machined parts, formed sheet, or cut-to-length extrusions that are less than 0.25 inch in nominal thickness and 6 inches or less in length.
Soak Time	-	The minimum length of time that parts or material must be held in heat treating equipment. The time is calculated with the maximum thickness of the part at the specified temperature range (see Section 8.2.1.b.). Also, soaking time, soaking period.
Solution Heat Treating	-	Heating an alloy at the specified temperature for sufficient time to evenly distribute the alloy elements through the material. This condition is a solid solution and is an unstable condition at room temperature because alloying elements tend to precipitate out of the solid solution. The solid solution can be kept if the quench is fast and the metal is then held in a freezer.
Standard Heat Treatment Terminology	-	Refer to ASTM A919
Temper Definitions	-	Refer to AA H35.1/H35.1M
Thickness	-	Unless specified differently, thickness is the minimum dimension of the thickest section at the time of heat treatment.
Uphill Quenching	-	A procedure to cool alloy parts in liquid nitrogen and then reverse quench them in steam.
Work Zone	-	The volume in the heat treating equipment where the process occurs. This excludes ductwork or heating element chambers. According to BAC5621, it is the working volume in the heat treating equipment set by the temperature uniformity survey.

8 MANUFACTURING CONTROL

WARNING

This specification involves the use of chemical substances which are hazardous. Boeing personnel must refer to the work area hazard communication information about health effects and control measures. Additional information is contained in the Globally Harmonized System (GHS) Safety Data Sheets (SDS), or Material Safety Data Sheets (MSDS). For disposition of hazardous waste materials, consult site environmental engineers for proper disposal methods.

Non-Boeing personnel should refer to manufacturer's Globally Harmonized System (GHS) Safety Data Sheets (SDS), or Material Safety Data Sheets (MSDS), and their employer's safety instructions.

8.1 GENERAL REQUIREMENTS

8.1.1 PROCESSING SEQUENCE

Processing sequences must be as follows:

a. Review the work order to identify the alloy for heat treatment.

b. Make sure that the material is clean and dry.

c. Heat at the specified temperature for the specified length of time.

d. Quench as specified for the type of alloy.

e. Rinse fully, when necessary.

f. Age as specified for the type of alloy.

8.1.2 SURFACE CONDITION - PRIOR TO HEAT TREATMENT

a. Before heat treatment, clean the parts to remove forming lubricants, marking fluids, or other unwanted material that can cause blistering, surface attack, or staining during subsequent processing. Remove anodized coating before heat treatment.

EXCEPTION: Do not remove anodized coating from rivets before heat treatment.

OPTION: It is permitted to not remove Protectsol 512 or identification marks on raw material before solution heat treating or precipitation hardening in air. The identification marks must not interfere with subsequent processing in accordance with Section 11.4.

b. Use the processes that follow for cleaning before heat treatment.

NOTE: It is not mandatory, but highly recommended, to use the chemicals and process controls in these specifications: BAC5765, BAC5750, BAC5408, BAC5763.

Alternative processes such as hot water rinsing are also permitted.

c. Before salt bath heat treatment, remove all liquids or coatings to prevent salt spatter or unfavorable reaction.

8.1.3 CONFIGURATION OF THE CHARGE FOR SOLUTION TREATMENT

a. Position and support parts to minimize distortion.

b. Configure the charge to keep a free circulation of heat and quenchant between the individual parts. Anywhere in the load, the part orientation must prevent quench degradation from steam generation. Unless specified differently in this section, the configuration must be in accordance with these requirements:

(1) Examine part separation visually. Measure only in cases of dispute.

(2) Unless specified differently in Section 8.1.3.b.(7), if the parts are 0.25 inch or less in thickness then separate them from each other by 1 inch or more. The edges are permitted to touch. For sections that are 0.10 inch or less in thickness, edge-to-planar surface touching is also permitted. The distance between planar surfaces that are approximately parallel (± 30 degrees) must not be less than 1 inch.

(3) Parts more than 0.25 inch in thickness must be separated by a minimum of 1 inch plus the material thickness.

(4) Fixtures and spacers must be designed for line or point contact to have minimum effect on the quench rate. The fixtures and spacers must not prevent access of the quenchant to the part . Area contact by fixtures or spacers (such as by flat steel racking bars) is not permitted.

(5) The load must be small enough to comply with the quenchant temperature requirements in accordance with Section 8.2.4.2.a., Section 8.2.4.3, Section 8.2.4.4, or Section 8.2.4.5 as applicable.

(6) Configure large parts made from thin sheet with sufficient support to prevent buckling. Buckling occurs because the material softens during solution heat treatment.

(7) For parts that meet the requirements of Table II and are in 45 degrees of vertical, it is permitted to use these space parameters:

(a) The minimum distance between surfaces that are approximately parallel (± 30 degrees) must be in the limits of Figure 1.

(b) Surface-to-surface contact between two parts is permitted if the quenchant has free access to the opposite surfaces of both parts. The distance between the next part that is approximately parallel must be at least 1 inch.

TABLE II - MAXIMUM GAGE THICKNESS (INCHES) FOR RACKING IN ACCORDANCE WITH Section 8.1.3, Section 8.1.3.b., Section 8.1.3.b.(7)

ALLOY	QUENCH MEDIA	
	WATER	28 PERCENT TYPE I GLYCOL
2000 series	0.064	0.032
6000 series	0.090	0.090
7000 series	0.125	0.125 FL 1
FL 1 Not Applicable to 7055.		

8.1.3 CONFIGURATION OF THE CHARGE FOR SOLUTION TREATMENT (Continued)

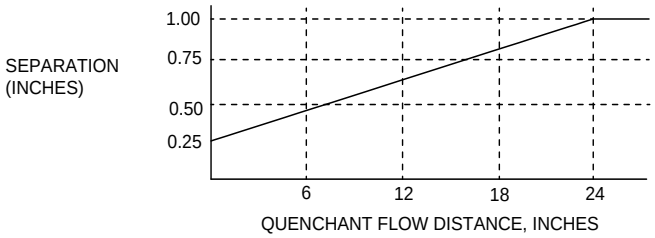

(See Figure 2 and Figure 3 for an explanation of Quenchant Flow Distance)

FIGURE 1 - SEPARATION REQUIREMENTS FOR 2000, 6000, AND 7000 SERIES ALLOYS IN THE LIMITS OF Table II

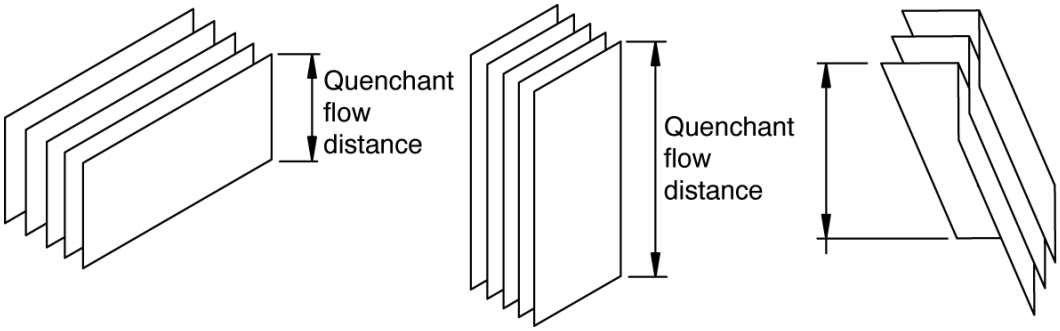

FIGURE 2 - QUENCHANT FLOW DISTANCE (LENGTH-TO-WIDTH RATIO OF 4 TO 1 OR LESS)

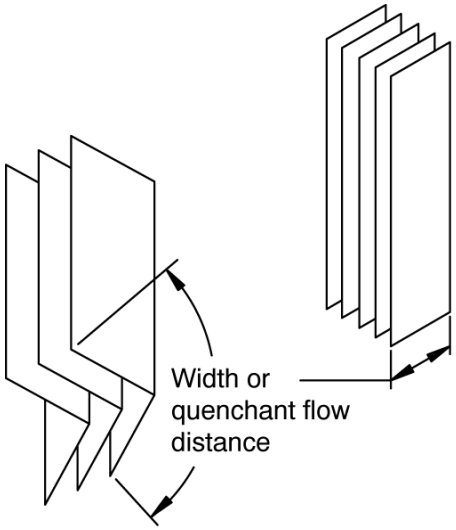

FIGURE 3 - QUENCHANT FLOW DISTANCE (LENGTH-TO-WIDTH RATIO GREATER THAN 4 TO 1)

c. Part spacing closer than that specified in Section 8.1.3.b. and Section 8.1.3.d. is permitted with Boeing approval. The applicable Boeing Research and Technology (BR&T) group approves the spacing procedure. To get approvals, include these items:

(1) Written description of the practice(s)

8.1.3 CONFIGURATION OF THE CHARGE FOR SOLUTION TREATMENT (Continued)

(2) Written description of the parts to which the procedure applies

(3) Photographs of typical parts that are racked according to the procedure.

After inspection of this information, Boeing can ask for more data and specimens. For example, alternative spacing procedures that involve sheet materials are likely to need specimens for corrosion tests.

d. Small parts such as machined parts, formed sheet, or cut to length extrusions can be heat treated in baskets in layers. The parts must be less than 0.25 inch in nominal thickness and 6 inches in length. The layers can be no more than 4 inches deep with no less than 4 inches between the layers. Configure the distance between parts as follows:

(1) The distance between parts must be at a minimum of 0.25 inch.

(2) Areas that are not more than one inch square are permitted to touch adjacent parts.

(3) Linear areas that are not more than 0.25 inch wide are permitted to touch.

(4) The parts must move and separate during quenching.

e. When round tooling rod is used, use the rod to make a separation measurement in accordance with Figure 1. It is permitted to use an average separation based on the diameter of the rod.

f. The previous requirements do not apply to rivets or small parts that are heat treated in containers in accordance with in Section 6.5.

g. When a sheet or strip is heat treated as a coil, put distance between the loops or wraps of individual coils. The distance between coils must meet the requirements listed above unless specified differently in Section 8.1.3.h. Adjacent coils of sheet material that is 0.080 inch or less in nominal thickness can touch if movement and separation occurs during quenching. Do not pack coils in a manner that prevents movement during quenching.

h. It is permitted to corrugate and coil 7055 and 7075 sheet for heat treatment if these conditions are satisfied:

(1) The sheet is less than 7 inches wide and is not more than 0.090 inch in thickness.

(2) The separation between the individual wraps conforms to Figure 1. Areas with one to three layers that touch are permitted if none of the area is more than 9 inches long.

(3) Straight and staggered two-coil high stacking is permitted. Do not put more coils on racks above these coils.

(4) The coils are racked with the coil axis no more than 10 degrees off vertical.

(5) The coils are water quenched in accordance with Section 8.2.4.2.a.

8.1.3 CONFIGURATION OF THE CHARGE FOR SOLUTION TREATMENT (Continued)

i. It is permitted to solution heat treat ducts of 6061 that will be heat treated to the -T42 or -T62 temper in baskets. No part of a duct or flange must be more than 0.25 inch in thickness. The baskets must not be more than 20 inches in height or diameter. Do not stack the baskets. The basket construction must not adversely change the heat up rate or quenching. Process these parts as follows:

(1) Load parts into baskets in a vertical position as much as possible.

(2) It is permitted to load multiple layers vertically to a maximum of three layers for each basket.

(3) Separate the parts with one screen for each layer, with a maximum of two screens per basket.

(4) The parts can project from the basket a maximum of 10 inches if more than half the length of the part is in the basket.

(5) Point and line contacts between parts is permitted.

8.1.4 CONFIGURATION OF THE CHARGE FOR PRECIPITATION TREATMENTS AND ANNEALING

It is permitted to nest parts for precipitation treatments and annealing to a maximum thickness of one inch. For all 2024 artificial aging or aging of 7055 and 7075 to a -T7X condition, only nest parts or materials that are less than 6 inches wide. Put the wider parts in equal distance positions according to Section 8.1.3.

8.2 HEAT TREATMENT

8.2.1 GENERAL REQUIREMENTS

a. When heat treating material in air above 700 F (371 C), high temperature oxidation is not permitted. To make sure there is no high temperature oxidation, use one of these methods:

(1) Check monthly for high temperature oxidation in accordance with Section 12.4.

(2) Use ammonium fluoborate (preferred) or sodium fluoborate in powder or granular form. Put the fluoborate in a secure open container on the heat treat rack/basket. Use a minimum of 1 ounce of fluoborate for each 1,000 cubic feet of furnace volume.

(a) Find the amount to use by experience. Post that amount at each furnace.

(b) For clad materials or annealing 6061, it is optional to use fluoborate.

(c) It is recommended to not use fluoborate on skin quality materials.

8.2.1 GENERAL REQUIREMENTS (Continued)

b. When furnace or salt bath temperatures fall below the specified temperature range, do not start the soaking period. Start the soaking period when the indications from all process thermocouples go back to the minimum of the specified temperature range. When salt bath temperatures do not fall below the specified range, the soaking period starts when the load is completely immersed in the salt bath.

c. Before parts are put into solution heat treatments, make sure the furnaces and salt baths are at the specified heat treating temperature.

d. Set the furnace controller at the mid-point of the specified temperature range.

e. After heat treatment, remove the salt from parts that were heated in a salt bath. Fully rinse them in the quench bath or a facility in accordance with Section 6.3.

f. It is permitted to heat treat parts with hidden surfaces in a salt bath. Check for entrapped salt. Remove all entrapped salt.

g. Heat treat parts as a whole. Do not heat treat partial areas of parts separately.

h. During solution heat treatment, soaking must be uninterrupted.

i. For annealing and precipitation treatments, interruptions of the soaking period for insertion or removal of parts are permitted under these conditions:

(1) No more than one interruption is permitted during aging treatments for 7000 series alloys at temperatures above 300 F (149 C).

(2) For annealing and all other aging treatments and alloys, a maximum of four interruptions are permitted.

(3) Interruptions (the period during which any furnace instrumentation show temperatures below the specified range) must not be more than 10 minutes in duration.

(4) The aging time is the sum of the times between interruptions.

j. All processing of 2524 (2xxx in accordance with BMS7-327 or BMS7-316) must be in accordance with the requirements which are applicable to alloy 2024.

8.2.2 ANNEALING

a. Anneal the materials in Table XIII and Table XIV only when approved in the Engineering Drawing.

b. Anneal wrought material in accordance with Table III.

c. It is optional to use partial annealing as specified in Table III followed by air cooling to remove forming stresses. If the heating material was salt, remove the remaining salt with a cold water rinse after the parts have cooled.

d. To anneal castings, heat them to 650 to 750 F (343 to 399 C) for approximately two hours and air cool.

8.2.2 ANNEALING (Continued)

e. Use temporary protective coatings as necessary to prevent material or part corrosion after annealing. Apply temporary protective coatings in accordance with BAC5034.

TABLE III - ANNEALING WROUGHT PRODUCTS

ALLOY	ANNEALING CYCLES	
	METHOD FOR PARTIAL ANNEAL	METHOD FOR FULL ANNEAL (CONDITION O)
1100	- - -	(1)
3003	- - -	(2)
5052 5056 5086 5456	- - -	(1)
2014 2017 2024 2117 2119 2219 4043 6061 FL 3 6063 6151	(1)	(3)
7050	- - -	(5) FL 2
7049 7075 7149 7175 7178	(4) FL 1	(5)

METHOD	ANNEALING METHODS
1	Heat to 630 to 660 F (333 to 349 C), soak for 0.5 to 1 hour and air cool to room temperature.
2	Heat to 730 to 760 F (388 to 404 C), soak for 0.5 to 1 hour and air cool to room temperature.
3	Heat to 750 to 800 F (399 to 427 C), soak 2 hours minimum, furnace cool at maximum rate of 50 F (28 C) per hour to 500 F (260 C) or less, air cool to room temperature.
4	Heat to 750 to 800 F (399 to 427 C), soak 2 hours minimum, air cool to 450 ± 25 F (232 ± 14 C) and hold for 2 hours minimum, air cool to room temperature.
5	Heat to 750 to 800 F (399 to 427 C), soak 2 hours minimum. OPTION: Heat to 775 to 825 F (413 to 441 C), soak 1 hour minimum. Furnace cool at 50 F (28 C) per hour to 450 ± 25 F (232 ± 14 C), hold 6 hours minimum and air cool to room temperature.

FL 1 Partial anneal in accordance with Method 1 when it is necessary to remove the effects of cold work to complete a forming operation.

8.2.2 ANNEALING (Continued)

FL 2 Manufacturer's Option: If the Engineering Drawing does not specify the "O" condition, Method 3 can be substituted for Method 5.

FL 3 For 6061 parts, Method 2 may also be used for partial annealing.

8.2.3 SOLUTION HEAT TREATMENT

a. Solution treatment soaking times and temperatures for different alloys are shown in Table IV, Table V, Table VI, and Table VII.

b. When solution heat treating clad material, obey the maximum and minimum time requirements of Table V. Charges that contain clad material of different thicknesses are permitted. Use the appropriate maximum soaking time listed in Table V. The maximum time of the material in the load must not be less than the minimum soaking time of other material in the load. Limit the number of heat treatments in accordance with Table XV.

c. Use a furnace charge distribution to make sure the furnace recovery rates are as specified in Section 6.1.3 when heat treating clad material.

d. When a charge consists of different thicknesses, assemblies, overlapping material, and does not include clad, use the soaking period for the thickest. Select thickness combinations so that this period is not more than four times the minimum requirement for the thinnest section.

8.2.3.1 Solution Heat Treatment and Soak Times for Various Products

See Table IV and Table V for solution treatment and soak times.

TABLE IV - SOLUTION TREATMENTS FOR VARIOUS PRODUCTS

ALLOY AND FORM	TEMP	THICKNESS OF MATERIAL FL 1	SOAKING PERIOD FL 2	RESULTING TEMPER	NOTES / RESTRICTIONS
2014 All Products except Forgings	925 to 945 F (496 to 508 C)	Refer to Table V		2014-W	- - -
2017 and 2117, All Products except Rivets				2017-W 2117-W	- - -
2119 and 2219 Bare and Clad Sheet and Plate, Extrusions and Tubing	985 to 1005 F (529 to 541 C)			2119-W 2219-W	For weldments use two times the minimum solution treatment soaking time.
2024 Bare and Clad Sheet, Plate, Bar, Extrusions and Tubing	910 to 930 F (487 to 499 C)			2024-W	- - -
6061 or 6062 All Products, 6063 Extrusions, 6951 FL 3	975 to 995 F (523 to 535 C)			6061-W 6062-W 6063-W 6951-W	- - -

8.2.3.1 Solution Heat Treatment and Soak Times for Various Products (Continued)

TABLE IV - SOLUTION TREATMENTS FOR VARIOUS PRODUCTS (Continued)

ALLOY AND FORM	TEMP	THICKNESS OF MATERIAL FL 1	SOAKING PERIOD FL 2	RESULTING TEMPER	NOTES / RESTRICTIONS
7050 Bare and Clad Sheet in accordance with BMS7-325	870 to 890 F (465 to 477 C)	Refer to Table V		7050-W	- - -
7050 Extrusions	880 to 900 F (471 to 483 C)			7050-W	Minimize the time between solution treatment and aging to minimize the risk of stress corrosion cracking.
7055 Sheet	865 to 885 F (462 to 474 C)			7055-W 7055-W Roll Reduced	Room temperature age of 96 hours minimum prior to elevated temperature aging. Minimize the time between solution treatment and aging to minimize the risk of stress corrosion cracking.
7075 Bare and Clad Sheet	910 to 930 F (487 to 499 C)			7075-W	For sheet material 0.051 inch and thicker in nominal thickness, it is permitted to use 860 to 880 F (460 to 472 C).
					For 0.10 inch nominal thickness and under that is solution heat treated in a continuous furnace, it is permitted to reduce soak times if: (1) The material is above 870 F (466 C) for a minimum of 3 minutes, and (2) The material must also be above 910 F (488 C) for a minimum of 2 of those 3 minutes. Start artificial aging any time after quenching.

ORIGINAL ISSUE 14-DEC-1941 REVISED (AH) 16-NOV-2020

8.2.3.1 Solution Heat Treatment and Soak Times for Various Products (Continued)

TABLE IV - SOLUTION TREATMENTS FOR VARIOUS PRODUCTS (Continued)

ALLOY AND FORM	TEMP	THICKNESS OF MATERIAL FL 1	SOAKING PERIOD FL 2	RESULTING TEMPER	NOTES / RESTRICTIONS
7075 Plate, Bar, Tubing and Extrusions	860 to 880 F (460 to 472 C)	Refer to Table V		7075-W	For plate 1.00 inch and less in nominal thickness, 910 to 930 F (487 to 499 C) can be used. Start artificial aging at any time after quenching.
7136-O Extrusions in Accordance with BMS7-371	870 to 890 F (465 to 477 C)			7136-W	Minimize the time between solution treatment and aging to minimize the risk of stress corrosion cracking.
7175 Extrusions	860 to 880 F (460 to 472 C)			7175-W	Start artificial aging at any time after quenching.
7178 All Products	860 to 880 F (460 to 472 C)			7178-W	Start artificial aging at any time after quenching.
Welded Assy's 356, A356, 357 or A357 to 6061	970 to 990 F (521 to 533 C)	- - -	6 hours	- - -	For solution treated 356 or A356 that are welded to 6061, it is permitted to decrease the solution treating time. It is permitted to decrease the time to 2 hours for the first 0.15 inch of thickness. Add 30 minutes for each added 0.5 inch or fraction thereof.
242	- - -	- - -	None	242-F	- - -
C355	970 to 990 F (521 to 533 C)	1 Inch Maximum	12 hours	C355-T4	For castings thicker than 1 inch, add 2 hours soak time for each additional 0.5 inch of thickness, or fraction thereof. 8 hour minimum delay at room temperature between quench and aging.
356	- - -	- - -	None	356-F	- - -

8.2.3.1 Solution Heat Treatment and Soak Times for Various Products (Continued)

TABLE IV - SOLUTION TREATMENTS FOR VARIOUS PRODUCTS (Continued)

ALLOY AND FORM	TEMP	THICKNESS OF MATERIAL FL 1	SOAKING PERIOD FL 2	RESULTING TEMPER	NOTES / RESTRICTIONS
356	990 to 1010 F (532 to 544 C)	1 Inch Maximum	8 hours for reheat treatment, 12 hours for initial heat treatment	356-T4	For castings thicker than 1 inch, add 2 hours soak time for each additional 0.5 inch of thickness, or fraction thereof.
A356	990 to 1010 F (532 to 544 C)	1 Inch Maximum	12 hours	A356-T4	For castings thicker than 1 inch, add 2 hours soak time for each additional 0.5 inch of thickness, or fraction thereof. Refer to Table X for minimum delay at room temperature between quench and aging for the specified final temper.
357, A357	990 to 1020 F (532 to 549 C)	1 Inch Maximum	12 hours	357-T4 A357-T4	For castings thicker than 1 inch, add 2 hours soak time for each additional 0.5 inch of thickness, or fraction thereof. 8 hour minimum delay at room temperature between quench and aging.
359	990 to 1010 F (532 to 544 C)	1 Inch Maximum	14 hours	359-T4	For castings thicker than 1 inch, add 2 hours soak time for each additional 0.5 inch of thickness, or fraction thereof. 8 hour minimum delay at room temperature between quench and aging.
520	800 to 820 F (426 to 438 C)	1 Inch Maximum	12 hours	520-W	For castings thicker than 1 inch, add 2 hours soak time for each additional 0.5 inch of thickness, or fraction thereof.
713	- - -	- - -	None	713-F	- - -

8.2.3.1 Solution Heat Treatment and Soak Times for Various Products (Continued)

FL 1 Thickness is the minimum dimension of thickest section at the time of heat treatment.

FL 2 See Section 8.2.1.b. to calculate the start of soaking times.

FL 3 Alloy 6951 is the core alloy for numbers 21, 22, 23, and 24 (MIL-B-20148 Class 21, 22, 23 and 24 respectively) clad aluminum brazing sheet.

TABLE V - SOLUTION HEAT TREATMENT SOAK TIMES FOR VARIOUS PRODUCTS

THICKNESS OF MATERIAL (INCH) FL 1	TIME AT TEMPERATURE (SOAKING PERIOD (MINUTES))			
	SALT BATH		AIR FURNACE	
	MINIMUM FL 3	MAXIMUM (FOR CLAD ONLY) FL 2	MINIMUM FL 3	MAXIMUM (FOR CLAD ONLY) FL 2
0.010 to 0.012	10	15	10	15
0.013 to 0.016	10	15	20	25
0.017 to 0.020	10	20	20	30
0.021 to 0.032	15	25	25	35
0.033 to 0.063	20	30	30	40
0.064 to 0.090	25	35	35	45
0.091 to 0.125	30	40	40	50
0.126 to 0.250	35	45	50	60
0.251 to 0.500	45	55	65	75
Over 0.500 inch	Add 20 minutes per additional 0.5 inch or fraction thereof in salt.		Add 30 minutes per additional 0.5 inch or fraction thereof in air.	

FL 1 Thickness is the minimum dimension of thickest section at the time of heat treatment.

FL 2 Soak times that are more than the maximum listed, but less than two times the maximum are permitted if the material can have one more heat treatment in accordance with Table XV. Such cases then become two heat treatments in accordance with Section 8.2.8.b. and Table XV.

FL 3 For non-clad material, the maximum permitted soak time is 4 times the minimum shown.

8.2.3.2 Solution Heat Treatment and Soak Times for Forgings

See Table VI for solution treatment and Table VII for soak times.

TABLE VI - SOLUTION HEAT TREATMENTS FOR FORGINGS FL 1

ALLOY	TEMP	TIME AT TEMPERATURE	WATER QUENCH TEMP FL 2	RESULTING TEMPER
2014	925 to 945 F (496 to 508 C)	Refer to Table VII	150 to 180 F (66 to 82 C)	2014-W
2219	985 to 1005 F (529 to 541 C)		140 to 160 F (60 to 72 C)	2219-W
6061	975 to 995 F (523 to 535 C)		140 to 160 F (60 to 72 C)	6061-W

8.2.3.2 Solution Heat Treatment and Soak Times for Forgings (Continued)

TABLE VI - SOLUTION HEAT TREATMENTS FOR FORGINGS FL 1 (Continued)

ALLOY	TEMP	TIME AT TEMPERATURE	WATER QUENCH TEMP FL 2	RESULTING TEMPER
6151	960 to 980 F (515 to 527 C)	Refer to Table VII	140 to 160 F (60 to 72 C)	6151-W 6151-T4
7049	865 to 885 F (462 to 474 C)		130 to 150 F (54 to 66 C)	7049-W
7050	870 to 890 F (465 to 477 C)		130 to 150 F (54 to 66 C)	7050-W
7075	860 to 880 F (460 to 472 C)		140 to 160 F (60 to 72 C)	7075-W
7149	865 to 885 F (462 to 474 C)		130 to 150 F (54 to 66 C)	7149-W

FL 1 The second time any forging is solution heat treated, it is permitted to use the soaking schedules in Table V (that is, for 7075 forgings use schedule for 7075 plate, bar, tubing and extrusions).

FL 2 Quenchant temperature must not increase more than 20 F (11 C) during quenching. Parts must stay in the quench for a minimum of 2 minutes for each inch of material thickness or fraction thereof. Calculate the quench time with the maximum section thickness.

TABLE VII - SOLUTION HEAT TREATMENT SOAK TIMES FOR FORGINGS

THICKNESS OF ORIGINAL BLOCK OR FORGING FROM WHICH PART WAS MADE (INCH)	THICKNESS AT TIME OF HEAT TREATING (INCH)	MINIMUM TIME AT TEMPERATURE (HOURS) FL 1
0 to 6	0.00 to 1.99	3
	2.00 to 3.99	4
	4.00 to 5.99	5
6 to 8	0.00 to 1.99	4
	2.00 to 3.99	5
	4.00 to 5.99	6
	6.00 to 7.99	7
8 to 10	0.00 to 1.99	5
	2.00 to 3.99	6
	4.00 to 5.99	7
	6.00 to 7.99	8
	8.00 to 9.99	9
10 to 12	0.00 to 1.99	6
	2.00 to 3.99	7
	4.00 to 5.99	8
	6.00 to 7.99	9
	8.00 to 9.99	10
	10.00 to 12.00	11

8.2.3.2 Solution Heat Treatment and Soak Times for Forgings (Continued)

TABLE VII - SOLUTION HEAT TREATMENT SOAK TIMES FOR FORGINGS (Continued)

THICKNESS OF ORIGINAL BLOCK OR FORGING FROM WHICH PART WAS MADE (INCH)	THICKNESS AT TIME OF HEAT TREATING (INCH)	MINIMUM TIME AT TEMPERATURE (HOURS) FL 1
12 to 14	0.00 to 1.99	7
	2.00 to 3.99	8
	4.00 to 5.99	9
	6.00 to 7.99	10
	8.00 to 9.99	11
	10.00 to 12.00	12
14 to 16	0.00 to 1.99	8
	2.00 to 3.99	9
	4.00 to 5.99	10
	6.00 to 7.99	11
	8.00 to 9.99	12
	10.00 to 12.00	13

FL 1 The second time any forging is solution heat treated, it is permitted to use the soaking schedules in Table V (that is, for 7075 forgings use schedule for 7075 plate, bar, tubing and extrusions).

8.2.4 QUENCHING

8.2.4.1 Quench Delay Requirements

a. Use fast and continuous quenching. Decrease quench delay time as much as possible. Table VIII specifies the maximum quench delay time. Measure quench delay time annually. Longer delay times are permitted if:

(1) The test shows that part temperatures do not fall below 900 F (482 C) before immersion for 2219 material, or below 775 F (413 C) for other alloys.

(2) Repeat quench delay tests after equipment repair or modifications that change the quench delay. Also repeat the tests when the quench delay time measured annually increases. Document the test results for Boeing approval.

b. Quench delay time in air furnaces starts when the door starts to open and ends when the last corner of the load is immersed in the quenchant. Quench delay time starts in salt baths when the first corner of the load or part emerges from the salt and ends when the last corner of the load or part is immersed in the quenchant.

c. For bottom-quench downdraft air furnaces, obey the processes that follow:

(1) Start the quench delay when the first one of these conditions occurs:

(a) The parts emerge from the work zone,

(b) Or the work zone temperature decreases below the minimum solution temperature.

8.2.4.1 Quench Delay Requirements (Continued)

(2) As part of the Temperature Uniformity Survey, find the temperature decrease characteristics in the work zone when the door opens. Do the tests again after equipment repair or after rework that could change the quench delay characteristics.

TABLE VIII - QUENCH DELAY TIME REQUIREMENTS FOR ALL PRODUCTS

MINIMUM THICKNESS (INCH) FL 2	MAXIMUM QUENCH DELAY (SECONDS)	
	2014, 2017, 2117, 2119, 2219, 2024, 6061, 7136, 7049, 7149, 7050, 7055, 7075, 7175, AND ALL CASTING ALLOYS	7178
0.010 to 0.015	4	FL 1
0.016 to 0.019	5	FL 1
0.020 to 0.031	7	5
0.032 to 0.062	10	7
0.063 to 0.089	10	10
0.090 and greater	15	15

FL 1 Heat treatment by the purchaser is not permitted.

FL 2 For permitted delays, thickness is the minimum dimension of the thinnest section of any part of the load.

8.2.4.2 Quenching of All Products Other Than Castings and Forgings

a. Unless specified differently in the items that follow, quench all alloys in water. The water temperature immediately before quenching must be at less than 90 F (32 C). During quenching the temperature must not increase to above 100 F (38 C), according to the temperature indicator. See Section 6.2.b.

b. Quench 6061 parts in hot water (maximum temperature 200 F (93 C)) if cold water causes too much distortion or internal stresses. Spray quench can be substituted when hot water quench is required. Use air quenching as permitted by the Engineering Drawing.

c. Spray or hot water quench only as permitted by the Engineering Drawing or by Boeing Research and Technology (BR&T) . Unless the BR&T approval is different, spray quench in accordance with the Engineering Drawing and use these cooling rates:

(1) A minimum of 800 F (444 C) per second for 7075 sheet up to 0.100 inch in thickness.

(2) A minimum of 1000 F (556 C) per second for all other applications.

d. Use glycol quenchants in accordance with Section 8.2.4.5.

e. For immersion quenching, fully immerse the parts into the quenchant.

(1) Keep the parts in the quenchant for:

8.2.4.2 Quenching of All Products Other Than Castings and Forgings (Continued)

(a) A minimum of 2 minutes for each inch of thickness or fraction thereof in the thickest section,

(b) Or at least 2 minutes after all signs of boiling stop.

(2) For parts that need cold storage, the maximum quench time must not be more than two times the minimum quench time.

f. After salt-heat treatment and drying, rinse parts in fresh water to remove the remaining salt. The rinse facility must be in accordance with Section 6.3.

g. When using Turco Aquasorb to remove water from the parts, put the parts fully in Turco Aquasorb for a minimum of 30 seconds. This removes the water and prevents ice formation in a freezer. No temperature control is necessary when using Turco Aquasorb. Drain water from the tank as needed to prevent the parts from being in contact with water.

h. For cold storage parts, the maximum delay from the quench removal to the cold storage is 15 minutes for 2000 series alloys other than 2219. For the 2219 alloy and all other alloys, the maximum delay is 30 minutes. If these delay times are longer, decrease the maximum permitted accumulative holding time, in accordance with BAC5300-2 or BAC5001-12, by the amount of excess delay time.

OPTION: Before cold storage, it is permitted to use cold liquid baths to accelerate cooling of the quenched material. Control and/or adjust the bath to temperatures of -20 F (-29 C) or lower. After the parts are at the approximate temperature of the liquid, transfer them to conventional refrigerated storage.

8.2.4.3 Quenching of Castings and Casting Weldments

Quench castings and casting weldments in water at a temperature of 140 to 200 F (60 to 93 C) or in glycol-water solutions in accordance with Section 8.2.4.5. Do not let the water temperature increase more than 20 F (11 C) as a result of quenching any load. The water temperature must not increase to more than 200 F (93 C).

8.2.4.4 Quenching of Forgings

a. Water temperatures for quenching forgings must be in accordance with Table VI. It is permitted to use glycol-water solutions to quench forgings in accordance with Section 8.2.4.5.

b. Forgings that will be in a stress relieved temper such as -TXX51, -TXX52, or -TXX54 can be quenched in cold water. With BR&T approval, quench other forgings in cold water if tests or past experience has proven that:

(1) Distortion is not a problem.

(2) Residual stresses will not decrease service performance.

(3) Adequate properties are difficult to get because of section thickness.

8.2.4.4 Quenching of Forgings (Continued)

c. Keep parts in the quenchant for a minimum of two minutes for each inch of thickness or fraction thereof. Use the maximum section thickness to calculate the minimum quench time.

8.2.4.5 Glycol Quenching

Polyalkalene glycol-water solutions can be used to quench these alloys: 2014, 2017, 2024, 2117, 2119, 2219, 6061, 7050, 7075, 7136, 7175, 7178, and all aluminum castings. When glycol solutions are used, obey the requirements that follow:

a. Quenchants must conform to Section 5.1.d. or Section 5.1.e. Maintain quenchants according to Section 9.2.

b. Thickness limitations for all concentrations of solutions must be in accordance with Table IX. Concentrations are percent by volume of the glycol polymer.

c. Do not mix Aqua Quench 364, Aqua Quench 251, Aquatensid BW/RB, or Aquatensid D, with each other or with any other glycol quenchant material. It is permitted to mix different batches/lots of material of the same product designator.

d. The temperature of the quenchant must not increase more than 20 F (11 C) from quenching one heat treatment load. The maximum quenchant temperature at the start of quench must be 90 F (32 C). The quenchant temperature must not be more than 100 F (38 C) at any time during the quench. Measure temperatures with the quench tank temperature indicator. See Section 6.2.b.

e. Start the agitation to make sure the concentration is fully mixed before the quench or performing sampling. The circulation of the quenchant must continue until the end of the quench.

f. Use an agitated cold water rinse to remove glycol films after quenching. Agitate the parts in a cold water immersion rinse for a minimum of 10 minutes, or as follows:

(1) Use cold water spray rinse for 2 minutes minimum. Surfaces must not be shielded from the spray by other parts. The sprayed water must directly strike all surfaces.

(2) Alternative rinsing procedures are permitted when documentation indicates removal of all glycol residue.

TABLE IX - LIMITS FOR QUENCHING IN GLYCOL-WATER SOLUTIONS

ALLOY	FORM	MAXIMUM NOMINAL THICKNESS (INCHES)	CONCENTRATION OF GLYCOL QUENCHANT (PERCENT BY VOLUME)	
			TYPE I	TYPE II
2014, 2017, 2024, 2117, 2119, 2219, 2524	All FL 1	0.040	34 max	34 max
		0.063	28 max	22 max
		0.071	22 max	16 max
		0.080	16 max	16 max

8.2.4.5 Glycol Quenching (Continued)

TABLE IX - LIMITS FOR QUENCHING IN GLYCOL-WATER SOLUTIONS (Continued)

ALLOY	FORM	MAXIMUM NOMINAL THICKNESS (INCHES)	CONCENTRATION OF GLYCOL QUENCHANT (PERCENT BY VOLUME)	
			TYPE I	TYPE II
6061, 6063, castings, and weld assemblies of castings to 6061	Sheet, Plate, Bar, Tubing, Extrusions, and Castings FL 2	0.032	40 max	40 max
		0.063	40 max	34 max
		0.080	34 max	34 max
		0.125	34 max	28 max
		0.190	28 max	20 max
		0.250	22 max	18 max
		0.630	16 max	N/A
7050, 7075, 7136, 7175, 7178	Sheet, Plate, Bar, Tubing, and Extrusions	0.032	40 max	40 max
		0.063	40 max	34 max
		0.080	34 max	34 max
		0.125	34 max	28 max
		0.190	28 max	20 max
		0.250	22 max	18 max
		0.630	16 max	N/A
6061, 7050	Forgings FL 3	1.5	35 max	22 max
		3.0	25 max	N/A
7075	Forgings FL 3	0.75	40 max	16 max
		1.5	28 max	16 max
		3.0	18 max	N/A

FL 1 When the final temper is T6, T62, or T8XXX, all product forms to a maximum thickness of 0.25 inch can be quenched in Type I or Type II glycol solutions. Glycol solutions must be at 22 percent maximum.

FL 2 When the final temper is T6XXX, all product forms to a maximum thickness of 0.500 inch can be quenched in 38 percent Type I glycol solution.

FL 3 Use of Aquatensid D-Water solutions are not permitted for quenching forgings or parts made from forgings.

8.2.5 PRECIPITATION TREATMENT (AGING)

a. Keep the material at a low temperature to slow the rate of natural aging and to keep the material in the relatively soft W condition. Keep materials that are to be formed in the W condition as specified in BAC5300-2.

b. Do precipitation treatment, whether natural or artificial, as shown in Table X, Table XI, or Table XII.

(1) Let all solution heat treated alloys naturally age before artificial aging. Minimum natural aging times are given in the notes to Table X, Table XI, and Table XII.

8.2.5 PRECIPITATION TREATMENT (AGING) (Continued)

(2) Many drawings use the designations T4 or T6 for user heat treated tempers. Tables in this specification include T4, T6, and T42 and T62 temper designations. In the scope of this specification, T4 is interchangeable with T42, and T6 is interchangeable with T62.

(3) When approved equipment and facilities are available (See Table I), warm the material to 125 F (52 C) or less as an alternative to natural aging. Use the aging times for natural aging, or age until the hardness and conductivity measurements are in the specified range.

8.2.5.1 Preciptation Treatments for Various Products

See Table X and Table XI for treatments.

TABLE X - PRECIPITATION TREATMENTS (AGING) FOR VARIOUS PRODUCTS FL 1

ALLOY AND FORM	INITIAL TEMPER FL 2	TEMP	TIME (HOURS) FL 3	FINAL TEMPER	NOTES / RESTRICTIONS
2014 All Products except Forgings	2014-W	Room	96	2014-T4, T42	If minimum acceptable hardness and conductivity occur prior to time shown, parts can be released for subsequent processing.
	2014-W, -T4, -T42	340 to 360F (171 to 183 C)	8 to 9	2014-T6, -T62	- - -
2017 and 2117 All Products except Rivets	2017-W	Room	96	2017-T4, -T42	If minimum acceptable hardness and conductivity occur prior to time shown, parts can be released for subsequent processing.
	2117-W			2117-T4, -T42	
2119 and 2219 Bare and Clad Sheet and Plate, Extrusions, and Tubing	2119-W	Room	96	2119-T42	If minimum acceptable hardness and conductivity occur prior to time shown, parts can be released for subsequent processing. T42 is an intermediate temper and must be artificially aged to T62 prior to use.
	2219-W			2219-T42	
	2119-W, -T42	365 to 385 F (185 to 197 C)	35 to 37	2119-T6, -T62	- - -
	2219-W, -T42			2219-T6, -T62	- - -
2024 Bare and Clad Sheet, Plate, Bar, Extrusions and Tubing	2024-W	Room	96	2024-T4, -T42	If minimum acceptable hardness and conductivity occur prior to time shown, parts can be released for subsequent processing.
6061 or 6062, All Products, 6063 Extrusions, 6951 FL 4	6061-W	Room	96	6061-T4, -T42	If minimum acceptable hardness and conductivity occur prior to time shown, parts can be released for subsequent processing.
	6062-W			6062-T4, -T42	
	6063-W			6063-T4, -T42	
	6951-W			6951-T4, -T42	
	6061-W, -T4, -T42 and T4XXX	340 to 360 F (171 to 183 C)	8 to 10	6061-T6, -T62 and T6XXX	- - -
	6062-W, -T4			6062-T6, -T62	

8.2.5.1 Preciptation Treatments for Various Products (Continued)

TABLE X - PRECIPITATION TREATMENTS (AGING) FOR VARIOUS PRODUCTS FL 1 (Continued)

ALLOY AND FORM	INITIAL TEMPER FL 2	TEMP	TIME (HOURS) FL 3	FINAL TEMPER	NOTES / RESTRICTIONS
6061 or 6062, All Products, 6063 Extrusions, 6951 FL 4	6063-W, -T4	340 to 360 F (171 to 183 C)	8 to 10	6063-T6, -T62	- - -
	6951-W, -T4, -T42	310 to 330 F (154 to 166 C)	17 to 19	6951-T6, -T62	
7050 Bare and Clad Sheet in accordance with BMS7-325	7050-W	240 to 260 F (115 to 127 C) - plus - 325 to 345 F (162 to 174 C)	3.5 to 4.5 at first temp - plus - 9 to 11 at second temp	7050-T762	- - -
7050 Extrusions	7050-W	240 to 260 F (115 to 127 C) - plus - 340 to 360 F (171 to 183 C)	6 to 8 at first temp - plus - 3.5 to 5.25 at second temp	7050-T76	Minimize the time between solution treatment and aging to minimize the risk of stress corrosion cracking. Soak at 340 to 360 F (171 to 183 C) for an additional 0.5 hour for each inch, or fraction thereof, in excess of 2 inches. See Table XI for additional aging provisions.
7055 Sheet	7055-W, 7055-W Roll Reduced	240 to 260 F (115 to 127 C) - plus - 310 to 330 F (154 to 166 C)	24 at first temp - plus - 4 at second temp	7055- T762	Minimize the time between solution treatment and aging in order to minimize the risk of stress corrosion cracking. Room temperature age of 96 hours minimum prior to elevated temperature aging.
7075 Bare and Clad Sheet	7075-W	240 to 260 F (115 to 127 C)	22 to 24	7075-T6, -T62	Artificial aging can begin at any time following quenching. See Table XI for additional aging provisions.
7075 Plate, Bar, Tubing and Extrusions					
7136-O Extrusions in accordance with BMS7-371	7136-W	240 to 260 F (115 to 127 C) - plus - 305 to 325 F (151 to 163 C)	12 to 14 at first temp - plus - 11 to 14 at second temp	7136- T762	Minimize the time between solution treatment and aging in order to minimize the risk of stress corrosion cracking.
7175 Extrusions	7175-W	240 to 260 F (115 to 127 C)	22 to 24	7175-T6, -T62	Artificial aging can begin at any time following quenching. See Table XI for additional aging provisions.
7178 All Products	7178-W			7178-T6, -T62	Artificial aging can begin at any time following quenching.
Welded Assy's 356, A356, 357 or A357 to 6061	- - -	310 to 330 F (154 to 166 C)	12	- - -	When the drawing specifies “Heat treat to T6 or T62,” the aging parameters for 6061-T62 can also be used.

8.2.5.1 Preciptation Treatments for Various Products (Continued)

TABLE X - PRECIPITATION TREATMENTS (AGING) FOR VARIOUS PRODUCTS FL 1 (Continued)

ALLOY AND FORM	INITIAL TEMPER FL 2	TEMP	TIME (HOURS) FL 3	FINAL TEMPER	NOTES / RESTRICTIONS
40E	Room Temp. 21 days. Opt. 345 to 365 F (173 to 185 C) for 8 hours				Use for sand castings only. Consult BR&T for other castings.
242	242-F	330 to 350 F (165 to 177 F)	22 to 26	242-T571	- - -
C355	C355-T4	300 to 320 F (148 to 160 C)	10 to 12	C355-T61	8 hour minimum delay at room temperature between quench and aging.
356	356-F	430 to 450 F (221 to 233 C)	6 to 12	356-T51	- - -
	356-T4	300 to 320 F (148 to 160 C)	3 to 5	356-T6	- - -
		390 to 410 F (198 to 210 C)	4	356-T7	Use for sand castings only. Consult BR&T for other castings.
		465 to 485 F (240 to 252 C)	3 to 5	356-T71	- - -
A356	A356-T4	300 to 320 F (148 to 160 C)	3 to 5	A356-T6	The -T6, -T61, and T62 precipitation treatments are interchangeable if mechanical property requirements are satisfied.
			6 to 10	A356-T61	8 hour minimum delay at room temperature between quench and aging. The -T6, -T61, and T62 precipitation treatments are interchangeable if mechanical property requirements are satisfied
		330 to 350 F (165 to 177 C)	3 to 8	A356-T62	
357, A357	357-T4 A357-T4	300 to 320 F (148 to 160 C)	10 to 12	A357-T61 357-T61	The -T6, -T61, and T62 precipitation treatments are interchangeable if mechanical property requirements are satisfied. 8 hour minimum delay at room temperature between quench and aging.
		330 to 350 F (165 to 177 C)	6 to 10	357-T62 A357-T62	
359	359-T4	300 to 320 F (148 to 160 C)	10 to 12	359-T61	The -T6, -T61, and T62 precipitation treatments are interchangeable if mechanical property requirements are satisfied. 8 hour minimum delay at room temperature between quench and aging.
		330 to 350 F (165 to 177 C)	6 to 10	359-T62	
520	520-W	Room	96	520-T4	- - -
713	713-F	Room	21 days	713-T5	- - -

8.2.5.1 Preciptation Treatments for Various Products (Continued)

TABLE X - PRECIPITATION TREATMENTS (AGING) FOR VARIOUS PRODUCTS FL 1 (Continued)

ALLOY AND FORM	INITIAL TEMPER FL 2	TEMP	TIME (HOURS) FL 3	FINAL TEMPER	NOTES / RESTRICTIONS
713	713-F	250 F (121 C)	10	713-T5	- - -

FL 1 For added precipitation treatments, see Table XI.

FL 2 Unless specified differently, age a minimum of 2 hours at room temperature before the start of artificial aging.

FL 3 See Section 8.2.1.b. for determining the beginning of soaking time. For castings more than 1 inch in thickness, add 2 hours soak time for each additional 0.5 inch of thickness, or fraction thereof. When a range is shown, the time of precipitation treatment must be in the specified range. When only one time is shown, it is a minimum value. For artificial aging only, the maximum time is plus 0.5 hour or plus 5 percent, whichever is less.

FL 4 Alloy 6951 is the core alloy for numbers 21, 22, 23, and 24 (MIL-B-20148 Class 21, 22, 23 and 24 respectively) clad aluminum brazing sheet.

TABLE XI - ADDED PRECIPITATION TREATMENTS FOR PRODUCTS OTHER THAN FORGINGS

ALLOY AND PRODUCT	ORIGINAL TEMPER DESIGNATION	TEMPERATURE (F)	TIME (HOURS) FL 1	FINAL TEMPER DESIGNATION
2024 Sheet, Plate (Bare and Clad)	2024-T3, -T351	365 to 385 (185 to 197 C)	11 to 13	2024-T81, -T851
	2024-T36, -T361		8 to 9	2024-T861
	2024, -W, -T4, -T42 FL 5		9 to 12	2024-T6, -T62
	2024-W, -T42 FL 5		16 to 18	2024-T72 FL 2
2024 Drawn Tube, Cold Finished Wire and Bar	2024-T3, T351		11 to 13	2024-T81, -T851
	2024-W, -T4 -T42		9 to 10	2024-T6, -T62
2024 Wire Extruded Bars, Shapes and Tubes	2024-T3		11 to 13	2024-T81
	2024-T3510		12 to 13	2024-T8510
	2024-T3511			2024-T8511
	2024-W, -T4, -T42 FL 5			2024-T6, -T62
2219 Plate, Bare and Clad	2219-T351 2219-T37	340 to 360 (171 to 183 C)	17 to 19	2219-T851 2219-T87
2219 Sheet, Bare and Clad	2219-T37	315 to 335 (157 to 169 C)	23 to 25	2219-T87
2219 Extruded and Drawn Bars, Shapes and Tubes	2219-T31 2219-T3510 2219-T3511	365 to 385 (185 to 197 C)	17 to 19	2219-T81 2219-T8510 2219-T8511
2219 (All)	2219-T4 2219-T42, -W FL 5	365 to 385 (185 to 197 C)	35 to 37	2219-T6 2219-T62
2219, Sheet	2219-T31	340 to 360 (171 to 183 C)	17 to 19	2219-T81

8.2.5.1 Preciptation Treatments for Various Products (Continued)

TABLE XI - ADDED PRECIPITATION TREATMENTS FOR PRODUCTS OTHER THAN FORGINGS
(Continued)

ALLOY AND PRODUCT	ORIGINAL TEMPER DESIGNATION	TEMPERATURE (F)	TIME (HOURS) FL 1	FINAL TEMPER DESIGNATION
6013 Sheet, (Bare and Clad)	6013-T4	365 to 385 (185 to 197 C)	4 to 5	6013-T6
7050 Extruded Bars, Shapes and Tubes	7050-W FL 7	240 to 260 plus 340 to 360 (115 to 127 C plus 171 to 183 C)	6 to 8 plus 9.5 to 10.5 FL 3	7050-T74 (T736)
	7050-T76 7050-T76511	340 to 360 (171 to 183 C)	7.5 to 8.5	7050-T73 7050-T73511
7075 Rolled and Cold Finished Bar	7075-W	215 to 235 plus 340 to 360 (101 to 113 C plus 171 to 183 C)	6 to 8 FL 3 plus 8 to 10 FL 4	7075-T73
	7075-T6	340 to 360 (171 to 183 C)	8 to 10 FL 4	7075-T73
	7075-T651			7075-T7351
7075 Extrusions	7075-W	215 to 235 plus 340 to 360 (101 to 113 C plus 171 to 183 C)	6 to 8 FL 3 plus 6 to 8 FL 4	7075-T73
	7075-W	240 to 260 plus 315 to 335 (115 to 127 C plus 157 to 169 C)	3 to 5 FL 3 plus 15 to 18	7075-T76
	7075-T6	340 to 360 (171 to 183 C)	6 to 8 FL 4	7075-T73
	7075-T6510			7075-T73510
	7075-T6511			7075-T73511
	7075-T6511	310 to 330 (154 to 166 C)	19 to 21	7075-T76511
	7075-T6510			7075-T76510
	7075-T6			7075-T76
7075 Bare and Clad, Sheet and Plate	7075-W	215 to 235 plus 315 to 335 FL 6 (101 to 113 C plus 157 to 169 C)	6 to 7 FL 3 plus 26 to 28 FL 4	7075-T73
	7075-T6	315 to 335 FL 6 (157 to 169 C)	26 to 28 FL 4	7075-T73
	7075-T651			7075-T7351
	7075-W	215 to 235 plus 315 to 335 (101 to 113 C plus 157 to 169 C)	6 to 8 FL 3 plus 16 to 18	7075-T76
	7075-T6	315 to 335 (157 to 169 C)	16 to 18	7075-T76
	7075-T651			7075-T7651

8.2.5.1 Preciptation Treatments for Various Products (Continued)

TABLE XI - ADDED PRECIPITATION TREATMENTS FOR PRODUCTS OTHER THAN FORGINGS
(Continued)

ALLOY AND PRODUCT	ORIGINAL TEMPER DESIGNATION	TEMPERATURE (F)	TIME (HOURS) FL 1	FINAL TEMPER DESIGNATION
7175 Extrusions	7175-W FL 5	215 to 235 plus 340 to 360 (101 to 113 C plus 171 to 183 C)	6 to 8 FL 3 plus 6 to 8 FL 4	7175-T73
	7175-T6	340 to 360 (171 to 183 C)	6 to 8 FL 4	7175-T73
	7175-T6510			7175-T73510
	7175-T6511	340 to 360 (171 to 183 C)		7175-T73511

FL 1 The times listed are for thicknesses up to 0.5 inch. Add 0.5 hour for each additional 0.5 inch or fraction thereof.

FL 2 Applicable only to sheet.

FL 3 All listed heat treatments are required. Although permitted, it is not necessary to remove the load from the furnace or to cool to room temperature between steps.

FL 4 Add an additional 0.5 hour of soak time to parts for each inch or fraction thereof more than two inches in thickness. Re-aging is permitted in accordance with Section 8.2.6.

FL 5 Unless specified differently, age a minimum of 2 hours at room temperature before the start of artificial aging.

FL 6 If furnace recovery time is less than 1 hour, it is permitted to age the parts at 340 to 360 F (171 to 183 C) for 8 to 10 hours as an alternative treatment to the specified treatment of 315 to 335 F (157 to 169 C) for 26 to 28 hours.

FL 7 Keep the time between solution treatment and aging at a minimum to decrease the risk of stress corrosion cracking.

8.2.5.2 Precipitation Treatments for Forgings

See Table XII for precipitation treatments of forgings.

8.2.5.2 Precipitation Treatments for Forgings (Continued)

TABLE XII - PRECIPITATION TREATMENTS (AGING) FOR FORGINGS

ALLOY AND STARTING TEMPER FL 5	TEMP	THICKNESS AT TIME OF HEAT TREATING (INCH)	TIME AT TEMP (HOURS) FL 1	RESULTING TEMPER	NOTES / RESTRICTIONS
2014-W 2014-T4	340 to 360 F (171 to 183 C)	0.00 to 1.99	8	2014-T6	Parts are in the W temper immediately after quenching. Parts are in the -T4 when a minimum of 96 hours at room temperature have elapsed after quenching. Artificial aging treatment can start immediately after quenching.
		2.00 to 3.99	9		
		4.00 to 5.99	10		
		6.00 to 7.99	11		
		8.00 to 9.99	12		
		10.00 to 12.00	13		
2219-W 2219-T4	365 to 385 F (185 to 197 C)	0.00 to 5.99	26	2219-T6	
		6.00 to 7.99	27		
		8.00 to 9.99	28		
		10.00 to 12.00	29		
2219-T352	340 to 360 F (171 to 183 C)	0.00 to 5.99	18	2219-T852	- - -
		6.00 to 7.99	19		
		8.00 to 9.99	20		
		10.00 to 12.00	21		
6061-W 6061-T4	340 to 360 F (171 to 183 C)	All thicknesses	8 to 10	6061-T6	Parts are in the W temper immediately after quenching. Parts are in the -T4 when a minimum of 96 hours at room temperature have elapsed after quenching. Artificial aging treatment can start immediately after quenching.
6151-W 6151-T4	330 to 350 F (165 to 177 C)	All thicknesses	10	6151-T6	
7049-W FL 2	Room Temperature	All thicknesses	48 to 72	7049-T23	All of the listed times and temperatures are required. It is not necessary to remove the load from the furnace or to cool to room temperature between steps, although this is permitted and does not cause damage.
	240 to 260 F (115 to 127 C)		24		
	310 to 330 F (154 to 166 C)		14		
7050-W	210 to 230 F (98 to 110 C)	0.00 to 1.99	4 to 5	7050-T74	All of the listed times and temperatures are required. It is not necessary to remove the load from the furnace or to cool to room temperature between steps, although this is permitted and does not cause damage. Keep the time between solution treatment and aging at a minimum to decrease the risk of stress corrosion cracking.
	240 to 260 F (115 to 127 C)		4 to 5		
	305 to 325 F (151 to 163 C)		3		
	340 to 360 F (171 to 183 C)		6 to 8 FL 3		
	210 to 230 F (98 to 110 C)	2.00 to 3.99	6 to 7		
	240 to 260 F (115 to 127 C)		6 to 7		
	305 to 325 F (151 to 163 C)		4		
	340 to 360 F (171 to 183 C)		6 to 8 FL 3		
	210 to 230 F (98 to 110 C)	4.00 to 12.00	8		
	240 to 260 F (115 to 127 C)		8		
	305 to 325 F (151 to 163 C)		5		
	340 to 360 F (171 to 183 C)		6 to 8 FL 3		

8.2.5.2 Precipitation Treatments for Forgings (Continued)

TABLE XII - PRECIPITATION TREATMENTS (AGING) FOR FORGINGS (Continued)

ALLOY AND STARTING TEMPER FL 5	TEMP	THICKNESS AT TIME OF HEAT TREATING (INCH)	TIME AT TEMP (HOURS) FL 1	RESULTING TEMPER	NOTES / RESTRICTIONS
7075-W	215 to 235 F (101 to 113 C)	All thicknesses	6 to 8 FL 4	7075-T73	All of the listed times and temperatures are required. It is not necessary to remove the load from the furnace or to cool to room temperature between steps, although this is permitted and does not cause damage.
	340 to 360 F (171 to 183 C)		8 to 10 FL 4		
7075-W	240 to 260 F (115 to 127 C)	0.00 to 5.99	24	7075-T6	- - -
		6.00 to 7.99	25		
		8.00 to 9.99	26		
		10.00 to 12.00	27		
7075-T6	340 to 360 F (171 to 183 C)	0.00 to 1.99	8	7075-T73	- - -
		2.00 to 3.99	9		
		4.00 to 5.99	10		
		6.00 to 7.99	11		
		8.00 to 9.99	12		
		10.00 to 12.00	13		
7075-T652	340 to 360 F (171 to 183 C)	0.00 to 1.99	6	7075-T7352	- - -
		2.00 to 3.99	7		
		4.00 to 5.99	8		
		6.00 to 7.99	9		
		8.00 to 9.99	10		
		10.00 to 12.00	11		
7149-W FL 2	Room Temp.	All thicknesses	48 to 72	7149-T73	All of the listed times and temperatures are required. It is not necessary to remove the load from the furnace or to cool to room temperature between steps. This is permitted and does not cause damage.
	240 to 260 F (115 to 127 C)		24		
	310 to 330 F (154 to 166 C)		14		

FL 1 When a range is shown, the time must be within the specified range. When a single time is shown, the time specified is a minimum. For artificial aging, the maximum time must be plus 0.5 hour or plus 5 percent, whichever is less.

FL 2 The two thermal treatments may be continuous. In such cases, the temperature must change (between temperature ranges) in one hour or less.

FL 3 Longer last step age times are permitted to lower the yield strength and/or increase conductivity with these conditions:

a. When production history documentation identifies a consistent need to re-age parts in accordance with Section 8.2.6.

8.2.5.2 Precipitation Treatments for Forgings (Continued)

b. Added age time must not be more than 4 hours. If after 4 hours of added aging, the material does not meet these requirements, it is permitted to give more aging in accordance with Section 8.2.6.

FL 4 Soak parts for 0.5 hour more for each added inch, or fraction thereof, that is more than 2 inches.

FL 5 Unless specified differently, age a minimum of 2 hours at room temperature before the start of artificial aging.

8.2.6 SUPPLEMENTAL ARTIFICAL (RE-AGING) FOR 7000 SERIES ALUMINUM ALLOYS

All 7000 series alloys heat treated to any T7X temper for the specified time can be re-aged. Re-aging is permitted if they are not in compliance with the minimum conductivity requirements of BAC5946 or Section 11.

NOTE: Re-aging of 7000 series alloys is not an interruption of the aging cycle.

a. Only re-age material that is a minimum of 2 HRB points more than the minimum requirement.

b. Re-age in cycles of 2 hours minimum plus 0.5 hour for each inch of thickness or fraction thereof for more than 2 inches.

c. Re-aging must meet the applicable specification requirements. Document re-aging as part of the production records. After each aging cycle, do the necessary tests to make sure the parts are in compliance with the applicable properties.

d. Re-aging temperatures for specified alloys are as follows:

(1) 7049 and 7149 Forgings - Re-age at 310 to 330 F (154 to 166 C)

(2) 7050 Alloys - Re-age at 340 to 360 F (171 to 183 C) or at 315 to 335 F (157 to 166 C)

(3) 7075 Sheet and Plate - Re-age at 315 to 335 F (157 to 169 C) or 340 to 360 F (171 to 183 C)

(4) 7075 Bar and Extrusions - Re-age at 340 to 360 F (171 to 183 C)

(5) 7175 Extrusions - Re-age at 340 to 360 F (171 to 183 C)

(6) 7136-T762 Extrusions - Re-age at 305 to 325 F (151 to 163 C).

8.2.7 STRESS RELIEF

8.2.7.1 Partial Stress Relief

It is permitted to partially stress relieve these aluminum alloys at 250 to 270 F (121 to 133 C) for a maximum accumulative time of one hour: 7049, 7050, 7075, 7175 and 7178, in any T7 temper such as T73, T7351, T74, T74X, T76.

8.2.7.2 Stress Relief of Cast Aluminum Parts

After rough machining, it is permitted to stress relieve cast aluminum alloy parts that have been solution treated and aged. Stress relieve them for a maximum accumulative time of 1 hour at a temperature 50 F (28 C) below the aging temperature.

8.2.7.3 Stress Relief by Uphill Quenching

If the Engineering Drawing specifies, stress relieve 7075-T73 alloy parts with uphill quenching. This minimizes machine distortion. The uphill quenching procedure first cools in liquid nitrogen and then reverse quenches in steam.

Condition of the part prior to uphill quenching:

a. Temper - The part must be in the -W temper, and must not have been exposed to room temperature for more than one hour.

b. Cold Storage - The part can be kept in storage at 0 F (-18 C) or colder to keep the -W temper. Do not keep the part in cold storage for more than 14 days prior to uphill quenching.

Process Control:

a. Time in Liquid Nitrogen - Put the part fully into the liquid nitrogen (-320 F (-196 C)) for the longest of these two options:

   (1) At least 10 minutes for each inch (or fraction thereof) of the maximum section thickness.

   (2) Until the liquid nitrogen stops bubbling.

b. Steam Delay - After the liquid nitrogen immersion, the time must not be more than 20 seconds between the first exposure of the part to air and the steam impingement. If the part has not yet been exposed to steam after 20 seconds, re-submerge the part in liquid nitrogen and reprocess it.

c. Maximum Steam Temperature - Do not expose the part to a steam temperature above 300 F (149 C). During exposure the part temperature must not be more than 250 F (121 C).

d. Maximum Steam Exposure - After removal from liquid nitrogen, do not expose the part to steam for longer than 2 minutes.

Process Verification:

On the first uphill quenched production lot of each part, do a longitudinal or long transverse tensile test from a prolongation, integral material, or a cut-up part. Report the tensile result, the test location thickness and grain direction, on the lot certification.

8.2.8 REHEAT TREATMENT

a. Certain tempers and forms of aluminum alloys are mechanically stress relieved or procured with increased mechanical properties due to cold working. These characteristics are permanently lost by subsequent annealing and/or re-solution heat treatments. Do not reheat-treat the tempers and forms shown in Table XIII or Table XIV unless the reheat-treated condition is required by the Engineering Drawing.

TABLE XIII - PRODUCTS SUBJECT TO LOSS OF PROPERTIES AFTER REHEAT TREATMENT

MATERIAL AND TEMPER	PRODUCT	REHEAT - TREAT CONDITION
1100, 3003, 5052, 5056, 5086, and 5456, in any "H" condition (-H26, -H28, -H32, et cetera)	All	-O
2014-T3, -T4, -T451, -T651	Clad Sheet or Plate	-T42 or -T62 (FL 1)
2014-T4, -T4510, -T4511, -T6, -T6510, -T6511	Extrusion	
2219-T31, -T81, -T37, -T351, -T851, -T87, -T3510, -T3511, -T8510, -T8511	Bare or Clad Sheet or Plate, Tube, Extrusions	
2024-T3, -T4, -T36, -T361, -T351, -T81, -T86, -T851, -T861	Bare or Clad Sheet or Plate, Tube, Bar	
2024-T4, -T3510, -T3511, -T81, -T8510, -T8511	Extrusion	
6061-T4, -T451, -T4510, -T4511	Sheet, Plate, Extrusion, Bar, Tube	
6063-T5	Extrusion	
6066-T4, -T4510, -T4511, -T6, -T6510, -T6511	Extrusion	

FL 1 Condition after re-solution heat treat and aging.

TABLE XIV - PRODUCTS SUBJECT TO LOSS OF STRESS RELIEVED CONDITION DURING REHEAT TREATMENT

MATERIAL AND TEMPER	PRODUCT	CONDITION AFTER RE-SOLUTION HEAT TREAT AND AGING
2014-T451, -T651	Bar	-T42 or -T62
2024-T351, -T3511, -T851 and -T8511	All Forms	
6061-T651 7075-T651, -T7351, -T7651, 7178-T651,	Bare or Clad Plate, Bar	-T62, -T73, or -T76
6061-T6510, -T6511, 7075-T6510, -T6511, -T73510, -T73511, -T76510, -T76511, 7175-T6510, -T6511, -T73510, -T73511, 7178-T6510, -T6511	Extrusion	
7050-T7452, -T74511, -T73511, -T76511, 7075-T652, -T7352	Extrusions, Die Forgings and Forged Block	-T62, -T73, -T74, or -T76

b. Do not heat-treat clad 2014, 2024, 2119, 2219, 7050, 7075 and 7178 more than the number of times shown in Table XV.

8.2.8 REHEAT TREATMENT (Continued)

TABLE XV - HEAT TREATMENT OF CLAD MATERIAL

THICKNESS OF MATERIAL (INCHES)	NUMBER OF PERMITTED HEAT TREATMENTS FL 1	
	FOR MATERIAL PURCHASED IN THE -O OR -F CONDITION	FOR MATERIAL PURCHASED IN THE -T CONDITION
Less than 0.025	1	0
0.025 to 0.125	2	1
More than 0.125	3	2

FL 1 Any solution treatments or annealing by Method 3, 4, or 5, as shown in Table III, are heat treatments. Solution soak times that are more than the maximum given in Table V, but less than two times that maximum, are considered two heat treatments.

8.2.9 ABORTED LOADS OF CLAD ALLOYS

a. An aborted load is counted as a heat treatment if the last process control instrument reading is at the minimum solution treating temperature in accordance with Table IV. Unless specified differently in Table XV, do a reheat treatment in accordance with the requirements of this specification. When reheat treatment is permitted in Table XV, a reheat treatment will be required to meet full specification requirements. When reheat treatment is prohibited by Table XV, reject the aborted loads.

b. Quench aborted loads of clad material that have come to the solution treating temperature in water or glycol. It is permitted to air cool loads that do not get to the solution treating temperature.

8.2.10 HEAT TREATMENT OF RIVETS

a. Solution heat treat 2024 rivets to the W condition in accordance with Section 8.2.10.1.

b. It is also permitted to heat treat nuts and other small parts in accordance with the requirements of this section.

8.2.10.1 Rivet Heat Treat Procedures

a. Unless special permission is given from BR&T, all facilities for rivet heat treatment must be in accordance with Section 6 of this specification. Qualification results must be available on request.

b. Heat treat rivets in an air furnace, salt bath or fluidized bed. Design and qualify containers, if used, in accordance with Section 6.5.

c. Heat treatment times and temperatures are listed in Table XVI.

8.2.10.1 Rivet Heat Treat Procedures (Continued)

TABLE XVI - HEAT TREATMENTS FOR RIVETS AND SELECTED SMALL PARTS

ALLOY (ANY TEMPER)	SOLUTION HEAT TREATMENT (HOLDING TIME AND TEMPERATURE)	AGING CYCLE	TEMPER
2024	910 to 930 F (487 to 499 C) for heat-up time plus soak 60 min. (30 minutes in fluidized bed)	96 hours minimum at room temperature	-T4
		None (Refrigerate within 4 minutes of quench in accordance with Section 8.2.10.1.f.)	-W

d. Holding times for salt bath, fluidized beds, and air furnaces are as follows:

(1) The hold time starts when the load enters the salt bath or fluidized bed.

(2) Hold time starts for air furnaces when all process temperature instrumentation gets to the minimum of the specified temperature range.

(3) Find the container heat up time according to Section 6.5.

(4) Hold the load for a minimum of the heat up time plus the soak time given in Table XVI.

e. Water quench as follows:

(1) Keep the quench delay to a minimum (not more than 15 seconds).

(2) The temperature of the quenching water must not be more than 90 F (32 C) before quenching, or 100 F (38 C) during the quenching.

(3) If the container is approved, heat treat the rivets in an air furnace and quench them in that same container. The depth of the rivets in the container must not be more than three inches. If the depth is more than three inches or if the containers do not let salt or quenchant touch the rivets, then:

(a) Dump the rivets into a perforated container that is submerged in water for quenching. This quickly quenches the rivets to prevent low mechanical properties or inter-granular corrosion.

(b) Hang each container in the water to permit free circulation of water.

f. Put 2024 rivets into cold storage as follows:

(1) Find the temperature of the rivets with a temperature test or use a thermocouple that is attached to the center of the charge. When the rivets get to the temperature of the quenchant, transfer them to a chilled denatured or isopropyl alcohol bath.

(a) The bath must be chilled to -40 ± 20 F (-40 ± 11 C). The alcohol bath must be able to decrease the temperature of the rivets to 0 F (-18 C) or below in 3 minutes or less.

(b) Hold the rivets in the chilled bath for at least 3 to 5 minutes, until the temperature is below -10 F (-23 C).

8.2.10.1 Rivet Heat Treat Procedures (Continued)

(c) Immediately transfer the rivets to cold storage. During transfer, do not let rivet temperature increase to more than -10 F (-23 C).

(2) Keep the rivets in storage at or below -10 F (-23 C), or to a maximum of 80 exposure units. Exposure from -10 to 0 F (-23 to -18 C) constitutes one exposure unit per hour or fraction thereof. Exposure from 0 to 32 F (-18 to 0 C) constitutes ten exposure units per hour or fraction thereof. Drive rivets in 15 minutes after exposure to temperatures above 32 F (0 C), according to this specification. Re-solution heat treat and quench, or reject rivets with more than 80 exposure units.

(3) Between quenching and driving, do not let the total elapsed time of rivet exposure to room temperature increase to more than 15 minutes. If rivets will be driven immediately after quenching, increase the total elapsed time of rivet exposure to room temperature to a maximum of 20 minutes.

g. Age, when required, in accordance with Table XVI.

h. After the heat treatment is complete, remove a representative sample of rivets for inspection in accordance with Section 10.5. Examine the nuts or equivalent small parts in accordance with Section 10.1 and Section 10.3.

8.2.11 ALTERNATIVE HEAT TREATMENT OF DIP BRAZED 6061 ALUMINUM ASSEMBLIES

a. Solution heat treatment of dip brazed assemblies of 6061 aluminum alloy is possible by quenching the assemblies after removal from the brazing flux bath. Preheat, braze, and quench temperatures and times must be in accordance with the procedure record submitted in accordance with BAC5941. The assembly transfer times from the brazing equipment to the quench must meet the requirements for quench delay in Section 8.2.4.1. It is permitted to extend the quench delay time after the transfer time tests. The transfer time must be documented as a part of the brazing procedure record. See Section 8.2.4.1.

b. Perform the precipitation treatments in accordance with Section 8.2.5.

9 MAINTENANCE CONTROL

9.1 SALT BATH CONTROL

a. Other than solution heat treatment in accordance with Section 8.2.11, use one of the compositions listed below in salt baths for heat treating aluminum alloys. There must be no negative or objectionable reactions with the materials in heat treatment.

(1) A mixture of sodium nitrate and potassium nitrate containing no less than 45 percent by weight of sodium nitrate (AMS2821, Class 2).

(2) A mixture of sodium nitrate and sodium nitrite, containing no less than 90 percent by weight sodium nitrate.

(3) 100 percent commercial grade (Chilean) sodium nitrate.

9.1 SALT BATH CONTROL (Continued)

(4) The 5000 series aluminum alloys have high magnesium alloy content. The salt bath sodium nitrate content must not be more than 90 percent for annealing these alloys.

b. A large but temporary quantity of bubbles occurs when fresh Chilean sodium nitrate is heated to the operating temperature. To decrease the risk of spatter from the tank, use the procedure that follows to recharge a tank with fresh Chilean sodium nitrate as necessary.

(1) Add only enough salt to the bath to fully submerge the heating coils. Increase the heat to the operating temperature. Do not overheat. If violent bubbling occurs, decrease the temperature until the bubbling is in control.

(2) After the initial bubbling has subsided add another increment of new and clean salt, and let the solution degas.

(3) Continue this procedure until operating level is reached.

(4) Do not let bath temperatures increase to more than 1000 F (538 C) during this procedure.

c. Clean and fill salt baths according to the recommendations of the salt supplier.

d. Clean the tanks to prevent sludge accumulation at the bottom of the tank that can submerge heating coils and cause local overheating.

(1) Pump the clean salt from the tank.

(2) Remove and discard sludge or foreign material.

(3) Clean the bath frequently to make sure there is temperature uniformity.

9.2 GLYCOL-WATER QUENCH BATH CONTROL

Measure the glycol-water quench solutions at least once every two weeks as follows:

9.2.1 QUENCHING FROM AIR FURNACES

Use one of these techniques for glycol concentration measurements in quench tanks only associated with air furnaces.

9.2.1.1 Elevated Temperature Separation

a. Fill a graduated cylinder with 100 milliliters of the glycol solution.

b. Put the cylinder in a bath at 180 to 200 F (82 to 94 C).

c. Find the volume of the glycol visually and convert it to a percentage.

9.2.1.2 Refractive Index Measurement

a. Use an optical or digital refractometer to measure the glycol concentration.

9.2.1.2 Refractive Index Measurement (Continued)

b. Calibrate the refractometer with known glycol-water concentrations in the glycol-water concentration usage range.

9.2.1.3 Kinematic Viscosity Measurement

a. Measure the kinematic viscosity to find the glycol concentration in accordance with ASTM D445.

b. Calibrate the viscosity measurements with known glycol-water concentrations in the glycol-water concentration usage range.

9.2.2 QUENCHING FROM SALT BATHS

To find the glycol concentration in quench tanks associated with salt baths or mixed air furnace/salt baths, use only the elevated temperature separation technique in Section 9.2.1.1.

9.2.3 SALT CONTAMINATION OF GLYCOL SOLUTIONS

The salt concentration of glycol quenchant solutions must not be more than 6 percent by weight.

a. Initially, do salt contamination tests a minimum of once a week on glycol quenchant used with salt bath furnaces.

b. The test frequency can decrease when the test data indicate continuous compliance with salt contamination requirements.

c. The test method is optional but calibrate the data from glycol solutions with known concentrations of salt.

10 QUALITY CONTROL

a. Assure that the requirements of this specification are met by monitoring the process and examining the end-items in accordance with established quality assurance provisions.

b. Reports that show quantitative results for all tests required by this specification must be available to Boeing Quality Assurance.

10.1 QUALITY CONFORMANCE INSPECTION AND DOCUMENTATION

a. Make sure the heat treat facilities have the correct instrumentation and certification in accordance with Section 6.

b. Make sure the charge is clean and the arrangement is correct immediately before the solution heat treatment in accordance with Section 8.1.2 and Section 8.1.3 respectively. Make sure that proper test samples are included with the load when required for acceptance.

c. Visually examine parts for blisters after solution heat treatment. Blisters are raised spots on the surface of the metal caused by expansion of gas in a subsurface zone during thermal treatment. Acceptance criteria are listed in Section 11.4.

10.1 QUALITY CONFORMANCE INSPECTION AND DOCUMENTATION (Continued)

d. Make sure that the temperature records show that cold storage units for rivets have been maintained at -10 F (-23 C) or below. Excursions not more than two minutes each when rivets are added or removed during cold storage are permitted.

e. Change circular charts when one cycle is complete. Over-recording is not permitted.

f. Confirm the identity of the alloys in each charge. Acceptable methods include, but are not limited to, checking of material markings or manufacturing plan acceptance.

g. Document these items on the work order/job planning paper work or electronic planning manufacturing record system:

(1) Heat treat load number

(2) Part numbers

(3) Work order/job number or other lot identification numbers

(4) Part quantities

(5) Alloy

(6) Quench medium

(7) Quench delay times

(8) Initial and final quenchant temperature.

h. Record the work order or job number and the ID of the inspector (responsible member of the organization doing the work) with time and temperature of the load, when it was actually put in the furnace. This information must be recorded in the paper or electronic temperature recording system.

i. If multiple work orders or jobs are in a single load, the load number and the corresponding work order or job numbers can be documented in a log. If the time and temperature meet the required range, put an indication of acceptance (stamp/ID) in the time and temperature records at the finish of the cycle. If multiple cycles are used, put an acceptance stamp on each individual cycle record.

(1) Do not accept parts if complete records, as described above, have not been accomplished.

(2) Keep the paper temperature recording charts or electronic data records in accordance with contractual record retention requirements.

j. Document acceptance of each solution heat treat and age-load in the applicable manufacturing process record.

10.2 ELECTRONIC PROGRAM CONTROL AND DATA ACQUISITION

a. If electronic programs are used, before the first production use there must be a system that:

10.2 ELECTRONIC PROGRAM CONTROL AND DATA ACQUISITION (Continued)

(1) Permits access only by designated personnel

(2) Keeps a revision record of all revisions/changes

(3) Verifies all process parameters.

b. The system must create electronic records that cannot be altered without detection.

10.2.1 AUTOMATED ACCEPTANCE OF FURNACE CYCLES

a. For computer self-inspection/acceptance to be acceptable, these provisions must be in place in the Quality Assurance system:

(1) The integrated control and data acquisition system must document all specification-required furnace parameters and tolerances. The system must monitor them at a sufficient frequency to detect and document any out-of-tolerance conditions. Recording frequency is governed by BAC5621 or AMS2750.

(2) The time and duration of any instances when these parameters are out of tolerance is recorded as part of the furnace processing record. The operator must be alerted to these conditions in some visual manner before the job is further processed.

(3) Each processing program is verified for accuracy to all specification parameters before use. A first article inspection of the first heat treat load is performed and documented to make sure the results are satisfactory.

b. If the applicable processing program is integrated into the job planning system through a bar coding or similar system that will prevent the operator from selecting the wrong program, then the computer self-inspection/acceptance is permitted. The QA System must document compliance to items a. 1 to 3 above, to verify that the proper program is embedded in the job planning.

c. When the program is selected by the operator, documented review and verification by Quality Assurance or other designated personnel is required. It is required to verify that the operator selected the correct automated program.

10.3 TEMPER VERIFICATION

Do a temper check of all parts and material in accordance with Table XVII. The cognizant Boeing Quality Assurance organization can authorize sample inspection. Sample inspection is not permitted for forgings or parts made from forgings.

TABLE XVII - REQUIRED TESTING FOR TEMPER VERIFICATION

PRODUCT FORM	ALLOY	TEMPER	REQUIRED TESTING FL 4, FL 5, FL 6
Extrusion	All 2000 series but not 2090	All	FL 1
	All 6000 series and 2090	All	FL 2
	7050	T7XXXX	FL 1, FL 3
	7075	T6XXX, T73XXX	FL 1
		T76XXX	FL 1, FL 3

10.3 TEMPER VERIFICATION (Continued)

TABLE XVII - REQUIRED TESTING FOR TEMPER VERIFICATION (Continued)

PRODUCT FORM	ALLOY	TEMPER	REQUIRED TESTING FL 4, FL 5, FL 6
Extrusion	7136	T762	FL 1
	7175	T6XXX, T73XXX	FL 1
	7178	T6XXX	FL 1
Sheet & Plate	All 2000 series but not 2090	All	FL 1
	All 6000 series and 2090	All	FL 2
	7050	T762	FL 1
	7055	T762	FL 3, FL 7
	7075	T6XX, T73XX	FL 1
		T76XX	FL 1, FL 3
	7178	T6X	FL 1
Forgings	All 2000 series	All	FL 1
	All 6000 series	All	FL 2
	7049, 7149	T73	FL 1, FL 3
	7050	T74	FL 1, FL 3
	7075	T6, T73	FL 1

FL 1 Measure the conductivity of all parts. Do a hardness test, as a minimum, on those two parts in each lot that have the maximum and minimum conductivities. Do 100 percent hardness tests on parts that cannot be conductivity tested. Also, for parts in T7XXX tempers that cannot be conductivity tested, use a specimen heat treated with the load for the conductivity test.

FL 2 Only hardness testing is required. Measure the hardness for all of the parts in the lot.

OPTION: If 6061 detail parts or material are heat treated to T42 to help handling or processing, only do the temper check with the heat treat inspection stamp and furnace records. Do this only if these conditions apply:

a. The part or material is on a welded assembly and it will be solution heat treated or aged to get the final temper. Hardness testing must be done on the final temper.

b. For assemblies only aged to T62, conductivity tests must be done on part details that are not easy to access for hardness tests. The conductivity tests can occur any time interval before the aging to T62 process.

FL 3 A tensile specimen in accordance with Section 10.4 must be processed with each heat treat lot, and tested in accordance with Section 12.2. Unless specified differently in the Engineering Drawing, use one tensile test specimen. The specimen can be the representative for multiple heat treat lots if:

a. The specimen satisfies the product form and thickness requirements of all lots.

b. All lots plus the specimen were processed through the complete heat treat cycle (solution treatment and all aging steps) together.

10.3 TEMPER VERIFICATION (Continued)

FL 4 The Engineering Drawing may require more testing.

FL 5 When hardness and/or conductivity testing cannot be done, use specimens in accordance with Section 10.4. Examples of conditions where hardness and/or conductivity testing cannot be done are part geometry, weld heat-affected zones, et cetera.

FL 6 The heat treat inspection records required by Section 10.1 must be used for temper verification of parts or material less than 0.026 inch thick.

FL 7 Examine all parts for conductivity. Measure the Rockwell B hardness of those two parts in each lot that have the maximum and minimum conductivities. Keep the results for BR&T review.

10.4 CONDUCTIVITY - HARDNESS - TENSILE TEST SPECIMENS

a. To represent the parts for tensile, hardness, and/or conductivity testing, use material that is:

(1) From the same product form

(2) The same thickness as the parts

(3) Preferably from the same heat lot.

It is permitted to use bare sheet specimens to represent clad sheet parts for the hardness and/or conductivity tests. It is permitted to use a bare 6061 sheet, plate, bar, or extruded specimen as a representative for the 6061 welded assemblies. It is also permitted to use it for parts made from 6061 tubing. The specimen must be as thick as the thickest location on the part.

b. Forging specimens can be remnants of a forging, forged block, or a prolongation. It can also be a section or prolongation that is cut from the forging after heat treatment.

c. Each heat treat lot must have a test specimen. Each specimen must be traceable to the heat treat lot by a part and manufacturing control number. The specimen must stay with the heat treat lot through all heat treatment operations.

d. Unless specified differently, make sure that the tensile specimens are in accordance with ASTM B557.

10.5 INSPECTION OF RIVETS

After the solution heat treatment, age a sample of rivets from each furnace load in accordance with Table XVI. Check the shear strength for compliance with BPS-R-131. Shear test 2024 rivets that are to be driven in the -W condition at any time interval after quenching. When the sample rivets meet the shear strength requirements of BPS-R-131 at minimum, release the related furnace load of rivets to production.

10.5.1 RIVET SAMPLE

a. Get all sample rivets from the center of the volume of the quenching basket. Get the rivets with the smallest diameter that can be double shear tested. If none of the rivets in the furnace load have the correct dimensions for double shear testing, get the smallest diameter rivets for single shear testing.

10.5.1 RIVET SAMPLE (Continued)

b. The sample size per furnace load must be in accordance with the lot sampling provisions of BPS-R-131.

11 REQUIREMENTS

Suppliers governed by a Boeing purchase agreement must meet the record retention requirements of the purchase contract. All other suppliers must meet the record retention requirements of The Boeing Company. Consult with the Boeing contract focal or the Boeing records focal, for specific information for retention requirements.

11.1 MECHANICAL PROPERTIES

When tested in accordance with Section 12.2, tensile strength must be, in sequence of precedence, as follows:

a. As specified by the Engineering Drawing.

b. The material specification given in the Engineering Drawing.

c. As specified in this standard.

11.2 HARDNESS - CONDUCTIVITY REQUIREMENTS

Unless specified differently in this standard, hardness and conductivity must be in accordance with BAC5946.

11.2.1 7075-T73XX AND 7175-T73XX PARTS

This material must meet the requirements of BAC5946 and as follows:

NOTE: See the internal reference document for requirements for 7175-T74(T736).

a. If the conductivity is 38.0 to 42.5 percent IACS and the hardness is HRB 79.5 to 89.0 or 135-154 HB (10 mm ball, 1000 Kg load), the material is satisfactory.

b. When conductivity is more than 42.5 percent IACS, the parts must be 100 percent hardness tested. Parts are acceptable if the hardness in the area of high conductivity is more than HRB 81.5 (HB 139). If hardness is not at the HRB 81.5 (HB 139) minimum, do a tensile test on material taken from the same area. The tensile test must be satisfactory in accordance with minimum strength requirements. Other parts from the same heat treat lot that are in the same condition are acceptable.

c. Re-age parts with conductivity readings less than 38 percent IACS in accordance with Section 8.2.6. Alternatively, re-solution heat treat the nonconforming parts and re-age.

11.2.2 7136-T762 EXTRUSIONS

When tested in accordance with Section 10.3, specimen properties must be as follows:

a. Electrical conductivity must be 36 percent IACS or more.

(1) If the conductivity is less than 36 percent IACS, re-age in accordance with Section 8.2.6.

11.2.2 7136-T762 EXTRUSIONS (Continued)

(2) Alternatively, for parts made from material that is less than 0.75 inch thick and the conductivity is less than 36 percent IACS, perform the exfoliation corrosion test in accordance with Section 12.5. The material is satisfactory if the exfoliation corrosion rating is EB or better.

b. Minimum Rockwell Hardness must be as follows:

(1) 89 for material thickness > 0.012 inch and < 0.040 inch according to the R15T scale.

(2) 89 for material thickness ≥ 0.040 inch according to the RB scale.

11.2.3 2524-T42 SHEET AND PLATE

When tested in accordance with Section 10.3, use the hardness and conductivity requirements for 2024-T4X in BAC5946 to accept the material.

11.3 CONDUCTIVITY - TENSILE TEST REQUIREMENTS

11.3.1 7049-T73 AND 7149-T73 FORGINGS

When tested in accordance with Section 10.3, properties of test specimens must be as follows:

a. If the electrical conductivity is below 38 percent IACS, re-age the material in accordance with Section 8.2.6.

b. The material is satisfactory if:

(1) The electrical conductivity is 38 percent IACS or more, and

(2) The results of tensile testing are in compliance with the specification requirements. Use the material thickness at time of heat treatment to find the tensile property requirements.

11.3.2 7050-T74 HAND FORGINGS AND DIE FORGINGS

After the tests in Section 10.3 for heat treat verification, the test specimen must satisfy the applicable specifications and these conditions:

a. If the electrical conductivity is below 38 percent IACS, re-age in accordance with Section 8.2.6.

b. If the Tensile Yield Strength (TYS) is more than these limits, re-age in accordance with Section 8.2.6:

(1) Longitudinal, 72 ksi

(2) Long Transverse, 69 ksi. Use this only when a longitudinal coupon is not available.

c. If the electrical conductivity is at least 40 percent IACS, and the longitudinal TYS is 72 ksi (69 ksi for long transverse) or less, then accept the forgings.

d. Forgings are acceptable if:

11.3.2 7050-T74 HAND FORGINGS AND DIE FORGINGS (Continued)

(1) The Electrical Conductivity (EC) is at least 38 but less than 40 percent IACS, and

(2) The TYS is less than or equal to 32 + EC (29 + EC for long transverse).

If both of these requirements are not met:

(3) Re-age the lot, together with some of the test coupons, in accordance with Section 8.2.6 or

(4) Re-solution heat treat and re-age the lot and test coupons.

11.3.3 7050-T76 AND 7050-T73XX EXTRUSIONS

a. When tested in accordance with Section 10.3, 7050-T76 coupons must have these properties:

(1) Minimum mechanical properties in the longitudinal grain direction:

(a) Ultimate Tensile Strength - 79 ksi

(b) TYS (0.2 percent offset) - 69 ksi

(c) Elongation (in 2 inches or 4D) - 7 percent.

(2) EC must be 37.0 percent IACS or more. If the EC is 37.0 to 38.9 percent IACS, then longitudinal tensile yield strength must be less than or equal to 36.0 + EC.

b. When tested in accordance with Section 10.3, 7050-T73XX specimens must have these properties:

(1) Minimum mechanical properties in the longitudinal grain direction:

(a) Ultimate Tensile Strength - 70 ksi

(b) TYS (0.2 percent offset) - 60 ksi

(c) Elongation (in 2 inches or 4D) - 8 percent.

(2) EC must be 40 percent IACS or more. If conductivity is at least 40 percent IACS but less than 41 percent IACS, the longitudinal TYS must not be more than 69 ksi. If conductivity is 41 percent IACS or greater, maximum yield strength is not restricted.

c. Re-age materials and test specimens in accordance with Section 8.2.6 that do not conform to Section 11.3.3.a. or Section 11.3.3.b. Alternatively, it is permitted to re-solution heat treat and age the material and specimens together.

11.3.4 7055-T762 SHEET

When tested in accordance with Section 10.3, specimen properties must be as follows:

a. EC must be 34.5 percent IACS or more.

b. A tensile specimen from the same 7055-0 raw-material heat lot must be:

11.3.4 7055-T762 SHEET (Continued)

(1) In the as-received thickness.

(2) Representative of either the Longitudinal (L) or Long Transverse (LT) orientation.

(3) Heat treated with the parts.

c. The tensile properties must be in accordance with BMS7-387.

11.3.5 7075-T76XX SHEET, PLATE AND EXTRUSIONS

When tested in accordance with Section 10.3, specimen properties must be as follows:

a. EC must be 38 percent IACS or more.

(1) If conductivity is less than 38 percent IACS, re-age in accordance with Section 8.2.6.

(2) Alternatively, for parts made from material that is less than 0.75 inch thick, perform the exfoliation corrosion test in accordance with Section 12.5. The material is satisfactory if the exfoliation corrosion rating is EB or better. This test can be performed when:

(a) EC is 36 percent IACS or more, and

(b) EC is less than 38 percent IACS.

b. Minimum mechanical properties must be in accordance with Table XVIII. Use a longitudinal or long transverse coupon for the mechanical property verification.

TABLE XVIII - MECHANICAL PROPERTIES FOR 7075-T76XX SHEET, PLATE AND EXTRUSIONS

MATERIAL FORM, DIRECTION, AND THICKNESS			UTS (KSI)	TYS (KSI)	PERCENT ELONG.
Bare Sheet & Plate	L		72	62	8
	LT		73	62	8
Clad Sheet	L	0.040 to 0.062	66	56	8
		0.063 to 0.187	67	57	8
		0.188 to 0.249	69	59	8
	LT	0.040 to 0.062	67	56	8
		0.063 to 0.187	68	57	8
		0.188 to 0.249	70	59	8
Extrusion	L	< 0.250	71	61	7
		0.250 to 1.000	75	65	7
	LT	< 0.250	68	57	7
		0.250 to 0.499	72	61	7
		0.500 to 0.749	71	60	7
		0.750 to 1.000	70	59	7

11.4 BLISTERS

a. Accept blisters on as-extruded surfaces if they are not more than 1/32 (0.03125) inch in length or width. Also there must be no more than 10 blisters per linear inch, or no more than 10 blisters in a 0.50 inch diameter circle. Do not accept parts with more blisters than the allowance. Analyze the parts with blisters for rework, as follows.

b. Rework to remove blisters is permitted if:

(1) The cross section and metallurgical analysis of the part in the lot with the most blistering confirms there is no eutectic melting.

(2) There are no voids that cannot be removed in the dimensional tolerance of the extrusion.

c. Rework parts by sanding in accordance with BAC5748 or chemical milling in accordance with BAC5772 Type II. Parts must be reinspected with the inspection method originally used to find the blisters.

d. Reject parts with blisters on machined surfaces, or that do not meet the criteria for rework.

e. Reject blisters on product forms other than extrusions.

12 TEST METHODS

12.1 ELECTRICAL CONDUCTIVITY TEST METHOD

Perform electrical conductivity testing in accordance with BAC5651.

12.2 TENSILE TEST METHOD

a. Machine the tensile test specimens in accordance with ASTM B557 to the largest size permitted by the part configuration.

b. Perform tensile testing in accordance with ASTM B557.

12.3 HARDNESS TEST METHOD

Perform hardness testing in accordance with BAC5650.

12.4 EUTECTIC MELTING AND HIGH TEMPERATURE OXIDATION TEST METHODS

a. Samples can consist of: broken tensile specimens, temper inspection coupons, production parts, or simulated production parts of the same alloy and product form. Clad samples must not represent bare aluminum production parts. When pulled tensile specimens are used, examine the specimen with the lowest yield strength. For material 0.020 inch or more in thickness, remove and examine a 1 by 3 inch strip. The strip must be from the same sheet as the tensile specimen with the lowest yield strength.

b. Section and polish the sample to a fineness for examination at 500X.

c. Examine the specimen at 500X as follows:

12.4 EUTECTIC MELTING AND HIGH TEMPERATURE OXIDATION TEST METHODS (Continued)

(1) Examine unetched to find indications of high temperature oxidation. Multiple voids in grain boundaries near the surface which are visible in more than two fields of view are evidence of high temperature oxidation.

(2) Etch mildly (approximately 2 seconds) in an etchant such as Keller's etch to find and examine for eutectic melting. See Figure 4 below for example of unacceptable microstructure:

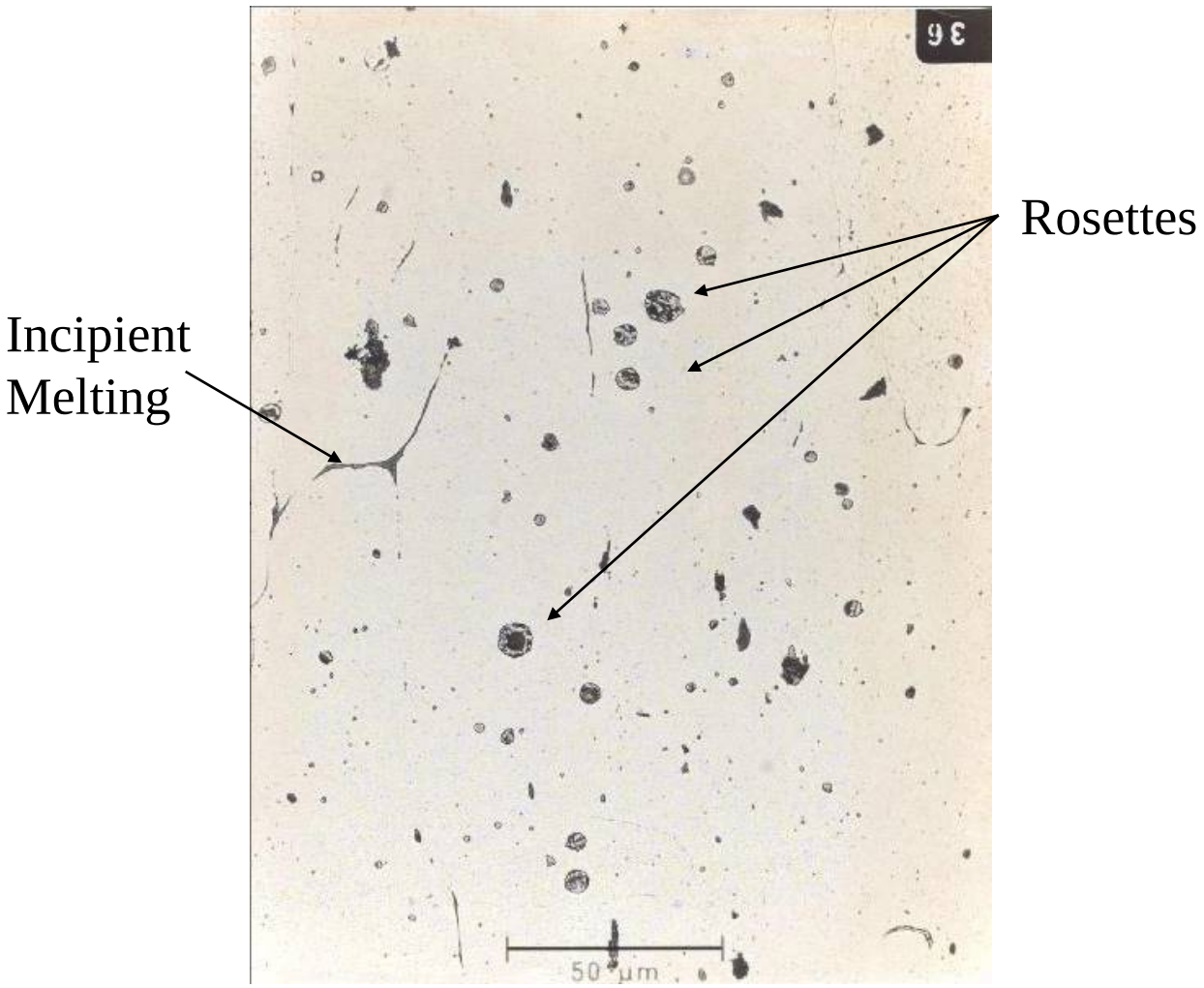

FIGURE 4 - MICROSTRUCTURAL EXAMPLES ASSOCIATED WITH EUTECTIC MELTING

12.5 EXFOLIATION CORROSION TEST METHODS

Perform exfoliation corrosion resistance testing in accordance with ASTM G34.

12.6 SHEAR STRENGTH

Perform the shear strength testing of rivets in accordance with BPS-R-131.

13 QUALIFICATION

Not applicable to this specification.

MOI UNIVERSITY

Telephone: +254 321 43170
Fax: +254 321 43170
E-mail: *deanengineering@mu.co.ke*

P. O. Box 3900
Eldoret,
KENYA

SCHOOL OF ENGINEERING

CERTIFICATE OF CORRECTIONS

This is to certify that all corrections proposed at the Board of Examiners meeting held on …**Monday**, **30th October 2023**…… in respect of MSc thesis of…

Robert Kipchumba Rutto….Reg No…**ENG/MIE/3988/20**…….

Titled ……**Investigation of microstructural cracking of riveted and Heat-treated Al7075 alloys under constant fatigue loading**……

……

Have been effected to my/our satisfaction and the thesis can now be prepared for binding.

Supervisor

Prof Diana Madara

Date: 13th November 2023

Moi University, Eldoret, Kenya

Supervisor

Dr J .K .Kiplagat

Date: 13th November 2023

Moi University, Eldoret, Kenya